

**Ubiquitin and ubiquitin-like systems
in *Saccharomyces cerevisiae***

Loes Andrea Leonora van de Pasch

ISBN 978-90-393-5855-9

Printed by Drukwerkconsultancy, Boereboom Grafische Bedrijven B.V., Utrecht

The research described in this thesis was financially supported by the Netherlands Organization for Scientific Research (NWO).

Ubiquitin and ubiquitin-like systems in *Saccharomyces cerevisiae*

Ubiquitine en ubiquitine-achtige systemen in *Saccharomyces cerevisiae*
(met een samenvatting in het Nederlands)

Proefschrift

ter verkrijging van de graad van doctor aan de Universiteit Utrecht
op gezag van de rector magnificus, prof.dr. G.J. van der Zwaan,
ingevolge het besluit van het college voor promoties in het openbaar te
verdedigen op maandag 5 november 2012 des middags te 12.45 uur

door

Loes Andrea Leonora van de Pasch

geboren op 1 februari 1982 te Horst

Promoter: Prof.dr. F.C.P. Holstege

Table of contents

Abbreviations		6
Chapter 1	General introduction	9
Chapter 2	Delineating ubiquitin and ubiquitin-like systems in <i>Saccharomyces cerevisiae</i> by gene expression profiling	33
Chapter 3	A gene expression signature for ubiquitin-proteasome system defects in <i>Saccharomyces cerevisiae</i>	65
Chapter 4	Centromere binding and a conserved role in chromosome stability for SUMO-dependent ubiquitin ligases	91
Chapter 5	Subunit-specific functions of the SUMO-targeted ubiquitin E3 ligase Slx5/8	119
Chapter 6	General discussion	135
Nederlandse samenvatting		149
Curriculum vitae		151
Publications		152
Dankwoord		153

Abbreviations

APC/C	anaphase promoting complex/cyclosome
BIR	break-induced replication
ChIP	chromatin immunoprecipitation
DSB	double-stranded DNA break
DUB	deubiquitinating enzyme
E1	ubiquitin(-like)-activating enzyme
E2	ubiquitin(-like)-conjugating enzyme
E3	ubiquitin(-like) protein ligase
ER	endoplasmic reticulum
ERAD	ER-associated protein degradation
ESCRT	endosomal sorting complex required for transport
FC	fold change
GO	gene ontology
HECT	'homologous to E6-associated protein C-terminus' domain
HR	homologous recombination
HU	hydroxyurea
Hub1	homologous to ubiquitin 1
MAPK	mitogen-activated protein kinase
MVB	multivesicular body
NMD	nonsense-mediated mRNA decay
PACE	proteasome-associated control element
PCNA	proliferating cell nuclear antigen
PE	phosphatidylethanolamine
PML	promyelocytic leukemia protein
RGR	relative growth rate
RING	'really interesting new gene' domain
RNF4	RING finger protein 4
Rub1	related to ubiquitin 1
SAC	spindle assembly checkpoint
SAGA	Spt-Ada-Gcn5-acetyltransferase complex
SAP	Sit4-associated protein
SCF	Skp1/Cul1/F-box protein complex
SIM	SUMO-interaction motif
SLIK	SAGA-like complex
SLX	Synthetic Lethal Unknown
SPOC	spindle position checkpoint
STUbL	SUMO-targeted ubiquitin ligase

SUMO	small ubiquitin-like modifier
TFBS	transcription factor binding site
TGN	trans-Golgi network
UBD	ubiquitin-binding domain
Ubl	ubiquitin-like modifier
ULP	ubiquitin-like protease
UPS	ubiquitin-proteasome system
UPR	unfolded protein response
Urm1	ubiquitin-related modifier 1
wt	wild type



1

General introduction

General introduction

Proteins are the building blocks of cells and play fundamental roles in virtually all cellular processes. The functionality of individual proteins is greatly expanded through posttranslational modifications. Protein modification is an efficient way for a cell to respond and adapt to a variety of cues. Intra- and extracellular stimuli can trigger the modification of specific proteins, allowing the cell to modulate cellular processes rapidly and reversibly, for example in cell cycle progression, transcription, DNA repair and vesicular transport. A large array of posttranslational modifications exists, including small-molecule modifications such as phosphorylation, acetylation and methylation, but there is also a class of proteinaceous modifications. The most well-known modifier of the latter category is the ubiquitin protein, the attachment of which can modify many proteins in all eukaryotic cells from yeast to human. Since the discovery of ubiquitin in the mid-1970s, an entire family of small protein modifiers known as ubiquitin-like modifiers (Ubls) has been identified. Selective protein modification with ubiquitin or Ubls is a complex process that involves intricate enzyme systems. In the budding yeast *Saccharomyces cerevisiae* these include the systems of ubiquitination, sumoylation, neddylation, urmylation, Hub1 modification and Atg8/Atg12 modification. This chapter gives a global overview of all the ubiquitin and ubiquitin-like systems, with a focus on ubiquitination and sumoylation in *S. cerevisiae*. A large part of the work described in this thesis will deal with the functional characterisation of a novel class of SUMO-targeted ubiquitin ligases (STUbls). Particular attention is therefore spent on the roles of STUbls, which highlights the diverse functional interactions between the systems of ubiquitination and sumoylation.

Ubiquitin and ubiquitin-like modifiers

Ubiquitin and ubiquitin-like modifiers are a

family of small proteins that are dedicated to the modification of other proteins. Ubiquitin(-like) proteins are widespread among all eukaryotes and are thought to have evolved from prokaryotic sulphurtransferase systems¹. All ubiquitin(-like) modifiers have a remarkably similar globular protein structure that contains the characteristic ubiquitin or β -grasp fold. At least eleven different ubiquitin(-like) proteins have been identified: ubiquitin, Atg8, Atg12, FAT10, FUB1, Hub1, ISG15, NEDD8, SUMO, UFM1 and Urm1, of which seven are conserved in *S. cerevisiae*^{1,2}. Recently, ubiquitin-like proteins have also been identified in prokaryotes (PUPs) and archaea (SAMPs)^{3,4}. Ubiquitin and SUMO (small ubiquitin-like modifier) are the two most common protein modifiers of a large number of substrates that take part in very diverse cellular pathways^{5,6}. Proteomics approaches have estimated that in *S. cerevisiae* around 250 to 1000 proteins are modified by ubiquitin and around 150 proteins are sumoylated out of 6300 genes⁷⁻¹⁰. The number of substrates of the other Ubls is far more limited and they have very specific condition-dependent functions. Also their means of conjugation to substrates has diverged from the evolutionarily conserved and analogous systems of ubiquitination and sumoylation. First the general molecular mechanisms and functions of ubiquitin(-like) modification will be described based on ubiquitination and sumoylation. The other ubiquitin-like systems of *S. cerevisiae* will be discussed separately at the end of this chapter.

The molecular mechanism of ubiquitination and sumoylation

Ubiquitin and SUMO are small polypeptides of 76 and 98 amino acids respectively, which are synthesised as inactive precursor modifier proteins. *S. cerevisiae* harbours four genes that encode for ubiquitin precursor proteins (*RPL40A*, *RPL40B*, *RPS31* and *UBI4*) and a single gene for the SUMO precursor (*SMT3*). The four ubiquitin-encoding genes produce identical ubiquitin proteins, but they are fused to ribosomal protein genes or multiple

repeats of ubiquitin genes. In order to produce a functional, conjugatable modifier, the ubiquitin precursor has to be proteolytically cleaved by deubiquitinating enzymes (DUBs). The C-terminus of SUMO is also cleaved by SUMO-specific ubiquitin-like proteases (ULPs). A hallmark of the processing step is that this exposes a C-terminal diglycine motif, which is used as future acceptor site for conjugation to target proteins. The attachment of the processed modifier to a substrate involves the concerted action of multiple enzymes called E1, E2 and E3 enzymes, which function in a consecutive order (Figure 1)^{2,11-13}. The first step is the activation of the modifier by the ubiquitin- or SUMO-activating enzyme, also known as E1 enzyme. The E1 enzyme adenylates the C-terminal glycine of the modifier using ATP and forms a high-energy thioester bond between the active-site cysteine of the E1 and ubiquitin or SUMO. Next, the modifier is transferred to the active-site cysteine of the E2 enzyme, which is also known as

ubiquitin- or SUMO-conjugating enzyme. The E2 enzyme can attach the modifier to a target protein, but it requires an E3 ligase, which provides the substrate specificity. The E3 ligase mediates the interaction between the substrate and the E2 enzyme, and allows the transfer of ubiquitin or SUMO from the active-site cysteine of the E2 to the substrate. In general, a lysine residue in the substrate is used as acceptor site for ubiquitin(-like) modification. However, also the terminal NH₂ group of a protein can be the site of modification. A key aspect of ubiquitination and sumoylation is that it is reversible. DUBs and ULPs can cleave the ubiquitin or SUMO moiety from a substrate, leaving the substrate unmodified and allowing the recycling of the ubiquitin(-like) protein for another round of conjugation¹⁴⁻¹⁶. This makes ubiquitination and sumoylation a dynamic process that is based on the balanced and regulated conjugation and deconjugation of a ubiquitin(-like) modifier to and from substrates (Figure 1).

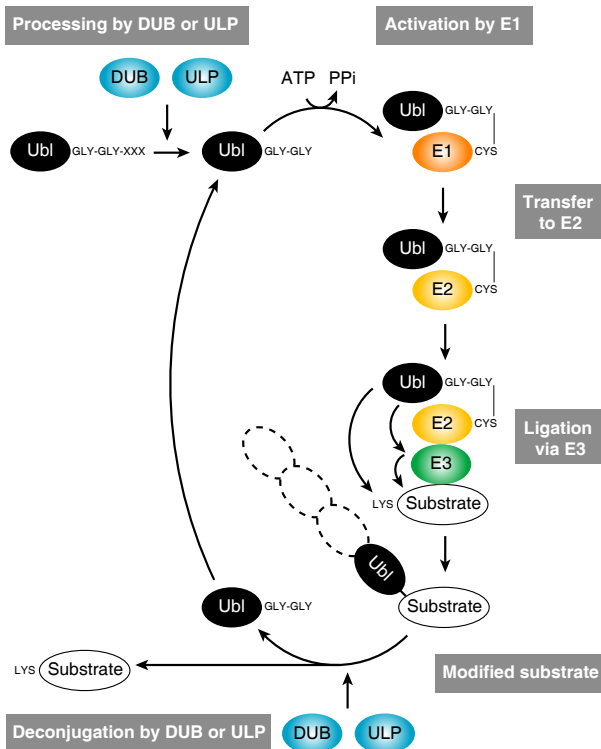


Figure 1. A generalised molecular mechanism for reversible ubiquitination and sumoylation.

Precursor ubiquitin and SUMO (Ubl) are processed by a deubiquitinating enzyme (DUB) or ubiquitin-like protease (ULP) to expose the C-terminal diglycine residues. The processed Ubl is adenylated at the C-terminal glycine and covalently attached to the catalytic cysteine of the Ubl-activating enzyme (E1). The Ubl is transferred to the catalytic cysteine of a Ubl-conjugating enzyme (E2), which can ligate the Ubl to a substrate. This is accomplished with an E3 ligase (E3), which mediates the interaction between the E2 and the substrate. The Ubl is either directly ligated to the substrate, usually at a lysine residue, or via an intermediate step where the Ubl is first transferred to the E3 and then to the substrate. Multiple rounds of ligation results in Ubl chain formation on a substrate, e.g. polyubiquitination and polysumoylation (indicated with dashed lines). Ubl modification is reversible due to Ubl deconjugation by DUBs and ULPs, which cleave the Ubl from the substrate. The free Ubl can be recycled for a new round of conjugation. Adapted from Kerscher *et al.* and Geiss-Friedlander *et al.*^{2,13}.

Besides functioning as monomeric protein modifier, ubiquitin and SUMO can also form polymeric chains on substrates. This is achieved by repeated conjugation of ubiquitin or SUMO to an internal lysine residue of the preceding modifier that is already attached to a substrate. Ubiquitin has seven lysine residues (K6, K11, K27, K29, K33, K48 and K63) that can all be used for polyubiquitin chain formation. The type of chain is dictated by the combination of specific E2 and E3 enzymes. Depending on the type of ubiquitin linkage, different conformations and lengths of ubiquitin chains can be generated, which create specific molecular signals¹⁷. In some specific cases, the elongation of polyubiquitin chains requires an E4 enzyme, which supports the assembly of ubiquitin chains^{18,19}. SUMO can also form chains^{20,21}. The capacity of yeast SUMO to form polymeres lies in the N-terminal portion of the protein, where at least three lysine residues (K11, K15 and K19) contribute to chain formation. However, yeast mutants that lack the lysine residues for SUMO polymerisation have no phenotypic defects²². The physiological role of SUMO chains remains therefore poorly understood.

Ubiquitin and SUMO system components in *S. cerevisiae*

The molecular process of ubiquitination involves a large number of catalytic components, which are organised in a complex system. Uba1 is the single ubiquitin-activating (E1) enzyme, which transfers ubiquitin to twelve different ubiquitin-conjugating (E2) enzymes (Table 1). The E2 enzymes specifically cooperate with one or more ubiquitin E3 ligases. Currently, over 30 distinct ubiquitin E3 ligases have been identified, which target different substrates and are therefore implicated in very diverse cellular processes (Table 2). Some E3 ligases function as monomers, whereas others function in large multi-protein complexes, such as the anaphase promoting complex/cyclosome (APC/C) and Skp1/Cul1/F-box protein (SCF) ubiquitin ligase complexes^{23,24}. Ubiquitin E3 ligases are characterised by the

presence of one of three defining protein domains required for ubiquitination. Most E3s belong to the RING (really interesting new gene) domain family. RING E3 ligases function as scaffolds that simultaneously bind the E2 and the substrate. They stimulate ubiquitination of the substrate by positioning the E2 and the substrate in proximity of each other²⁵. The U-box is a domain that is structurally and functionally similar to the RING domain and is found in ubiquitin E3 and E4 ligases²⁶. In contrast to the RING and U-box E3s, ubiquitin E3 ligases with a so-called HECT (homologous to E6-associated protein C-terminus) domain actively participate in the enzymatic ubiquitination reaction. HECT E3s contain a conserved cysteine residue that temporarily binds ubiquitin prior to its attachment to a substrate²⁷.

At least 18 deubiquitinating enzymes exist, which are involved in ubiquitin processing or in the removal of ubiquitin from ubiquitin-protein conjugates (Table 3). In *S. cerevisiae*, they comprise cysteine proteases of three distinct subfamilies, the UBP (ubiquitin-specific processing protease), UCH (ubiquitin carboxy-terminal hydrolase) and OTU (ovarian tumour-related protease) subfamily, and one metalloprotease (Rpn11), all with different modes of action¹⁶. In contrast to the majority of E2 and E3 enzymes, the mechanisms and physiological roles of most DUBs are still very poorly characterised²⁸.

The basic organisational structure of the sumoylation system is very similar to that of the ubiquitin system, but it involves much less enzymes (Table 4). In *S. cerevisiae* and most other species, the SUMO system comprises one heterodimeric E1 enzyme complex (Aos1/Uba2) and only one SUMO-specific E2 enzyme (Ubc9)^{29,30}. Sumoylation by Ubc9 does not necessarily require an E3 ligase. Many substrates for sumoylation contain a sumoylation consensus motif (I/V/L)-K-X-(D/E), where X is any amino acid. *In vitro* studies have shown that Ubc9 binds directly to this motif and that it can sumoylate proteins in the absence of E3s^{31,32}. Nonetheless, at least four SUMO-specific E3 ligases (Cst9, Mms21,

Nfn1 and Siz1) facilitate sumoylation by Ubc9 *in vivo* towards specific substrates in *S. cerevisiae*^{33–36}. Ulp1, Ulp2 and Wss1 are three SUMO-specific proteases in *S. cerevisiae*. Ulp1 localises to the nuclear pore complex and is required for SUMO precursor processing and for cleaving SUMO conjugates. Ulp2 resides in the nucleus and does not cleave the precursor SUMO, but desumoylates a distinct set of conjugates^{14,15}. Wss1 is implicated in the deconjugation of polysumoylated proteins³⁷.

The ubiquitin and sumoylation systems are not restricted to the E1, E2, E3 and deconjugating enzymes. Besides the catalytic components, there are also many adapter proteins that contribute to the substrate specificity of E3s, the interaction between E2s and E3s or the subcellular location of the

enzymes. Many of these proteins contain ubiquitin-binding domains (UBDs) or SUMO-interaction motifs (SIMs) for transient, noncovalent interactions with ubiquitin and SUMO moieties on substrates^{38,39}. These molecular interaction events function as signalling pathways to downstream effector proteins in order to regulate cellular processes.

Cellular functions of ubiquitination and sumoylation

The functional consequences of ubiquitin or SUMO modification vary per substrate. In general, the modification either promotes or inhibits the interaction of the modified substrate with other proteins. This is important for the assembly of multi-

Table 1. Overview of ubiquitin E1 and E2 enzymes and their function in *S. cerevisiae*

Gene	Description ¹
<i>UBA1</i>	Ubiquitin activating enzyme (E1); involved in ubiquitin-mediated protein degradation and essential for viability
<i>UBC1</i>	Ubiquitin-conjugating enzyme (E2); mediates selective degradation of short-lived and abnormal proteins; plays a role in vesicle biogenesis and ERAD; component of the cellular stress response
<i>RAD6</i> (<i>UBC2</i>)	Ubiquitin-conjugating enzyme (E2); involved in postreplication repair (as a heterodimer with Rad18), DSB repair and checkpoint control (as a heterodimer with Bre1), ubiquitin-mediated N-end rule protein degradation (as a heterodimer with Ubr1)
<i>CDC34</i> (<i>UBC3</i>)	Ubiquitin-conjugating enzyme (E2) and catalytic subunit of SCF ubiquitin-protein ligase complex (together with Skp1, Rbx1, Cdc53, and an F-box protein); regulates cell cycle progression by targeting key substrates for degradation
<i>UBC4</i>	Ubiquitin-conjugating enzyme (E2); mediates degradation of abnormal or excess proteins, including calmodulin and histone H3; interacts with many SCF ubiquitin protein ligases; component of the cellular stress response
<i>UBC5</i>	Ubiquitin-conjugating enzyme (E2); mediates selective degradation of short-lived, abnormal, or excess proteins, including histone H3; central component of the cellular stress response; expression is heat inducible
<i>UBC6</i>	Ubiquitin-conjugating enzyme (E2); involved in ERAD; located at the cytosolic side of the ER membrane; tail region contains a transmembrane segment at the C-terminus; substrate of the ubiquitin-proteasome pathway
<i>UBC7</i>	Ubiquitin-conjugating enzyme (E2); involved in ERAD; requires Cue1 for recruitment to the ER membrane; proposed to be involved in chromatin assembly
<i>UBC8</i>	Ubiquitin-conjugating enzyme (E2); negatively regulates gluconeogenesis by mediating the glucose-induced ubiquitination of fructose-1,6-bisphosphatase (FBPase); cytoplasmic enzyme that catalyses the ubiquitination of histones <i>in vitro</i>
<i>PEX4</i> (<i>UBC10</i>)	Peroxisomal ubiquitin-conjugating enzyme (E2); required for peroxisomal matrix protein import and peroxisome biogenesis
<i>UBC11</i>	Ubiquitin-conjugating enzyme (E2); most similar in sequence to <i>Xenopus</i> ubiquitin-conjugating enzyme E2-C, but not a true functional homologue of this E2; unlike E2-C, not required for the degradation of mitotic cyclin Clb2
<i>UBC13</i>	Ubiquitin-conjugating enzyme (E2); involved in error-free DNA postreplication repair; interacts with Mms2 to assemble ubiquitin chains at the Ub Lys63 residue; DNA damage triggers redistribution from the cytoplasm to the nucleus
<i>MMS2</i>	Ubiquitin-conjugating enzyme variant; involved in error-free DNA postreplication repair; forms a heteromeric complex with Ubc13, an active ubiquitin-conjugating enzyme; cooperates with chromatin-associated RING finger proteins Rad18 and Rad5

¹ Obtained from the Saccharomyces Genome Database (www.yeastgenome.org)

protein complexes or the localisation of proteins to specific subcellular locations. A classic example is RanGAP1, which was the first characterised sumoylated protein in mammalian cells. Unmodified RanGAP1 is cytosolic, but upon sumoylation becomes tethered to the nuclear pore complex to regulate nuclear import^{40,41}. Ubiquitination and sumoylation are both implicated in numerous proteolytic and nonproteolytic processes in various cellular pathways. A brief summary of a selection of cellular pathways in *S. cerevisiae* that depend on ubiquitination or sumoylation is given below.

The ubiquitin-proteasome system

The most well-known function of ubiquitination is targeting of proteins to the proteasome for proteolysis. The proteasome is a ~ 2.5 MDa protein complex that consists of at least 33 subunits in *S. cerevisiae*. It can be subdivided in two subcomplexes, known as the 20S or core particle and the 19S or regulatory particle. The core particle is a barrel-shaped structure, which contains a cavity that harbours the peptidolytic activity. The regulatory particle is associated with both ends of the core particle and regulates the recognition of ubiquitinated substrates, protein unfolding and opening of the core particle pore^{42,43}. The targeting of proteins to the proteasome is mostly based on the recognition of substrates modified with K48-linked polyubiquitin chains. The regulatory particle of the proteasome contains several polyubiquitin receptors, such as Rpn10, Rpn13 and UBD-containing accessory proteins, to bind polyubiquitinated substrates. Some substrate-bound E3 enzymes also associate directly with the regulatory particle to recruit the substrate to the proteasome themselves^{44,45}. Next, the regulatory particle unfolds the substrate and translocates it into the proteasomal cavity, where the substrate is deubiquitinated and ultimately degraded⁴⁶. The ubiquitin-proteasome system (UPS) is therefore crucial for regulating protein turnover, which is important for the removal of misfolded, damaged or excess proteins, but also for the selective degradation of certain proteins.

ER-associated protein degradation

A cellular process that very much depends on the UPS is endoplasmic reticulum (ER)-associated protein degradation (ERAD). Newly synthesised, unfolded proteins are translocated to the ER and folded with the assistance of chaperones to form mature proteins. Misfolded proteins on the other hand need to be eliminated by the UPS⁴⁷. In *S. cerevisiae*, three ubiquitin E2 enzymes (Ubc1, Ubc6 and Ubc7) participate in ERAD. They cooperate with two ubiquitin E3 ligases, the Ssm4 and Hrd1 complexes, which target distinct ERAD substrates^{48,49}. The ubiquitinated proteins are actively extracted from the ER by the ATPase complex Cdc48/Npl4/Ufd1 or they are bound in the cytoplasmic lumen after passage through the ER-membrane^{50,51}. Cdc48/Npl4/Ufd1 ultimately escorts the substrates to the proteasome for degradation⁵².

Ubiquitin-dependent vesicular transport

Vacuolar protein degradation is a second major route for protein degradation and is independent of the proteasome. The yeast vacuole, equivalent to the mammalian lysosome, can receive intracellular and extracellular material via various secretory pathways, one of which is the ubiquitin-dependent multivesicular body (MVB) pathway. A major class of proteins that are regulated by the MVB pathway are yeast permeases, which are transmembrane transporters for nutrients. *S. cerevisiae* harbours almost one hundred permeases, which function under specific conditions and are tightly regulated to adapt to changes in nutrient availability. Monoubiquitination or short K63-linked ubiquitin chain modification of permeases and other membrane-bound proteins by the ubiquitin E3 ligase Rsp5 induces their internalisation from the plasma membrane to specific endosomes, known as multivesicular bodies (MVBs). These MVBs ultimately fuse with the vacuole to degrade their content⁵³. The 'endosomal sorting complex required for transport' (ESCRT), which actually consists of five distinct cooperating protein complexes, has a key role in the recognition of ubiquitinated

Table 2. Overview of (putative) ubiquitin E3 and E4 ligases and their function in *S. cerevisiae*

E3 or E4 ligase (complex)	Description¹	Associated genes
Anaphase promoting complex (APC/C)	Ubiquitin ligase complex that degrades mitotic cyclins and anaphase inhibitory protein, thereby triggering sister chromatid separation and exit from mitosis; substrate recognition by APC/C occurs through degradation signals, the most common of which is termed the Dbox degradation motif, originally discovered in cyclin B	<i>AMA1, APC1, APC2, APC4, APC5, APC9, APC11*, CDC16, CDC20, CDC23, CDC26, CDC27, CDH1, DOC1, MND2, SWM1</i>
Asi1, Asi2, Asi3	Putative integral membrane ubiquitin ligase that ensures the fidelity of SPS-sensor signalling by maintaining the dormant repressed state of gene expression in the absence of inducing signals	<i>ASI1*, ASI2, ASI3*</i>
Asr1	Ubiquitin ligase that modifies and regulates RNA polymerase II; involved in a putative alcohol-responsive signalling pathway; accumulates in the nucleus under alcohol stress; contains a RING/PHD finger domain similar to the mammalian rA9 protein	<i>ASR1*</i>
Bre1	Ubiquitin ligase that forms heterodimer with Rad6 to monoubiquitinate histone H2B-K123, which is required for the subsequent methylation of histone H3-K4 and H3-K79; required for DSB repair, transcription, silencing and checkpoint control	<i>BRE1*</i>
Ccr4-Not complex	Mot2 is the ubiquitin ligase subunit of the Ccr4-Not complex; with Ubc4, ubiquitinates nascent polypeptide-associated complex subunits and histone demethylase Jhd2; Ccr4-Not has roles in transcription regulation, mRNA degradation and post-transcriptional modifications	<i>CAF40, CAF130, CCR4, CDC36, CDC39, MOT2*, NOT3, NOT5, POP2</i>
Cul3-RING ubiquitin ligase complex	Ubiquitin ligase complex in which a cullin from the Cul3 subfamily and a RING domain protein form the catalytic core; substrate specificity is conferred by a BTB-domain-containing protein	<i>CUL3*, ELA1, ELC1, RAD16, RAD7</i>
Cul8-RING ubiquitin ligase complex	Ubiquitin ligase complex in which a cullin from the Cul8 subfamily and a RING domain protein form the catalytic core; in <i>S. cerevisiae</i> , Mms1 acts as the adaptor protein and substrate specificity is conferred by any of a number of different proteins.	<i>MMS1, MMS21, RTT101*, RTT107</i>
Dma1, Dma2	Two functionally redundant ubiquitin ligases; control septin dynamics and the spindle position checkpoint (SPOC) by regulating the recruitment of Elm1 to the bud neck; regulate levels of the translation initiation factor eIF2 subunit Gcd11, as well as abundance, localisation and ubiquitination of Cdk inhibitory kinase Swe1; orthologue of human RNF8 protein, with sequence similarity to human Chfr; contain FHA and RING finger domains	<i>DMA1, DMA2</i>
Doa10 ubiquitin ligase complex	Multi-protein complex that recognises and ubiquitinates membrane proteins with misfolded cytosolic domains during ERAD	<i>CDC48, CUE1, NPL4, SSM4*, UBX2</i>
GID complex	Protein complex with ubiquitin ligase activity that is involved in proteasomal degradation of fructose-1,6-bisphosphatase (FBPase) and phosphoenolpyruvate carboxykinase during the transition from gluconeogenic to glycolytic growth conditions	<i>FYV10, GID7, GID8, RMD5*, VID24</i>
Hrd1 ubiquitin ligase ERAD-L and ERAD-M complex	Two multiprotein complexes that recognise and ubiquitinate proteins with misfolded luminal domains during ERAD	<i>DER1, DFM1, HRD1*, HRD3, USA1, YOS9</i>
Hul4	Protein with similarity to HECT domain ubiquitin ligases; found in association with Trf4 in TRAMP complex	<i>HUL4*</i>
Hul5	Multiubiquitin chain assembly factor (E4); proteasome processivity factor that elongates polyubiquitin chains on substrates, opposing Ubp6, a branched polyubiquitin protease; required for retrograde transport of misfolded proteins during ERAD	<i>HUL5</i>
Peroxisomal translocation subcomplex	Peroxisomal protein complex, consisting of three RING-type ubiquitin ligase proteins; required for Ubc4-dependent Pex5 ubiquitination and peroxisomal matrix protein import	<i>PEX2*, PEX10*, PEX12*</i>
Pib1	RING-type ubiquitin ligase of the endosomal and vacuolar membranes; binds phosphatidylinositol(3)-phosphate; contains a FYVE finger domain	<i>PIB1*</i>
Prp19 complex	Protein complex consisting of Prp19 and associated proteins that is involved in the transition from the precatalytic spliceosome to the activated form that catalyses step 1 of splicing, and which remains associated with the spliceosome through the second catalytic step; widely conserved, found in both yeast and mammals, though the exact composition varies	<i>CEF1, CLF1, CWC2, ISY1, NTC20, PRP19*, PRP46, SNT309, SYF1, SYF2</i>

Table 2. Continued

E3 or E4 ligase (complex)	Description¹	Associated genes
Psh1	Ubiquitin ligase; mediates polyubiquitination and degradation of centromere-binding protein Cse4 and prevents Cse4 from mislocalising to euchromatin	<i>PSH1*</i>
Rad5	DNA helicase; proposed to promote replication fork regression during postreplication repair by template switching; RING finger containing ubiquitin ligase; stimulates the synthesis of free and PCNA-bound polyubiquitin chains by Ubc13p-Mms2p	<i>RAD5</i>
Rad18	Ubiquitin ligase; forms heterodimer with Rad6 to monoubiquitinate PCNA-K164; heterodimer binds single-stranded DNA and has single-stranded DNA dependent ATPase activity; required for postreplication repair	<i>RAD18*</i>
Rkr1	RING domain ubiquitin ligase; involved in the ubiquitin-mediated degradation of non-stop proteins; functional connections to chromatin modification; nuclear protein that also co-localises with ribosomes; homologue of mouse Listerin, whose mutation has been reported to cause neurodegeneration in mice	<i>RKR1*</i>
Rsp5 ubiquitin E3 ligase complex	Ubiquitin ligase of the NEDD4 family; involved in regulating many cellular processes, including MVB sorting, heat shock response, transcription, endocytosis, and ribosome stability; human homologue is involved in Liddle syndrome; mutant tolerates aneuploidy; ubiquitinates Sec23	<i>BUL1, BUL2, RSP5*</i>
San1	Ubiquitin ligase; involved in the proteasome-dependent degradation of aberrant nuclear proteins; targets substrates with regions of exposed hydrophobicity containing 5 or more contiguous hydrophobic residues; contains intrinsically disordered regions that contribute to substrate recognition	<i>SAN1*</i>
SCF complex	Ubiquitin ligase complex in which a cullin from the Cul1 subfamily and a RING domain protein form the catalytic core; substrate specificity is conferred by a Skp1 adaptor and an F-box protein; involved in targeting proteins for degradation by the proteasome	<i>CDC34*, CDC4, CDC53, DAS1, DIA2, GRR1, HRT1, HRT3, MDM30, MET30, MFB1, SAF1, SKP1, SKP2, UFO1, YDR131C, YDR306C, YLR224W, YLR352W</i>
Slx5/Slx8 STUbL complex	SUMO-targeted ubiquitin ligase (STUbL) complex; stimulated by prior attachment of SUMO to the substrate; Slx5 and Slx8 contain a C-terminal RING domain	<i>SLX5, SLX8*</i>
Tom1	Ubiquitin ligase of the HECT-domain class; has a role in mRNA export from the nucleus and may regulate transcriptional coactivators; involved in degradation of excess histones	<i>TOM1*</i>
Tul1	Golgi-localised RING-finger ubiquitin ligase; involved in ubiquitinating and sorting membrane proteins that contain polar transmembrane domains to multivesicular bodies for delivery to the vacuole for quality control purposes	<i>TUL1*</i>
Ubr1	Ubiquitin ligase (N-recognin); forms heterodimer with Rad6 to ubiquitinate substrates in the N-end rule pathway; regulates peptide transport via Cup9 ubiquitination	<i>UBR1*</i>
Ubr2/Mub1 ubiquitin ligase	Cytoplasmic ubiquitin ligase; required for ubiquitination of Rpn4; mediates formation of a Mub1-Ubr2-Rad6 complex	<i>MUB1, UBR2*</i>
Ufd2	Ubiquitin chain assembly factor (E4); also functions as an E3	<i>UFD2*</i>
Ufd4	Ubiquitin ligase; interacts with Rpt4 and Rpt6, two subunits of the 19S particle of the 26S proteasome; cytoplasmic E3 involved in the degradation of ubiquitin fusion proteins	<i>UFD4*</i>
Uls1	RING finger protein involved in proteolytic control of sumoylated substrates; interacts with SUMO (Smt3); member of the SWI/SNF family of DNA-dependent ATPases; plays a role in antagonising silencing during mating-type switching	<i>ULS1</i>

¹ Obtained from the Saccharomyces Genome Database (www.yeastgenome.org)

* Protein with ubiquitin ligase activity (GO:0004842)

cargo proteins and the formation of MVBs⁵⁴. Ubiquitinated substrates have to be deubiquitinated before delivery to the vacuole. This is catalysed by the DUB Doa4 and is important for repletion of the ubiquitin pool²⁸.

Ubiquitination is not only important in the late stages of vesicular sorting into MVBs. It also contributes to endocytosis of permeases and receptors, such as the pheromone receptors Ste2 and Ste4^{55,56}. Also the trafficking of newly synthesised proteins that follow the secretory pathway in the trans-Golgi network (TGN) is a ubiquitin-

dependent process. This for example directs the transport of the amino acid transporter Gap1 to either the plasma membrane or the vacuole⁵⁷. There is no direct evidence that sumoylation is implicated in any secretory pathways.

Histone modification

Ubiquitin and SUMO are also involved in diverse nuclear processes. One of the ways this is achieved is through modification of histones. Histones are subjected to a large number of posttranslational modifications, including acetylation, methylation,

Table 3. Overview of deubiquitinating enzymes and their function in *S. cerevisiae*

Gene	Description ¹
<i>UBP1</i>	Ubiquitin-specific protease that removes ubiquitin from ubiquitinated proteins; cleaves at the C-terminus of ubiquitin fusions irrespective of their size; capable of cleaving polyubiquitin chains
<i>UBP2</i>	Ubiquitin-specific protease that removes ubiquitin from ubiquitinated proteins; interacts with Rsp5 and is required for MVB sorting of membrane proteins; can cleave polyubiquitin and has isopeptidase activity
<i>UBP3</i>	Ubiquitin-specific protease involved in transport and osmotic response; interacts with Bre5 to co-regulate anterograde and retrograde transport between the ER and Golgi; involved in transcription elongation in response to osmotic stress through phosphorylation at Ser695 by Hog1; inhibitor of gene silencing; cleaves ubiquitin fusions but not polyubiquitin; also has mRNA binding activity
<i>DOA4</i> (<i>UBP4</i>)	Ubiquitin isopeptidase; required for recycling ubiquitin from proteasome-bound ubiquitinated intermediates; acts at the late endosome/prevacuolar compartment to recover ubiquitin from ubiquitinated membrane proteins en route to the vacuole
<i>UBP5</i>	Putative ubiquitin-specific protease; closest paralogue of Doa4 but has no functional overlap; concentrates at the bud neck
<i>UBP6</i>	Ubiquitin-specific protease situated in the base subcomplex of the 26S proteasome, releases free ubiquitin from branched polyubiquitin chains; works in opposition to Hul5 polyubiquitin elongation activity; mutant has aneuploidy tolerance
<i>UBP7</i>	Ubiquitin-specific protease that cleaves ubiquitin-protein fusions
<i>UBP8</i>	Ubiquitin-specific protease that is a component of the SAGA complex; required for SAGA-mediated deubiquitination of histone H2B
<i>UBP9</i>	Ubiquitin carboxyl-terminal hydrolase; cleaves ubiquitin-protein fusions
<i>UBP10</i> (<i>DOT4</i>)	Ubiquitin-specific protease that deubiquitinates ubiquitin-protein moieties; may regulate silencing by acting on Sir4; involved in posttranscriptionally regulating Gap1 and possibly other transporters; primarily located in the nucleus
<i>UBP11</i>	Ubiquitin-specific protease that cleaves ubiquitin from ubiquitinated proteins
<i>UBP12</i>	Ubiquitin carboxyl-terminal hydrolase; ubiquitin-specific protease present in the nucleus and cytoplasm that cleaves ubiquitin from ubiquitinated proteins
<i>UBP13</i>	Putative ubiquitin carboxyl-terminal hydrolase; ubiquitin-specific protease that cleaves ubiquitin-protein fusions
<i>UBP14</i>	Ubiquitin-specific protease that specifically disassembles unanchored ubiquitin chains; involved in fructose-1,6-bisphosphatase degradation; similar to human isopeptidase T
<i>UBP15</i>	Ubiquitin-specific protease involved in protein deubiquitination; catalytic activity regulated by an N-terminal TRAF-like domain and C-terminal sequences; physically interacts with APC/C activator Cdh1
<i>UBP16</i>	Deubiquitinating enzyme anchored to the outer mitochondrial membrane; probably not important for general mitochondrial functioning, but may perform a more specialised function at mitochondria
<i>OTU1</i>	Deubiquitinating enzyme that binds to the chaperone-ATPase Cdc48; may contribute to regulation of protein degradation by deubiquitinating substrates that have been ubiquitinated by Ufd2; member of the Ovarian Tumour (OTU) family

¹ Obtained from the Saccharomyces Genome Database (www.yeastgenome.org)

phosphorylation, ubiquitination and sumoylation. Modifications or combination of modifications are recognised by different proteins, which determine downstream consequences. This is crucial for many chromatin-related processes, such as transcription, DNA replication, DNA repair and cell cycle progression^{58,59}. An important modification for transcription is the monoubiquitination of histone H2B at lysine 123 (K123) by the E2 enzyme Rad6 and the E3 ligase Bre1. This is a prerequisite for the establishment of a tri-methyl group on histone H3K4 and H3K79^{60,61}. H2B ubiquitination is counteracted by the Spt-Ada-Gcn5-acetyltransferase (SAGA) and SAGA-like (SLIK) complexes, which both contain the DUB subunit Ubp8. Another DUB Ubp10 also deubiquitinates H2B, but its targeted genomic loci are distinct from Ubp8. Ubp8 and Ubp10 are therefore thought to act on distinct pools of H2B. Ubp10 is mostly involved in transcriptional silencing of telomeres and rDNA, whereas Ubp8 has an activating function in SAGA/SLIK-mediated transcription⁶²⁻⁶⁵.

The centromeric H3 variant Cse4 is also ubiquitinated. Cse4 ubiquitination is mediated by the ubiquitin E3 ligase Psh1, resulting in Cse4 degradation. This prevents Cse4 incorporation in euchromatin to achieve an exclusively centromeric localisation^{66,67}. Furthermore, all four core histones H2A, H2B, H3 and H4 are known to be sumoylated. Histone sumoylation is linked to transcriptional repression in *S. cerevisiae*, but its exact contribution to transcription regulation is still unclear^{68,69}.

Transcription factor regulation

Besides histone modification, ubiquitin and SUMO are also involved in regulation of transcription in other ways. For example, many gene-specific transcription factors, basal transcription factors and transcription coregulators are targets of ubiquitination and sumoylation. The functional effect of transcription factor ubiquitination or sumoylation is very diverse and different per substrate⁷⁰. In many cases, ubiquitination promotes the degradation of a transcription factor via the UPS to modulate the

turnover of a transcription factor. For example, the transcriptional activator Gcn4 is ubiquitinated and proteasomally degraded to prevent the transcription and biosynthesis of amino acids and purines under nutrient-rich growth conditions. During cellular starvation Gcn4 degradation is inhibited, leading to activation of amino acid biosynthesis genes⁷¹. Several transcription factors are regulated in a similar manner, e.g. Cup9, MAT α 2, Rpn4 and Yap9⁷²⁻⁷⁵.

Ubiquitination and sumoylation can also have a nonproteolytic effect on transcription factors to alter their activity. For example, the transcriptional activator Met4 is ubiquitinated by the ubiquitin ligase Cdc34/SCF^{Met30}. Ubiquitinated Met4 can associate with gene promoters, but is incapable of forming a functional transcription complex resulting in transcription repression⁷⁶. Sumoylation of Gcn4 promotes its dissociation from gene promoters and reduces transcription activation⁷⁷. Sumoylation also regulates the relocation of transcription factors to distinct subcellular compartments, for example through regulation of the nucleo-cytoplasmic shuttling of transcription factors or the sequestering of transcription regulatory proteins into so-called promyelocytic leukemia (PML) nuclear bodies in mammalian cells⁷⁸⁻⁸⁰. Global analysis of sumoylated substrates using proteomics approaches in *S. cerevisiae* have indicated that there are still many uncharacterised sumoylated substrates implicated in transcription, including subunits of RNA polymerase I, II, and III, as well as various components implicated in mRNA processing^{8,81,82}. The exact contribution of sumoylation in transcription regulation remains to be resolved for most of these substrates.

Maintenance of genome stability

Another nuclear process that requires sumoylation is the maintenance of genome stability. This involves a large and diverse group of cellular processes, including maintenance of higher-order chromatin structure, cell cycle progression, DNA replication, DNA repair, mitosis and meiosis. In response to genotoxic stress, cells activate the DNA damage

response and specific checkpoints to coordinate a cell cycle arrest and DNA repair⁵. The ubiquitin system intersects with the SUMO system, as it also directly contributes to the cellular processes described above, in particular in ubiquitin-mediated degradation of key proteins. Any defects in these processes can lead to genome instability due to DNA damage or inaccurate segregation of chromosomes, which is very disadvantageous for cells and directly associated with many diseases, such as cancer⁸³. Of course cancer is nonexistent in unicellular organisms such as *S. cerevisiae*, but many yeast mutants of SUMO components display severe phenotypic defects as a consequence of loss of genome integrity. This is also underscored by the fact that most SUMO system components are essential for viability in yeast and other eukaryotes⁵. The maintenance of genome stability is very complex. It is beyond the scope of this introduction to describe all molecular processes involving sumoylation or ubiquitination, but some processes are highlighted below.

The most deleterious type of DNA damage is a double-stranded DNA break (DSB), which can occur at a stalled DNA replication fork. In order to repair the DSB, cells have evolved several repair mechanisms, such as homologous recombination (HR) and break-induced replication (BIR). The SUMO-specific E3 ligase Mms21 is a component of the Smc5-Smc6 complex, which contributes to HR-mediated DNA repair and is essential for the correct structural organisation of chromatin^{34,35,84}. Furthermore, the stalling of DNA replication forks triggers the monoubiquitination of the replication processivity factor Proliferating Cell Nuclear Antigen (PCNA), mediated by the E2/E3 pair Rad6/Rad18, or polyubiquitination of PCNA by the E2/E3 complex Ubc13-Mms2/Rad5, which direct two distinct post-replication repair pathways to bypass the DNA damage site. PCNA can also be modified at the same lysine residue with SUMO, mediated by the SUMO E3 ligase Siz1, which directs a third alternate function of PCNA in DNA repair⁸⁵. DNA damage

Table 4. Overview of SUMO-specific E1, E2, E3 and deconjugating enzymes, and their function in *S. cerevisiae*

Gene	Description ¹
<i>AOS1</i>	Subunit of a heterodimeric nuclear SUMO-activating enzyme (E1) with Uba2; activates Smt3 (SUMO) before its conjugation to proteins, which may play a role in protein targeting; essential for viability
<i>UBA2</i>	Subunit of a heterodimeric nuclear SUMO activating enzyme (E1) with Aos1; activates Smt3 (SUMO) before its conjugation to proteins, which may play a role in protein targeting; essential for viability
<i>UBC9</i>	SUMO-conjugating enzyme (E2); involved in the Smt3 conjugation pathway; nuclear protein required for S- and M-phase cyclin degradation and mitotic control; involved in proteolysis mediated by the APC/C
<i>CST9</i>	SUMO E3 ligase; required for synaptonemal complex formation; localises to synapsis initiation sites on meiotic chromosomes; potential Cdc28 substrate
<i>MMS21</i>	SUMO E3 ligase and component of the SMC5-SMC6 complex; this complex plays a key role in the removal of X-shaped DNA structures that arise between sister chromatids during DNA replication and repair; mutants are sensitive to methyl methanesulfonate and show increased spontaneous mutation and mitotic recombination
<i>NFI1</i>	SUMO E3 ligase; catalyses the covalent attachment of Smt3 (SUMO) to proteins; primary E3 ligase for Sir4; sumoylates Yku70/Yku80 and Sir4 in vivo to promote chromatin anchoring; promotes telomere anchoring to the nuclear envelope; involved in maintenance of proper telomere length
<i>SIZ1</i>	SUMO E3 ligase that promotes the attachment of Smt3 (SUMO) to proteins; binds Ubc9 and may bind septins; specifically required for sumoylation of septins in vivo; localised to the septin ring
<i>ULP1</i>	Protease that specifically cleaves Smt3-protein conjugates; required for cell cycle progression; associates with nucleoporins and may interact with septin rings during telophase; sequestered to the nucleolus under stress conditions
<i>ULP2</i>	Peptidase that deconjugates Smt3 (SUMO) peptides from proteins; plays a role in chromosome cohesion at centromeric regions and recovery from checkpoint arrest induced by DNA damage or DNA replication defects; potential Cdc28 substrate
<i>WSS1</i>	Sumoylated protein that localises to a single spot on the nuclear periphery of mother cells but not daughters; interacts genetically with SMT3; UV-sensitive mutant phenotype and genetic interactions suggest a role in the DNA damage response

¹ Obtained from the Saccharomyces Genome Database (www.yeastgenome.org)

can also result in stalling of RNA polymerase II complexes while transcribing genes. Def1 stimulates the ubiquitination and degradation of such stalled RNA polymerase II⁸⁶.

Another well-known protein targeted by the SUMO system is DNA topoisomerase II (Top2). Top2 sumoylation is highly conserved in various species and required for recruitment of Top2 to centromeres. This is crucial for DNA decatenation and centromeric cohesion for accurate chromosome segregation^{87–89}. Also the kinetochore, which resides at the centromere, is a target of sumoylation and ubiquitination, which is thought to contribute to chromosome segregation. The SUMO protein-encoding gene *SMT3* ('Suppressor of Mif Two') was originally identified as a high-copy suppressor of a mutation in the centromere protein Mif2⁹⁰. Mammalian cells lacking the SUMO protease SENP6 have an aberrant kinetochore composition, lacking the inner kinetochore CENP-H/I/K complex⁹¹. Furthermore, CENP-I is ubiquitinated and proteasomally degraded, which is antagonised by SENP6⁹¹. In yeast, several kinetochore subunits are reported to be sumoylated or ubiquitinated, which affects the mitotic spindle function and chromosome segregation^{92–94}.

Sumoylation and especially ubiquitination are also important for cell cycle progression, which is orchestrated by a coordinated degradation of specific proteins, such as cyclins. The induced degradation of cyclins during specific cell cycle phases changes the activity of specific cyclin-dependent kinases, which guide the cell through G1-, S-, G2- and M-phase. Cyclin degradation is primarily regulated through the UPS and is mediated by two ubiquitin ligases, the SCF complex and APC/C. Both can associate to various adaptor proteins, which determine the substrate specificity during a certain cell cycle stage. The SCF and APC/C can also act in response to certain cellular signals, such as DNA damage or the misattachment of chromosomes to the mitotic spindle. This activates cell cycle checkpoints that halt the progression through the cell cycle, which is crucial to enable DNA repair and to maintain

genome stability^{23,95,96}. Lastly, the SUMO E3 ligase Siz1 targets several members of the septin family of cytoskeletal proteins in the yeast bud neck, which are the most abundant sumoylated proteins in yeast during M-phase. Septin sumoylation only occurs during mitosis and is thought to coordinate the removal of the septin ring structure from the site of cell division after completion of cytokinesis^{33,97}.

STUBls and SUMO-dependent ubiquitination

Although ubiquitination and sumoylation have been regarded as separate systems that function in parallel to each other, it has recently become clear that there are many functional interactions between the two pathways^{98,99}. There are several examples of proteins that can be modified with both ubiquitin and SUMO, which can have different effects on a protein. For example, an interesting regulatory mechanism has been uncovered for IκBα (inhibitor of transcription factor NF-κB). IκBα can be ubiquitinated and subsequently proteasomally degraded, but SUMO-modification of IκBα occurs at the same lysine residue as ubiquitination and therefore antagonises its degradation¹⁰⁰. Recently, it was discovered that cells also have a regulatory mechanism to polyubiquitinate and proteasomally degrade proteins that are specifically modified with polySUMO chains. This novel proteolytic pathway, known as SUMO-dependent ubiquitination, again underscores that ubiquitination and sumoylation are tightly interconnected systems^{101–103}.

SUMO-dependent ubiquitination was first characterised in *S. cerevisiae* and *S. pombe*. In 2001, several genes essential for cell viability in the absence of the DNA helicase *SGS1* were identified in *S. cerevisiae*. These genes were referred to as 'Synthetic Lethal Unknown' (*SLX*). Among the *SLX* genes were *SLX5* and *SLX8*, which were found to encode RING domain proteins that function as a heterodimeric complex¹⁰⁴. In the past decade, much effort has been put into the characterisation of the biochemical function of the Slx5/8 complex.

Initially, all evidence pointed to a role for Slx5/8 as a SUMO-specific E3 ligase. Genetic studies of *SLX5* and *SLX8* revealed that they had several synthetic lethal and sick genetic interactions, as well as protein interactions with sumoylating enzymes, indicating that Slx5/8 is a component of the sumoylation system^{105,106}. Intriguingly, loss of Slx5/8 results in accumulation of SUMO-conjugated proteins, rather than the expected decrease in sumoylation¹⁰⁵. Also *in vitro* sumoylation assays did not support a role for Slx5/8 as a true SUMO E3 ligase. Although Slx5/8

could stimulate *in vitro* sumoylation, this was fully independent of the RING domain of both Slx5 and Slx8¹⁰⁶. The studies by Uzunova *et al.* and Xie *et al.* finally shed light on the matter, uncovering that Slx5/8 is in fact a ubiquitin E3 ligase complex that specifically targets sumoylated proteins^{107,108}. These novel E3 enzymes are therefore known as SUMO-targeted ubiquitin ligases (STUbLs). Orthologous STUbLs have been identified from yeast to mammals, indicating an evolutionary conserved and important role for proteasomal degradation of sumoylated

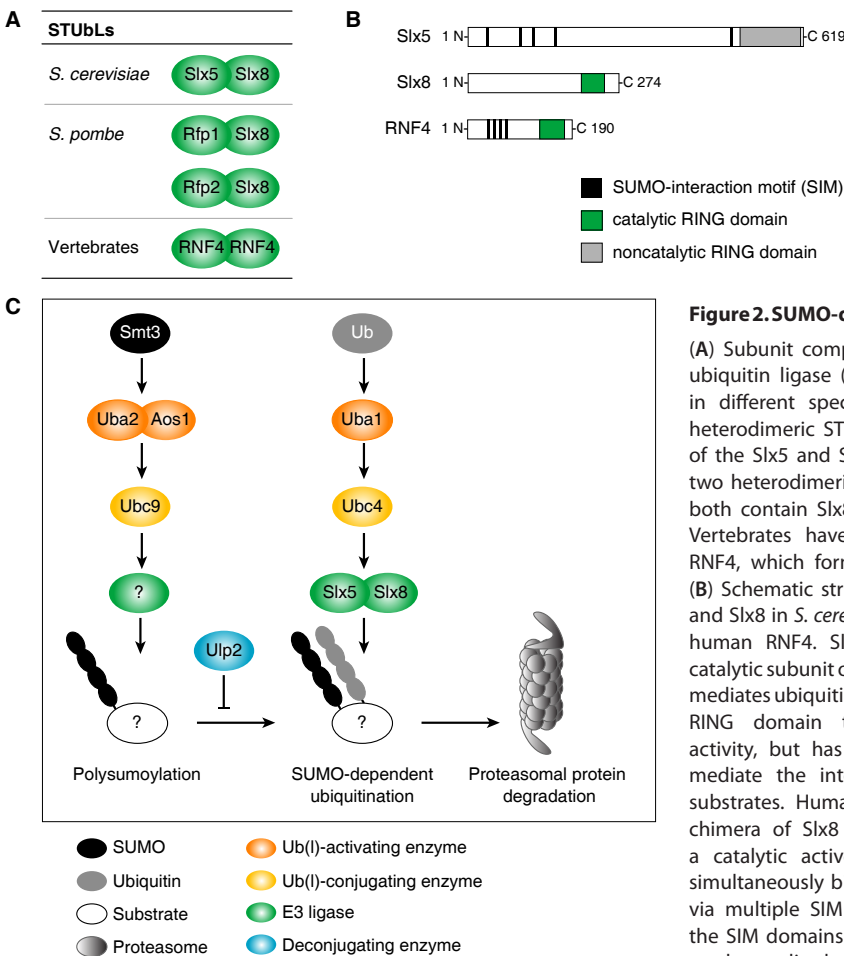


Figure 2. SUMO-dependent ubiquitination.

(A) Subunit composition of SUMO-targeted ubiquitin ligase (STUbL) protein complexes in different species. *S. cerevisiae* has one heterodimeric STUbL complex that consists of the Slx5 and Slx8 proteins. *S. pombe* has two heterodimeric STUbL complexes, which both contain Slx8 and either Rfp1 or Rfp2. Vertebrates have a single STUbL protein RNF4, which forms a homodimeric STUbL. (B) Schematic structure of the proteins Slx5 and Slx8 in *S. cerevisiae* and the orthologous human RNF4. Slx8 is thought to be the catalytic subunit of the Slx5/8 complex, which mediates ubiquitination. Slx5 has a C-terminal RING domain that lacks ubiquitination activity, but has five SIM domains, which mediate the interaction with sumoylated substrates. Human RNF4 is regarded as a chimera of Slx8 and Slx5, because it has a catalytic active RING domain and can simultaneously bind to sumoylated proteins via multiple SIM domains. The position of the SIM domains in Slx5 and RNF4 is based on the studies by Xie *et al.* and Tatham *et al.*^{108,111,113}. (C) Schematic representation of the molecular mechanism of SUMO-dependent ubiquitination in *S. cerevisiae*. See text for details.

proteins^{109–112}.

STUbLs are thought to function as dimeric protein complexes and are similar in their protein domain composition in different species (Figure 2A and 2B). They have a C-terminal RING domain, which mediates ubiquitination. Secondly, they have multiple SIMs, which contribute to binding to polysumoylated proteins. Slx5 in *S. cerevisiae* is found to have at least five SIMs, but the RING domain of Slx5 has no ubiquitinating activity. By forming a heterodimer with Slx8, which has a catalytically active RING but no SIMs, they form a functional SUMO-dependent ubiquitin E3 ligase complex^{107,108,113}. Contrary to yeast, vertebrates have a single STUbL, called RING finger protein 4 (RNF4), which forms a homodimeric complex¹¹⁴. RNF4 also contains a RING domain and multiple SIM domains¹¹¹. RNF4 can completely rescue the phenotypic defects of STUbL mutants in yeast, indicating that RNF4 is a functional chimera of both yeast STUbL subunits^{109,110,115}.

The molecular mechanism of SUMO-dependent ubiquitination in *S. cerevisiae* is thought to occur as follows (Figure 2C). The SUMO protein Smt3 is activated by the SUMO-specific E1 Aos1/Uba2 and conjugated to a substrate by the E2 enzyme Ubc9. Repeated conjugation of SUMO to internal lysine residues of the previous SUMO moiety results in the formation of a polySUMO chain. Until to date, there is no evidence that a specific SUMO E3 ligase contributes to the formation of a polySUMO chain. Polysumoylation is antagonised by the SUMO-isopeptidase Ulp2²². The polysumoylated proteins are recognised by the STUbL Slx5/8, which engage in a physical interaction with the polySUMO chain via the SIM domains of Slx5. Slx8 mediates the formation of K48-linked polyubiquitin chains on the polysumoylated substrate via the ubiquitin-specific E2 enzyme Ubc4, which targets them to the proteasome for degradation^{107,108}. Other E2s, including Ubc1, Ubc5, Ubc6 and Ubc13, have also been shown to have ubiquitinating activity with Slx5/8 *in vitro*, but their functional relevance *in vivo* remains to be established¹¹⁶. Strikingly,

the transcription MAT α 2 is also known to be ubiquitinated by Slx5/8 in a SUMO-independent way, suggesting that STUbLs are not fully dependent on polySUMO chains for substrate recognition¹¹³.

The physiological role of STUbLs is less well characterised. *SLX5* and *SLX8* were originally identified in a screen for genes that are synthetic lethal with deletion of *SGS1*, a DNA helicase of the RecQ family, indicating a role for Slx5/8 in genome stability¹⁰⁴. Inactivation of STUbLs leads to a broad spectrum of genome instability phenotypes in *S. cerevisiae* and *S. pombe*. These include a strong cell cycle delay, DNA damage checkpoint activation, sensitivity to genotoxic stress, gross chromosomal rearrangements and increased rates of DNA mutation and recombination^{109,110,117–120}. The Slx5/8 complex resides at sites of DNA damage and replication, and contributes to DNA repair by relocating DNA breaks to the nuclear pore^{118,119,121}. STUbLs are also implicated in transcription regulation. The first identified *in vivo* substrate of a STUbL is the human promyelocytic leukemia (PML) protein, which is ubiquitinated by hRNF4 in a SUMO-dependent manner^{111,112,122}. Additional *in vivo* substrates of STUbLs are still few in number and so far include the transcriptional regulators PEA3, HIF-2 α , PARP-1, Mot1, MAT α 1 and MAT α 2^{113,123–127}. In budding yeast, this is supported with evidence for Slx5/8 to contribute to telomeric silencing¹²⁸. Strikingly, the predominant function of Slx5/8 in *S. cerevisiae* appears to be the maintenance of genome stability for which no *in vivo* target has been identified yet.

Other ubiquitin-like systems in *S. cerevisiae*

Neddylation

Rub1 (related to ubiquitin 1) is the yeast orthologue of the mammalian ubiquitin-like protein NEDD8¹²⁹. Rub1-conjugation to substrates is therefore known as neddylation. The process of neddylation is similar to that of ubiquitination and sumoylation (Figure 3). Rub1 has a C-terminal diglycine sequence that requires processing and ATP-dependent

activation. The E1-like Rub1-activating enzyme is the heterodimeric Ula1/Uba3 complex and Ubc12 is the Rub1-specific E2 enzyme¹²⁹. Dcn1 is the only known E3 ligase for Rub1¹³⁰. The major class of neddylation substrates in yeast and other species are cullin proteins^{129–132}. Interestingly, cullins are subunits of the family of cullin-RING ubiquitin ligases, such as the SCF complex, which are large multi-protein complexes that polyubiquitinate substrates for proteasomal degradation¹³³. This indicates that there are tight functional links between the neddylation and ubiquitin-proteasome system, although the nature of these interactions are still poorly understood. Neddylation is reversible through the action of the Signalosome, which is a highly conserved multi-subunit protein complex that mediates deneddylation of cullins^{134–136}. In almost all model organisms, except *S. cerevisiae*, neddylation is crucial for cell viability, as it is involved in several early developmental processes, such as embryogenesis of *Drosophila* and *Arabidopsis*^{137,138}. In the nematode *Caenorhabditis elegans*, neddylation modulates the cytoskeleton during embryonic cell divisions¹³⁹. Strikingly, disruption of Rub1 or any other enzymatic neddylation component is not associated with any particular phenotype in *S. cerevisiae*, despite aberrant Rub1-modified cullins^{129,136}. The role of neddylation in *S. cerevisiae* is therefore largely unknown.

Atg8 and Atg12 modification

The formation of autophagosomes during autophagy is dependent on two related ubiquitin-like systems, which is based on substrate modification with the ubiquitin-like proteins Atg8 and Atg12^{140,141}. Autophagy is a cellular process during which cells deliver intracellular material to the vacuole, which is a yeast organelle that is equivalent to the mammalian lysosome with an important function in degradation. During autophagy, a cell forms a double-membrane structure that envelopes part of the cytoplasm to form a vesicular structure called the autophagosome. The autophagosome can contain proteins or lipids, but also entire organelles, such as mitochondria or

peroxisomes. The autophagosome ultimately fuses with the vacuole in order to degrade its content by use of vacuolar enzymes. The degradation products, such as amino acids, are recycled and are therefore a valuable nutrient source for the cell¹⁴². Autophagy is particularly important during starvation, when yeast cells are deprived from nutrients¹⁴³. Substrate modification with the ubiquitin-like proteins Atg8 and Atg12 is essential for autophagosome formation. Mutants that lack any Atg system component are therefore unable to survive in starvation conditions¹⁴⁴. Homologous genes of the Atg8 and Atg12 conjugation systems are also existent in mammals and are required for autophagy as well^{141,142}.

Atg8 and Atg12 have little sequence similarity to each other or to ubiquitin, but their conjugation to substrates is similar to ubiquitination (Figure 3). Atg8 is synthesised as an inactive precursor protein that is processed by the cysteine protease Atg4 to expose a C-terminal glycine residue¹⁴⁵. Atg8 is activated by the E1-like enzyme Atg7, transferred to the E2-like enzyme Atg3, and finally attached to its substrate phosphatidylethanolamine (PE), which is an abundant lipid of cellular membranes¹⁴⁶. The attachment of Atg8 to PE promotes membrane tethering and hemifusion of liposomes *in vitro*. This can be modulated by Atg4, the deconjugating enzyme that removes Atg8 from PE, which also contributes to autophagosome biogenesis *in vivo*^{145,147,148}. Contrary to Atg8, the ubiquitin-like modifier Atg12 is synthesised with an already exposed C-terminal glycine residue and therefore does not require processing. Atg12 is activated by Atg7, which is the same E1-like enzyme as for Atg8¹⁴⁹. Atg7 is the only known E1 enzyme that is found to be capable of activation of two distinct ubiquitin-like modifiers. Next, Atg12 is transferred to its specific E2-like enzyme Atg10 and conjugated to its substrate Atg5^{149,150}. Intriguingly, this Atg12-Atg5 conjugate is found to possess an E3-like function, as it promotes the transfer of Atg8 from the E2-like enzyme Atg3 to the substrate PE¹⁵¹. This demonstrates that the two conjugation systems are closely related to each other and may even be regarded as one functional system.

Urmylation

Urm1 (ubiquitin-related modifier 1) is a ubiquitin-like protein with the unique property that it also functions as sulphur carrier^{152,153}. The transfer of sulphur is integrated in the enzymatic cascade that catalyses the conjugation of Urm1 to substrates, also known as urmylation (Figure 3)¹⁵⁴. Structural and phylogenetic analyses have revealed that Urm1 is likely the most ancient ubiquitin-like protein and that it represents the evolutionary link between ATP-dependent protein conjugation in eukaryotes and ATP-dependent cofactor sulfuration in prokaryotes¹⁵⁵. Urm1 has no sequence resemblance to eukaryotic ubiquitin. In contrast, Urm1 is very similar to the prokaryotic proteins MoaD and ThiS, which are sulphur carrier proteins needed for the biosynthesis of the cofactors molybdopterin and thiamin¹⁵⁶. Urm1, MoaD and ThiS have the characteristic β -grasp fold domain, like all eukaryotic ubiquitin(-like) proteins. Moreover, they are activated at their C-terminal

glycine residue via ATP-dependent adenylation by sulfurtransferases, resembling the activation of ubiquitin by an E1 enzyme. The Urm1-specific E1-like enzyme in *S. cerevisiae* is Uba4¹²⁹. There is no evidence for the existence of Urm1-specific E2-like, E3-like or deconjugating enzymes, but Uba4 has been proposed to function as a hybrid of an E1 and E2 enzyme¹⁵⁷. After adenylation, Uba4 transfers a sulphur molecule to Urm1 to form a thiocarboxylate at its C-terminus. This thiocarboxylate group is essential for Urm1-conjugation to substrates¹⁵⁴. It also fulfils a second function as sulphur donor for the modification of specific tRNAs, which is independent of the function of Urm1 as ubiquitin-like protein modifier^{158,159}. Until to date, only one substrate of Urm1 is identified in *S. cerevisiae*. The peroxiredoxin Ahp1 is modified with a single Urm1 polypeptide at a specific lysine residue¹⁶⁰. Urmylated proteins are lowly abundant under normal conditions, but oxidative stress greatly induces urmylation to

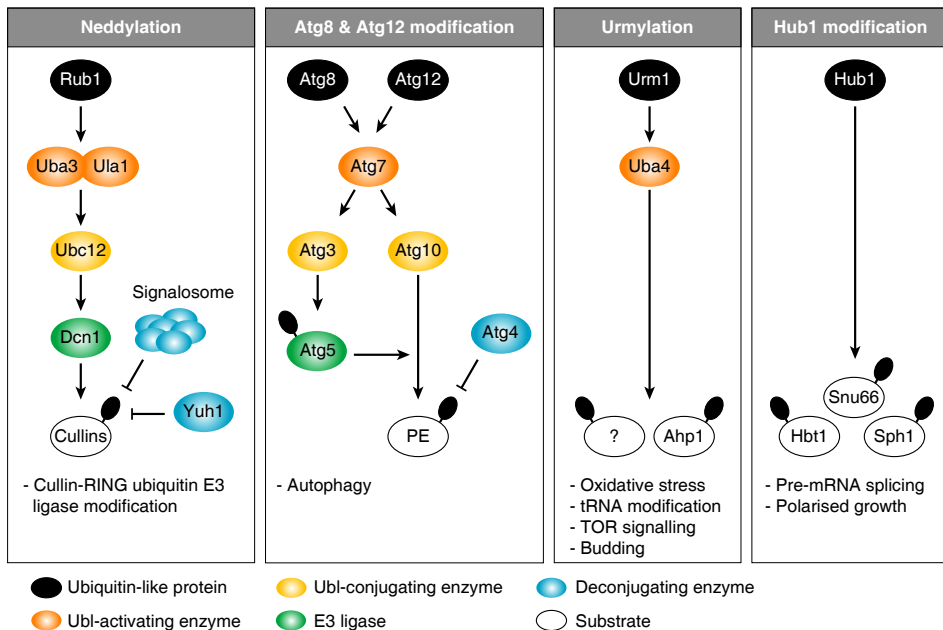


Figure 3. Ubiquitin-like systems in *S. cerevisiae*.

Schematic representation of the four ubiquitin-like systems that exist in parallel to ubiquitination and sumoylation in *S. cerevisiae*. For simplicity, the processing step of the ubiquitin-like proteins is not visualised. See text for details of the enzymatic processes per system.

multiple substrates¹⁵⁴. These additional substrates are still uncharacterised, but they are likely to take part in several cellular processes, such as tRNA modification, the oxidative stress response, budding, invasive growth and TOR signalling^{154,158,160–162}. The urmylation pathway is highly conserved in humans. Several human substrates have been identified and found to be urmylated during oxidative stress as well¹⁵⁴. The human orthologues of the UBL Urm1 and E1-like enzyme Uba4 are MOCS2A and MOCS3, respectively. Functionally and mechanistically they perform the same cellular processes as in *S. cerevisiae* and are required for the biosynthesis of the molybdenum cofactor and tRNA modification¹⁶³.

Hub1 modification

Hub1 (homologous to ubiquitin 1) is a ubiquitin-like modifier that is distantly related to ubiquitin. Hub1 has a similar protein structure as ubiquitin and contains the typical β -grasp fold domain¹⁶⁴. Currently, Hub1 is known to be covalently conjugated to two substrates, Sph1 and Hbt1, which is required for polarised growth during mating and bud-site selection in diploids (Figure 3)¹⁶⁵. Surprisingly, most studies point to a role for Hub1 as a noncovalent protein modifier^{166–169}. Hub1 interacts noncovalently with the spliceosome protein Snu66, which is required for splice site selection in pre-mRNAs for alternative splicing^{167,169}. Hub1 also contributes to pre-mRNA splicing in fission yeast, but unlike in *S. cerevisiae*, the function of Hub1 is essential in *S. pombe*¹⁶⁸. Hub1 is also conserved in higher eukaryotes, including humans, but the cellular functions of these orthologous genes have not been characterised yet¹⁶⁸. In general, Hub1 modification of a substrate, either covalently or noncovalently, contributes to the correct subcellular localisation of that substrate^{165,167}. Currently, no E1-, E2-, E3-like, deconjugating or processing enzymes have been identified for Hub1. It is the only ubiquitin-like modifier that lacks a C-terminal glycine residue, but instead it has a double tyrosine (YY) motif. The YY motif has been proposed to act as the site for Hub1-processing, similar to ubiquitin-processing at

the diglycine motif, prior to substrate conjugation¹⁶⁵. However, Hub1-conjugates can be formed in yeast mutants lacking the YY motif and the process does not require ATP¹⁶⁶. These observations, in combination with the lack of identified enzymes, agree with the hypothesis that Hub1 functions as a noncovalent protein modifier. This makes Hub1 a unique member of the ubiquitin-like protein family, as it is the only ubiquitin-like protein that may modify substrates through an entirely non-enzymatic pathway and through a noncovalent protein interaction.

Aim and scope of the work described in this thesis

Ubiquitination, sumoylation and other ubiquitin-like systems are well-known to be of fundamental importance to a large number of cellular pathways. Insight in these molecular processes has mostly been obtained through biochemical approaches, for instance to unravel the subunit composition of enzyme complexes, determine protein interactions between E2 and E3 enzymes, identify substrates, or characterise the type of ubiquitin(-like) chains formed. Our knowledge about ubiquitin(-like) modification systems relies for a large part on the collected *in vitro* data, which may not necessarily be representative for the *in vivo* situation. We therefore aimed to characterise all the ubiquitin and ubiquitin-like systems in the *in vivo* context. For this we have employed the yeast model organism *S. cerevisiae*, whose availability of mutants and relative ease to genetically manipulate allows the performance of large-scale experiments for a systematic approach that simultaneously addresses all ubiquitin(-like) system components. Rather than focussing on the biochemical events, we investigated the phenotypes of yeast deletion mutants using genome-wide microarray expression profiles to assess the gene expression changes upon disruption of genes implicated in ubiquitin(-like) modification. Changes in gene expression upon deletion of components can reveal which cellular processes are affected and

can therefore be used for attributing functions to ubiquitin(-like) system components. Our ultimate goal is to build a comprehensive biological network that integrates the functional relationships between all ubiquitin(-like) system components in *S. cerevisiae*.

Chapter 2 provides an extensive phenotypic study of yeast mutants implicated in ubiquitin(-like) modification by genome-wide mRNA expression profiling. The mutant expression phenotypes are explored in detail and uncover known and novel cellular functions of specific ubiquitin(-like) pathways and reveal numerous functional relationships among the genes. **Chapter 3** describes a unique mRNA expression phenotype for mutants with ubiquitin-proteasome system defects. The central player in this transcriptional response is the gene-specific transcription factor Rpn4. We have characterised the Rpn4 regulon and exploit this gene expression signature to identify mutants with ubiquitin-proteasome system defects. The work in **Chapter 4** is an in-depth functional study of the SUMO-targeted ubiquitin E3 ligase Slx5/8 in yeast and its human orthologue RNF4. We reveal that Slx5 is exclusively located to centromeres and describe a conserved mitotic function for Slx5/8 and RNF4 that is crucial for accurate chromosome segregation. In **Chapter 5** we show detailed functional analyses of the individual Slx5 and Slx8 subunits. These results provide mechanistic insight into the role of the Slx5/8 complex as SUMO-targeted ubiquitin ligase. Finally, **Chapter 6** is a general discussion of the work described in this thesis and its implications for our understanding of the ubiquitin and ubiquitin-like systems.

REFERENCES

- Hochstrasser, M. Origin and function of ubiquitin-like proteins. *Nature* **458**, 422–429 (2009).
- Kerscher, O., Felberbaum, R. & Hochstrasser, M. Modification of proteins by ubiquitin and ubiquitin-like proteins. *Annu. Rev. Cell Dev. Biol.* **22**, 159–180 (2006).
- Humbard, M. A. *et al.* Ubiquitin-like small archaeal modifier proteins (SAMPs) in *Haloflex volcanii*. *Nature* **463**, 54–60 (2010).
- Pearce, M. J., Mintseris, J., Ferreyra, J., Gygi, S. P. & Darwin, K. H. Ubiquitin-like protein involved in the proteasome pathway of *Mycobacterium tuberculosis*. *Science* **322**, 1104–1107 (2008).
- Johnson, E. S. Protein modification by SUMO. *Annu. Rev. Biochem.* **73**, 355–382 (2004).
- Komander, D. & Rape, M. The ubiquitin code. *Annu. Rev. Biochem.* **81**, 203–229 (2012).
- Peng, J. *et al.* A proteomics approach to understanding protein ubiquitination. *Nat. Biotechnol.* **21**, 921–926 (2003).
- Panse, V. G., Hardeland, U., Werner, T., Kuster, B. & Hurt, E. A proteome-wide approach identifies sumoylated substrate proteins in yeast. *J. Biol. Chem.* **279**, 41346–41351 (2004).
- Hannich, J. T. *et al.* Defining the SUMO-modified proteome by multiple approaches in *Saccharomyces cerevisiae*. *J. Biol. Chem.* **280**, 4102–4110 (2005).
- Tagwerker, C. *et al.* A tandem affinity tag for two-step purification under fully denaturing conditions: application in ubiquitin profiling and protein complex identification combined with in vivo cross-linking. *Mol. Cell Proteomics* **5**, 737–748 (2006).
- Pickart, C. M. Mechanisms underlying ubiquitination. *Annu. Rev. Biochem.* **70**, 503–533 (2001).
- Welchman, R. L., Gordon, C. & Mayer, R. J. Ubiquitin and ubiquitin-like proteins as multifunctional signals. *Nat. Rev. Mol. Cell Biol.* **6**, 599–609 (2005).
- Geiss-Friedlander, R. & Melchior, F. Concepts in sumoylation: a decade on. *Nat. Rev. Mol. Cell Biol.* **8**, 947–956 (2007).
- Li, S. J. & Hochstrasser, M. A new protease required for cell-cycle progression in yeast. *Nature* **398**, 246–251 (1999).
- Li, S. J. & Hochstrasser, M. The yeast ULP2 (SMT4) gene encodes a novel protease specific for the ubiquitin-like Smt3 protein. *Mol. Cell Biol.* **20**, 2367–2377 (2000).
- Amerik, A. Y. & Hochstrasser, M. Mechanism and function of deubiquitinating enzymes. *Biochim. Biophys. Acta* **1695**, 189–207 (2004).
- Ikeda, F. & Dikic, I. Atypical ubiquitin chains: new molecular signals. ‘Protein Modifications: Beyond the Usual Suspects’ review series. *EMBO Rep.* **9**, 536–542 (2008).
- Crosas, B. *et al.* Ubiquitin chains are remodeled at the proteasome by opposing ubiquitin ligase and deubiquitinating activities. *Cell* **127**, 1401–1413 (2006).
- Koegl, M. *et al.* A novel ubiquitination factor, E4, is involved in multiubiquitin chain assembly. *Cell* **96**, 635–644 (1999).
- Ulrich, H. D. The fast-growing business of SUMO chains. *Mol. Cell* **32**, 301–305 (2008).

21. Verteegaal, A. C. O. SUMO chains: polymeric signals. *Biochem. Soc. Trans.* **38**, 46–49 (2010).
22. Bylebyl, G. R., Belichenko, I. & Johnson, E. S. The SUMO isopeptidase Ulp2 prevents accumulation of SUMO chains in yeast. *J. Biol. Chem.* **278**, 44113–44120 (2003).
23. Barford, D. Structure, function and mechanism of the anaphase promoting complex (APC/C). *Q. Rev. Biophys.* **44**, 153–190 (2011).
24. Deshaies, R. J. SCF and Cullin/Ring H2-based ubiquitin ligases. *Annu. Rev. Cell Dev. Biol.* **15**, 435–467 (1999).
25. Joazeiro, C. A. & Weissman, A. M. RING finger proteins: mediators of ubiquitin ligase activity. *Cell* **102**, 549–552 (2000).
26. Hatakeyama, S. & Nakayama, K. I. U-box proteins as a new family of ubiquitin ligases. *Biochem. Biophys. Res. Commun.* **302**, 635–645 (2003).
27. Rotin, D. & Kumar, S. Physiological functions of the HECT family of ubiquitin ligases. *Nat. Rev. Mol. Cell Biol.* **10**, 398–409 (2009).
28. Amerik, A. Y., Li, S. J. & Hochstrasser, M. Analysis of the deubiquitinating enzymes of the yeast *Saccharomyces cerevisiae*. *Biol. Chem* **381**, 981–992 (2000).
29. Johnson, E. S. & Blobel, G. Ubc9p is the conjugating enzyme for the ubiquitin-like protein Smt3p. *J. Biol. Chem.* **272**, 26799–26802 (1997).
30. Johnson, E. S., Schwienhorst, I., Dohmen, R. J. & Blobel, G. The ubiquitin-like protein Smt3p is activated for conjugation to other proteins by an Aos1p/Uba2p heterodimer. *EMBO J.* **16**, 5509–5519 (1997).
31. Desterro, J. M., Rodriguez, M. S., Kemp, G. D. & Hay, R. T. Identification of the enzyme required for activation of the small ubiquitin-like protein SUMO-1. *J. Biol. Chem.* **274**, 10618–10624 (1999).
32. Bernier-Villamor, V., Sampson, D. A., Matunis, M. J. & Lima, C. D. Structural basis for E2-mediated SUMO conjugation revealed by a complex between ubiquitin-conjugating enzyme Ubc9 and RanGAP1. *Cell* **108**, 345–356 (2002).
33. Johnson, E. S. & Gupta, A. A. An E3-like factor that promotes SUMO conjugation to the yeast septins. *Cell* **106**, 735–744 (2001).
34. Takahashi, Y., Kahyo, T., Toh-E, A., Yasuda, H. & Kikuchi, Y. Yeast Ull1/Siz1 is a novel SUMO1/Smt3 ligase for septin components and functions as an adaptor between conjugating enzyme and substrates. *J. Biol. Chem.* **276**, 48973–48977 (2001).
35. Zhao, X. & Blobel, G. A SUMO ligase is part of a nuclear multiprotein complex that affects DNA repair and chromosomal organization. *Proc. Natl. Acad. Sci. U.S.A.* **102**, 4777–4782 (2005).
36. Cheng, C.-H. *et al.* SUMO modifications control assembly of synaptonemal complex and polycomplex in meiosis of *Saccharomyces cerevisiae*. *Genes Dev.* **20**, 2067–2081 (2006).
37. Mullen, J. R., Chen, C.-F. & Brill, S. J. Wss1 is a SUMO-dependent isopeptidase that interacts genetically with the Slx5-Slx8 SUMO-targeted ubiquitin ligase. *Mol. Cell. Biol.* **30**, 3737–3748 (2010).
38. Song, J., Durrin, L. K., Wilkinson, T. A., Krontiris, T. G. & Chen, Y. Identification of a SUMO-binding motif that recognizes SUMO-modified proteins. *Proc. Natl. Acad. Sci. U.S.A.* **101**, 14373–14378 (2004).
39. Dikic, I., Wakatsuki, S. & Walters, K. J. Ubiquitin-binding domains - from structures to functions. *Nat. Rev. Mol. Cell Biol.* **10**, 659–671 (2009).
40. Mahajan, R., Delphin, C., Guan, T., Gerace, L. & Melchior, F. A small ubiquitin-related polypeptide involved in targeting RanGAP1 to nuclear pore complex protein RanBP2. *Cell* **88**, 97–107 (1997).
41. Matunis, M. J., Coutavas, E. & Blobel, G. A novel ubiquitin-like modification modulates the partitioning of the Ran-GTPase-activating protein RanGAP1 between the cytosol and the nuclear pore complex. *J. Cell Biol.* **135**, 1457–1470 (1996).
42. Hanna, J. & Finley, D. A proteasome for all occasions. *FEBS Lett.* **581**, 2854–2861 (2007).
43. Pickart, C. M. & Cohen, R. E. Proteasomes and their kin: proteases in the machine age. *Nat. Rev. Mol. Cell Biol.* **5**, 177–187 (2004).
44. Xie, Y. & Varshavsky, A. UFD4 lacking the proteasome-binding region catalyses ubiquitination but is impaired in proteolysis. *Nat. Cell Biol.* **4**, 1003–1007 (2002).
45. Leggett, D. S. *et al.* Multiple associated proteins regulate proteasome structure and function. *Mol. Cell* **10**, 495–507 (2002).
46. Finley, D. Recognition and processing of ubiquitin-protein conjugates by the proteasome. *Annu. Rev. Biochem.* **78**, 477–513 (2009).
47. Meusser, B., Hirsch, C., Jarosch, E. & Sommer, T. ERAD: the long road to destruction. *Nat. Cell Biol.* **7**, 766–772 (2005).
48. Swanson, R., Locher, M. & Hochstrasser, M. A conserved ubiquitin ligase of the nuclear envelope/endoplasmic reticulum that functions in both ER-associated and Matalpha2 repressor degradation. *Genes Dev* **15**, 2660–2674 (2001).
49. Carvalho, P., Goder, V. & Rapoport, T. A. Distinct ubiquitin-ligase complexes define convergent pathways for the degradation of ER proteins. *Cell* **126**, 361–373 (2006).
50. Ye, Y., Meyer, H. H. & Rapoport, T. A. The AAA ATPase Cdc48/p97 and its partners transport proteins from the ER into the cytosol. *Nature* **414**, 652–656 (2001).
51. Jarosch, E. *et al.* Protein dislocation from the ER requires polyubiquitination and the AAA-ATPase Cdc48. *Nat. Cell Biol.* **4**, 134–139 (2002).
52. Richly, H. *et al.* A series of ubiquitin binding factors connects CDC48/p97 to substrate multiubiquitylation and proteasomal targeting. *Cell* **120**, 73–84 (2005).
53. Piper, R. C. & Katzmman, D. J. Biogenesis and function of multivesicular bodies. *Annu. Rev. Cell Dev. Biol.* **23**, 519–547 (2007).
54. Henne, W. M., Buchkovich, N. J. & Emr, S. D. The ESCRT pathway. *Dev. Cell* **21**, 77–91 (2011).
55. Hicke, L. & Riezman, H. Ubiquitination of a yeast plasma membrane receptor signals its ligand-stimulated endocytosis. *Cell* **84**, 277–287 (1996).
56. Zhu, M., Torres, M. P., Kelley, J. B., Dohlman, H. G. & Wang, Y. Pheromone- and RSP5-dependent ubiquitination of the G protein beta subunit Ste4 in yeast. *J. Biol. Chem.* **286**, 27147–27155 (2011).
57. Scott, P. M. *et al.* GGA proteins bind ubiquitin to facilitate sorting at the trans-Golgi network. *Nat. Cell Biol.* **6**, 252–259 (2004).
58. Strahl, B. D. & Allis, C. D. The language of covalent histone modifications. *Nature* **403**, 41–45 (2000).
59. Atanassov, B. S., Koutelou, E. & Dent, S. Y. The role of deubiquitinating enzymes in chromatin regulation.

- FEBS Lett* (2010).doi:10.1016/j.febslet.2010.10.042
60. Wood, A. *et al.* Bre1, an E3 ubiquitin ligase required for recruitment and substrate selection of Rad6 at a promoter. *Mol. Cell* **11**, 267–274 (2003).
 61. Sun, Z.-W. & Allis, C. D. Ubiquitination of histone H2B regulates H3 methylation and gene silencing in yeast. *Nature* **418**, 104–108 (2002).
 62. Gardner, R. G., Nelson, Z. W. & Gottschling, D. E. Ubp10/Dot4p regulates the persistence of ubiquitinated histone H2B: distinct roles in telomeric silencing and general chromatin. *Mol. Cell. Biol.* **25**, 6123–6139 (2005).
 63. Schulze, J. M. *et al.* Splitting the task: Ubp8 and Ubp10 deubiquitinate different cellular pools of H2BK123. *Genes Dev.* **25**, 2242–2247 (2011).
 64. Emre, N. C. T. *et al.* Maintenance of low histone ubiquitylation by Ubp10 correlates with telomere-proximal Sir2 association and gene silencing. *Mol. Cell* **17**, 585–594 (2005).
 65. Daniel, J. A. *et al.* Deubiquitination of histone H2B by a yeast acetyltransferase complex regulates transcription. *J. Biol. Chem.* **279**, 1867–1871 (2004).
 66. Hewawasam, G. *et al.* Psh1 is an E3 ubiquitin ligase that targets the centromeric histone variant Cse4. *Mol. Cell* **40**, 444–454 (2010).
 67. Ranjitkar, P. *et al.* An E3 ubiquitin ligase prevents ectopic localization of the centromeric histone H3 variant via the centromere targeting domain. *Mol. Cell* **40**, 455–464 (2010).
 68. Shiio, Y. & Eisenman, R. N. Histone sumoylation is associated with transcriptional repression. *Proc. Natl. Acad. Sci. U.S.A.* **100**, 13225–13230 (2003).
 69. Nathan, D. *et al.* Histone sumoylation is a negative regulator in *Saccharomyces cerevisiae* and shows dynamic interplay with positive-acting histone modifications. *Genes Dev.* **20**, 966–976 (2006).
 70. Gill, G. SUMO and ubiquitin in the nucleus: different functions, similar mechanisms? *Genes Dev.* **18**, 2046–2059 (2004).
 71. Kornitzer, D., Raboy, B., Kulka, R. G. & Fink, G. R. Regulated degradation of the transcription factor Gcn4. *EMBO J.* **13**, 6021–6030 (1994).
 72. Byrd, C., Turner, G. C. & Varshavsky, A. The N-end rule pathway controls the import of peptides through degradation of a transcriptional repressor. *EMBO J.* **17**, 269–277 (1998).
 73. Laney, J. D. & Hochstrasser, M. Ubiquitin-dependent degradation of the yeast Mat(alpha)2 repressor enables a switch in developmental state. *Genes Dev.* **17**, 2259–2270 (2003).
 74. Wang, L., Mao, X., Ju, D. & Xie, Y. Rpn4 is a physiological substrate of the Ubr2 ubiquitin ligase. *J. Biol. Chem.* **279**, 55218–55223 (2004).
 75. Gulshan, K., Thommandru, B. & Moye-Rowley, W. S. Proteolytic degradation of the Yap1 transcription factor is regulated by subcellular localization and the E3 ubiquitin ligase Not4. *The Journal of biological chemistry* (2012).doi:10.1074/jbc.M112.384719
 76. Kaiser, P., Flick, K., Wittenberg, C. & Reed, S. I. Regulation of transcription by ubiquitination without proteolysis: Cdc34/SCF(Met30)-mediated inactivation of the transcription factor Met4. *Cell* **102**, 303–314 (2000).
 77. Rosonina, E., Duncan, S. M. & Manley, J. L. Sumoylation of transcription factor Gcn4 facilitates its Srb10-mediated clearance from promoters in yeast. *Genes Dev.* **26**, 350–355 (2012).
 78. Bernardi, R. & Pandolfi, P. P. Structure, dynamics and functions of promyelocytic leukaemia nuclear bodies. *Nat. Rev. Mol. Cell Biol.* **8**, 1006–1016 (2007).
 79. Zhong, S., Salomoni, P. & Pandolfi, P. P. The transcriptional role of PML and the nuclear body. *Nat. Cell Biol.* **2**, E85–90 (2000).
 80. Salinas, S. *et al.* SUMOylation regulates nucleocytoplasmic shuttling of Elk-1. *J. Cell Biol.* **165**, 767–773 (2004).
 81. Wohlschlegel, J. A., Johnson, E. S., Reed, S. I. & Yates, J. R., 3rd Global analysis of protein sumoylation in *Saccharomyces cerevisiae*. *J. Biol. Chem.* **279**, 45662–45668 (2004).
 82. Zhou, W., Ryan, J. J. & Zhou, H. Global analyses of sumoylated proteins in *Saccharomyces cerevisiae*. Induction of protein sumoylation by cellular stresses. *J. Biol. Chem.* **279**, 32262–32268 (2004).
 83. Hoesjmakers, J. H. Genome maintenance mechanisms for preventing cancer. *Nature* **411**, 366–374 (2001).
 84. De Piccoli, G., Torres-Rosell, J. & Aragón, L. The unnamed complex: what do we know about Smc5-Smc6? *Chromosome Res.* **17**, 251–263 (2009).
 85. Hoege, C., Pfander, B., Moldovan, G.-L., Pyrowolakis, G. & Jentsch, S. RAD6-dependent DNA repair is linked to modification of PCNA by ubiquitin and SUMO. *Nature* **419**, 135–141 (2002).
 86. Somesh, B. P. *et al.* Multiple mechanisms confining RNA polymerase II ubiquitylation to polymerases undergoing transcriptional arrest. *Cell* **121**, 913–923 (2005).
 87. Takahashi, Y. & Strunnikov, A. In vivo modeling of polysumoylation uncovers targeting of Topoisomerase II to the nucleolus via optimal level of SUMO modification. *Chromosoma* **117**, 189–198 (2008).
 88. Bachant, J., Alcasabas, A., Blat, Y., Kleckner, N. & Elledge, S. J. The SUMO-1 isopeptidase Smt4 is linked to centromeric cohesion through SUMO-1 modification of DNA topoisomerase II. *Mol. Cell* **9**, 1169–1182 (2002).
 89. Dawlaty, M. M. *et al.* Resolution of sister centromeres requires RanBP2-mediated SUMOylation of topoisomerase IIalpha. *Cell* **133**, 103–115 (2008).
 90. Meluh, P. B. & Koshland, D. Evidence that the MIF2 gene of *Saccharomyces cerevisiae* encodes a centromere protein with homology to the mammalian centromere protein CENP-C. *Mol. Biol. Cell* **6**, 793–807 (1995).
 91. Mukhopadhyay, D., Arnautov, A. & Dasso, M. The SUMO protease SENP6 is essential for inner kinetochore assembly. *J. Cell Biol* **188**, 681–692 (2010).
 92. Yoon, H. J. & Carbon, J. Genetic and biochemical interactions between an essential kinetochore protein, Cbf2p/Ndc10p, and the CDC34 ubiquitin-conjugating enzyme. *Mol. Cell. Biol* **15**, 4835–4842 (1995).
 93. Montpetit, B., Hazbun, T. R., Fields, S. & Hieter, P. Sumoylation of the budding yeast kinetochore protein Ndc10 is required for Ndc10 spindle localization and regulation of anaphase spindle elongation. *J. Cell Biol* **174**, 653–663 (2006).
 94. Vizeacoumar, F. J. *et al.* Integrating high-throughput genetic interaction mapping and high-content screening to explore yeast spindle morphogenesis. *J. Cell Biol* **188**, 69–81 (2010).

95. Cardozo, T. & Pagano, M. The SCF ubiquitin ligase: insights into a molecular machine. *Nat. Rev. Mol. Cell Biol.* **5**, 739–751 (2004).
96. Silverman, J. S., Skaar, J. R. & Pagano, M. SCF ubiquitin ligases in the maintenance of genome stability. *Trends Biochem. Sci.* **37**, 66–73 (2012).
97. Johnson, E. S. & Blobel, G. Cell cycle-regulated attachment of the ubiquitin-related protein SUMO to the yeast septins. *J. Cell Biol.* **147**, 981–994 (1999).
98. Ulrich, H. D. Mutual interactions between the SUMO and ubiquitin systems: a plea of no contest. *Trends Cell Biol.* **15**, 525–532 (2005).
99. Praefcke, G. J. K., Hofmann, K. & Dohmen, R. J. SUMO playing tag with ubiquitin. *Trends Biochem. Sci.* **37**, 23–31 (2012).
100. Desterro, J. M., Rodriguez, M. S. & Hay, R. T. SUMO-1 modification of I κ B α inhibits NF- κ B activation. *Mol. Cell* **2**, 233–239 (1998).
101. Perry, J. J. P., Tainer, J. A. & Boddy, M. N. A SIM-ultaneous role for SUMO and ubiquitin. *Trends Biochem. Sci.* **33**, 201–208 (2008).
102. Geoffroy, M.-C. & Hay, R. T. An additional role for SUMO in ubiquitin-mediated proteolysis. *Nat. Rev. Mol. Cell Biol.* **10**, 564–568 (2009).
103. Miteva, M., Keusekotten, K., Hofmann, K., Praefcke, G. J. K. & Dohmen, R. J. Sumoylation as a signal for polyubiquitylation and proteasomal degradation. *Subcell. Biochem.* **54**, 195–214 (2010).
104. Mullen, J. R., Kaliraman, V., Ibrahim, S. S. & Brill, S. J. Requirement for three novel protein complexes in the absence of the Sgs1 DNA helicase in *Saccharomyces cerevisiae*. *Genetics* **157**, 103–118 (2001).
105. Wang, Z., Jones, G. M. & Prelich, G. Genetic analysis connects SLX5 and SLX8 to the SUMO pathway in *Saccharomyces cerevisiae*. *Genetics* **172**, 1499–1509 (2006).
106. Ii, T., Mullen, J. R., Slagle, C. E. & Brill, S. J. Stimulation of in vitro sumoylation by Slx5-Slx8: evidence for a functional interaction with the SUMO pathway. *DNA Repair (Amst.)* **6**, 1679–1691 (2007).
107. Uzunova, K. *et al.* Ubiquitin-dependent proteolytic control of SUMO conjugates. *J. Biol. Chem.* **282**, 34167–34175 (2007).
108. Xie, Y. *et al.* The yeast Hex3-Slx8 heterodimer is a ubiquitin ligase stimulated by substrate sumoylation. *J. Biol. Chem.* **282**, 34176–34184 (2007).
109. Sun, H., Levenson, J. D. & Hunter, T. Conserved function of RNF4 family proteins in eukaryotes: targeting a ubiquitin ligase to SUMOylated proteins. *EMBO J* **26**, 4102–4112 (2007).
110. Prudden, J. *et al.* SUMO-targeted ubiquitin ligases in genome stability. *EMBO J* **26**, 4089–4101 (2007).
111. Tatham, M. H. *et al.* RNF4 is a poly-SUMO-specific E3 ubiquitin ligase required for arsenic-induced PML degradation. *Nat. Cell Biol.* **10**, 538–546 (2008).
112. Lallemand-Breitenbach, V. *et al.* Arsenic degrades PML or PML-RAR α through a SUMO-triggered RNF4/ubiquitin-mediated pathway. *Nat. Cell Biol.* **10**, 547–555 (2008).
113. Xie, Y., Rubenstein, E. M., Matt, T. & Hochstrasser, M. SUMO-independent in vivo activity of a SUMO-targeted ubiquitin ligase toward a short-lived transcription factor. *Genes Dev.* **24**, 893–903 (2010).
114. Liew, C. W., Sun, H., Hunter, T. & Day, C. L. RING domain dimerization is essential for RNF4 function. *Biochem. J* **431**, 23–29 (2010).
115. Mullen, J. R., Das, M. & Brill, S. J. Genetic evidence that polysumoylation bypasses the need for a SUMO-targeted Ub ligase. *Genetics* **187**, 73–87 (2011).
116. Ii, T., Fung, J., Mullen, J. R. & Brill, S. J. The yeast Slx5-Slx8 DNA integrity complex displays ubiquitin ligase activity. *Cell Cycle* **6**, 2800–2809 (2007).
117. Zhang, C., Roberts, T. M., Yang, J., Desai, R. & Brown, G. W. Suppression of genomic instability by SLX5 and SLX8 in *Saccharomyces cerevisiae*. *DNA Repair (Amst.)* **5**, 336–346 (2006).
118. Burgess, R. C., Rahman, S., Lisby, M., Rothstein, R. & Zhao, X. The Slx5-Slx8 complex affects sumoylation of DNA repair proteins and negatively regulates recombination. *Mol. Cell. Biol.* **27**, 6153–6162 (2007).
119. Nagai, S. *et al.* Functional targeting of DNA damage to a nuclear pore-associated SUMO-dependent ubiquitin ligase. *Science* **322**, 597–602 (2008).
120. Kosoy, A., Calonge, T. M., Outwin, E. A. & O'Connell, M. J. Fission yeast Rnf4 homologs are required for DNA repair. *J. Biol. Chem.* **282**, 20388–20394 (2007).
121. Cook, C. E., Hochstrasser, M. & Kerscher, O. The SUMO-targeted ubiquitin ligase subunit Slx5 resides in nuclear foci and at sites of DNA breaks. *Cell Cycle* **8**, 1080–1089 (2009).
122. Weisshaar, S. R. *et al.* Arsenic trioxide stimulates SUMO-2/3 modification leading to RNF4-dependent proteolytic targeting of PML. *FEBS Lett* **582**, 3174–3178 (2008).
123. Guo, B. & Sharrocks, A. D. Extracellular signal-regulated kinase mitogen-activated protein kinase signaling initiates a dynamic interplay between sumoylation and ubiquitination to regulate the activity of the transcriptional activator PEA3. *Mol. Cell. Biol.* **29**, 3204–3218 (2009).
124. van Hagen, M., Overmeer, R. M., Abolvardi, S. S. & Vertegaal, A. C. O. RNF4 and VHL regulate the proteasomal degradation of SUMO-conjugated Hypoxia-Inducible Factor-2 α . *Nucleic Acids Res* **38**, 1922–1931 (2010).
125. Martin, N. *et al.* PARP-1 transcriptional activity is regulated by sumoylation upon heat shock. *EMBO J* **28**, 3534–3548 (2009).
126. Wang, Z. & Prelich, G. Quality control of a transcriptional regulator by SUMO-targeted degradation. *Mol. Cell. Biol.* **29**, 1694–1706 (2009).
127. Nixon, C. E., Wilcox, A. J. & Laney, J. D. Degradation of the *Saccharomyces cerevisiae* mating-type regulator alpha1: genetic dissection of cis-determinants and trans-acting pathways. *Genetics* **185**, 497–511 (2010).
128. Darst, R. P., Garcia, S. N., Koch, M. R. & Pillus, L. Slx5 promotes transcriptional silencing and is required for robust growth in the absence of Sir2. *Mol. Cell. Biol.* **28**, 1361–1372 (2008).
129. Liakopoulos, D., Doenges, G., Matuschewski, K. & Jentsch, S. A novel protein modification pathway related to the ubiquitin system. *EMBO J.* **17**, 2208–2214 (1998).
130. Kurz, T. *et al.* The conserved protein DCN-1/Dcn1p is required for cullin neddylation in *C. elegans* and *S. cerevisiae*. *Nature* **435**, 1257–1261 (2005).
131. Lammer, D. *et al.* Modification of Yeast Cdc53p by the Ubiquitin-Related Protein Rub1p Affects Function of the SCFCdc4 Complex. *Genes Dev.* **12**, 914–926 (1998).

132. Wu, J.-T., Lin, H.-C., Hu, Y.-C. & Chien, C.-T. Neddylation and deneddylation regulate Cull1 and Cul3 protein accumulation. *Nat. Cell Biol.* **7**, 1014–1020 (2005).
133. Petroski, M. D. & Deshaies, R. J. Function and regulation of cullin-RING ubiquitin ligases. *Nat. Rev. Mol. Cell Biol.* **6**, 9–20 (2005).
134. Lyapina, S. *et al.* Promotion of NEDD-CUL1 conjugate cleavage by COP9 signalosome. *Science* **292**, 1382–1385 (2001).
135. Cope, G. A. *et al.* Role of predicted metalloprotease motif of Jab1/Csn5 in cleavage of Nedd8 from Cull1. *Science* **298**, 608–611 (2002).
136. Wee, S., Hetfeld, B., Dubiel, W. & Wolf, D. A. Conservation of the COP9/signalosome in budding yeast. *BMC Genet.* **3**, 15 (2002).
137. Ou, C.-Y., Lin, Y.-F., Chen, Y.-J. & Chien, C.-T. Distinct protein degradation mechanisms mediated by Cull1 and Cul3 controlling Ci stability in *Drosophila* eye development. *Genes Dev.* **16**, 2403–2414 (2002).
138. Dharmasiri, S., Dharmasiri, N., Hellmann, H. & Estelle, M. The RUB/Nedd8 conjugation pathway is required for early development in *Arabidopsis*. *EMBO J.* **22**, 1762–1770 (2003).
139. Kurz, T. *et al.* Cytoskeletal regulation by the Nedd8 ubiquitin-like protein modification pathway. *Science* **295**, 1294–1298 (2002).
140. Ohsumi, Y. Molecular dissection of autophagy: two ubiquitin-like systems. *Nat. Rev. Mol. Cell Biol.* **2**, 211–216 (2001).
141. Mizushima, N., Yoshimori, T. & Ohsumi, Y. The role of Atg proteins in autophagosome formation. *Annu. Rev. Cell Dev. Biol.* **27**, 107–132 (2011).
142. Rubinsztein, D. C., Shpilka, T. & Elazar, Z. Mechanisms of autophagosome biogenesis. *Curr. Biol.* **22**, R29–34 (2012).
143. Cebollero, E. & Reggiori, F. Regulation of autophagy in yeast *Saccharomyces cerevisiae*. *Biochim. Biophys. Acta* **1793**, 1413–1421 (2009).
144. Tsukada, M. & Ohsumi, Y. Isolation and characterization of autophagy-defective mutants of *Saccharomyces cerevisiae*. *FEBS Lett.* **333**, 169–174 (1993).
145. Kirisako, T. *et al.* The reversible modification regulates the membrane-binding state of Apg8/Aut7 essential for autophagy and the cytoplasm to vacuole targeting pathway. *J. Cell Biol.* **151**, 263–276 (2000).
146. Ichimura, Y. *et al.* A ubiquitin-like system mediates protein lipidation. *Nature* **408**, 488–492 (2000).
147. Nakatogawa, H., Ichimura, Y. & Ohsumi, Y. Atg8, a ubiquitin-like protein required for autophagosome formation, mediates membrane tethering and hemifusion. *Cell* **130**, 165–178 (2007).
148. Nair, U. *et al.* A role for Atg8-PE deconjugation in autophagosome biogenesis. *Autophagy* **8**, (2012).
149. Mizushima, N. *et al.* A protein conjugation system essential for autophagy. *Nature* **395**, 395–398 (1998).
150. Shintani, T. *et al.* Apg10p, a novel protein-conjugating enzyme essential for autophagy in yeast. *EMBO J.* **18**, 5234–5241 (1999).
151. Hanada, T. *et al.* The Atg12-Atg5 conjugate has a novel E3-like activity for protein lipidation in autophagy. *J. Biol. Chem.* **282**, 37298–37302 (2007).
152. Pedrioli, P. G. A., Leidel, S. & Hofmann, K. Urm1 at the crossroad of modifications. 'Protein Modifications: Beyond the Usual Suspects' Review Series. *EMBO Rep.* **9**, 1196–1202 (2008).
153. Wang, F., Liu, M., Qiu, R. & Ji, C. The dual role of ubiquitin-like protein Urm1 as a protein modifier and sulfur carrier. *Protein Cell* **2**, 612–619 (2011).
154. Van der Veen, A. G. *et al.* Role of the ubiquitin-like protein Urm1 as a noncanonical lysine-directed protein modifier. *Proc. Natl. Acad. Sci. U.S.A.* **108**, 1763–1770 (2011).
155. Xu, J. *et al.* Solution structure of Urm1 and its implications for the origin of protein modifiers. *Proc. Natl. Acad. Sci. U.S.A.* **103**, 11625–11630 (2006).
156. Furukawa, K., Mizushima, N., Noda, T. & Ohsumi, Y. A protein conjugation system in yeast with homology to biosynthetic enzyme reaction of prokaryotes. *J. Biol. Chem.* **275**, 7462–7465 (2000).
157. Hochstrasser, M. Evolution and function of ubiquitin-like protein-conjugation systems. *Nat. Cell Biol.* **2**, E153–157 (2000).
158. Leidel, S. *et al.* Ubiquitin-related modifier Urm1 acts as a sulphur carrier in thiolation of eukaryotic transfer RNA. *Nature* **458**, 228–232 (2009).
159. Noma, A., Sakaguchi, Y. & Suzuki, T. Mechanistic characterization of the sulfur-relay system for eukaryotic 2-thiouridine biogenesis at tRNA wobble positions. *Nucleic Acids Res.* **37**, 1335–1352 (2009).
160. Goehring, A. S., Rivers, D. M. & Sprague, G. F., Jr Attachment of the ubiquitin-related protein Urm1p to the antioxidant protein Ahp1p. *Eukaryotic Cell* **2**, 930–936 (2003).
161. Goehring, A. S., Rivers, D. M. & Sprague, G. F., Jr Urm1ylation: a ubiquitin-like pathway that functions during invasive growth and budding in yeast. *Mol. Biol. Cell* **14**, 4329–4341 (2003).
162. Rubio-Teixeira, M. Urm1ylation controls Nil1p and Gln3p-dependent expression of nitrogen-catabolite repressed genes in *Saccharomyces cerevisiae*. *FEBS Lett* **581**, 541–550 (2007).
163. Chowdhury, M. M., Dosche, C., Löhmannsröben, H.-G. & Leimkühler, S. Dual role of the molybdenum cofactor biosynthesis protein MOCS3 in tRNA thiolation and molybdenum cofactor biosynthesis in humans. *J. Biol. Chem.* **287**, 17297–17307 (2012).
164. Ramelot, T. A. *et al.* Solution structure of the yeast ubiquitin-like modifier protein Hub1. *J. Struct. Funct. Genomics* **4**, 25–30 (2003).
165. Dittmar, G. A. G., Wilkinson, C. R. M., Jedrzejewski, P. T. & Finley, D. Role of a ubiquitin-like modification in polarized morphogenesis. *Science* **295**, 2442–2446 (2002).
166. Lüders, J., Pyrowolakis, G. & Jentsch, S. The ubiquitin-like protein HUB1 forms SDS-resistant complexes with cellular proteins in the absence of ATP. *EMBO Rep.* **4**, 1169–1174 (2003).
167. Wilkinson, C. R. M. *et al.* Ubiquitin-like protein Hub1 is required for pre-mRNA splicing and localization of an essential splicing factor in fission yeast. *Curr. Biol.* **14**, 2283–2288 (2004).
168. Yashiroda, H. & Tanaka, K. Hub1 is an essential ubiquitin-like protein without functioning as a typical modifier in fission yeast. *Genes Cells* **9**, 1189–1197 (2004).
169. Mishra, S. K. *et al.* Role of the ubiquitin-like protein Hub1 in splice-site usage and alternative splicing. *Nature* **474**, 173–178 (2011).



Delineating ubiquitin and ubiquitin-like systems in *Saccharomyces cerevisiae* by gene expression profiling

Loes A.L. van de Pasch, Thanasis Margaritis, Mehdi Kashani, Giannis Ampatziadis, Sake van Wageningen, Tineke L. Lenstra, Dik van Leenen, Marian J.A. Groot Koerkamp and Frank C.P. Holstege

Delineating ubiquitin and ubiquitin-like systems in *Saccharomyces cerevisiae* by gene expression profiling

Loes A.L. van de Pasch*, Thanasis Margaritis*, Mehdi Kashani, Giannis Ampatziadis, Sake van Wageningen, Tineke L. Lenstra, Dik van Leenen, Marian J.A. Groot Koerkamp and Frank C.P. Holstege

Molecular Cancer Research, University Medical Centre Utrecht, Universiteitsweg 100, 3508 AB, Utrecht, The Netherlands

*These authors contributed equally to this work

Manuscript in preparation

ABSTRACT

Cellular processes are regulated through diverse posttranslational modifications, including phosphorylation, ubiquitination and ubiquitin-like modification. The way the different components of such pathways interact to form complex regulatory systems is still poorly understood. To investigate ubiquitination and ubiquitin-like modification pathways, we have generated genome-wide expression profiles of 224 *Saccharomyces cerevisiae* mutants bearing deletions of genes involved in these systems. Disruption of genes involved in ubiquitination, sumoylation and urmylation, elicits highly specific transcriptional responses, reflecting which cellular processes are targeted. The expression profiles can be used for detailed phenotypic characterisation of yeast mutants and identifies established and novel functional relationships between genes. These include shared protein complex subunits, same cellular pathway components, E2-E3 interacting pairs, and signalling across ubiquitin(-like) modification and phosphorylation systems. The data reveal new characteristics of individual components and demonstrate that expression profiling is a powerful tool to gain insight in the *in vivo* functions of the ubiquitin and ubiquitin-like systems.

INTRODUCTION

Appropriate regulation of gene expression is pivotal to most cellular processes. Transcription regulation is achieved by an intimate interplay between gene-specific transcription factors, general transcription factors and complexes that influence chromatin. Signal transduction pathways impinge on this machinery through a variety of posttranslational modifications of downstream effector proteins that ultimately control the expression of specific genes. An important posttranslational modification in eukaryotic cells is the conjugation of the highly conserved ubiquitin protein^{1,2}. Ubiquitin is a small 76-residue polypeptide that can be covalently attached to proteins, thereby modulating protein

functionality by changing protein conformation, altering protein activity, creating protein interaction surfaces, targeting proteins to specific subcellular locations or by serving as a marker for protein degradation through the proteasome. The covalent attachment of ubiquitin to a substrate is a multi-step process, involving several enzymes that function in consecutive order. First, the ubiquitin modifier is synthesised as an inactive precursor protein, which is then processed by a deubiquitinase (DUB). Next, a ubiquitin-activating enzyme (E1) forms a thiol ester bond with the processed modifier. The modifier is then transferred to a ubiquitin-conjugating enzyme (E2) that, together with a ubiquitin ligase (E3), mediates the attachment of ubiquitin to a lysine residue of a substrate. The modification is

reversible due to the action of DUBs that remove the modifier from the substrate, making ubiquitination a highly dynamic system that depends on a balanced attachment and removal of ubiquitin to and from substrates³⁻⁵. The diversity in effects of protein ubiquitination is also reflected by the large variety in types of ubiquitin modification. These include modifications with a single ubiquitin moiety or with polyubiquitin chains that differ in length and linkages⁶.

Besides ubiquitin, a family of structurally related ubiquitin-like proteins has been identified⁷. Similar to ubiquitin, these peptides function as posttranslational modifiers of substrates in ubiquitin-like systems. In the yeast *Saccharomyces cerevisiae*, these systems include sumoylation, neddylation, urmylation, Atg8 and Atg12 modification, as well as Hub1 modification⁸⁻¹⁴. Each ubiquitin and ubiquitin-like system has their own unique set of enzymes, resulting in a complex network to ensure correct modification of specific substrates. Despite this enzymatic separation, there is evidence for signalling across these systems. For instance, sumoylation of I κ B α and PCNA antagonises ubiquitination by competing for a lysine residue, thereby inhibiting ubiquitin-dependent proteasomal degradation or altering protein function^{15,16}. Furthermore, sumoylated proteins can be ubiquitinated by SUMO-dependent ubiquitin E3 ligases, leading to proteasomal degradation^{17,18}. The organisational structure of the ubiquitin(-like) systems is complex due to the large number of enzymes involved, the variety of cellular processes they regulate and the possibility of crosstalk, making it challenging to understand how these systems function together in parallel.

We have used the model organism *S. cerevisiae* to systematically analyse ubiquitin and ubiquitin-like pathways. Yeast mutants bearing deletions of ubiquitin(-like) system components were investigated using microarray expression profiles. The expression patterns of the mutants give detailed information about the cellular response caused by disruption of ubiquitin(-like) system-dependent

cellular pathways. The gene expression profiles are used for phenotypic characterisation of the mutants, revealing known and novel functions of the components. Moreover, functional relationships among the different components can be derived from the expression patterns. This improves our insight in the function of the individual components in the context of the entire system of ubiquitin and ubiquitin-like modification.

RESULTS and DISCUSSION

Expression profiles of yeast deletion mutants of ubiquitin(-like) systems

We have investigated the genome-wide expression patterns of 224 yeast deletion mutants for which the disrupted gene is implicated in ubiquitin or ubiquitin-like modification. The mutants were selected based on the association of the deleted gene with specific Gene Ontology (GO) terms related to ubiquitin(-like) modification (Supplementary Table S1). In addition, the set of genes with a (putative) role as E3 ligase was expanded by including all genes containing specific protein domains commonly found in E3 ligases, namely the RING finger domain, HECT domain, U-box and F-box¹⁹⁻²³.

DNA microarray expression profiles were generated for all available deletion mutants, which were grown alongside a wild type (wt) strain under a single growth condition. For every mutant, four DNA microarray expression profiles were generated from two biological replicates derived from independent yeast colonies. Mutant RNA samples were hybridised on dual-channel microarrays versus a single batch of wt RNA as common reference. The mRNA expression changes were assessed by comparing the mutant expression profiles to a collection of 200 wt profiles generated in the same manner²⁴. Mutants with chromosomal aneuploidy or bearing incorrect deletions were remade and profiled again, resulting in a total of 224 mutants that passed all quality controls. Equivalent studies under identical conditions have been performed previously using deletion mutants of kinases, phosphatases and

chromatin regulators^{24,25}. The mutants described in this study provide a complementary set of expression profiles that can be directly compared to these earlier studies (Figure 1A).

Changes in mRNA expression upon disruption of ubiquitination, sumoylation and urmylation

For each individual mutant the four DNA microarray profiles were averaged and the number of differentially expressed genes was assessed. When comparing the expression levels of a mutant to that of wt, a *p*-value of <0.05 and a fold change (FC) of >1.7 were applied as thresholds to call a transcript significantly changed in expression ('significant gene'). The number of significant genes ranged from zero to maximally 755 genes in *mot2Δ* (Figure 1B), lacking the Mot2 subunit of the Ccr4-Not ubiquitin E3 ligase²⁶. Of the 89 wts that were grown in parallel to the deletion mutants, only six had five or more significantly changing genes (Figure 1B). This was applied as a threshold for calling a mutant profile different from wt. In this way, 108 mutants (48%) were assigned as having a significant expression phenotype (Figure 1B). The group of mutants analysed encompasses 93% of all the established nonessential components directly implicated in ubiquitin(-like) modification (Supplementary Table S2). The majority of the mutants represent components of the ubiquitin system (Figure 1C). Significant expression phenotypes (different than wt) were identified for various mutants with deletions of E2 enzymes, E3 ligases, DUBs, but also for mutants with deletions

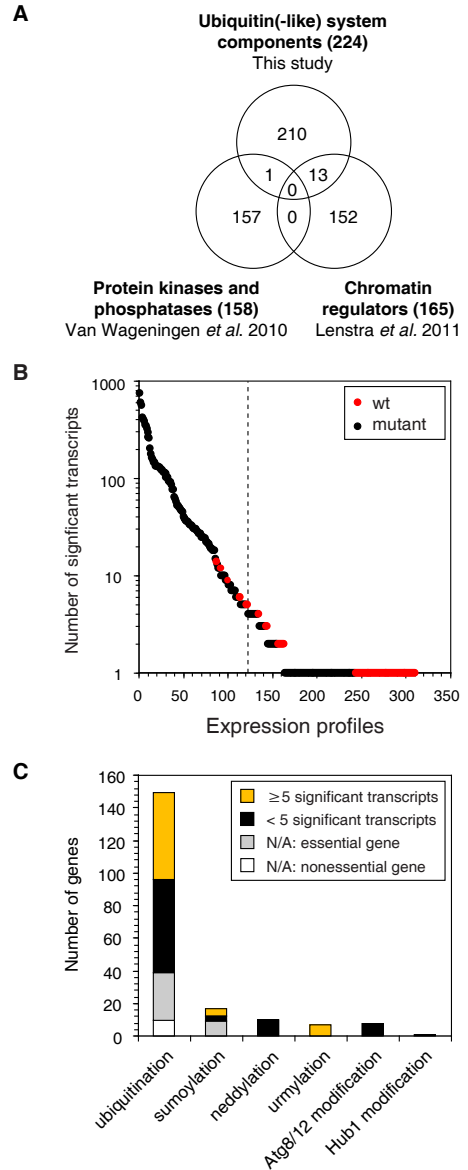


Figure 1. Disruption of ubiquitin and ubiquitin-like modification pathways results in mRNA expression changes.

(A) Venn diagram of the number of unique yeast deletion mutants described here, in comparison to two other similar large-scale microarray studies performed under identical experimental conditions. (B) Gene expression profiles of 224 mutants and 89 wts that were grown in parallel, showing the number of differentially expressed transcripts (FC > 1.7, *p* < 0.05) compared to wt. Dashed line indicates the significance threshold applied here to distinguish mutants with a significant expression phenotype (≥ 5 significant transcripts) from mutants without a significant phenotype. Strains without significant transcripts are represented as having one transcript changing in order to allow data representation on a logarithmic scale. (C) Stacked histogram showing the number of genes per ubiquitin(-like) system. Genes are categorised in distinct ubiquitin(-like) systems based on the GO terms specified in Supplementary Table S2. Genes associated with a significant expression phenotype (≥ 5 genes, FC > 1.7, *p* < 0.05) are shown in yellow. Genes without a significant expression phenotype (< 5 genes, FC > 1.7, *p* < 0.05) are shown in black. Genes that were not profiled, mostly due to inviability of the mutant, are marked as not available (N/A)

of non-catalytic subunits associated with E3 ligase or DUB protein complexes (Table 1). The number of nonessential genes in *S. cerevisiae* that represent the ubiquitin-like systems is quite small compared to the ubiquitin system (Figure 1C). For the ubiquitin-like systems, significant expression phenotypes were only identified in deletion mutants with a role in sumoylation and urmylation (Table 1). Disruption of genes involved in neddylation, Atg8/12 modification or Hub1 modification did not significantly affect gene expression, as these mutants showed expression

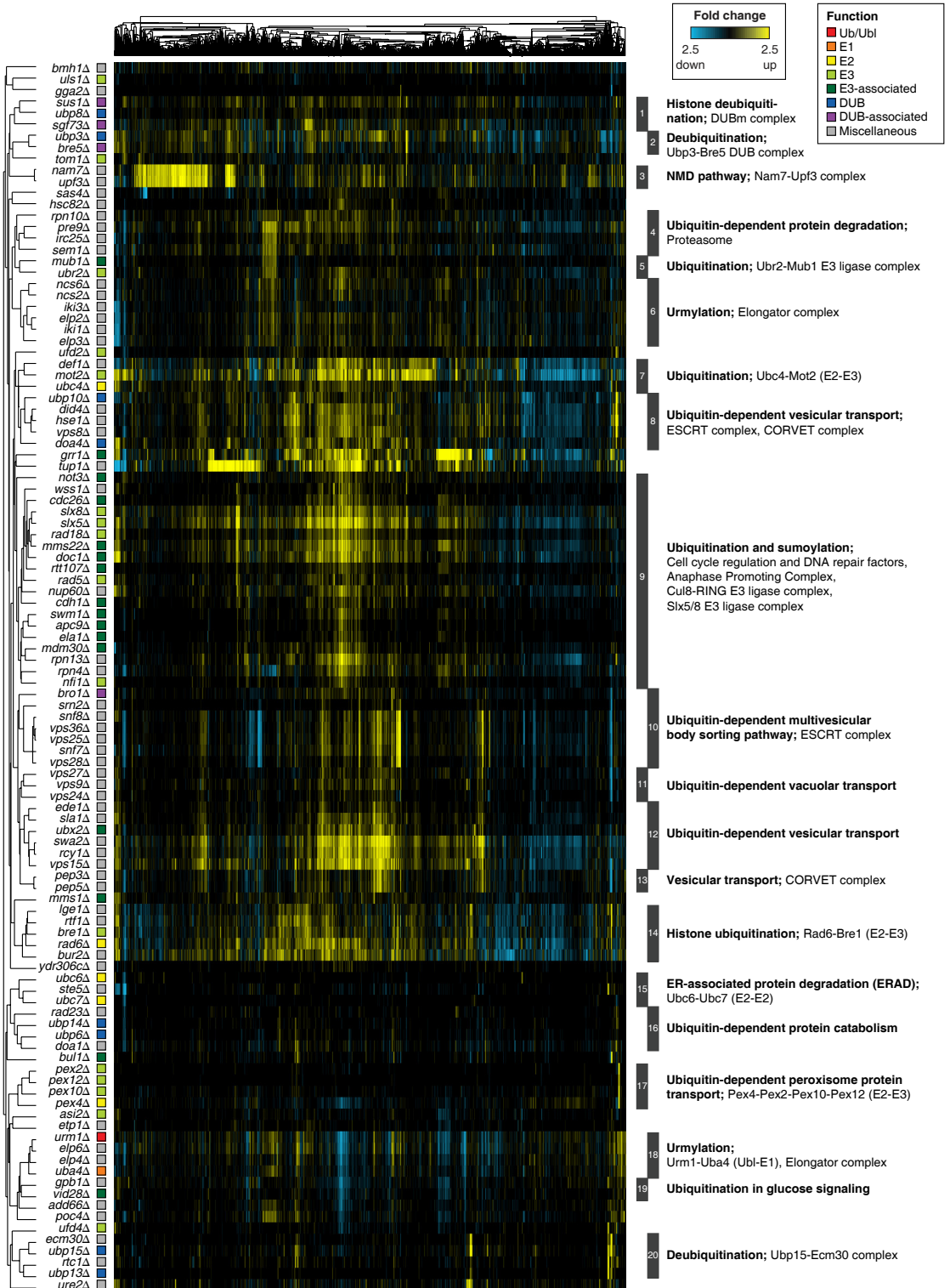
profiles that were equivalent to wt. Likely reasons for a lack of an expression phenotype are redundancy and condition-dependency. The latter can apply to an entire ubiquitin-like system. For example, genes involved in Atg8/12 modification are required for regulation of autophagy under starvation conditions¹¹. A complete overview of all genes with a (putative) role in ubiquitin(-like) modification and whether they are associated with an expression phenotype upon deletion is provided in Supplementary Table S3.

Table 1. Overview of the major ubiquitin(-like) system components and their association to an expression phenotype upon deletion

Ubiquitin system	Phenotype	No phenotype
Modifier		<i>ubi4Δ</i>
E1		
E2	<i>pex4Δ rad6Δ ubc4Δ ubc6Δ ubc7Δ</i>	<i>mms2Δ ubc5Δ ubc8Δ ubc11Δ</i>
E3	<i>asi2Δ bre1Δ mot2Δ pex2Δ pex10Δ pex12Δ rad5Δ rad18Δ slx5Δ slx8Δ tom1Δ ubr2Δ ufd2Δ ufd4Δ uls1Δ</i>	<i>asi1Δ asi3Δ asr1Δ cul3Δ dma1Δ dma2Δ hrd1Δ hul4Δ hul5Δ pib1Δ psh1Δ rkr1Δ rmd5Δ san1Δ ssm4Δ tul1Δ ubr1Δ</i>
E3-associated	<i>apc9Δ bul1Δ cdc26Δ cdh1Δ doc1Δ ela1Δ grr1Δ mdm30Δ mms1Δ mss22Δ mub1Δ not3Δ rtt107Δ swm1Δ ubx2Δ vid28Δ ydr306cΔ</i>	<i>ama1Δ bul2Δ cue1Δ das1Δ der1Δ elc1Δ hrd3Δ hrt3Δ mfb1Δ mnd2Δ rad7Δ rad16Δ saf1Δ skp2Δ ufo1Δ usa1Δ vid24Δ vid30Δ ydr131cΔ ylr224wΔ ylr352wΔ yos9Δ</i>
DUB	<i>doa4Δ ubp3Δ ubp6Δ ubp8Δ ubp10Δ ubp13Δ ubp14Δ ubp15Δ</i>	<i>otu1Δ ubp1Δ ubp2Δ ubp5Δ ubp7Δ ubp9Δ ubp11Δ ubp12Δ ubp16Δ yuh1Δ</i>
DUB-associated	<i>bre5Δ bro1Δ ecm30Δ sgf73Δ sus1Δ</i>	<i>rup1Δ sgf11Δ</i>
Ubiquitin-like systems	Phenotype	No phenotype
Modifier	<i>urm1Δ</i>	<i>atg8Δ atg12Δ hub1Δ rub1Δ</i>
E1	<i>uba4Δ</i>	<i>atg7Δ ula1Δ</i>
E2		<i>atg3Δ atg10Δ ubc12Δ</i>
E3	<i>nfi1Δ</i>	<i>atg5Δ cst9Δ dcn1Δ siz1Δ</i>
ULP		<i>atg4Δ rri1Δ</i>
ULP-associated		<i>csi1Δ csn9Δ pci8Δ rri2Δ</i>

Figure 2. Deletion of ubiquitin(-like) system components results in specific gene expression responses that define cellular pathways and protein complexes.

Heatmap and cluster diagram of the expression profiles of 109 yeast deletion mutants with a significant expression phenotype (≥ 5 genes, $FC > 1.7$, $p < 0.05$). The mutants are implicated in ubiquitination or ubiquitin-like modification and are colour-coded according to their function. The heatmap displays all genes that change significantly at least once in any mutant. Fold change expression levels are indicated by the colour scale, with yellow for upregulation, blue for downregulation and black for no change. Mutants are subdivided in subclusters (labelled 1-20), based on the clustering indicated by the dendrogram. The subclusters are functionally annotated based on common function in one cellular pathway and/or protein complex. See also Supplementary Figure S1.



Disruption of ubiquitin(-like) system components results in highly specific expression responses that are shared among functionally related mutants

A two-dimensional hierarchical cluster diagram was generated to compare the expression profiles of all mutants with five or more significant genes. The cluster diagram reveals that the mutants separate in at least 20 groups based on their gene expression patterns (Figure 2 and Supplementary Figure S1). As has been demonstrated previously, mutants that cluster together are functionally related, e.g. part of the same protein complex or cellular pathway^{24,25,27}. For example, mutants with functions in various (ubiquitin-dependent) vesicular transport pathways are represented by five distinct expression signatures (cluster #8, #10, #11, #12, #13) (Figure 2, shown in more detail in Supplementary Figure S1), such as the CORVET complex (cluster #13; *pep3Δ*, *pep8Δ*) and components of the multivesicular body sorting pathway (cluster #10; *snf7Δ*, *snf8Δ*, *vps25Δ*, *vps28Δ*, *vps36Δ*, *srn2Δ*, *bro1Δ*). Mutants with a common function in histone ubiquitination also cluster tightly together (cluster #14; *rad6Δ*, *bre1Δ*, *lge1Δ*, *rtf1Δ*, *bur2Δ*). Furthermore, mutants of proteasome subunits and proteasome assembly factors strongly resemble each other (cluster #4; *rpn10Δ*, *pre9Δ*,

irc25Δ, *sem1Δ*). The largest cluster represents mutants with roles in cell cycle regulation and/or DNA repair (cluster #9), and includes components of the anaphase promoting complex (*apc9Δ*, *cdh1Δ*, *cdc26Δ*, *doc1Δ*, *swm1Δ*), the Cul8-RING ubiquitin ligase (*mms22Δ*, *rtt107Δ*), the ubiquitin E3 ligases Rad5 and Rad18 (*rad5Δ*, *rad18Δ*), the SUMO-dependent ubiquitin E3 ligase complex Slx5/Slx8 (*slx5Δ*, *slx8Δ*), as well as other mutants implicated in sumoylation (*nfi1Δ*, *nup60Δ*, *wss1Δ*). The number of changing transcripts is highly dependent on which pathway is disrupted, ranging from very few (e.g. cluster #17; 30 transcripts; *pex2Δ*, *pex4Δ*, *pex10Δ*, *pex12Δ*) to many significant genes (e.g. cluster #12; 562 transcripts; *rcy1Δ*, *sla1Δ*, *swa2Δ*, *ubx2Δ*, *vps15Δ*) (Supplementary Figure S1).

The specificity of the transcriptional responses of the clustered mutants was exploited to define in which pathway the protein encoded by the deleted gene may take part (Figure 2). Generally, the cellular functions, as derived from co-clustering, agree with previously established functions. There are also exceptions. For example, the strong resemblance of the expression profile of *ubx2Δ* to that of *rcy1Δ*, *sla1Δ*, *swa2Δ* and *vps15Δ* is unexpected (Figure 3A). *Ubx2* is involved in ER-associated protein degradation (ERAD), mediated by the ubiquitin

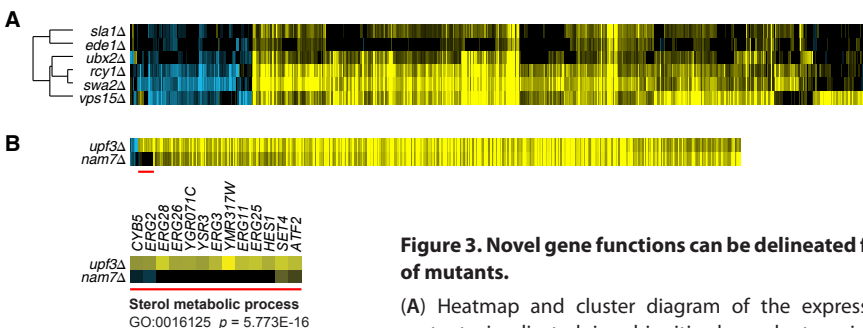


Figure 3. Novel gene functions can be delineated from expression profiles of mutants.

(A) Heatmap and cluster diagram of the expression profiles of deletion mutants implicated in ubiquitin-dependent vesicular transport (see also Figure 2, cluster #12). The expression profile of ERAD component *ubx2Δ* is similar to profiles of vesicular transport mutants *sla1Δ*, *ede1Δ*, *rcy1Δ*, *swa2Δ* and *vps15Δ*. (B) Heatmap of expression profiles of mutants *upf3Δ* and *nam7Δ* with a common function in nonsense-mediated mRNA decay (see also Figure 2, cluster #3). Bottom panel is a magnification of the gene cluster in the upper heatmap that is marked with a red line. *Upf3Δ* shows induction of transcripts associated to GO 'sterol metabolic process'.

E3 ligases Hrd1 and Ssm4²⁸. Disruption of ERAD components has only little effect on gene expression (*hrd1Δ*: 1 significant gene, *ssm4Δ*: 4 significant genes). In contrast, deletion of *UBX2* affects the expression of 103 genes, indicating that Ubx2 has a second function that is separate from ERAD. The similarity in expression response of *ubx2Δ* to mutants defective in endocytosis (*rcy1Δ*, *sla1Δ*), clathrin-coated vesicle transport (*swa2Δ*) and vacuolar transport (*vps15Δ*) (Figure 3A), predicts that Ubx2 has an uncharacterised function in vesicular transport.

Individual genes may function in more than one cellular pathway. Linking mutants to specific protein complexes or cellular pathways can therefore also be based on a subset of differentially expressed genes. For instance, the expression profiles of *nam7Δ* and *upf3Δ* are virtually identical, with the exception of a small block of transcripts that is uniquely induced in *upf3Δ* (Figure 3B). Nam7 and Upf3 function together in the nonsense-mediated mRNA decay (NMD) pathway²⁹. Deletion of any of these components results in a strong upregulation of ~400 transcripts (Figure 3B), which agrees with the function of Nam7/Upf3 in mRNA degradation. Strikingly, *upf3Δ* also shows induction of transcripts with a common function in sterol biosynthesis, suggesting that Upf3 has an uncharacterised function related to sterol metabolism that is independent of the NMD pathway (see also Supplementary Figure S2).

Functional interactions between E2 and E3 enzymes can be derived from gene expression signatures

The central players of the ubiquitin system are reasonably well-defined in *S. cerevisiae*. There is one E1, twelve E2s, at least 36 E3 enzymes (not taking into account E3 complex-associated subunits) and 25 DUB(-associated) proteins. In order to study this enzymatic system, the expression profiles of the corresponding deletion mutants were analysed in detail to characterise the *in vivo* function of the deleted gene and to delineate known and novel

relationships between these components. Five out of nine profiled E2 mutants (*pex4Δ*, *rad6Δ*, *ubc4Δ*, *ubc6Δ*, *ubc7Δ*) displayed a significant effect on gene expression (≥ 5 genes, FC > 1.7, $p < 0.05$) (Figure 4A). In all cases, the E2 mutant could be linked to one or more E3 deletion mutants based on a (partial) overlap in differentially expressed genes (Figure 4B-E). A clear example is the E2 mutant *pex4Δ* (Figure 4B). Pex4 cooperates with three ubiquitin E3 ligases, namely Pex2, Pex10 and Pex12, and is involved in the biogenesis of peroxisomes and peroxisomal protein import^{30,31}. Comparison of the expression profile of *pex4Δ* with that of *pex2Δ*, *pex10Δ* and *pex12Δ* reveals a remarkable overlap in their upregulated genes, showing induction of the lysine metabolic pathway (Figure 4B). This gene signature is characteristic for mutants with a peroxisome deficiency and is not identified in any other ubiquitin(-like) system component deletion mutant (Figure 2)³². This specific gene signature therefore confirms the established functional link between Pex2, Pex4, Pex10 and Pex12.

Similarly, deletion of the functionally related ubiquitin E2 enzymes *UBC6* and *UBC7* results in a small but significant effect on nine and six genes respectively (Figure 4C). *Ubc6Δ* and *ubc7Δ* share five downregulated genes that are associated with mating, which agrees with the function of Ubc6 and Ubc7 in MAT α 2 degradation and ERAD³³. Cue1 recruits Ubc7 to the ER and indeed the expression phenotype of *cue1Δ* resembles that of *ubc6Δ* and *ubc7Δ* (Figure 4C)³⁴. Ubc6 and Ubc7 have been reported to cooperate with two distinct ubiquitin E3 ligases, namely Hrd1 and Ssm4, which target different ERAD pathways³⁵. The E3 mutant *ssm4Δ* displays the same downregulated genes as seen in *ubc6Δ* and *ubc7Δ* (Figure 4C). The mutant *hrd1Δ* or other Hrd1 E3 ligase complex deletion mutants (*hrd3Δ*, *usa1Δ*, *yos9Δ*, *der1Δ*) does not affect gene expression (Figure 4C and Supplementary Table S3). This suggests that the differentially expressed genes seen in *ubc6Δ* and *ubc7Δ* are predominantly due to a defect in Ssm4-mediated rather than Hrd1-mediated ubiquitination.

Ubc4 and Ubc5 are two homologous and functionally redundant ubiquitin E2 enzymes that take part in numerous (poly-)ubiquitination pathways through interactions with multiple E3 ligases, including the Ccr4-Not complex^{26,36}. Expression of the genes *UBC4* and *UBC5* is highly regulated, with high expression of *UBC4* and low expression of *UBC5* under normal growth conditions in mid-log phase³⁶. In agreement with this observation, deletion of *UBC5* under our growth condition does not affect gene expression, whereas *ubc4Δ* displays altered expression of 45 genes (Figure 4D). The expression changes in *ubc4Δ* are almost completely recapitulated as a subset of the profile of the Ccr4-Not mutant *mot2Δ* (Figure 4D). This again confirms that functionally interacting E2-E3 pairs can be identified, in this case Ubc4 and Mot2, based

on overlap in expression patterns upon deletion of the corresponding genes. Among the upregulated genes in *mot2Δ* are *UBC4* and *UBC5* (Figure 4D), suggesting feedback leading to activation of Ubc4/Ubc5-dependent ubiquitination pathways. Since the phenotype of *mot2Δ* is much stronger than observed for *ubc4Δ*, this suggests that other Ubc4/Ubc5-independent pathways are also affected in *mot2Δ*.

A more complex example of functional interactions between E2s and E3s is observed for the E2 mutant *rad6Δ*. Of all E2 mutants tested, *rad6Δ* displays the strongest effect on gene expression, with 268 significant gene expression changes (Figure 4A). Rad6 is a versatile ubiquitin E2 that functions with different E3 ligases that target distinct cellular pathways^{37–39}. Direct comparison of the expression profile of *rad6Δ* with four E3 deletion mutants

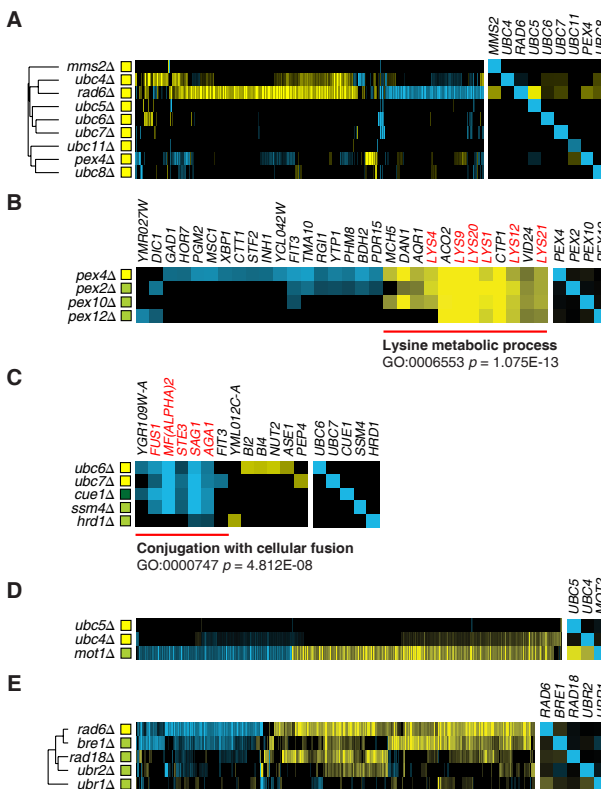


Figure 4. Functional relationships between ubiquitin-conjugating enzymes and ubiquitin protein ligases can be derived from gene expression profiles.

(A) Heatmap and cluster diagram of the expression profiles of mutants with deletions of ubiquitin-conjugating (E2) enzymes. *Pex4Δ*, *rad6Δ*, *ubc4Δ*, *ubc6Δ* and *ubc7Δ* have ≥ 5 significant genes ($FC > 1.7$, $p < 0.05$) and are therefore annotated as having a significant expression phenotype. The colour-coding is as shown in Figure 2. The right-hand panel shows the expression levels of the E2 encoding genes, showing loss of expression in the respective deletion mutants. (B) Heatmap of the expression profiles of the E2 mutant *pex4Δ* and the E3 mutants *pex2Δ*, *pex10Δ* and *pex12Δ*. Upregulated genes, indicated in red, are associated to GO 'lysine metabolic process'. The colour-coding is as shown in Figure 2. The right-hand panel shows the expression levels of the E2 encoding genes, showing loss of expression in the respective deletion mutants. (C) Heatmap of the expression profiles of the E2 mutants *ubc6Δ* and *ubc7Δ* and the E3(-associated) mutants *cue1Δ*, *ssm4Δ* and *hrd1Δ*. Note that *cue1Δ*, *ssm4Δ* and *hrd1Δ* have a weak expression phenotype that is below our significance cut-off (< 5 genes) and are therefore not displayed in Figure 2. Downregulated transcripts, associated to GO 'conjugation with cellular fusion' are shown in red. (D) Heatmap of the expression profiles of the E2 mutants *ubc4Δ* and *ubc5Δ* and the E3 mutant *mot2Δ*. Note that the expression of *UBC4* and *UBC5* is induced in *mot2Δ*. (E) Heatmap and cluster diagram of the expression profiles of the E2 mutant *rad6Δ* and the E3 mutants *bre1Δ*, *rad18Δ*, *ubr1Δ* and *ubr2Δ*.

shows that the *rad6Δ* expression profile is similar to a merged expression profile of the four individual E3 mutant profiles (Figure 4E). This additive effect in *rad6Δ* can be interpreted as the combined disruption of at least four parallel ubiquitination pathways. The largest part of the *rad6Δ* profile is constituted of genes that also change in *bre1Δ* and/or *rad18Δ* (Figure 4E), suggesting that histone ubiquitination and DNA repair are defective in *rad6Δ* and predominantly responsible for the expression phenotype in *rad6Δ*. The examples of Pex4, Ubc4, Ubc6, Ubc7, Rad6 and their respective ubiquitin E3 ligases demonstrate that similarity in gene expression changes upon deletion of the enzyme can be used to delineate functionally interacting E2-E2, E2-E3 and E3-E3 pairs. More complex relationships between one E2 and multiple E3s representing different cellular pathways, as seen in *rad6Δ*, can be identified based on a partial overlap in differentially expressed genes.

Differentially expressed genes can be used for phenotypic characterisation of DUB mutants

DUBs are required for ubiquitin processing and the removal of ubiquitin moieties from substrates⁴⁰. None of the DUBs in *S. cerevisiae* are essential and most of them are not associated with any severe growth defects or phenotypes upon deletion under normal growth conditions⁴¹. Expression profiles were generated for 25 mutants with deletions of DUBs or DUB-associated genes, of which 13 mutants display significant gene expression changes (Figure 5A). Clustering of the expression profiles of the DUB mutants shows that the responding genes cluster in separate blocks, which were systematically analysed using GO enrichment analysis. Each block of co-expressed genes is enriched for different GO terms, which are indicative for the cellular pathways affected by the deletion (Figure 5A).

Correlation analysis shows that some DUB mutants correlate highly with each other, reflecting that these deletions are part of the same protein complex or cellular pathway (Figure 5B). For example, the expression profile of *ubp8Δ* correlates with *sgf11Δ*, *sgf73Δ* and *sus1Δ*. The DUB Ubp8 and

the associated factors Sgf11, Sgf73 and Sus1 form a protein module in the transcription regulator complex SAGA/SLIK with a role in histone deubiquitination⁴². Deletion of *UBP8* or *SGF11* however only affects a small number of genes (Figure 5C), suggesting a minor role in global gene transcription, separate from the other submodules of the complex²⁵. A second example of correlated DUB mutants whose deleted genes have a shared function in one DUB complex are *ubp3Δ* and *bre5Δ* (Figure 5D). Ubp3 is a ubiquitin protease that forms a heterotetrameric deubiquitinating protein complex with its cofactor Bre5^{43,44}. A third group of highly correlated mutants is *ubp13Δ*, *ubp15Δ* and *ecm30Δ*. Ubp15 is a poorly characterised deubiquitinating enzyme⁴⁵. Previously, we have shown that Ubp15 interacts physically with Ecm30, a protein with a putative role in cell wall biosynthesis^{27,46}. The expression profiles of *ubp15Δ* and *ecm30Δ* correlate well (Figure 5B), as expected for mutants with deletions of the same protein complex. Strikingly, a large part of the changed genes observed in *ubp15Δ* and *ecm30Δ* are also identified in *ubp13Δ* (Figure 5E). This suggests that Ubp13, Ubp15 and Ecm30 have a shared function in the same cellular pathway or protein complex. To characterise the putatively shared *in vivo* function of Ubp13, Ubp15 and Ecm30, the differentially expressed genes of the deletion mutants were analysed for GO enrichment. All three mutants show enrichment for GO 'cellular amino acid process' (Figure 5E), which may indicate a defect in ubiquitin-dependent trafficking of certain amino acid receptors. It also demonstrates that the differentially expressed genes can be used for phenotypic characterisation of mutants and that this approach gives insights in the potential underlying cellular defects.

Functional characterisation of the Ubp3/Bre5 ubiquitin protease complex

The transcription responses of some mutants are enriched for multiple GO terms (Figure 5A). In these cases, the deletion is likely to disrupt multiple cellular pathways. This is for instance the case in

ubp3Δ and *bre5Δ*. Ubp3/Bre5 is a versatile ubiquitin protease complex that is involved in transcription, response to osmotic stress, the pheromone response pathway, vesicular transport, and ribophagy^{43,46-53}. The expression patterns of *ubp3Δ* and *bre5Δ* were further dissected in order to investigate the functions of Ubp3/Bre5. Deletion of *ubp3Δ* or *bre5Δ* results in the differential expression of 200 and 93 genes respectively (Figure 5D). The affected genes are enriched for cellular processes related to cell wall, reproduction, transport and small molecule metabolic process. Among the genes involved in transport, several genes of the ER-Golgi secretory pathway are identified, which agrees with the role of Ubp3/Bre5 in anterograde and retrograde transport between the ER and Golgi (Figure 6A). Currently, two substrates of Ubp3/Bre5 have been identified in this pathway, namely the COPII protein Sec23 and the COPI protein Sec27^{43,52}. Strikingly, several genes that encode COPI and COPII vesicle coat proteins transcriptionally respond to *UBP3* or *BRE5* disruption, including the substrate-encoding genes *SEC23* and *SEC27* (Figure 6A). The genes are downregulated, suggesting that the cell represses the ER-Golgi secretory pathway due to accumulation of ubiquitinated Sec23 and Sec27 upon loss of Ubp3/Bre5 function.

Ubp3Δ and *bre5Δ* also display downregulation of genes involved in late and post-Golgi vesicular transport. This may be an indirect response of the cell to the ER-Golgi transport defect and the consequential missorting of proteins in downstream vesicular transport pathways. Alternatively, this downregulation may reflect the existence of additional unidentified substrates of Ubp3/Bre5 in the late or post-Golgi vesicular transport pathways. Other cellular processes that are found to respond to *UBP3* or *BRE5* deletion are ERAD and translation (Figure 6A). *Ubp3Δ*, and not *bre5Δ*, displays induction of genes involved in protein folding and ERAD, which potentially indicates a Bre5-independent function of Ubp3. *Ubp3Δ* also displays downregulation of ribosomal protein genes, which may be related to a defect in ribophagy (Kraft

et al, 2008). Strikingly, a large number of tRNA synthetases are repressed in expression in *ubp3Δ* and to a lesser extent in *bre5Δ* (Figure 6A). We therefore hypothesise a function for Ubp3/Bre5 in protein translation, possibly by targeting the tRNA synthetase system.

Functional interactions across systems: signalling between the ubiquitination and phosphorylation systems

Previously, a collection of expression profiles of kinase and phosphatase deletion mutants was generated under the same condition as this study²⁴. The availability of these expression profiles allows an investigation of additional regulatory interactions between the phosphorylation and the ubiquitination system. An example includes the interactions between the DUB Ubp3 and mitogen-activated protein kinases (MAPKs). The activity of Ubp3 is under the regulatory control of the Hog1 MAPK. During osmotic stress, Ubp3 is phosphorylated by Hog1 and is recruited to osmoreponsive genes where it modulates the transcriptional response to osmotic stress⁵⁰. Ubp3 is also involved in deubiquitination of another MAPK kinase, namely Ste7 (MAPKK), which is part of the pheromone response pathway. Deletion of *UBP3* results in accumulation of polyubiquitinated Ste7 upon pheromone treatment and increases Ste7 protein stability, indicating that Ubp3 promotes ubiquitin-dependent degradation of Ste7⁵¹. These interactions are reflected in the overlaps between the corresponding expression profiles (Figure 6B). Alignment of the expression profiles of *ubp3Δ* and *bre5Δ* to those of the MAPK deletion mutants shows an overlap that encompasses the pheromone response genes, confirming the role of Ubp3/Bre5 in the pheromone response pathway. The pheromone response genes are upregulated in *ubp3Δ* and *bre5Δ*, but also in the Hog1 pathway mutants *ssk2Δ* (MAPKKK), *pbs2Δ* (MAPKK) and *hog1Δ* (MAPK), which agrees with Ubp3 being a downstream target of Hog1 (Figure 6B and 6C). The same genes are downregulated in the pheromone response pathway mutants *ste20Δ*, *ste11Δ*

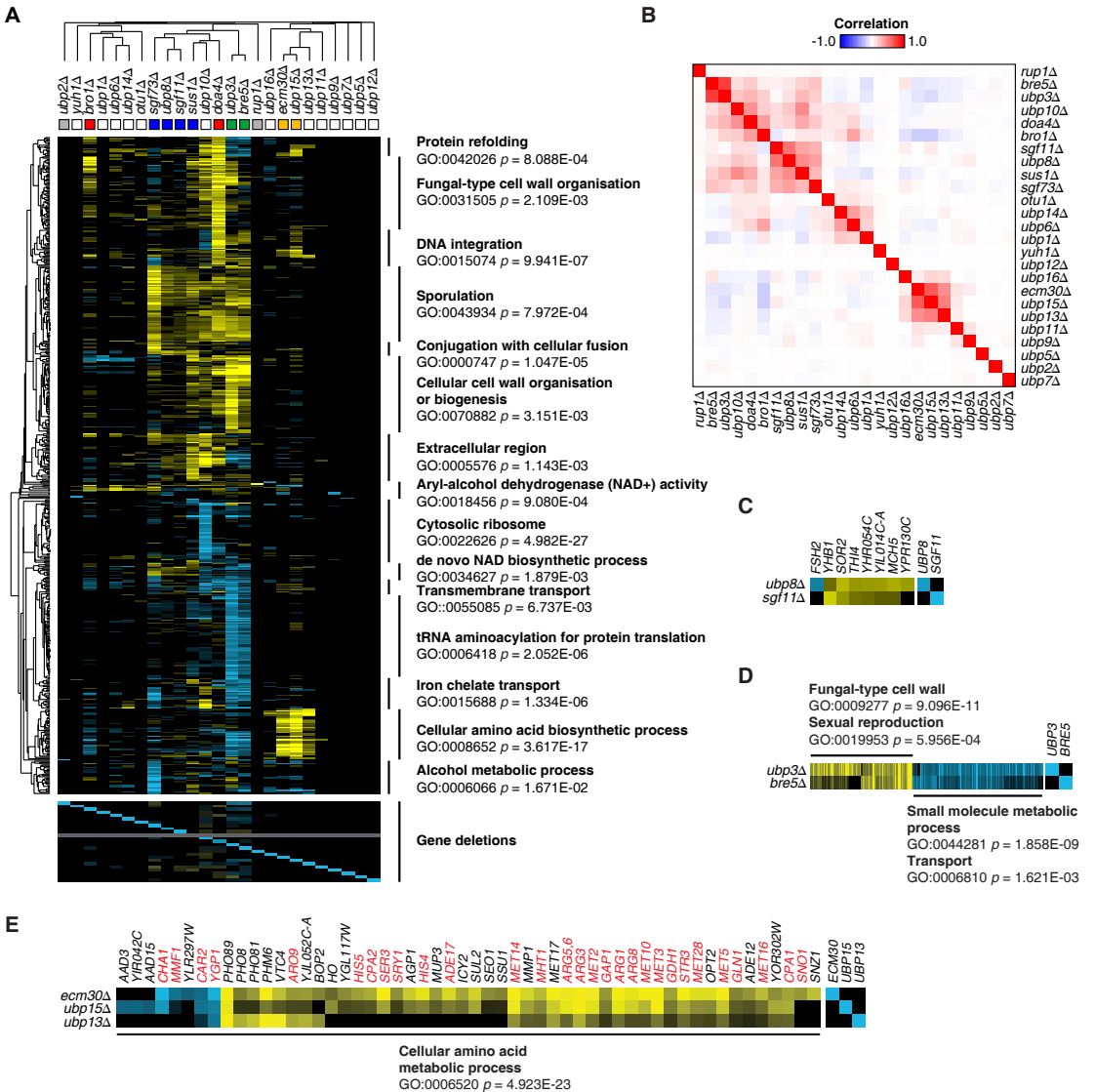
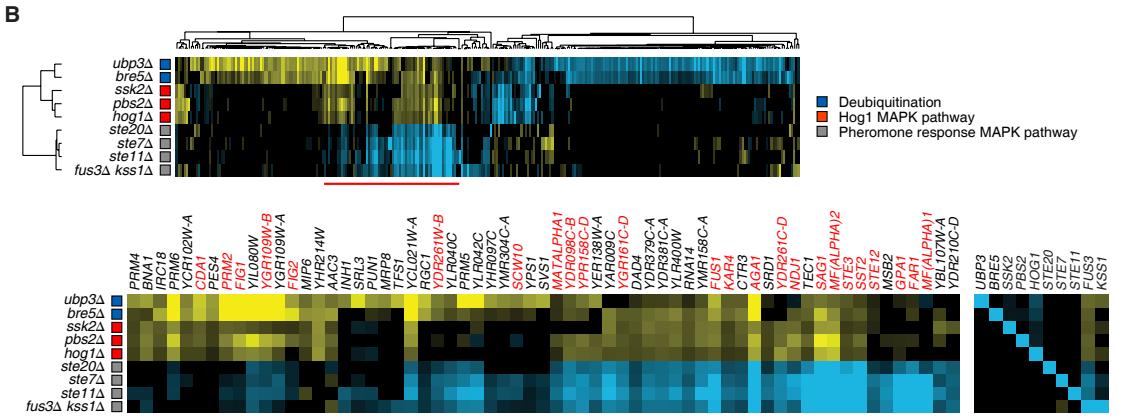
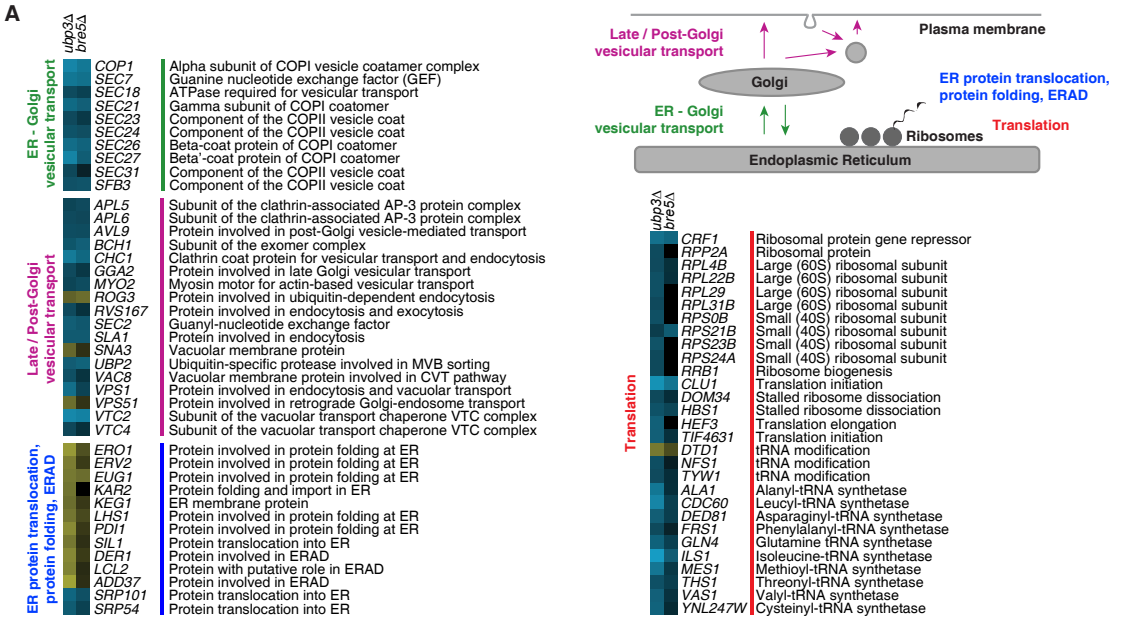
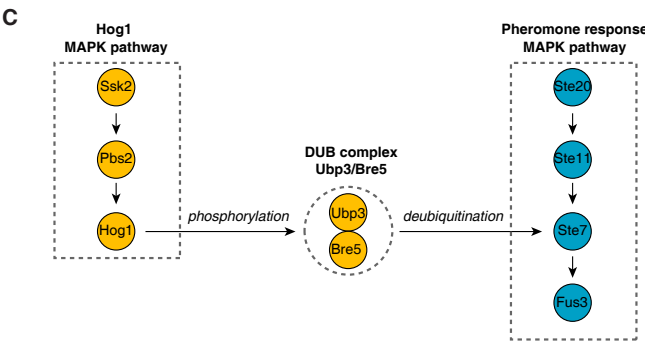


Figure 5. Functional characterisation of expression signatures in DUB mutants.

(A) Heatmap and cluster diagram of the expression profiles of DUB(-associated) deletion mutants. Gene products with physical protein interactions between are colour-coded (red: Doa4-Bro1; blue: SAGA complex; green: Ubp3-Bre5; grey: Ubp2-Rup1; yellow: Ubp15-Ecm30). The heatmap displays all genes that change significantly ($FC > 1.7, p < 0.05$) at least once in any mutant. Co-expressed genes are functionally annotated using GO term enrichment analysis. Bottom panel shows the expression levels of the DUB(-associated) encoding genes, showing loss of expression in the respective deletion mutants. Note that *SUS1* is not represented on the microarray and therefore its transcript is displayed in grey. (B) Correlation matrix of the expression profiles of all DUB(-associated) deletion mutants, shown in A. (C) Heatmap of the expression profiles of the DUB mutant *ubp8Δ* and *sgf11Δ*. Note that *sgf11Δ* has a weak expression phenotype that is below our significance cut-off (< 5 significant transcripts). (D) Heatmap of the expression profiles of the DUB mutant *ubp3Δ* and the DUB-associated mutant *bre5Δ*. GO terms associated with either up- or downregulated transcripts are indicated. (E) Heatmap and cluster diagram of the gene expression profiles of the DUB(-associated) mutants *ecm30Δ*, *ubp15Δ* and *ubp13Δ*. Transcripts associated to GO 'cellular amino acid metabolic process' are indicated in red.



Reproduction
 GO:0000003 $p = 1.442E-10$



(MAPKKK), *ste7* Δ (MAPKK) and *fus3* Δ *kss1* Δ (MAPK). Deletion of the substrate *STE7* is expected to have the opposite effect compared to deletion of *UPB3* where *Ste7* is stabilised. This example demonstrates that the comparison of expression profiles across different systems is a potentially useful way of exploring regulatory relationships.

Functional interactions across systems: signalling between the urmylation and phosphorylation systems

Urmylation is the process of attachment of the ubiquitin-related modifier Urm1 to substrates. The components of the urmylation system are poorly characterised. The only enzyme implicated in this process in *S. cerevisiae* is the E1 activating enzyme Uba4¹³. Interestingly, several genes, including Elongator complex components, have been shown to modulate urmylated protein levels through an as yet undefined mechanism⁵⁴. Expression profiles were generated for all deletion mutants that are associated to the urmylation system or Elongator complex. All eleven mutants have a significant expression phenotype that upon clustering separate into three distinct phenotype groups (Fig. 7A). The expression profiles of *urm1* Δ and *uba4* Δ are very similar, as expected for mutants of the same cellular pathway. Urmylation has been linked to multiple biological processes, including the oxidative stress response, nitrogen-catabolite repression, TOR signalling, response to nutrients, budding, invasive growth and tRNA modification⁵⁴⁻⁵⁸. GO enrichment analysis agrees with some of the previously established

functions of urmylation, showing enrichment for GO 'oxidative-reduction process' in the downregulated genes and enrichment for 'cellular amino acid metabolic process' in the upregulated genes (Figure 7D).

Strikingly, the *urm1* Δ and *uba4* Δ expression profiles are virtually indistinguishable from those of the Elongator mutants *elp4* Δ and *elp6* Δ (Figure 7B), indicating a very close functional relationship. The other Elongator mutants *elp2* Δ , *elp3* Δ , *iki1* Δ and *iki3* Δ cluster separately and share their expression phenotype with *nsc2* Δ and *nsc6* Δ (Figure 7A). Both *Ncs2* and *Ncs6* have an unknown function in urmylation⁵⁴. Purification of the Elongator complex has revealed that it exists as a six-subunit complex with two modules of respectively *Elp2/Elp3/Iki3* and *Elp4/Elp6/Iki1*⁵⁹. Our expression profiles reflect the existence of the two modules and indicate that both modules have different functions. However, based on the overlap in expression responses, we propose that the *Iki1* subunit is likely to function with the *Elp2/Elp3/Iki3* module, rather than with *Elp4/Elp6* (Figure 7A). Possibly, *Iki1* may function to anchor the *Elp2/Elp3/Iki3* submodule to the entire complex.

Three other mutants were identified in our collection of expression profiles that correlated with the above mentioned Elongator subunits: *kti12* Δ , *sit4* Δ and the double deletion mutant *sap185* Δ *sap190* Δ (Figure 7B). *Kti12* is a known interactor of Elongator⁶⁰. *Sit4* is the catalytic subunit of a PP2A phosphatase, whose specificity depends on other *Sit4*-associated proteins (*SAP*; *Sap4*, *Sap155*, *Sap185*, *Sap190*). The redundant *Sap185* and *Sap190*

Figure 6. Cellular processes affected in *ubp3* Δ and *bre5* Δ are identified by expression profiling and reveal regulatory interactions with MAP kinases.

(A) *Ubp3* Δ and *bre5* Δ show changed expression of genes involved in ER-Golgi vesicular transport, late/post Golgi vesicular transport, ER protein translocation, protein folding, ERAD and translation. Upper right panel shows a schematic representation of the affected cellular processes, with the colours relating to the specific groups of transcripts. The transcripts are a subset of all genes affected in *ubp3* Δ and *bre5* Δ , and are differentially expressed in one or both mutants (FC > 1.5, $p < 0.01$). (B) Expression phenotype comparison of *ubp3* Δ , *bre5* Δ and MAP kinase deletion mutants of the Hog1 and pheromone response MAPK pathways. The heatmap displays all genes that change significantly (FC > 1.7, $p < 0.05$) at least once in any mutant. The differentially expressed genes of the MAPK mutants are functionally enriched for reproduction and overlap with a subset of the genes affected in *ubp3* Δ and *bre5* Δ . Genes associated to GO 'reproduction' are indicated in red. (C) Schematic representation of the regulatory interactions between *Ubp3/Bre5* and the Hog1 and pheromone MAP kinase pathway components. The components are colour-coded based on the (partial) similarity in expression phenotype upon deletion, as shown in B.

subunits coordinate the specificity of Sit4 towards Elongator for dephosphorylation of Iki3⁶¹. The other SAP subunits target different cellular pathways. This agrees with our observations that the expression profile of *sap185Δ sap190Δ* correlates better with Elongator deletion mutants than *sit4Δ*, since the expression profile of *sit4Δ* includes the loss of all

parallel SAP pathways (Figure 7B). The expression profile of *sit4Δ* can partially be explained as the merge of the expression patterns seen in *sap155Δ* and *sap185Δ sap190Δ*, reflecting inactivation of at least two parallel cellular pathways (Figure 7C). *Sap4Δ*, *sap185Δ* and *sap190Δ* have no or a weak expression phenotype (Figure 7C), which agrees

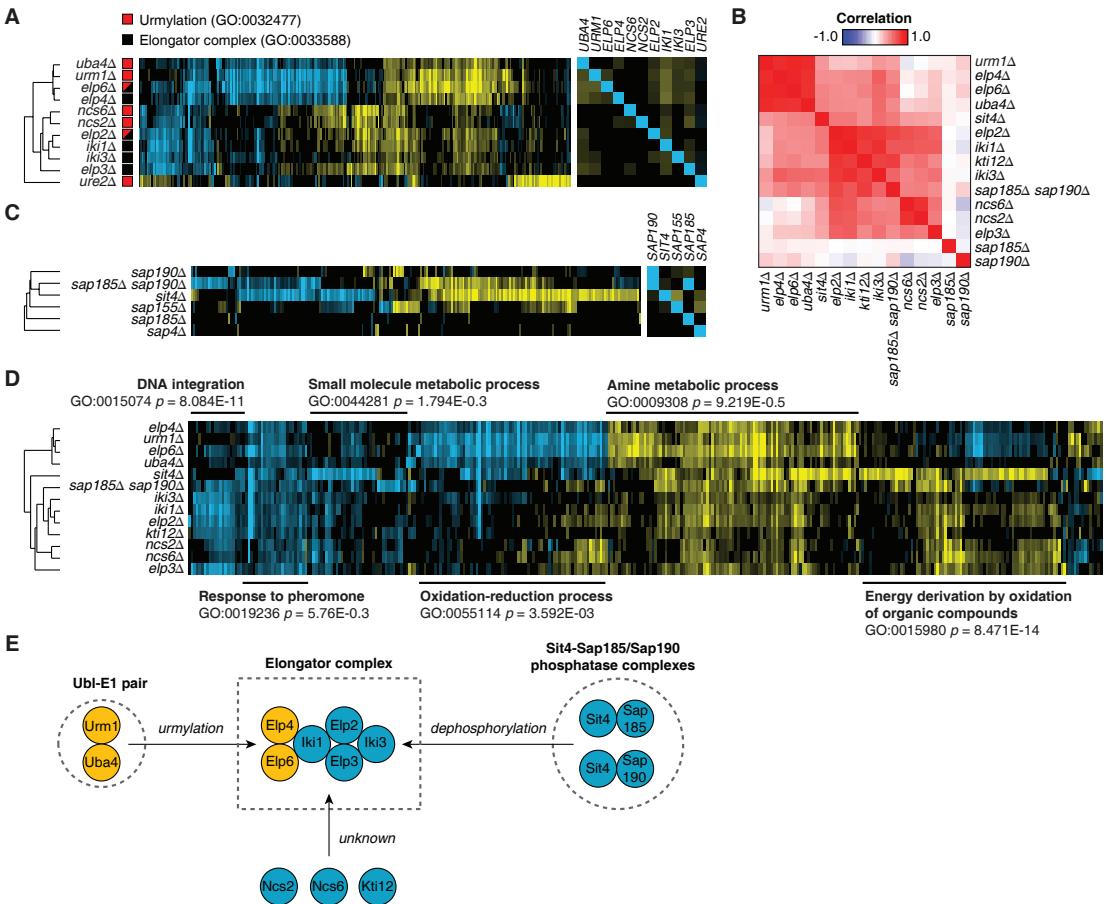


Figure 7. Expression patterns in mutants indicate regulatory control of the Elongator complex via the urmylation and phosphorylation systems.

(A) Expression profiles of deletion mutants implicated in urmylation or Elongator complex function. The heatmap displays all genes that change significantly ($FC > 1.7$, $p < 0.05$) at least once in any mutant. (B) Correlation matrix of the expression profiles shown in A. (C) Expression profiles of PP2A phosphatase subunit deletion mutants. *SIT4* is the catalytic phosphatase subunit. *SAP4*, *SAP155*, *SAP185* and *SAP190* encode the regulatory subunits of PP2A. The heatmap displays all genes that change significantly ($FC > 1.7$, $p < 0.05$) at least once in any mutant. (D) Expression phenotype comparison of mutants with gene deletions implicated in urmylation, Elongator and PP2A (Sit4-Sap185/190) function. The heatmap displays all genes that change significantly ($FC > 1.7$, $p < 0.05$) at least once in any mutant. Differentially expressed genes are functionally annotated using GO enrichment analysis. (E) Schematic representation of the regulatory interactions between the Elongator complex, urmylation components and the Sit4/Sap185 and Sit4/Sap190 phosphatase complexes. The components are colour-coded based on the (partial) similarity in expression phenotype upon deletion, as shown in D.

with redundancy effects among the SAP subunits⁶². The close functional relationships between Elongator and the Sit4/Sap185 and Sit4/Sap190 phosphatases is preserved in the expression profiles (Figure 7D). It reflects that the functional Elongator module Elp2/Elp3/Iki1/Iki3 is downstream of the Sit4/Sap185 and Sit4/Sap190 phosphatases. Although speculative, extrapolation of this observation to the urmylation components Urm1 and Uba4, suggests that the Elp2/Elp4 module is targeted by the urmylation system as these deletion mutants resemble each other most (Figure 7D and 7E).

Concluding remarks

The ubiquitin and ubiquitin-like systems consist of complex regulatory pathways that involve many proteins. This study describes the phenotypes of ubiquitin(-like) system mutants at the level of mRNA expression. In almost half of the cases we observe highly specific transcriptional responses upon gene disruption. The number of potential phenotypes can be increased, for instance by including double mutants for redundant genes, including point mutants for essential genes or by altering growth conditions. The annotation of mutants to have an expression phenotype is based on an arbitrary threshold of significant genes. There are many examples of mutants not mentioned here with minor expression phenotypes below the significance cut-off. These phenotypes have been ignored here, but are still interesting for future studies. Detailed analysis of the individual mutant profiles demonstrates that the differentially expressed genes are highly informative about the disrupted cellular responses, which provides many possibilities for future functional experiments to uncover new gene function.

Each mutant expression profile can be regarded as the transcription response to disruption of one or more cellular pathways. Mutants that share phenotypes in terms of expression are likely to take part in the same cellular pathway. This can either be based on completely overlapping profiles or on a subset of transcripts. Future challenges lie in the

interpretation of the expression data in terms of functional regulatory interactions. While predictions on interactions can be made based on overlap in phenotype, it is difficult to establish at what level these functional interactions may take place. The examples in this study show that these range from direct physical interactions such as protein complex components and enzyme-substrate interactions to components that indirectly take part in the same cellular pathway. These established interactions are needed as benchmark for interpretation of unknown regulatory interactions. Valuable information about epistatic relationships between genes can be obtained by analysing double mutants. The increasing amount of available expression data from other sources and the availability of double mutants from high-throughput synthetic genetic interaction screens will therefore contribute to a better understanding of the entire network of ubiquitin and ubiquitin-like system components.

MATERIALS and METHODS

Yeast strains

All yeast strains are isogenic to S288c (BY4742; MAT α *his3 Δ 1 leu2 Δ lys2 Δ lys2 Δ ura3 Δ*). Strains are from the *Saccharomyces* Genome Deletion libraries of Open Biosystems (Huntsville, USA) and Euroscarf (Frankfurt, Germany). Yeast strains and genotypes are listed in Supplementary Table S4. Technical issues with strains from the commercial collections, such as aneuploidy, no downregulation of the deleted gene or deletion of the wrong gene, were occasionally encountered. In these cases, the strains were remade by PCR-based gene disruption using the pFA6a-KanMX6 or pFA6aNatMX6 deletion cassettes in the genetic background of the wt parental strain BY4742 and reprofiled⁶³.

Yeast growth for expression profiling

Yeast growth was performed as described previously (ArrayExpress accession P-UMCU-36)^{24,25}. Strains were streaked from -80°C stocks onto plates and grown for 3-5 days depending on growth rate. Liquid cultures were inoculated with independent colonies and grown overnight in Synthetic Complete (SC) medium: 2 g/L Drop-out mix Complete and 6.71 g/L Yeast Nitrogen Base without AA, Carbohydrate & w/ AS (YNB) from US Biologicals (Swampscott, USA) with 2% D-glucose. Overnight cultures were diluted to an OD₆₀₀ of 0.15 in 60 ml medium in 250 ml Erlenmeyer flasks and grown at 30°C, 230 rpm in a shaking incubator. Growth curves were made for the mutant cultures (two cultures from two isolates)

as well as for two wt inoculates, grown in parallel. Mutant and wt cells were harvested in mid-log phase at an OD_{600} of 0.6 by centrifugation for 3 min at 4000 rpm. Pellets were frozen immediately in liquid nitrogen after removal of supernatant. During the course of this study, the protocol for yeast growth was optimised to grow more mutants on the same day in a less labour intensive way. A slightly different protocol for yeast growth was thus used for the mutants *bur2Δ*, *eps1Δ*, *mms1Δ*, *mms22Δ*, *nam7Δ*, *nmd2Δ*, *rtt107Δ* and *upf3Δ*, which were grown in a Tecan plate reader (ArrayExpress accession P-UMCU-50). This protocol differed in culture volume, equipment and used an automated method for RNA purification. Overnight cultures were diluted to an OD_{600} of 0.15 in 1.5 ml medium and grown at 30°C in a 24-well plate in a Tecan Infinite F200 under continuous shaking. Mutant and wt cells were harvested in mid-log phase at an OD_{600} of 0.6 by centrifugation for 3 min at 6100 rpm. Detailed comparative analysis of the same mutants grown with both protocols revealed no difference in expression²⁵.

RNA extraction and purification

RNA was isolated as described previously^{24,25}. In brief, frozen cells (-80°C) were resuspended in 500 μ l Acid Phenol Chloroform (Sigma, 5:1, pH 4.7). Equal volume of TES-buffer (TES: 10 mM Tris pH 7.5, 10 mM EDTA, 0.5% SDS) was added. Samples were vortexed for 20 seconds and incubated 10 min at 65°C and vortexed again, followed by 50 min incubation in a thermomixer at 65°C, 1400 rpm. Samples were centrifuged for 20 min at 14000 rpm at 4°C. Phenol extraction was repeated once, followed by a Chloroform:Isoamyl-alcohol (25:1) extraction. RNA was precipitated with sodium acetate (3 M, pH 5.2) and ethanol (96%, -20°C). The pellet was washed with ethanol and dissolved in Milli-Q water, snapfrozen and stored at -80°C. Phenol extracted total RNA from mutants grown in Erlenmeyer flasks was cleaned up using Qiagen's RNAeasy kit. RNA purification of total RNA from mutants grown in the Tecan plate reader was performed on a customised Sciclone ALH 3000 Workstation (Caliper LifeSciences) that included a PCR PTC-200 (Bio-Rad Laboratories), SpectraMax 190 spectrophotometer (Molecular Devices) and a magnetic bead-locator (Beckman) (ArrayExpress accession P-UMCU-37 and P-UMCU-51).

RNA amplification, labelling and hybridisation

RNA was amplified and labelled as described before^{24,25}. In the course of this study, the protocol was changed from a manual procedure (ArrayExpress accession P-UMCU-7) to an automated, robotic procedure in a 96-wells plate (4titude, Bioke) on a customised Sciclone ALH 3000 Workstation (Caliper LifeSciences) that included a PCR PTC-200 (Bio-Rad Laboratories), SpectraMax 190 spectrophotometer (Molecular Devices) and a magnetic bead-locator (Beckman) (ArrayExpress accession P-UMCU-38). RNA was hybridised on two-channel DNA microarrays containing 70-mer oligonucleotides from the Operon Array-Ready Oligo Set (Operon Biotechnologies, Huntsville, USA) (ArrayExpress accession A-UMCU-10). RNA isolated from a single, large

culture of wt yeast was used as common reference. This reference was used in one of the channels for each hybridisation and used in the statistical analysis to obtain an average expression profile for each deletion mutant relative to the wt. Per mutant, two independent cultures were hybridised on two separate microarrays (ArrayExpress accession P-UMCU-39). For the first hybridisation the Cy5 (red) labelled cRNA from the deletion mutant was hybridised together with the Cy3 (green) labelled cRNA from the common reference. For the replicate hybridisation, the labels were swapped. Each gene probe is represented twice on the microarray, resulting in four measurements per mutant. In addition, the array contains 2838 control features for external control normalisation and quality control⁶⁴. Slides were scanned using a G2565AA scanner (Agilent, California, USA) at 100% laser power and 30% PMT (ArrayExpress accession P-UMCU-40). After scanning, the intensities for the Cy5 (Red) and Cy3 (Green) channels were automatically extracted using the batch-processing module in ImaGene 8.0.1 (Biodiscovery, California, USA) (ArrayExpress accession P-UMCU-42). Hybridisation quality control was performed as described previously²⁵.

Data normalisation, statistical analysis and data analysis

Microarray data normalisation was performed on mean intensity values using a print-tip LOESS algorithm (*marray* R package version 1.20.0), using no background subtraction, a window span of 0.4 and excluding genes with (nearly) saturated signals (i.e. mean intensity $> 2^{15}$) for the LOESS curve estimation⁶⁵. Normalised data was corrected for gene-specific dye bias effects (*dyebias* R package version 1.4.3)⁶⁶. For each mutant the replicate hybridisations were compared to wt cultures grown on the same day to assess day-to-day variance and compared to a pool of 200 wt replicates grown throughout the project (ArrayExpress accession E-TABM-773 and E-TABM-984) through a common reference. *P*-values were obtained (*limma* R package version 2.12.0) after Benjamini-Hochberg FDR correction⁶⁷. Genes were considered significantly changed when the fold change (FC) was > 1.7 and the *p*-value < 0.05 . A set of 58 genes that changes frequently irrespective of the targeted deletion and in the collection of wt profiles (wt variable genes) was excluded from further downstream analysis²⁵. Unsupervised clustering of the microarray expression profiles was performed using the cosine correlation, including all genes with $FC > 1.7$ and $p < 0.05$ that changed expression at least once in any mutant, after replacing insignificant genes ($p > 0.05$) with zero and excluding wt variable genes and deleted genes. Correlation matrices are based on all significant genes with $p < 0.05$ in at least once in any mutant and after replacement of insignificant genes ($p > 0.05$) with zero and excluding wt variable genes and deleted genes. The data is visualised using JavaTreeview⁶⁸. Enrichment analysis of GO terms was performed on significant genes ($FC > 1.7$, $p < 0.05$), excluding wt variable genes and deleted genes⁶⁹. The background gene population was set to 6,182 (the number of genes represented on the microarray) and *p*-values are Bonferroni-corrected for multiple testing.

ACKNOWLEDGEMENTS

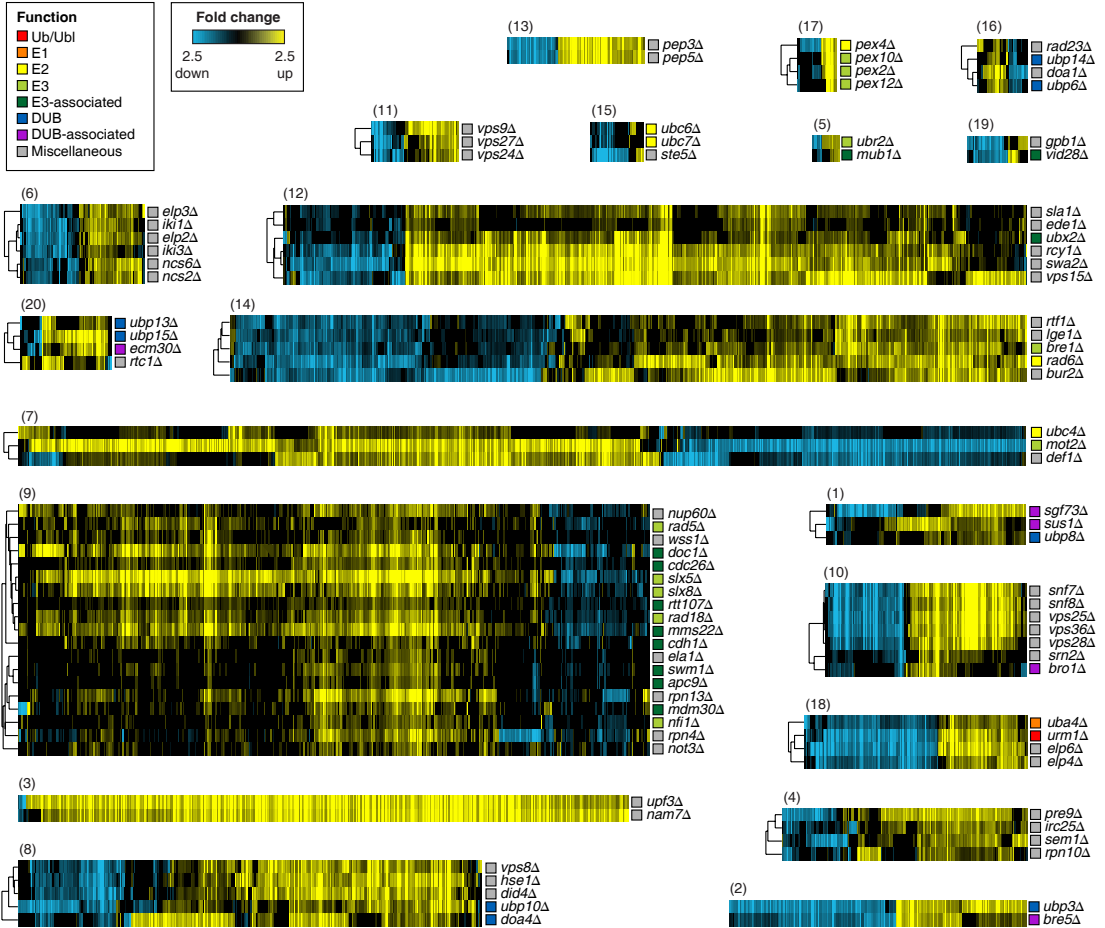
We thank Eva Apweiler, Nathalie Brabers and Joris Benschop for contributing microarray data; Cheuk Ko for technical assistance; Patrick Kemmeren, Sander van Hooff, Philip Lijnzaad and Katrin Sameith for bioinformatics.

REFERENCES

1. Ciechanover, A., Heller, H., Elias, S., Haas, A. L. & Hershko, A. ATP-dependent conjugation of reticulocyte proteins with the polypeptide required for protein degradation. *Proc. Natl. Acad. Sci. U.S.A.* **77**, 1365–1368 (1980).
2. Wilkinson, K. D., Urban, M. K. & Haas, A. L. Ubiquitin is the ATP-dependent proteolysis factor I of rabbit reticulocytes. *J. Biol. Chem.* **255**, 7529–7532 (1980).
3. Pickart, C. M. Mechanisms underlying ubiquitination. *Annu. Rev. Biochem.* **70**, 503–533 (2001).
4. Welchman, R. L., Gordon, C. & Mayer, R. J. Ubiquitin and ubiquitin-like proteins as multifunctional signals. *Nat. Rev. Mol. Cell Biol.* **6**, 599–609 (2005).
5. Kerscher, O., Felberbaum, R. & Hochstrasser, M. Modification of proteins by ubiquitin and ubiquitin-like proteins. *Annu. Rev. Cell Dev. Biol.* **22**, 159–180 (2006).
6. Ikeda, F. & Dikic, I. Atypical ubiquitin chains: new molecular signals. 'Protein Modifications: Beyond the Usual Suspects' review series. *EMBO Rep.* **9**, 536–542 (2008).
7. Hochstrasser, M. Origin and function of ubiquitin-like proteins. *Nature* **458**, 422–429 (2009).
8. Matunis, M. J., Coutavas, E. & Blobel, G. A novel ubiquitin-like modification modulates the partitioning of the Ran-GTPase-activating protein RanGAP1 between the cytosol and the nuclear pore complex. *J. Cell Biol.* **135**, 1457–1470 (1996).
9. Mahajan, R., Delphin, C., Guan, T., Gerace, L. & Melchior, F. A small ubiquitin-related polypeptide involved in targeting RanGAP1 to nuclear pore complex protein RanBP2. *Cell* **88**, 97–107 (1997).
10. Liakopoulos, D., Doenges, G., Matuschewski, K. & Jentsch, S. A novel protein modification pathway related to the ubiquitin system. *EMBO J.* **17**, 2208–2214 (1998).
11. Mizushima, N. *et al.* A protein conjugation system essential for autophagy. *Nature* **395**, 395–398 (1998).
12. Ichimura, Y. *et al.* A ubiquitin-like system mediates protein lipidation. *Nature* **408**, 488–492 (2000).
13. Furukawa, K., Mizushima, N., Noda, T. & Ohsumi, Y. A protein conjugation system in yeast with homology to biosynthetic enzyme reaction of prokaryotes. *J. Biol. Chem.* **275**, 7462–7465 (2000).
14. Dittmar, G. A. G., Wilkinson, C. R. M., Jedrzejewski, P. T. & Finley, D. Role of a ubiquitin-like modification in polarized morphogenesis. *Science* **295**, 2442–2446 (2002).
15. Desterro, J. M., Rodriguez, M. S. & Hay, R. T. SUMO-1 modification of I κ B α inhibits NF- κ B activation. *Mol. Cell* **2**, 233–239 (1998).
16. Hoegge, C., Pfander, B., Moldovan, G.-L., Pyrowolakis, G. & Jentsch, S. RAD6-dependent DNA repair is linked to modification of PCNA by ubiquitin and SUMO. *Nature* **419**, 135–141 (2002).
17. Uzunova, K. *et al.* Ubiquitin-dependent proteolytic control of SUMO conjugates. *J. Biol. Chem.* **282**, 34167–34175 (2007).
18. Lallemand-Breitenbach, V. *et al.* Arsenic degrades PML or PML-RAR α through a SUMO-triggered RNFA4/ubiquitin-mediated pathway. *Nat. Cell Biol.* **10**, 547–555 (2008).
19. Joazeiro, C. A. & Weissman, A. M. RING finger proteins: mediators of ubiquitin ligase activity. *Cell* **102**, 549–552 (2000).
20. Rotin, D. & Kumar, S. Physiological functions of the HECT family of ubiquitin ligases. *Nat. Rev. Mol. Cell Biol.* **10**, 398–409 (2009).
21. Hatakeyama, S. & Nakayama, K. I. U-box proteins as a new family of ubiquitin ligases. *Biochem. Biophys. Res. Commun.* **302**, 635–645 (2003).
22. Craig, K. L. & Tyers, M. The F-box: a new motif for ubiquitin dependent proteolysis in cell cycle regulation and signal transduction. *Prog. Biophys. Mol. Biol.* **72**, 299–328 (1999).
23. Kipreos, E. T. & Pagano, M. The F-box protein family. *Genome Biol.* **1**, REVIEWS3002 (2000).
24. van Wageningen, S. *et al.* Functional overlap and regulatory links shape genetic interactions between signaling pathways. *Cell* **143**, 991–1004 (2010).
25. Lenstra, T. L. *et al.* The specificity and topology of chromatin interaction pathways in yeast. *Mol. Cell* **42**, 536–549 (2011).
26. Mulder, K. W. *et al.* Modulation of Ubc4p/Ubc5p-mediated stress responses by the RING-finger-dependent ubiquitin-protein ligase Not4p in *Saccharomyces cerevisiae*. *Genetics* **176**, 181–192 (2007).
27. Benschop, J. J. *et al.* A consensus of core protein complex compositions for *Saccharomyces cerevisiae*. *Mol. Cell* **38**, 916–928 (2010).
28. Schubert, C. & Buchberger, A. Membrane-bound Ubx2 recruits Cdc48 to ubiquitin ligases and their substrates to ensure efficient ER-associated protein degradation. *Nat. Cell Biol.* **7**, 999–1006 (2005).
29. He, F., Brown, A. H. & Jacobson, A. Upf1p, Nmd2p, and Upf3p are interacting components of the yeast nonsense-mediated mRNA decay pathway. *Mol. Cell Biol.* **17**, 1580–1594 (1997).
30. Williams, C., van den Berg, M., Sprenger, R. R. & Distel, B. A conserved cysteine is essential for Pex4p-dependent ubiquitination of the peroxisomal import receptor Pex5p. *J. Biol. Chem.* **282**, 22534–22543 (2007).
31. Smith, J. J. & Aitchison, J. D. Regulation of peroxisome dynamics. *Curr. Opin. Cell Biol.* **21**, 119–126 (2009).
32. Breitling, R., Sharif, O., Hartman, M. L. & Krisans, S. K. Loss of compartmentalization causes misregulation of lysine biosynthesis in peroxisome-deficient yeast cells. *Eukaryotic Cell* **1**, 978–986 (2002).
33. Swanson, R., Locher, M. & Hochstrasser, M. A conserved ubiquitin ligase of the nuclear envelope/endoplasmic reticulum that functions in both ER-associated and Matalpha2 repressor degradation. *Genes Dev.* **15**, 2660–2674 (2001).
34. Biederer, T., Volkwein, C. & Sommer, T. Role of Cue1p in ubiquitination and degradation at the ER surface. *Science* **278**, 1806–1809 (1997).
35. Carvalho, P., Goder, V. & Rapoport, T. A. Distinct ubiquitin-ligase complexes define convergent pathways for the degradation of ER proteins. *Cell* **126**, 361–373 (2006).

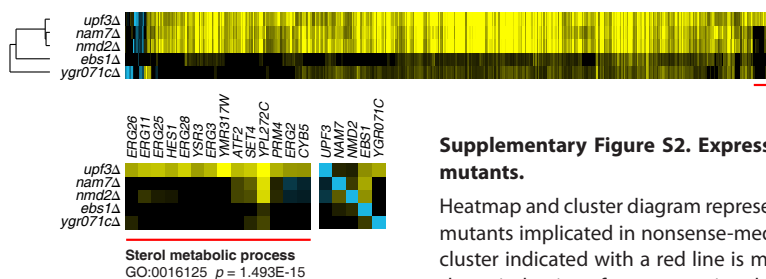
36. Seufert, W. & Jentsch, S. Ubiquitin-conjugating enzymes UBC4 and UBC5 mediate selective degradation of short-lived and abnormal proteins. *EMBO J.* **9**, 543–550 (1990).
37. Bailly, V., Lamb, J., Sung, P., Prakash, S. & Prakash, L. Specific complex formation between yeast RAD6 and RAD18 proteins: a potential mechanism for targeting RAD6 ubiquitin-conjugating activity to DNA damage sites. *Genes Dev.* **8**, 811–820 (1994).
38. Wang, L., Mao, X., Ju, D. & Xie, Y. Rpn4 is a physiological substrate of the Ubr2 ubiquitin ligase. *J. Biol. Chem.* **279**, 55218–55223 (2004).
39. Wood, A. *et al.* Bre1, an E3 ubiquitin ligase required for recruitment and substrate selection of Rad6 at a promoter. *Mol. Cell* **11**, 267–274 (2003).
40. Amerik, A. Y. & Hochstrasser, M. Mechanism and function of deubiquitinating enzymes. *Biochim. Biophys. Acta* **1695**, 189–207 (2004).
41. Amerik, A. Y., Li, S. J. & Hochstrasser, M. Analysis of the deubiquitinating enzymes of the yeast *Saccharomyces cerevisiae*. *Biol. Chem* **381**, 981–992 (2000).
42. Henry, K. W. *et al.* Transcriptional activation via sequential histone H2B ubiquitylation and deubiquitylation, mediated by SAGA-associated Ubp8. *Genes Dev.* **17**, 2648–2663 (2003).
43. Cohen, M., Stutz, F., Belgareh, N., Haguenuer-Tsapis, R. & Dargemont, C. Ubp3 requires a cofactor, Bre5, to specifically de-ubiquitinate the COPII protein, Sec23. *Nat. Cell Biol* **5**, 661–667 (2003).
44. Li, K., Ossareh-Nazari, B., Liu, X., Dargemont, C. & Marmorstein, R. Molecular basis for bre5 cofactor recognition by the ubp3 deubiquitylating enzyme. *J. Mol. Biol* **372**, 194–204 (2007).
45. Bozza, W. P. & Zhuang, Z. Biochemical characterization of a multidomain deubiquitinating enzyme ubp15 and the regulatory role of its terminal domains. *Biochemistry* **50**, 6423–6432 (2011).
46. Moazed, D. & Johnson, D. A deubiquitinating enzyme interacts with SIR4 and regulates silencing in *S. cerevisiae*. *Cell* **86**, 667–677 (1996).
47. Auty, R. *et al.* Purification of active TFIID from *Saccharomyces cerevisiae*. Extensive promoter contacts and co-activator function. *J. Biol. Chem* **279**, 49973–49981 (2004).
48. Kvint, K. *et al.* Reversal of RNA polymerase II ubiquitylation by the ubiquitin protease Ubp3. *Mol. Cell* **30**, 498–506 (2008).
49. Chew, B. S., Siew, W. L., Xiao, B. & Lehming, N. Transcriptional activation requires protection of the TATA-binding protein Tbp1 by the ubiquitin-specific protease Ubp3. *Biochem. J* **431**, 391–399 (2010).
50. Solé, C. *et al.* Control of Ubp3 ubiquitin protease activity by the Hog1 SAPK modulates transcription upon osmotic stress. *EMBO J* (2011).doi:10.1038/emboj.2011.227
51. Wang, Y. & Dohlman, H. G. Pheromone-dependent ubiquitination of the mitogen-activated protein kinase Ste7. *J. Biol. Chem* **277**, 15766–15772 (2002).
52. Cohen, M., Stutz, F. & Dargemont, C. Deubiquitination, a new player in Golgi to endoplasmic reticulum retrograde transport. *J. Biol. Chem* **278**, 51989–51992 (2003).
53. Kraft, C., Deplazes, A., Sohrmann, M. & Peter, M. Mature ribosomes are selectively degraded upon starvation by an autophagy pathway requiring the Ubp3p/Bre5p ubiquitin protease. *Nat. Cell Biol* **10**, 602–610 (2008).
54. Goehring, A. S., Rivers, D. M. & Sprague, G. F., Jr Urm1ylation: a ubiquitin-like pathway that functions during invasive growth and budding in yeast. *Mol. Biol. Cell* **14**, 4329–4341 (2003).
55. Goehring, A. S., Rivers, D. M. & Sprague, G. F., Jr Attachment of the ubiquitin-related protein Urm1p to the antioxidant protein Ahp1p. *Eukaryotic Cell* **2**, 930–936 (2003).
56. Rubio-Teixeira, M. Urm1ylation controls Nillp and Gln3p-dependent expression of nitrogen-catabolite repressed genes in *Saccharomyces cerevisiae*. *FEBS Lett* **581**, 541–550 (2007).
57. Noma, A., Sakaguchi, Y. & Suzuki, T. Mechanistic characterization of the sulfur-relay system for eukaryotic 2-thiouridine biogenesis at tRNA wobble positions. *Nucleic Acids Res.* **37**, 1335–1352 (2009).
58. Van der Veen, A. G. *et al.* Role of the ubiquitin-like protein Urm1 as a noncanonical lysine-directed protein modifier. *Proc. Natl. Acad. Sci. U.S.A* **108**, 1763–1770 (2011).
59. Krogan, N. J. & Greenblatt, J. F. Characterization of a six-subunit holo-elongator complex required for the regulated expression of a group of genes in *Saccharomyces cerevisiae*. *Mol. Cell. Biol* **21**, 8203–8212 (2001).
60. Petrakis, T. G., Søgaard, T. M. M., Erdjument-Bromage, H., Tempst, P. & Svejstrup, J. Q. Physical and functional interaction between Elongator and the chromatin-associated Kti12 protein. *J. Biol. Chem* **280**, 19454–19460 (2005).
61. Jablonowski, D., Täubert, J.-E., Bär, C., Stark, M. J. R. & Schaffrath, R. Distinct subsets of Sit4 holophosphatases are required for inhibition of *Saccharomyces cerevisiae* growth by rapamycin and zymocin. *Eukaryotic Cell* **8**, 1637–1647 (2009).
62. Luke, M. M. *et al.* The SAP, a new family of proteins, associate and function positively with the SIT4 phosphatase. *Mol. Cell. Biol* **16**, 2744–2755 (1996).
63. Longtine, M. S. *et al.* Additional modules for versatile and economical PCR-based gene deletion and modification in *Saccharomyces cerevisiae*. *Yeast* **14**, 953–961 (1998).
64. van de Peppel, J. *et al.* Monitoring global messenger RNA changes in externally controlled microarray experiments. *EMBO Rep.* **4**, 387–393 (2003).
65. Yang, Y. H. *et al.* Normalization for cDNA microarray data: a robust composite method addressing single and multiple slide systematic variation. *Nucleic Acids Res.* **30**, e15 (2002).
66. Margaritis, T. *et al.* Adaptable gene-specific dye bias correction for two-channel DNA microarrays. *Mol. Syst. Biol* **5**, 266 (2009).
67. Smyth, G. K., Michaud, J. & Scott, H. S. Use of within-array replicate spots for assessing differential expression in microarray experiments. *Bioinformatics* **21**, 2067–2075 (2005).
68. Saldanha, A. J. Java Treeview--extensible visualization of microarray data. *Bioinformatics* **20**, 3246–3248 (2004).
69. Ashburner, M. *et al.* Gene ontology: tool for the unification of biology. The Gene Ontology Consortium. *Nat. Genet* **25**, 25–29 (2000).
70. Ricarte, F. *et al.* A genome-wide immunodetection screen in *S. cerevisiae* uncovers novel genes involved in lysosomal vacuole function and morphology. *PLoS ONE* **6**, e23696 (2011).

SUPPLEMENTAL INFORMATION



Supplementary Figure S1. Expression phenotypes of mutants of ubiquitin and ubiquitin-like system components.

The heatmaps and cluster diagrams represent the expression profiles of 20 groups of mutants implicated in ubiquitin(-like) modification. The mutants are subdivided in groups (labelled 1-20), based on the cluster shown in Figure 2. Mutants are colour-coded according to their function. Each heatmap displays all genes that change significantly (FC > 1.7, $p < 0.05$) at least once in any mutant in that cluster. Fold change expression levels are indicated by the colour scale, with yellow for upregulation, blue for downregulation and black for no change.



Supplementary Figure S2. Expression phenotypes of NMD pathway mutants.

Heatmap and cluster diagram represent the expression profiles of deletion mutants implicated in nonsense-mediated mRNA decay (NMD). The gene cluster indicated with a red line is magnified in the bottom panel. *Upf3Δ* shows induction of genes associated to GO 'sterol metabolic process', which is likely independent of the NMD pathway. *YGR071C* is a gene of unknown function and is proposed to be involved in vacuolar protein processing⁷⁰. *YGR071C* may be a new NMD pathway member, based on the overlap in expression phenotype of *ygr071cΔ* with *upf3Δ*, *nam7Δ*, *nmd2Δ* and *ebs1Δ*.

Supplementary Table S1. Selection criteria of genes with a (putative) role in ubiquitin(-like) modification

GO term or protein domain ¹	Description	Associated genes ²	Expression profiles ³
<i>Molecular Function</i>			
GO:0019787	Small conjugating protein ligase activity	69 (89)	64
GO:0032182	Small conjugating protein binding	33 (43)	28
GO:0019783	Small conjugating protein-specific protease activity	19 (22)	19
GO:0004221	Ubiquitin thiolesterase activity	18 (19)	18
GO:0031386	Protein tag	7 (9)	5
GO:0008641	Small protein activating activity	4 (7)	3
GO:0019776	ATG8 ligase activity	4 (4)	3
<i>Cellular Component</i>			
GO:0000151	Ubiquitin ligase complex	45 (64)	41
GO:0000502	Proteasome complex	19 (50)	15
GO:0008180	Signalosome	6 (7)	6
GO:0033588	Elongator holoenzyme complex	6 (6)	8
<i>Biological Process</i>			
GO:0006511	Ubiquitin-dependent protein catabolic process	138 (195)	99
GO:0070647	Protein modification by small protein conjugation	111 (147)	103
GO:0043248	Proteasome assembly	15 (27)	9
<i>Domain</i>			
IPR001841	RING-type zinc finger domain	36 (40)	36
IPR001810	F-box domain	9 (11)	8
IPR000569	HECT domain	4 (5)	4
IPR004181	MIZ-type zinc finger domain	3 (4)	3
IPR003613	U-box domain	1 (2)	1
<i>Other⁴</i>		10 (10)	10
Total		277 (361)	224

¹GO terms related to ubiquitin(-like) modification are obtained from the AmiGO Gene Ontology (GO) project (www.amigo.geneontology.org). E3-specific protein domains are obtained from the InterPro (IPR) database (www.ebi.ac.uk/interpro/).

²Number of nonessential genes that is associated with at least one of the given GO terms or protein domains. Number in parentheses represents the total number of associated genes, including essential genes.

³Number of mutants with deletions of genes in the specified category for which microarray expression profiles were generated that passed all QC criteria.

⁴Ten genes categorised as 'Other' did not meet the GO term or protein domain criteria, but were included after manual curation of the gene list.

Supplementary Table S2. GO term classification of genes into distinct ubiquitin(-like) systems

Ubiquitin(-like) system	GO term	Description	Associated genes ¹	Expression profiles ²
Ubiquitination	GO:0016567	Protein ubiquitination	120 (149)	111
	GO:0016579	Protein deubiquitination		
	GO:0004839	Ubiquitin activating enzyme activity		
	GO:0004842	Ubiquitin-protein ligase activity		
	GO:0000151	Ubiquitin ligase complex		
Sumoylation	GO:0004221	Ubiquitin thiolesterase activity	8 (17)	8
	GO:0016925	Protein sumoylation		
	GO:0016926	Protein desumoylation		
	GO:0019948	SUMO activating enzyme activity		
Neddylation	GO:0019789	SUMO ligase activity	10 (12)	8
	GO:0045116	Protein neddylation		
	GO:0000338	Protein deneddylation		
	GO:0019781	NEDD8 activating enzyme activity		
Urmylation	GO:0019788	NEDD8 ligase activity	7 (7)	7
	GO:0032447	Protein urmylation		
	GO:0042292	URM1 activating enzyme activity		
Atg8/Atg12	GO:0042294	URM1 conjugating enzyme activity	8 (8) ³	7
	GO:0019776	Atg8 ligase activity		
	GO:0019777	Atg12 ligase activity		
	GO:0019778	APG12 activating enzyme activity		
Hub1	GO:0019779	APG8 activating enzyme activity	1 (1) ⁴	1
	GO:0042293	Hub1 activating enzyme		

¹Number of nonessential genes that is associated with at least one of the given GO terms. Number in parentheses represents the total number of GO associated genes, including essential genes.

²Number of mutants with deletions of genes in the specified ubiquitin(-like) system for which microarray expression profiles were generated that passed all QC criteria.

³Manually included *ATG4* and *ATG8*.

⁴Manually included *HUB1*.

Supplementary Table S3. Overview of all genes with a (putative) role in ubiquitin(-like) modification and their association with an expression phenotype upon deletion

Gene ¹	Systematic name ¹	System ²	Function ³	Domain ³	Viable ³	Factor value ⁴	Profile ⁵
<i>ACM1</i>	<i>YPL267W</i>	UB			yes	acm1-del	2
<i>ADD37</i>	<i>YMR184W</i>				yes		
<i>ADD66</i>	<i>YKL206C</i>				yes	add66-del	20
<i>AMA1</i>	<i>YGR225W</i>	UB	E3-ass.		yes	ama1-del; TI	1
<i>AOS1</i>	<i>YPR180W</i>	SUMO	E1		no		
<i>APC1</i>	<i>YNL172W</i>	UB	E3-ass.		no		
<i>APC2</i>	<i>YLR127C</i>	UB	E3-ass.		no		
<i>APC4</i>	<i>YDR118W</i>	UB	E3-ass.		no		
<i>APC5</i>	<i>YOR249C</i>	UB	E3-ass.		no		
<i>APC9</i>	<i>YLR102C</i>	UB	E3-ass.		yes	apc9-del	6
<i>APC11</i>	<i>YDL008W</i>	UB	E3	RING	no		
<i>ARC40</i>	<i>YBR234C</i>				no		
<i>ASI1</i>	<i>YMR119W</i>	UB	E3		yes	asi1-del	1
<i>ASI2</i>	<i>YNL159C</i>				yes	asi2-del	9
<i>ASI3</i>	<i>YNL008C</i>	UB	E3		yes	asi3-del	3
<i>ASR1</i>	<i>YPR093C</i>	UB	E3	RING	yes	asr1-del	1
<i>ATE1</i>	<i>YGL017W</i>				yes		
<i>ATG3</i>	<i>YNR007C</i>	APG	E2		yes	atg3-del	0
<i>ATG4</i>	<i>YNL223W</i>	APG	ULP		yes	atg4-del	1

Supplementary Table S3. Continued

Gene ¹	Systematic name ¹	System ²	Function ³	Domain ³	Viable ³	Factor value ⁴	Profile ⁵
ATG5	YPL149W	APG			yes	atg5-del	1
ATG6	YPL120W				yes		
ATG7	YHR171W	APG	E1		yes	atg7-del	1
ATG8	YBL078C	APG	modifier		yes	atg8-del	0
ATG10	YLL042C	APG	E2		yes	atg10-del; TI	4
ATG12	YBR217W	APG	modifier		yes	atg12-del	0
ATG14	YBR128C				yes		
ATG16	YMR159C	APG			yes		
ATG18	YFR021W				yes		
ATG19	YOL082W				yes		
BLM10	YFL007W				yes	TI	
BMH1	YER177W	UB			yes	bmh1-del	36
BMH2	YDR099W	UB			yes	bmh2-del	0
BRE1	YDL074C	UB	E3	RING	yes	bre1-del	129
BRE5	YNR051C	UB	DUB-ass.		yes	bre5-del	93
BRO1	YPL084W	UB	DUB-ass.		yes	bro1-del	26
BSD2	YBR290W				yes	bsd2-del	3
BST1	YFL025C				yes		
BUB3	YOR026W				yes	TI	
BUL1	YMR275C	UB	E3-ass.		yes	bul1-del	22
BUL2	YML111W	UB	E3-ass.		yes	bul2-del	0
BUR2	YLR226W	UB			yes	bur2-del	346
CDC4	YFL009W	UB			no		
CDC16	YKL022C	UB	E3-ass.		no		
CDC20	YGL116W	UB	E3-ass.		no		
CDC23	YHR166C	UB	E3-ass.		no		
CDC26	YFR036W	UB	E3-ass.		yes	cdc26-del	36
CDC27	YBL084C	UB	E3-ass.		no		
CDC31	YOR257W				no		
CDC34	YDR054C	UB	E2		no		
CDC36	YDL165W	UB	E3-ass.		no		
CDC48	YDL126C	UB	E3-ass.		no		
CDC53	YDL132W	UB	E3-ass.		no		
CDH1	YGL003W	UB	E3-ass.		yes	cdh1-del	19
CIC1	YHR052W				no		
CKS1	YBR135W				no		
CNE1	YAL058W				yes		
COP1	YDL145C				no		
CSI1	YMR025W	NEDD	ULP-ass.		yes	csi1-del	1
CSN9	YDR179C	NEDD	ULP-ass.		yes	csn9-del	1
CSN12	YJR084W				yes	csn12-del	1
CSR1	YLR380W				yes		
CST9	YLR394W	SUMO	E3	RING	yes	cst9-del	1
CUE1	YMR264W	UB	E3-ass.		yes	cue1-del	4
CUE2	YKL090W				yes	cue2-del	0
CUE3	YGL110C				yes	cue3-del	0
CUE4	YML101C				yes	cue4-del	0
CUE5	YOR042W				yes	cue5-del	2
CUL3	YGR003W	UB	E3		yes	cul3-del	0
CWC24	YLR323C			RING	no		
DAS1	YJL149W	UB	E3-ass.	F-box	yes	das1-del	0
DCN1	YLR128W	NEDD/UB	E3		yes	dcn1-del	0
DDI1	YER143W				yes	ddi1-del	0
DEF1	YKL054C				yes	def1-del	297
DER1	YBR201W	UB	E3-ass.		yes	der1-del	1
DFM1	YDR411C	UB	E3-ass.		yes		
DIA2	YOR080W	UB	E3-ass.	F-box	yes	TI	
DID4	YKL002W				yes	did4-del	144
DMA1	YHR115C	UB	E3	RING	yes	chf1-del	4
DMA2	YNL116W	UB	E3	RING	yes	chf2-del	0
DOA1	YKL213C				yes	doa1-del	30

Supplementary Table S3. Continued

Gene ¹	Systematic name ¹	System ²	Function ³	Domain ³	Viable ³	Factor value ⁴	Profile ⁵
DOA4	YDR069C	UB	DUB		yes	doa4-del	146
DOC1	YGL240W	UB	E3-ass.		yes	doc1-del; TI	176
DOG2	YHR043C				yes		
DON1	YDR273W				yes	don1-del	1
DSK2	YMR276W				yes	dsk2-del	0
DUF1	YOL087C				yes	duf1-del	3
EAR1	YMR171C				yes		
ECM29	YHL030W				yes	TI	
ECM30	YLR436C		DUB-ass.		yes	ecm30-del	28
EDE1	YBL047C				yes	ede1-del	22
ELA1	YNL230C	UB	E3-ass.	F-box	yes	ela1-del	9
ELC1	YPL046C	UB	E3-ass.		yes	elc1-del	4
ELP2	YGR200C	URM			yes	elp2-del	39
ELP3	YPL086C				yes	hpa1-del; TI	39
ELP4	YPL101W				yes	elp4-del	61
ELP6	YMR312W	URM			yes	elp6-del	132
EPS1	YIL005W				yes		
ESS1	YJR017C	UB			no		
ETP1	YHL010C			RING	yes	yh1010c-del	5
FAP1	YNL023C			RING	yes	fap1-del	0
FAR1	YJL157C			RING	yes	far1-del	0
FYV10	YIL097W		E3-ass.		yes		
GGA1	YDR358W				yes	gga1-del	1
GGA2	YHR108W				yes	gga2-del	6
GID7	YCL039W		E3-ass		yes		
GID8	YMR135C		E3-ass		yes		
GPB1	YOR371C	UB			yes	krh1-del	32
GRR1	YJR090C	UB	E3-ass.	F-box	yes	grr1-del	566
GTS1	YGL181W				yes	gts1-del	0
HLJ1	YMR161W				yes		
HRD1	YOL013C	UB	E3	RING	yes	hrd1-del	1
HRD3	YLR207W	UB	E3-ass.		yes	hrd3-del	0
HRT1	YOL133W	UB	E3	RING	no		
HRT3	YLR097C	UB	E3-ass.		yes	hrt3-del	0
HSC82	YMR186W				yes	hsc82-del	7
HSE1	YHL002W				yes	hse1-del	162
HSM3	YBR272C				yes	TI	
HSP82	YPL240C				yes	TI	
HUB1	YNR032C-A	HUB1	modifier		yes	hub1-del	0
HUL4	YJR036C	UB	E3	HECT	yes	hul4-del	1
HUL5	YGL141W	UB	E3	HECT	yes	hul5-del	1
IKI1	YHR187W				yes	iki1-del	36
IKI3	YLR384C				yes	iki3-del	24
IRC20	YLR247C			RING	yes	irc20-del	1
IRC25	YLR021W				yes	irc25-del	24
ITT1	YML068W			RING	yes	itt1-del	5
JEM1	YJL073W				yes	jem1-del	0
KAP95	YLR347C	SUMO			no		
KAR2	YLR034W				no		
LAG2	YOL025W	UB			no		
LCL2	YLR104W				yes		
LGE1	YPL055C	UB			yes	lge1-del	76
MAG2	YLR427W			RING	yes	mag2-del	1
MDM30	YLR368W	UB	E3-ass.	F-box	yes	mdm30-del	29
MDV1	YJL112W				yes		
MET30	YIL046W	UB	E3-ass.	F-box	no		
MFB1	YDR219C	UB	E3-ass.	F-box	yes	mfb1-del	4
MGS1	YNL218W				yes	mgs1-del	0
MMS1	YPR164W	UB	E3-ass.		yes	mms1-del	18
MMS2	YGL087C	UB	E2		yes	mms2-del	1
MMS21	YEL019C	SUMO	E3	RING	no		

Supplementary Table S3. Continued

Gene ¹	Systematic name ¹	System ²	Function ³	Domain ³	Viable ³	Factor value ⁴	Profile ⁵
MMS22	YLR320W	UB	E3-ass.		yes	mms22-del	155
MND2	YIR025W	UB	E3-ass.		yes	mnd2-del	1
MNL1	YHR204W				yes		
MNS1	YJR131W				yes		
MOT2	YER068W	UB	E3	RING	yes	not4-del	755
MUB1	YMR100W	UB	E3-ass.		yes	mub1-del	7
MVB12	YGR206W				yes	mvb12-del	2
NAM7	YMR080C	UB			yes	nam7-del	383
NAS2	YIL007C				yes	TI	
NAS6	YGR232W				yes	nas6-del	0
NCS2	YNL119W	URM			yes	ncs2-del	25
NCS6	YGL211W	URM			yes	ncs6-de	40
NFI1	YOR156C	SUMO	E3	RING	yes	nfi1-del	10
NOB1	YOR056C				no		
NOT3	YIL038C	UB	E3-ass.		yes	not3-del	18
NOT5	YPR072W	UB	E3-ass.		yes	TI	
NPL4	YBR170C	UB	E3-ass.		yes	TI	
NUP53	YMR153W	SUMO			yes	nup53-del	1
NUP60	YAR002W	SUMO			yes	nup60-del; TI	57
OTU1	YFL044C	UB	DUB		yes	otu1-del	1
PAN2	YGL094C				yes	pan2-del	0
PBA1	YLR199C	UB			yes	pba1-del	4
PBN1	YCL052C				no		
PCI8	YIL071C	NEDD	ULP-ass.		yes	pci8-del	0
PEP1	YBL017C				yes		
PEP3	YLR148W			RING	yes	pep3-del	92
PEP5	YMR231W			RING	yes	pep5-del	86
PEX2	YJL210W		E3	RING	yes	pex2-del	10
PEX4	YGR133W	UB	E2		yes	pex4-del	27
PEX10	YDR265W	UB	E3	RING	yes	pex10-del	12
PEX12	YMR026C		E3		yes	pex12-del	7
PIB1	YDR313C	UB	E3	RING	yes	pib1-del	0
PMT1	YDL095W				yes		
PMT2	YAL023C				yes		
POC4	YPL144W				yes	poc4-del	30
PRE1	YER012W				no		
PRE2	YPR103W				no		
PRE3	YJL001W				no		
PRE4	YFR050C				no		
PRE5	YMR314W				no		
PRE6	YOL038W				no		
PRE7	YBL041W				no		
PRE8	YML092C				no		
PRE9	YGR135W				yes	pre9-del	126
PRE10	YOR362C				no		
PRP19	YLL036C	UB	E3	U-box	no		
PSE1	YMR308C	SUMO			no		
PSH1	YOL054W	UB	E3	RING	yes	psh1-del	1
PTH2	YBL057C				yes	pth2-del	4
PUP1	YOR157C				no		
PUP2	YGR253C				no		
PUP3	YER094C				no		
RAD4	YER162C				yes	TI	
RAD5	YLR032W	UB	E3	RING	yes	rad5-del	31
RAD6	YGL058W	UB		E2	yes	rad6-del	264
RAD7	YJR052W	UB	E3-ass.		yes	rad7-del	2
RAD16	YBR114W	UB	E3-ass.	RING	yes	rad16-del	1
RAD18	YCR066W	UB	E3	RING	yes	rad18-del	64
RAD23	YEL037C				yes	rad23-del	8
RCY1	YJL204C			F-box	yes	rcy1-del	261
RFA1	YAR007C	UB			no		

Supplementary Table S3. Continued

Gene ¹	Systematic name ¹	System ²	Function ³	Domain ³	Viable ³	Factor value ⁴	Profile ⁵
RFA2	YNL312W	UB			no		
RFA3	YJL173C	UB			no		
RKR1	YMR247C	UB	E3	RING	yes	rkr1-del	1
RMD5	YDR255C	UB	E3		yes	rmd5-del	1
RPL40A	YIL148W	UB	modifier		yes		
RPL40B	YKR094C	UB	modifier		yes		
RPN1	YHR027C				no		
RPN2	YIL075C				no		
RPN3	YER021W				no		
RPN4	YDL020C				yes	rpn4-del	92
RPN5	YDL147W	NEDD			no		
RPN6	YDL097C				no		
RPN7	YPR108W				no		
RPN8	YOR261C				no		
RPN9	YDR427W				no		
RPN10	YHR200W				yes	rpn10-del	35
RPN11	YFR004W	UB	DUB		no		
RPN12	YFR052W				no		
RPN13	YLR421C				yes	rpn13-del	112
RPN14	YGL004C				yes	rpn14-del	0
RPS31	YLR167W		modifier		no		
RPT1	YKL145W				no		
RPT2	YDL007W				no		
RPT3	YDR394W				no		
RPT4	YOR259C				no		
RPT5	YOR117W				no		
RPT6	YGL048C				no		
RRI1	YDL216C	NEDD	ULP		yes	rri1-del	0
RRI2	YOL117W	NEDD	ULP-ass.		yes	rri2-del	1
RSP5	YER125W	UB	E3	HECT	no		
RTC1	YOL138C			RING	yes	yol138c-del	25
RTF1	YGL244W	UB			yes	rtf1-del	132
RTT101	YJL047C	UB			yes	TI	
RTT107	YHR154W	UB	E3-ass.		yes	rtt107-del	6
RUB1	YDR139C	NEDD	modifier		yes	rub1-del	0
RUP1	YOR138C	UB	DUB-ass.		yes	rup1-del	1
SAD1	YFR005C	UB			no		
SAF1	YBR280C	UB	E3-ass.		yes	saf1-del	0
SAN1	YDR143C	UB	E3	RING	yes	san1-del	4
SAS4	YDR181C	UB			yes	sas4-del	34
SCJ1	YMR214W				yes		
SCL1	YGL011C				no		
SCM3	YDL139C	UB			no		
SEC27	YGL137W				no		
SEC61	YLR378C				no		
SEM1	YDR363W-A				yes	sem1-del	52
SGF11	YPL047W	UB	DUB-ass.		yes	sgf11-del	2
SGF73	YGL066W	UB	DUB-ass.		yes	sgf73-del	102
SGT1	YOR057W	UB			no		
SHP1	YBL058W				yes	TI	
SIZ1	YDR409W	SUMO	E3	RING	yes	siz1-del	1
SKP1	YDR328C	NEDD/UB	E3-ass.		no		
SKP2	YNL311C	UB	E3-ass.		yes	skp2-del	3
SLA1	YBL007C				yes	sla1-del	47
SLX5	YDL013W	SUMO/UB	E3	RING	yes	slx5-del	321
SLX8	YER116C	SUMO/UB	E3	RING	yes	slx8-del	132
SMT3	YDR510W	SUMO	modifier		no		
SNF7	YLR025W				yes	snf7-del	116
SNF8	YPL002C				yes	snf8-del	103
SNT2	YGL131C			RING	yes	snt2-del	3
SRN2	YLR119W				yes	srn2-del	18

Supplementary Table S3. Continued

Gene ¹	Systematic name ¹	System ²	Function ³	Domain ³	Viable ³	Factor value ⁴	Profile ⁵
<i>SSH4</i>	<i>YKL124W</i>				yes		
<i>SSM4</i>	<i>YIL030C</i>	UB	E3	RING	yes	ssm4-del	4
<i>STES</i>	<i>YDR103W</i>			RING	yes	ste5-del	33
<i>STP22</i>	<i>YCL008C</i>				yes	TI	
<i>STS1</i>	<i>YIR011C</i>				no		
<i>SUS1</i>	<i>YBR111W-A</i>	UB	DUB-ass		yes	sus1-del; TI	53
<i>SWA2</i>	<i>YDR320C</i>				yes	swa2-del; TI	403
<i>SWM1</i>	<i>YDR260C</i>	UB	E3-ass.		yes	swm1-del	21
<i>SWP82</i>	<i>YFL049W</i>				yes	TI	
<i>TAF5</i>	<i>YBR198C</i>				no		
<i>TFB3</i>	<i>YDR460W</i>			RING	no		
<i>TOM1</i>	<i>YDR457W</i>	UB	E3		yes	tom1-del	24
<i>TRE1</i>	<i>YPL176C</i>				yes	tre1-del	0
<i>TRE2</i>	<i>YOR256C</i>				no		
<i>TUL1</i>	<i>YKL034W</i>	UB	E3	HECT	yes	tul1-del	3
<i>TUP1</i>	<i>YCR084C</i>				yes	tup1-del	607
<i>UBA1</i>	<i>YKL210W</i>	UB	E1		no		
<i>UBA2</i>	<i>YDR390C</i>	SUMO	E1		no		
<i>UBA3</i>	<i>YPR066W</i>	NEDD	E1		yes	uba3-del; TI	
<i>UBA4</i>	<i>YHR111W</i>	URM	E1		yes	uba4-del	29
<i>UBC1</i>	<i>YDR177W</i>	UB	E2		no		
<i>UBC4</i>	<i>YBR082C</i>	UB	E2		yes	ubc4-del	45
<i>UBC5</i>	<i>YDR059C</i>	UB	E2		yes	ubc5-del	1
<i>UBC6</i>	<i>YER100W</i>	UB	E2		yes	ubc6-del	7
<i>UBC7</i>	<i>YMR022W</i>	UB	E2		yes	ubc7-del	6
<i>UBC8</i>	<i>YEL012W</i>	UB	E2		yes	ubc8-del	4
<i>UBC9</i>	<i>YDL064W</i>	SUMO	E2		no		
<i>UBC11</i>	<i>YOR339C</i>	UB	E2		yes	ubc11-del	0
<i>UBC12</i>	<i>YLR306W</i>	NEDD	E2		yes	ubc12-del	1
<i>UBC13</i>	<i>YDR092W</i>	UB	E2		yes	TI	
<i>UBI4</i>	<i>YLL039C</i>	UB	modifier		yes	ubi4-del; TI	0
<i>UBP1</i>	<i>YDL122W</i>	UB	DUB		yes	ubp1-del	4
<i>UBP2</i>	<i>YOR124C</i>	UB	DUB		yes	ubp2-del	0
<i>UBP3</i>	<i>YER151C</i>	UB	DUB		yes	ubp3-del	200
<i>UBP5</i>	<i>YER144C</i>	UB	DUB		yes	ubp5-del	0
<i>UBP6</i>	<i>YFR010W</i>	UB	DUB		yes	ubp6-del	8
<i>UBP7</i>	<i>YIL156W</i>	UB	DUB		yes	ubp7-del	1
<i>UBP8</i>	<i>YMR223W</i>	UB	DUB		yes	ubp8-del	7
<i>UBP9</i>	<i>YER098W</i>	UB	DUB		yes	ubp9-del	2
<i>UBP10</i>	<i>YNL186W</i>	UB	DUB		yes	ubp10-del	119
<i>UBP11</i>	<i>YKR098C</i>	UB	DUB		yes	ubp11-del	0
<i>UBP12</i>	<i>YJL197W</i>	UB	DUB		yes	ubp12-del	0
<i>UBP13</i>	<i>YBL067C</i>	UB	DUB		yes	ubp13-del	13
<i>UBP14</i>	<i>YBR058C</i>	UB	DUB		yes	ubp14-del	7
<i>UBP15</i>	<i>YMR304W</i>	UB	DUB		yes	ubp15-del	49
<i>UBP16</i>	<i>YPL072W</i>	UB	DUB		yes	ubp16-del	4
<i>UBR1</i>	<i>YGR184C</i>	UB	E3	RING	yes	ubr1-del	8
<i>UBR2</i>	<i>YLR024C</i>	UB	E3	RING	yes	ubr2-del	19
<i>UBS1</i>	<i>YBR165W</i>	UB			yes	ubs1-del	1
<i>UBX2</i>	<i>YML013W</i>	UB	E3-ass.		yes	ubx2-del	103
<i>UBX3</i>	<i>YDL091C</i>				yes	ubx3-del	3
<i>UBX4</i>	<i>YMR067C</i>				yes	ubx4-del	2
<i>UBX5</i>	<i>YDR330W</i>				yes	ubx5-del	1
<i>UBX6</i>	<i>YJL048C</i>				yes	ubx6-del	0
<i>UBX7</i>	<i>YBR273C</i>				yes	ubx7-del	1
<i>UFD1</i>	<i>YGR048W</i>				no		
<i>UFD2</i>	<i>YDL190C</i>	UB	E3	U-box	yes	ufd2-del	15
<i>UFD4</i>	<i>YKL010C</i>	UB	E3	HECT	yes	ufd4-del	12
<i>UFO1</i>	<i>YML088W</i>	UB	E3-ass.	F-box	yes	ufo1-del	1
<i>UIP4</i>	<i>YPL186C</i>				yes	uip4-del	0
<i>ULA1</i>	<i>YPL003W</i>	NEDD	E1		yes	ula1-del	1

Supplementary Table S3. Continued

Gene ¹	Systematic name ¹	System ²	Function ³	Domain ³	Viable ³	Factor value ⁴	Profile ⁵
<i>ULS1</i>	<i>YOR191W</i>			RING	yes	ris1-del	5
<i>ULP1</i>	<i>YPL020C</i>	SUMO	ULP		no		
<i>ULP2</i>	<i>YIL031W</i>	SUMO	ULP		no		
<i>UMP1</i>	<i>YBR173C</i>				yes	Tl	
<i>UPF3</i>	<i>YGR072W</i>	UB			yes	upf3-del	420
<i>URE2</i>	<i>YNL229C</i>	URM			yes	ure2-del	50
<i>URH1</i>	<i>YDR400W</i>				yes		
<i>URM1</i>	<i>YIL008W</i>	URM	modifier		yes	urm1-del	111
<i>USA1</i>	<i>YML029W</i>	UB	E3-ass.		yes	usa1-del	4
<i>VID24</i>	<i>YBR105C</i>		E3-ass.		yes	vid24-del	1
<i>VID28</i>	<i>YIL017C</i>		E3-ass.		yes	vid28-del	25
<i>VID30</i>	<i>YGL227W</i>		E3-ass.		yes	vid30-del	1
<i>VMS1</i>	<i>YDR049W</i>				yes		
<i>VPS8</i>	<i>YAL002W</i>			RING	yes	vps8-del	128
<i>VPS9</i>	<i>YML097C</i>				yes	vps9-del	46
<i>VPS15</i>	<i>YBR097W</i>				yes	vps15-del	353
<i>VPS20</i>	<i>YMR077C</i>				yes	Tl	
<i>VPS24</i>	<i>YKL041W</i>				yes	vps24-del	21
<i>VPS25</i>	<i>YJR102C</i>				yes	vps25-del	121
<i>VPS27</i>	<i>YNR006W</i>				yes	vps27-del	33
<i>VPS28</i>	<i>YPL065W</i>				yes	vps28-del	76
<i>VPS36</i>	<i>YLR417W</i>				yes	vps36-del	113
<i>VPS38</i>	<i>YLR360W</i>				yes		
<i>WSS1</i>	<i>YHR134W</i>	SUMO			yes	wss1-del	27
<i>YBR062C</i>	<i>YBR062C</i>			RING	yes	ybr062c-del	2
<i>YDJ1</i>	<i>YNL064C</i>				yes		
<i>YDR131C</i>	<i>YDR131C</i>	UB	E3-ass.	F-box	yes	ydr131c-del	2
<i>YDR161W</i>	<i>YDR161W</i>				yes		
<i>YDR266C</i>	<i>YDR266C</i>			RING	yes	ydr266c-del	2
<i>YDR306C</i>	<i>YDR306C</i>	UB	E3-ass.	F-box	yes	ydr306c-del	5
<i>YKR017C</i>	<i>YKR017C</i>			RING	yes	ykr017c-del	2
<i>YLR224W</i>	<i>YLR224W</i>	UB	E3-ass.	F-box	yes	ylr224w-del	4
<i>YLR352W</i>	<i>YLR352W</i>	UB	E3-ass.	F-box	yes	ylr352w-del	0
<i>YOS9</i>	<i>YDR057W</i>	UB			yes	yos9-del	1
<i>YRB1</i>	<i>YDR002W</i>				no		
<i>YUH1</i>	<i>YJR099W</i>	UB	DUB		yes	yuh1-del	1
<i>ZIP1</i>	<i>YDR285W</i>				yes	zip1-del	0

¹ Genes are selected based on the GO and protein domain criteria defined in Supplementary Table S1.

² Genes are classified in specific ubiquitin(-like) systems ('System'), based on the GO terms specified in Supplementary Table S2.

³ Information about Gene function ('Function'), protein domains ('Domain') and viability of the deletion mutant ('Viable') was retrieved from SGD (www.yeastgenome.org) and InterPro (www.ebi.ac.uk/interpro).

⁴ Genes for which deletion mutants were analysed by microarray expression profiling are annotated with specific expression profile IDs ('Factor value'). Genes marked with Tl (technical issue) are described below.

⁵ The value represents the number of significant genes ('Profile') observed in the deletion mutant. The number is based on total number of differentially expressed genes (mutant vs. wt, FC > 1.7, $p < 0.05$), excluding the deleted gene, wt variable genes and mitochondrial genes.

Tl: The expression profiles of *blm10Δ*, *hsm3Δ*, *rad4Δ*, *rtt101Δ*, *swp82Δ*, *uba3Δ*, *ubc13Δ* and *vps20Δ* were excluded because of aneuploidy or wrong deletion. Repeated attempts to create viable, euploid mutants for *bub3Δ*, *dia2Δ*, *ecm29Δ*, *hsp82Δ*, *nas2Δ*, *not5Δ*, *npl4Δ*, *shp1Δ*, *stp22Δ* and *ump1Δ* were unsuccessful. *Elp3Δ* was a MATa strain and was included using a MATa wt pool for statistical analysis. *Atg10Δ* showed mitochondrial aneuploidy and was included. The mutants *ama1Δ*, *doc1Δ*, *nup60Δ*, *sus1Δ*, *swa2Δ* and *ubi4Δ* did not show significant downregulation of the deleted gene, but were included after PCR analysis verified proper disruption of the gene.

Supplementary Table S4. Yeast strains

Mutant	Genotype	Source	Mutant	Genotype	Source
<i>acm1</i> Δ	<i>ACM1::KanMX4</i>	OBS	<i>fus3</i> Δ + <i>kss1</i> Δ	<i>FUS3::NatMX6</i>	This study*
<i>add66</i> Δ	<i>ADD66::KanMX4</i>	OBS		<i>KSS1::KanMX6</i>	
<i>ama1</i> Δ	<i>AMA1::KanMX6</i>	This study	<i>gga1</i> Δ	<i>GGA1::KanMX4</i>	OBS
<i>apc9</i> Δ	<i>APC9::KanMX4</i>	OBS	<i>gga2</i> Δ	<i>GGA2::KanMX4</i>	OBS
<i>asi1</i> Δ	<i>ASI1::KanMX4</i>	OBS	<i>krh1</i> Δ	<i>GPB1::KanMX4</i>	ES
<i>asi2</i> Δ	<i>ASI2::KanMX4</i>	OBS	<i>grr1</i> Δ	<i>GRR1::KanMX6</i>	This study
<i>asi3</i> Δ	<i>ASI3::KanMX4</i>	OBS	<i>gts1</i> Δ	<i>GTS1::KanMX4</i>	OBS
<i>asr1</i> Δ	<i>ASR1::KanMX4</i>	OBS	<i>hog1</i> Δ	<i>HOG1::KanMX4</i>	ES*
<i>atg3</i> Δ	<i>ATG3::KanMX4</i>	ES	<i>hrd1</i> Δ	<i>HRD1::KanMX4</i>	ES
<i>atg4</i> Δ	<i>ATG4::KanMX6</i>	This study	<i>hrd3</i> Δ	<i>HRD3::KanMX4</i>	OBS
<i>atg5</i> Δ	<i>ATG5::KanMX4</i>	OBS	<i>hrt3</i> Δ	<i>HRT3::KanMX4</i>	OBS
<i>atg7</i> Δ	<i>ATG7::KanMX4</i>	OBS	<i>hsc82</i> Δ	<i>HSC82::KanMX4</i>	OBS
<i>atg8</i> Δ	<i>ATG8::KanMX4</i>	OBS	<i>hse1</i> Δ	<i>HSE1::KanMX4</i>	OBS
<i>atg10</i> Δ	<i>ATG10::KanMX4</i>	ES	<i>hub1</i> Δ	<i>HUB1::KanMX4</i>	OBS
<i>atg12</i> Δ	<i>ATG12::KanMX4</i>	OBS	<i>hul4</i> Δ	<i>HUL4::KanMX4</i>	OBS
<i>bmh1</i> Δ	<i>BMH1::KanMX4</i>	ES	<i>hul5</i> Δ	<i>HUL5::KanMX4</i>	OBS
<i>bmh2</i> Δ	<i>BMH2::KanMX4</i>	ES	<i>iki1</i> Δ	<i>IKI1::KanMX4</i>	OBS
<i>bre1</i> Δ	<i>BRE1::KanMX4</i>	ES*	<i>iki3</i> Δ	<i>IKI3::KanMX4</i>	OBS
<i>bre5</i> Δ	<i>BRE5::KanMX4</i>	OBS	<i>irc20</i> Δ	<i>IRC20::KanMX4</i>	ES
<i>bro1</i> Δ	<i>BRO1::KanMX4</i>	OBS	<i>irc25</i> Δ	<i>IRC25::KanMX4</i>	OBS
<i>bsd2</i> Δ	<i>BSD2::KanMX6</i>	This study	<i>itt1</i> Δ	<i>ITT1::KanMX4</i>	ES
<i>bul1</i> Δ	<i>BUL1::KanMX4</i>	OBS	<i>jem1</i> Δ	<i>JEM1::KanMX4</i>	OBS
<i>bul2</i> Δ	<i>BUL2::KanMX4</i>	OBS	<i>kti12</i> Δ	<i>KTI12::KanMX4</i>	OBS
<i>bur2</i> Δ	<i>BUR2::KanMX4</i>	ES*	<i>lge1</i> Δ	<i>LGE1::KanMX4</i>	OBS*
<i>cdc26</i> Δ	<i>CDC26::KanMX4</i>	OBS	<i>mag2</i> Δ	<i>MAG2::KanMX4</i>	ES
<i>cdh1</i> Δ	<i>CDH1::KanMX4</i>	OBS	<i>mdm30</i> Δ	<i>MDM30::KanMX4</i>	OBS
<i>chf1</i> Δ	<i>CHF1::KanMX4</i>	ES	<i>mf1</i> Δ	<i>MFB1::KanMX4</i>	OBS
<i>chf2</i> Δ	<i>CHF2::KanMX4</i>	ES	<i>mgs1</i> Δ	<i>MGS1::KanMX4</i>	OBS
<i>csn9</i> Δ	<i>CSN9::KanMX4</i>	OBS	<i>mms1</i> Δ	<i>MMS1::KanMX4</i>	OBS
<i>csn12</i> Δ	<i>CSN12::KanMX4</i>	OBS	<i>mms2</i> Δ	<i>MMS2::KanMX4</i>	ES
<i>cst9</i> Δ	<i>CST9::KanMX6</i>	This study	<i>mms22</i> Δ	<i>MMS22::KanMX4</i>	OBS
<i>cue1</i> Δ	<i>CUE1::KanMX4</i>	OBS	<i>mnd2</i> Δ	<i>MND2::KanMX4</i>	OBS
<i>cue2</i> Δ	<i>CUE2::KanMX4</i>	OBS	<i>mot2</i> Δ	<i>MOT2::KanMX6</i>	This study*
<i>cue3</i> Δ	<i>CUE3::KanMX4</i>	OBS	<i>mub1</i> Δ	<i>MUB1::KanMX4</i>	OBS
<i>cue4</i> Δ	<i>CUE4::KanMX4</i>	OBS	<i>mvb12</i> Δ	<i>MVB12::KanMX4</i>	OBS
<i>cue5</i> Δ	<i>CUE5::KanMX4</i>	OBS	<i>nas6</i> Δ	<i>NAS6::KanMX4</i>	OBS
<i>cul3</i> Δ	<i>CUL3::KanMX4</i>	OBS	<i>nam7</i> Δ	<i>NAM7::KanMX4</i>	OBS
<i>das1</i> Δ	<i>DAS1::KanMX6</i>	This study	<i>ncs2</i> Δ	<i>NCS2::KanMX4</i>	OBS
<i>dcn1</i> Δ	<i>DCN1::KanMX4</i>	OBS	<i>ncs6</i> Δ	<i>NCS6::KanMX4</i>	OBS
<i>ddi1</i> Δ	<i>DDI1::KanMX4</i>	OBS	<i>nfi1</i> Δ	<i>NFI1::KanMX4</i>	OBS
<i>def1</i> Δ	<i>DEF1::KanMX6</i>	This study	<i>nmd2</i> Δ	<i>NMD2::KanMX4</i>	OBS
<i>der1</i> Δ	<i>DER1::KanMX4</i>	OBS	<i>not3</i> Δ	<i>NOT3::KanMX6</i>	This study*
<i>did4</i> Δ	<i>DID4::KanMX4</i>	OBS	<i>nup53</i> Δ	<i>NUP53::KanMX4</i>	OBS
<i>doa1</i> Δ	<i>DOA1::KanMX4</i>	OBS	<i>nup60</i> Δ	<i>NUP60::KanMX4</i>	OBS
<i>doa4</i> Δ	<i>DOA4::KanMX6</i>	This study	<i>otu1</i> Δ	<i>OTU1::KanMX4</i>	OBS
<i>doc1</i> Δ	<i>DOC1::KanMX4</i>	OBS	<i>pan2</i> Δ	<i>PAN2::KanMX4</i>	OBS
<i>don1</i> Δ	<i>DON1::KanMX4</i>	OBS	<i>pba1</i> Δ	<i>PBA1::KanMX4</i>	OBS
<i>dsk2</i> Δ	<i>DSK2::KanMX4</i>	OBS	<i>pbs2</i> Δ	<i>PBS2::KanMX4</i>	ES*
<i>duf1</i> Δ	<i>DUF1::KanMX4</i>	OBS	<i>pci8</i> Δ	<i>PCI8::KanMX4</i>	OBS
<i>ebs1</i> Δ	<i>EBS1::KanMX4</i>	OBS	<i>pep3</i> Δ	<i>PEP3::KanMX4</i>	ES
<i>ecm30</i> Δ	<i>ECM30::KanMX4</i>	OBS	<i>pep5</i> Δ	<i>PEP5::KanMX4</i>	ES
<i>ede1</i> Δ	<i>EDE1::KanMX4</i>	OBS	<i>pex2</i> Δ	<i>PEX2::KanMX6</i>	This study
<i>ela1</i> Δ	<i>ELA1::KanMX4</i>	OBS	<i>pex4</i> Δ	<i>PEX4::KanMX4</i>	ES
<i>elc1</i> Δ	<i>ELC1::KanMX4</i>	OBS	<i>pex10</i> Δ	<i>PEX10::KanMX4</i>	ES
<i>elp2</i> Δ	<i>ELP2::KanMX4</i>	OBS	<i>pex12</i> Δ	<i>PEX12::KanMX4</i>	OBS
<i>hpa1</i> Δ	<i>ELP3::KanMX4</i>	ES	<i>pib1</i> Δ	<i>PIB1::KanMX4</i>	ES
<i>elp4</i> Δ	<i>ELP4::KanMX4</i>	OBS	<i>poc4</i> Δ	<i>POC4::KanMX4</i>	OBS
<i>elp6</i> Δ	<i>ELP6::KanMX4</i>	OBS	<i>pre9</i> Δ	<i>PRE9::KanMX4</i>	OBS
<i>etp1</i> Δ	<i>ETP1::KanMX4</i>	ES	<i>psh1</i> Δ	<i>PSH1::KanMX4</i>	OBS
<i>fap1</i> Δ	<i>FAP1::KanMX4</i>	ES	<i>pth2</i> Δ	<i>PTH2::KanMX4</i>	OBS
<i>far1</i> Δ	<i>FAR1::KanMX4</i>	ES	<i>rad5</i> Δ	<i>RAD5::KanMX4</i>	ES

Supplementary Table S4. Continued

Mutant	Genotype	Source	Mutant	Genotype	Source
<i>rad6Δ</i>	<i>RAD6::KanMX6</i>	This study*	<i>ubc12Δ</i>	<i>UBC12::KanMX4</i>	ES
<i>rad7Δ</i>	<i>RAD7::KanMX4</i>	OBS	<i>ubi4Δ</i>	<i>UBI4::KanMX4</i>	OBS
<i>rad16Δ</i>	<i>RAD16::KanMX4</i>	ES	<i>ubp1Δ</i>	<i>UBP1::KanMX4</i>	ES
<i>rad18Δ</i>	<i>RAD18::KanMX4</i>	OBS	<i>ubp2Δ</i>	<i>UBP2::KanMX4</i>	ES
<i>rad23Δ</i>	<i>RAD23::KanMX4</i>	OBS	<i>ubp3Δ</i>	<i>UBP3::KanMX4</i>	ES
<i>rcy1Δ</i>	<i>RCY1::KanMX4</i>	ES	<i>ubp5Δ</i>	<i>UBP5::KanMX4</i>	ES
<i>rkr1Δ</i>	<i>RKR1::KanMX4</i>	ES	<i>ubp6Δ</i>	<i>UBP6::KanMX4</i>	OBS
<i>rmd5Δ</i>	<i>RMD5::KanMX4</i>	OBS	<i>ubp7Δ</i>	<i>UBP7::KanMX4</i>	ES
<i>rpn4Δ</i>	<i>RPN4::KanMX4</i>	OBS	<i>ubp8Δ</i>	<i>UBP8::KanMX4</i>	ES*
<i>rpn10Δ</i>	<i>RPN10::KanMX4</i>	OBS	<i>ubp9Δ</i>	<i>UBP9::KanMX4</i>	ES
<i>rpn13Δ</i>	<i>RPN13::NatMX6</i>	This study	<i>ubp10Δ</i>	<i>UBP10::KanMX6</i>	This study
<i>rpn14Δ</i>	<i>RPN14::KanMX4</i>	OBS	<i>ubp11Δ</i>	<i>UBP11::KanMX4</i>	ES
<i>rri1Δ</i>	<i>RRI1::KanMX4</i>	OBS	<i>ubp12Δ</i>	<i>UBP12::KanMX4</i>	OBS
<i>rri2Δ</i>	<i>RRI2::KanMX4</i>	OBS	<i>ubp13Δ</i>	<i>UBP13::KanMX4</i>	OBS
<i>rtc1Δ</i>	<i>RTC1::KanMX4</i>	ES	<i>ubp14Δ</i>	<i>UBP14::KanMX4</i>	OBS
<i>rtf1Δ</i>	<i>RTF1::KanMX4</i>	OBS*	<i>ubp15Δ</i>	<i>UBP15::KanMX4</i>	ES
<i>rtt107Δ</i>	<i>RTT107::KanMX4</i>	OBS	<i>ubr1Δ</i>	<i>UBR1::KanMX4</i>	ES
<i>rub1Δ</i>	<i>RUB1::NatMX6</i>	This study	<i>ubr2Δ</i>	<i>UBR2::KanMX4</i>	ES
<i>rup1Δ</i>	<i>RUP1::KanMX4</i>	OBS	<i>ubs1Δ</i>	<i>UBS1::KanMX4</i>	OBS
<i>saf1Δ</i>	<i>SAF1::KanMX4</i>	OBS	<i>ubx2Δ</i>	<i>UBX2::KanMX4</i>	OBS
<i>san1Δ</i>	<i>SAN1::KanMX4</i>	ES	<i>ubx3Δ</i>	<i>UBX3::KanMX4</i>	OBS
<i>sas4Δ</i>	<i>SAS4::KanMX4</i>	OBS*	<i>ubx4Δ</i>	<i>UBX4::KanMX4</i>	OBS
<i>sap4Δ</i>	<i>SAP4::KanMX4</i>	ES	<i>ubx5Δ</i>	<i>UBX5::KanMX4</i>	OBS
<i>sap155Δ</i>	<i>SAP155::KanMX4</i>	ES	<i>ubx6Δ</i>	<i>UBX6::KanMX4</i>	OBS
<i>sap185Δ</i>	<i>SAP185::KanMX4</i>	OBS	<i>ubx7Δ</i>	<i>UBX7::KanMX4</i>	OBS
<i>sap190Δ</i>	<i>SAP190::KanMX4</i>	ES	<i>ufd2Δ</i>	<i>UFD2::KanMX4</i>	OBS
<i>sap185Δ+ sap190Δ</i>	<i>SAP185::KanMX6</i>	This study	<i>ufd4Δ</i>	<i>UFD4::KanMX4</i>	ES
	<i>SAP190::NatMX6</i>		<i>ufo1Δ</i>	<i>UFO1::KanMX4</i>	OBS
<i>sem1Δ</i>	<i>SEM1::KanMX4</i>	OBS	<i>uip4Δ</i>	<i>UIP4::KanMX4</i>	OBS
<i>sgf11Δ</i>	<i>SGF11::KanMX4</i>	OBS*	<i>ula1Δ</i>	<i>ULA1::KanMX4</i>	OBS
<i>sgf73Δ</i>	<i>SGF73::KanMX4</i>	OBS*	<i>uls1Δ</i>	<i>ULS1::KanMX4</i>	OBS
<i>sit4Δ</i>	<i>SIT4::KanMX4</i>	ES*	<i>upf3Δ</i>	<i>UPF3::KanMX4</i>	OBS
<i>siz1Δ</i>	<i>SIZ1::KanMX4</i>	ES	<i>ure2Δ</i>	<i>URE2::KanMX4</i>	OBS
<i>skp2Δ</i>	<i>SKP2::KanMX4</i>	OBS	<i>urm1Δ</i>	<i>URM1::KanMX4</i>	OBS
<i>sla1Δ</i>	<i>SLA1::KanMX4</i>	OBS	<i>usa1Δ</i>	<i>USA1::KanMX4</i>	OBS
<i>slx5Δ</i>	<i>SLX5::KanMX6</i>	This study	<i>vid24Δ</i>	<i>VID24::KanMX4</i>	OBS
<i>slx8Δ</i>	<i>SLX8::KanMX4</i>	ES	<i>vid28Δ</i>	<i>VID28::KanMX4</i>	OBS
<i>snf7Δ</i>	<i>SNF7::KanMX4</i>	OBS	<i>vid30Δ</i>	<i>VID30::KanMX4</i>	OBS
<i>snf8Δ</i>	<i>SNF8::KanMX4</i>	OBS	<i>vps8Δ</i>	<i>VPS8::KanMX4</i>	OBS
<i>snt2Δ</i>	<i>SNT2::KanMX4</i>	ES	<i>vps9Δ</i>	<i>VPS9::KanMX4</i>	OBS
<i>srn2Δ</i>	<i>SRN2::KanMX4</i>	OBS	<i>vps15Δ</i>	<i>VPS15::KanMX4</i>	ES*
<i>ssk2Δ</i>	<i>SSK2::KanMX4</i>	ES*	<i>vps24Δ</i>	<i>VPS24::KanMX4</i>	OBS
<i>ssm4Δ</i>	<i>SSM4::KanMX4</i>	OBS	<i>vps25Δ</i>	<i>VPS25::KanMX4</i>	OBS
<i>ste5Δ</i>	<i>STE5::KanMX4</i>	ES	<i>vps27Δ</i>	<i>VPS27::KanMX4</i>	OBS
<i>ste7Δ</i>	<i>STE7::KanMX4</i>	ES*	<i>vps28Δ</i>	<i>VPS28::KanMX4</i>	OBS
<i>ste11Δ</i>	<i>STE11::KanMX6</i>	This study*	<i>vps36Δ</i>	<i>VPS36::KanMX4</i>	OBS
<i>ste20Δ</i>	<i>STE20::KanMX4</i>	ES*	<i>wss1Δ</i>	<i>WSS1::KanMX4</i>	OBS
<i>sus1Δ</i>	<i>SUS1::KanMX4</i>	OBS*	<i>ybr062cΔ</i>	<i>YBR062C::KanMX4</i>	ES
<i>swa2Δ</i>	<i>SWA2::KanMX6</i>	This study	<i>ydr131cΔ</i>	<i>YDR131C::KanMX4</i>	OBS
<i>swm1Δ</i>	<i>SWM1::KanMX4</i>	OBS	<i>ydr266cΔ</i>	<i>YDR266C::KanMX4</i>	ES
<i>tom1Δ</i>	<i>TOM1::KanMX4</i>	ES	<i>ydr306cΔ</i>	<i>YDR306C::KanMX4</i>	OBS
<i>tre1Δ</i>	<i>TRE1::KanMX4</i>	OBS	<i>ygr071cΔ</i>	<i>YGR071C::KanMX4</i>	OBS
<i>tul1Δ</i>	<i>TUL1::KanMX4</i>	ES	<i>ykr017cΔ</i>	<i>YKR017C::KanMX4</i>	ES
<i>tup1Δ</i>	<i>TUP1::KanMX6</i>	This study*	<i>ylr224wΔ</i>	<i>YLR224W::KanMX4</i>	OBS
<i>uba4Δ</i>	<i>UBA4::KanMX6</i>	OBS	<i>ylr352wΔ</i>	<i>YLR352W::KanMX4</i>	OBS
<i>ubc4Δ</i>	<i>UBC4::KanMX6</i>	This study	<i>yos9Δ</i>	<i>YOS9::KanMX4</i>	OBS
<i>ubc5Δ</i>	<i>UBC5::KanMX4</i>	ES	<i>yuh1Δ</i>	<i>YUH1::KanMX4</i>	OBS
<i>ubc6Δ</i>	<i>UBC6::KanMX6</i>	This study	<i>zip1Δ</i>	<i>ZIP1::KanMX4</i>	OBS
<i>ubc7Δ</i>	<i>UBC7::KanMX4</i>	ES			
<i>ubc8Δ</i>	<i>UBC8::KanMX4</i>	ES			
<i>ubc11Δ</i>	<i>UBC11::KanMX4</i>	ES			

Overview of all strains used in this study, including their genotype and source (Open Biosystems: OBS, Euroscarf: ES).

* Previously published expression profiles ^{24,25}.



A gene expression signature for ubiquitin-proteasome defects in *Saccharomyces cerevisiae*

Loes A.L. van de Pasch, Thanasis Margaritis,
Giannis Ampatziadis and Frank C.P. Holstege

A gene expression signature for ubiquitin-proteasome system defects in *Saccharomyces cerevisiae*

Loes A.L. van de Pasch*, Thanasis Margaritis*, Giannis Ampatziadis and Frank C.P. Holstege

Molecular Cancer Research, University Medical Centre Utrecht, Universiteitsweg 100, 3508 AB, Utrecht, The Netherlands

*These authors contributed equally to this work

ABSTRACT

The proteasome is a multi-subunit protein complex with a key function in the selective degradation of ubiquitinated proteins. The expression of genes encoding proteasome subunits in *Saccharomyces cerevisiae* is under the regulatory control of the transcription activator Rpn4. Many cellular pathways depend on proteasomal degradation of substrates, but it is unclear how changes in pathway function influence the ubiquitin-proteasome system (UPS). Here we analyse a comprehensive collection of yeast deletion mutants and show that mutants involved in the UPS display a constitutive elevated expression of the proteasome regulon. Detailed characterisation of this gene expression signature reveals that genes involved in protein folding and DNA repair are coregulated with proteasome genes. Changed proteasome regulon expression in mutants is frequently associated with sensitivity to drugs that interfere in proteasome function and protein folding, and is therefore indicative for UPS defects. The proteasome expression signature is used to screen for mutants with UPS defects and identifies several established and novel components. These include members of the Rpn4 transcription regulatory pathway, proteasome and proteasome-folding factors, ubiquitination and urmylation system components. We place the mutants with defective proteasome function in a model that integrates feedback from various cellular pathways to the proteasome via Rpn4.

INTRODUCTION

The proteasome is a large, evolutionarily conserved multi-subunit protein complex¹⁻⁴. It plays a central role in the ubiquitin-proteasome system (UPS), which is a major protein degradation pathway both for misfolded or excess proteins and for induced degradation of specific targets. Protein targeting to the proteasome for proteolysis requires the attachment of a polyubiquitin chain to a substrate. This involves the concerted action of a ubiquitin-activating (E1) enzyme, ubiquitin-conjugating (E2) enzyme and a ubiquitin E3 ligase that together mediate the covalent attachment of ubiquitin to a specific lysine residue of the target protein⁵⁻⁷. Multiple rounds of these enzymatic reactions,

in which ubiquitin is sequentially attached to a previous ubiquitin moiety, results in the formation of polyubiquitin chains. Depending on the type of ubiquitin linkage, different conformations and lengths of chains are generated, which create specific molecular signals. K48-linked ubiquitin chains are the most abundant and serve as the main recognition signal for the proteasome complex^{8,9}. Alternatively, proteasome targeting of proteins can also be mediated by E3 ligases that interact directly with the proteasome, rather than via the ubiquitin chain of the targeted substrate^{10,11}.

The proteasome can structurally be divided into two subcomplexes. The core or 20S particle has a characteristic barrel-shaped structure with a cavity that harbours the peptidolytic activity^{12,13}.

The regulatory or 19S particle is associated with both ends of the core particle and comprises a modular 'base' structure that supports a horseshoe-shaped 'lid' ¹⁴. Proteins that are targeted to the proteasome bind to the regulatory particle, which is involved in polyubiquitin chain recognition, protein unfolding and core particle pore opening ⁵. The proteins enter the proteasomal cavity and are degraded into small oligopeptides by hydrolysis of the peptide bonds. The UPS therefore plays a key role in protein turnover, which is an important regulatory mechanism for controlling cellular protein levels.

A crucial determinant of proteasome function is the absolute cellular level of active proteasome complexes ⁷. This is regulated at the level of transcription ¹⁵⁻¹⁷. In *S. cerevisiae*, the genes encoding the subunits of the proteasome complex are under the regulatory control of a single transcription activator Rpn4. Rpn4 binds directly to DNA sequences called proteasome-associated control elements (PACE), which are present in promoter regions of most proteasome subunit-encoding genes ¹⁵. Interestingly, Rpn4 itself is also subjected to proteasomal degradation, resulting in a negative feedback circuit between Rpn4 and the proteasome. Proteasome-mediated proteolysis of Rpn4 results in reduced transcription of proteasome genes and lowers proteasome production. Consequently, Rpn4 protein levels increase and proteasome gene transcription and proteasome formation is promoted, thereby balancing cellular proteasome levels ¹⁸⁻²¹. Rpn4 is required for constitutive transcription of proteasome genes, but can also be actively induced under a variety of stress conditions associated with proteotoxic stress, such as oxidative stress and DNA damage, as well as in cells with defective proteasome function due to mutations or chemical inhibition of the proteasome ²².

We have used the model organism *S. cerevisiae* to analyse the cellular responses of mutants to disruption of various ubiquitin and ubiquitin-like pathways at the level of gene expression (Chapter 2, this thesis). A large collection of deletion mutants was screened for expression changes of genes

involved in ubiquitin(-like) modification. A subset of the mutants exhibit changes in gene expression in proteasome genes, indicative of transcriptional feedback. The expression changes of the proteasome regulon are used as a gene expression signature to screen for mutants with defects associated with UPS activation. This results in identification of known and novel components of the UPS. From this we delineate a model that integrates the transcription regulatory pathway of Rpn4. This improves our understanding of the adaptive transcription response of cells to proteotoxic stress and underscores the central role of the proteasome in various cellular pathways.

RESULTS

Disruption of ubiquitin(-like) system components and transcriptional feedback

Previously, we have generated DNA microarray expression profiles for yeast mutants, bearing deletions of genes encoding enzymes involved in ubiquitin(-like) modification (Chapter 2, this thesis). The mutants represent 71 nonessential E1, E2, E3 and deconjugating enzymes. The mutants were grown as liquid cultures alongside a wild type (wt) strain under a normal growth condition. RNA samples were hybridised on dual-channel microarrays versus a single batch of wt RNA as common reference. For every strain, four DNA microarray expression profiles were generated from two biological replicates derived from independent yeast colonies. The four DNA microarray profiles were averaged for each individual mutant and the mRNA expression changes were assessed by comparing the mutant profile to a collection of 200 wt profiles that were generated in the same manner ²³.

Disruption of various biological pathways can result in highly specific expression changes that reflect the affected cellular processes in the mutants ²³⁻²⁵. For example, the expression profiles of ubiquitin(-like) system mutants reveal that components which act in the same cellular pathway, such as E3 ligase complex subunits or E2-E3 enzyme pairs, have highly similar expression responses

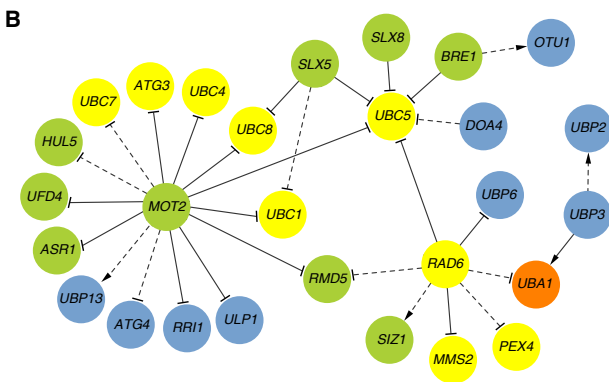
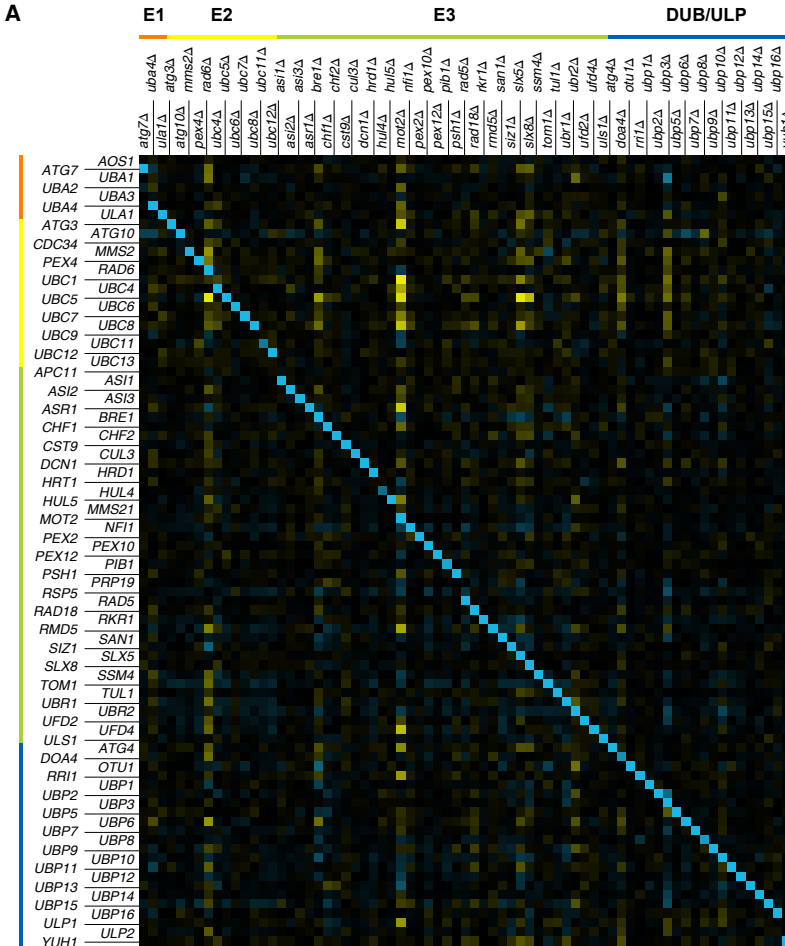


Figure 1. Disruption of ubiquitin(-like) pathways leads to transcriptional feedback among the catalytic components of ubiquitin(-like) systems.

(A) Heatmap of the mRNA expression profiles of yeast deletion mutants of E1 enzymes (orange), E2 enzymes (yellow), E3 ligases (green), deubiquitinases (DUBs; blue) and ubiquitin-like proteases (ULPs; blue). The heatmap displays the expression ratios (mutant vs. wt) of the catalytic ubiquitin(-like) system components in these mutants. Fold change (FC) expression levels are

indicated by the colour scale, with yellow for upregulation, blue for downregulation and black for no change. The diagonal blue line represents the loss of expression of the deleted gene in the corresponding mutant. Note that some genes are essential and that the corresponding deletion mutants could therefore not be profiled. (B) Disruption network of the catalytic components of the ubiquitin(-like) systems, shown in (A). Edges drawn from gene A to gene B denote a significant change in expression ($p < 0.05$, solid line: $FC > 1.7$, dashed line: $FC > 1.5$) of gene B upon deletion of gene A (\perp for upregulation, \rightarrow for downregulation). Colours of the nodes indicate the gene function, as described in (A).

(Chapter 2, this thesis). To investigate whether there is also transcriptional feedback to the genes encoding ubiquitin(-like) system components themselves, the mRNA expression ratios of all enzyme-encoding genes with a role in ubiquitin(-like) modification (86 in total, including essential genes) were systematically analysed in the mutants (Figure 1A). When comparing the expression levels of a mutant to that of wt, a p -value of < 0.05 and a fold change (FC) of > 1.7 were applied as thresholds to call a transcript significantly changed in expression. Strikingly, deletion of ubiquitin(-like) system enzymes results in few expression changes in other enzyme-encoding genes (Figure 1B). Expression changes (FC > 1.7 , $p < 0.05$) for the ubiquitin(-like) system enzymes were observed in 6 out of 71 mutants (8%) and only 13 out of the 86 transcripts (15%) changed at least once. This indicates that there is little transcriptional feedback among the catalytic components of the ubiquitin(-like) systems under the condition tested here.

The changes in gene expression were examined to determine relationships between the function of the gene that is deleted and the genes that respond. Deletion of the ubiquitin E2 enzyme *RAD6* or the ubiquitin E3 ligase *MOT2* results in changed expression of a variety of ubiquitin(-like) system components, such as the transcripts of several E2, E3 and deconjugating enzymes (Figure 1A and 1B). Since both mutants show upregulation of different enzymatic pathway components, this suggests that distinct ubiquitin(-like) pathways are induced upon loss of a single E2 or E3 enzyme. Furthermore, several mutants show increased expression of the E2 enzyme *UBC5* (*rad6Δ*, *bre1Δ*, *mot2Δ*, *slx5Δ* and *doa4Δ*), which likely results from activation of the general stress response²⁶. Deletion of the deubiquitinating enzyme *UBP3*

leads to downregulation of *UBA1*, that encodes the ubiquitin-activating (E1) enzyme (Figure 1A and 1B). Possibly, downregulation of *UBA1* is required to suppress all ubiquitination pathways, which may be beneficial for cells to counteract further accumulation of ubiquitinated proteins due to loss of Ubp3-dependent deubiquitination. The reverse may be true for the E2 mutant *rad6Δ*. Upregulation of *UBA1* in *rad6Δ* may be a transcriptional feedback mechanism to stimulate ubiquitination upon loss of ubiquitin-conjugation by Rad6.

Expression changes of ubiquitin(-like) system genes result largely from activation of the general stress response and UPS defects

To increase the number of represented cellular pathways, the microarray dataset was expanded with expression profiles of mutants with functions in phosphorylation and chromatin regulation. The profiles of these additional mutants were generated in an identical manner as described above^{23,25}. We also added mutants of non-catalytic ubiquitin(-like) system components and genes that are associated to ubiquitin(-like) modification, based on Gene Ontology (GO) terms and protein domains related to ubiquitin(-like) modification (Supplementary Table S1). In total 533 mutants were screened for expression changes in 361 genes with a (putative) role in ubiquitin(-like) modification. Changed expression (FC > 1.7 , $p < 0.05$) of at least one ubiquitin(-like) system gene was observed in 134 out of 533 mutants (25%) and for 175 out of 361 transcripts (48%).

A two-dimensional hierarchical cluster of the mutants with significant expression changes reveals that the mutants display a variety of responses, involving different ubiquitin(-like) system components (Figure 2). Two major transcript clusters

Figure 2. Perturbation of cellular pathways related to ubiquitin(-like) modification, phosphorylation and chromatin regulation, results in expression changes of specific ubiquitin(-like) system genes.

Heatmap and cluster diagram of the expression profiles of 134 mutants with significant expression changes (FC > 1.7 , $p < 0.05$). The heatmap displays 175 ubiquitin(-like) system transcripts that change significantly at least once in any mutant. The mutants and transcripts, implicated in ubiquitin(-like) modification, are colour-coded according to their function.

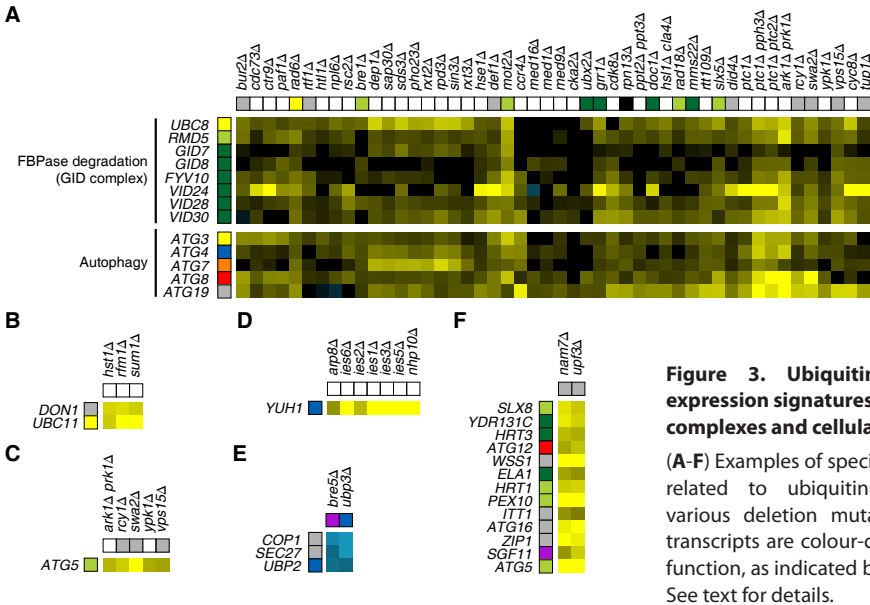


Figure 3. Ubiquitin(-like) system gene expression signatures are specific for protein complexes and cellular pathways.

(A-F) Examples of specific expression responses related to ubiquitin(-like) modification in various deletion mutants. The mutants and transcripts are colour-coded according to their function, as indicated by the legend in Figure 2. See text for details.

can be distinguished that involve a large number of coexpressed ubiquitin(-like) system genes (Figure 2). One cluster consists largely of genes encoding proteasome subunits and proteasome-associated factors. This cluster is further characterised in detail below. The second and largest block of coexpressed genes is likely associated with the activation of the general stress response in these mutants (Figure 2). It encompasses several upregulated ubiquitin system components, such as ubiquitin-conjugating enzymes (*UBC5*, *UBC8*), ubiquitin E3 ligases (*HULA*, *PIB1*, *RMD5*, *UFD4*, *DCN1*) and DUBs (*UBP5*, *UBP9*, *UBP11*). Also genes involved in proteasomal degradation of fructose-1,6-bisphosphatase for suppression of gluconeogenesis, such as subunits of the GID E3 ligase complex, and genes involved in autophagy, such as components of the Atg8/Atg12 ubiquitin-like systems, are part of this expression response (Figure 3A)^{27,28}. The mutants that display this expression phenotype do not have a common cellular function, but share a slow growth defect (data not shown), which is likely accompanied with metabolic stress.

Besides the two general expression responses, there are also several much more specific expression

responses in only a few mutants (Figure 2). For example, *Sum1/Rfm1/Hst1* complex mutants, involved in chromatin silencing of meiotic genes, show upregulation of the ubiquitin E2 enzyme *UBC11* and the RING protein *DON1* (Figure 3B). *Don1* is a meiosis-specific component of the spindle pole body²⁹. This function agrees with its derepression in *sum1Δ*, *rfm1Δ* and *hst1Δ*. The coexpression of *DON1* and *UBC11* suggests that *UBC11* may also have a meiosis-specific function. Another example is *ATG5*, an E3-like protein with a role in the cytoplasm-to-vacuole targeting (CVT) pathway³⁰. *ATG5* is specifically induced in mutants implicated in vesicular transport (Figure 3C), suggesting activation of the CVT pathway in these mutants. Seven mutants of the Ino8 chromatin remodelling complex show upregulation of the deubiquitinase *YUH1* (Figure 3D). Mutants of the DUB complex *Ubp3/Bre5*, with a role in ER-Golgi vesicular transport, show downregulation of *COP1* and *SEC27*, both encoding *COP1* vesicle coatamer proteins required for retrograde Golgi-ER transport (Figure 3E). Moreover, *SEC27* is a known target of *Ubp3/Bre5*^{31,32}. *Ubp3Δ* and *bre5Δ* also show downregulation of the DUB *UBP2*, which has a

role in the multi-vesicular body sorting pathway and has not been functionally linked to Ubp3/Bre5 before³³. And lastly, the mutants *nam7Δ* and *upf3Δ* show upregulation of several ubiquitin(-like) system genes, which is likely due to loss of nonsense-mediate mRNA decay of the transcripts of these genes (Figure 3F)³⁴. In summary, the expression of several ubiquitin(-like) system components change upon deletion of other pathway components. In some cases this may indicate direct regulation (e.g. *UBC11*), whereas in others the response may involve feedback (e.g. *ATG5*). Half of the mutants however can be distinguished based on two general expression responses involving either proteasome genes or genes implicated in a general stress response.

Proteasome genes are coexpressed with genes implicated in protein degradation, protein folding and DNA repair

The genes encoding proteasome subunits are under the regulatory control of the gene-specific transcription activator Rpn4^{15,18}. The cluster of coexpressed genes that largely consists of proteasome genes (Figure 2) is therefore likely to represent a proteasome regulon. To better characterise this transcript cluster, we first investigated which

other genes are coexpressed with the proteasome genes. For this, all expression changes in the 533 mutants were investigated, using a slightly lower significance threshold ($FC > 1.5, p < 0.01$). In a two-dimensional hierarchical cluster diagram, a subcluster of coexpressed genes is identified that comprises the proteasome and several other genes (Figure 4). Strikingly, mutants that show elevated expression of this transcript cluster are implicated in proteasome function. They include mutants of proteasome subunits (*pre9Δ*, *sem1Δ* and *rpn10Δ*), chaperones for proteasome assembly of the (*pba1Δ*, *poc4Δ* and *irc25Δ*), and a subunit of the ubiquitin E3 ligase Ubr2/Mub1, involved in Rpn4 ubiquitination (*mub1Δ*) (Figure 4).

To investigate whether the cluster of coregulated genes indeed represents a single regulon, their expression changes upon deletion of *RPN4* were examined. Most of these genes are downregulated in *rpn4Δ*, confirming that this cluster represents the proteasome regulon that is controlled by Rpn4 (Figure 4). As expected, the gene cluster is enriched for Rpn4 transcription factor binding sites ($p = 3.325E-12$) and proteasome complex components (GO:0000502: $p = 3.364E-54$), but also for several processes related to proteolysis

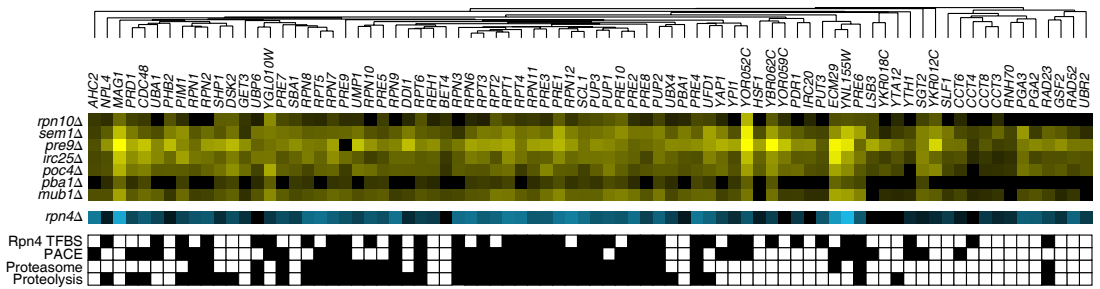


Figure 4. Mutants implicated in proteasome function and Rpn4 function are characterised by proteasome regulon expression changes.

Heatmap of the proteasome regulon in mutants bearing deletions of proteasome subunits (*pre9Δ*, *rpn10Δ*, *sem1Δ*), proteasome assembly factors (*pba1Δ*, *poc4Δ*, *irc25Δ*) and the Ubr2/Mub1 ubiquitin E3 ligase (*mub1Δ*, *ubr2Δ*). The genes are downregulated in *rpn4Δ*, bearing a deletion of the proteasome regulon transcription activator Rpn4. Genes associated to Rpn4 transcription factor binding sites (TFBS), PACE elements, proteasome complex components (GO:0000502) or proteolysis (GO:0006508) are indicated in black. The expression ratios for deleted genes and genes with $p > 0.01$ are replaced with zero.

(GO:0006508; $p = 9.222E-33$), such as ER-associated protein degradation (ERAD), mitochondrial protein degradation, protein folding and ubiquitination (Table 1)^{35,36}. For example, the proteasome mutants show increased expression of Cdc48-Npl4-Ufd1 complex subunits and Ubx4, which are all involved in ERAD^{37,38}. This suggests that mutants with proteasome dysfunction try to relieve the proteotoxic stress by increasing the levels of Cdc48-Npl4-Ufd1 to promote proteasomal degradation of misfolded proteins. This is accompanied with induction of genes involved in protein folding, which also may be a secondary response to compensate for the accumulation of unfolded proteins. Interestingly, these include four genes encoding subunits of the cytosolic chaperonin Cct ring complex (*CCT3*, *CCT4*, *CCT6*, *CCT8*), which is involved in tubulin and actin folding³⁹. *CCT4* is bound by Rpn4 and *CCT6* bears a PACE element in its promoter, suggesting that both genes are directly targeted by Rpn4 (Figure 4, Supplementary Table S2). The coexpression of Cct subunits with proteasome regulon genes suggests that Cct is also implicated in the UPS.

Rpn4 is also implicated in the DNA damage

response through modulation of the expression of the base excision repair gene *MAG1* and nucleotide excision repair gene *RAD23*⁴⁰. Indeed, *MAG1* and *RAD23* are coexpressed with proteasome genes, as are *RAD52* and *IRC20* (Figure 4). The latter two are implicated in double stranded DNA break repair, indicating that Rpn4 contributes to at least three different DNA repair pathways: base excision repair, nucleotide excision and double stranded break repair.

Proteasome regulon expression changes are associated with UPS defects

Elevated expression of the proteasome regulon is characteristic for mutants implicated in proteasome function (Figure 4). Intriguingly, several other mutants that are not known to be directly involved in proteasome function also display changed expression of the proteasome regulon (Figure 5A). To investigate whether altered expression of the proteasome regulon in these mutants is also linked to a UPS defect, 33 mutants with various degrees of proteasome regulon expression changes were selected for further investigation. The expression

Table 1. Functional characterisation of the proteasome regulon

Function	Transcripts
Proteasome complex	<i>PRE1 PRE2 PRE3 PRE4 PRE5 PRE6 PRE7 PRE8 PRE9 PRE10 PUP1 PUP2 PUP3 RPN1 RPN2 RPN3 PRN6 RPN7 RPN8 RPN9 RPN10 RPN11 RPN12 RPT1 RPT2 RPT3 RPT4 RPT5 RPT6 SCL1</i>
Protein folding	<i>CCT3 CCT4 CCT6 CCT8 GSF2 PHB2 SBA1 SGT2</i>
DNA repair	<i>IRC20 MAG1 RAD23 RAD52</i>
Transcription factor	<i>HSF1 PDR1 PUT3 YAP1</i>
ERAD	<i>CDC48 NPL4 UBX4 UFD1</i>
Proteasome assembly	<i>ECM29 PBA1 UMP1</i>
Ubiquitination	<i>SHF1 UBA1 UBR2</i>
Mitochondrial protein degradation	<i>PIM1 PRD1 YTA12</i>
Vesicular transport	<i>BET4 DDI1 GET3</i>
Proteasome-associated factor	<i>DSK2 UBP6</i>
Protein transport	<i>PGA2 PGA3</i>
RNA binding	<i>SLF1 YTH1</i>
RNA processing	<i>RNH70</i>
Histone acetylation	<i>AHC2</i>
Metabolism	<i>YPI1</i>
Ribosome biogenesis	<i>REH1</i>
Unknown	<i>LSB3 YBR062C YGL010W YKR012C YKR018C YNL155W YOR052C YOR059C</i>

of the proteasome regulon in these mutants was compared to a wt and three mutants (*med5Δ*, *rpn14Δ* and *hog1Δ*) that had wt-like expression of the proteasome regulon. Upregulation of the proteasome regulon is strongest in mutants that are directly implicated in proteasome function (*pre9Δ*, *irc25Δ*, *sem1Δ*, *poc4Δ*, *ubr2Δ*, *mub1Δ* and *rad6Δ*), but also in *mot2Δ* (Figure 5A). Proteasome regulon upregulation in *mot2Δ* is likely to be functionally relevant, because Mot2 is reported to interact with the proteasome and is important for proteasome stability⁴¹.

To assess whether mutants with minor expression changes of the proteasome regulon are also associated with a UPS defect, their sensitivity to MG132 and canavanine was tested (Figure 5B, 5C and 5D). MG132 is an inhibitor of the chymotryptic activity of the proteasome and canavanine is an arginine analogue that causes protein misfolding. Sensitivity to either drug is often associated with UPS defects. Yeast cells are relatively impermeable for MG132, but this can be enhanced by growing the cells in a low concentration of the detergent sodium dodecyl sulfate (SDS) to permeabilise the cell wall⁴². MG132 sensitivity was therefore assessed by quantifying the yeast growth rate in liquid medium (0.01% SDS) with either 50 μM MG132 or the control carrier dimethyl sulfoxide (DMSO) (Figure 5B). The relative growth rate (RGR) of the mutants compared to wt upon MG132 treatment ranged from strong growth inhibition (RGR <90%: *rpn4Δ*, *mot2Δ*, *paf1Δ*, *def1Δ*, *rad6Δ*, *ccr4Δ*, *ctr9Δ*, *med18Δ*, *rpn10Δ*, *pre9Δ*, *med2Δ*, *ubr2Δ*, *mub1Δ*, *irc25Δ* and *poc4Δ*), mild inhibition (RGR 90%-95%: *elp3Δ*, *swd3Δ*, *mck1Δ*, *iki1Δ*, *urm1Δ* and *elp2Δ*) to no effect (RGR >95%: *cdc73Δ*, *ncs2Δ*, *iki3Δ*, *sem1Δ*, *elp6Δ*, *ncs6Δ*, *bre1Δ*, *pba1Δ*, *uba4Δ* and *slx5Δ*) (Figure 5C). The mutants that are MG132 insensitive also include the control strains *med5Δ*, *rpn14Δ* and *hog1Δ*, which did not display changed expression of the proteasome regulon.

Similarly, sensitivity to canavanine was assessed by growing the strains on solid medium with and without canavanine (Figure 5D). Most

mutants that are highly sensitive (*mot2Δ*, *def1Δ*, *med2Δ*, *ccr4Δ* and *rad6Δ*) or moderately sensitive (*rpn4Δ*, *ctr9Δ*, *mck1Δ*, *sem1Δ* and *iki3Δ*) to canavanine are also sensitive to MG132, with the exception of *sem1Δ* and *iki3Δ*. This indicates that both assays are quite analogous to each other with perhaps a greater sensitivity or additional defects upon MG132 treatment. At least 24 out of 33 mutants (73%) with changed proteasome regulon expression are associated with sensitivity to MG132 and/or canavanine (Figure 5E). This indicates that mutants with changed proteasome regulon expression are highly likely to suffer from a perturbed UPS. Strikingly, *pba1Δ* and *add66Δ* are insensitive to MG132 and canavanine, but are characterised by a weak but significant upregulation (FC = 1.2) of the proteasome regulon. Pba1 and Add66 form a heterodimeric complex that contributes to proteasome assembly⁴³. Neither of the two deletion mutants are sensitive to MG132 or canavanine. This indicates that subtle UPS defects, which remain undetected by conventional phenotype assays based on drug sensitivity, can be identified by microarray expression profiling.

Identification of novel UPS components derived from proteasome regulon expression changes

The high sensitivity of the microarray expression profiles in detecting putative UPS defects was further exploited to identify more mutants in an additional set of 1400 different mutant expression profiles (unpublished data). The expression level of the proteasome regulon was measured for each mutant by calculating the average expression level of the 45 regulon genes. The expression level of the proteasome regulon is expressed as M_{pr} value, which is the average Log_2 fold change expression of the 45 genes. An M_{pr} threshold of >0.2 or <-0.2 was used to distinguish mutants with elevated or reduced proteasome regulon expression from those without significant changes. The specificity of the expression changes was assessed with a Student's *t*-test by comparing the expression levels of the

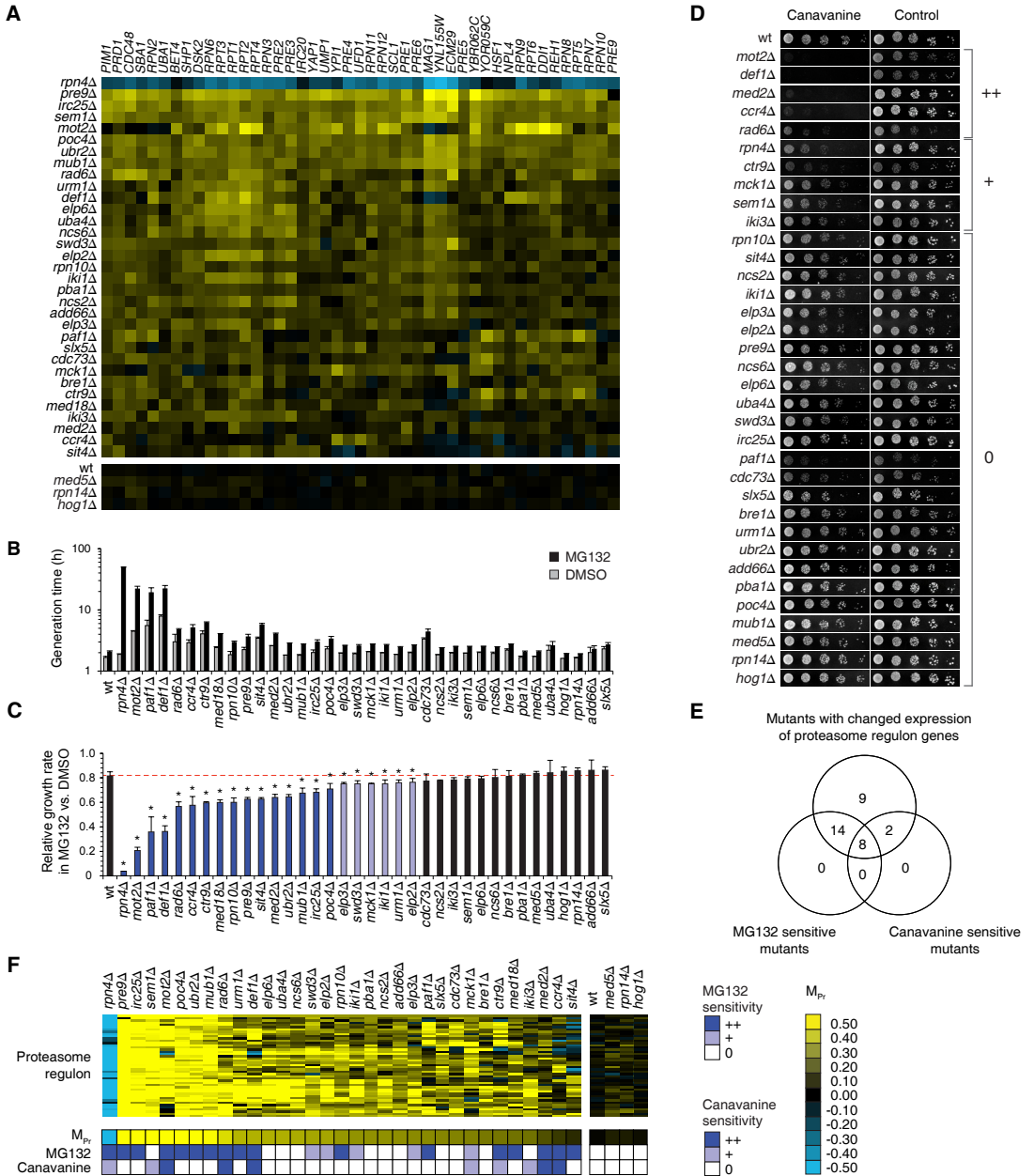


Figure 5. Proteasome regulon expression changes are generally associated to UPS defects. (A) Heatmap of the proteasome regulon expression levels in a collection of mutants with various degrees of expression changes. The FC ratio for deleted genes and genes with $p > 0.05$ is replaced with zero. Negative control strains *med5Δ*, *rpn14Δ* and *hog1Δ* show no significant expression changes of the proteasome regulon compared to wt. (B) Growth rate assay of exponentially growing cells in liquid media complemented with 50 μ M MG132 or DMSO. (C) Relative growth rate (RGR) of cells grown in MG132 compared to DMSO. Dashed red line indicates the RGR of wt (0.81 ± 0.03). Mutants with a significant growth inhibition (assessed by Student's t-test: mutant vs. wt, $p < 0.05$, indicated with asterisk) are annotated as being strongly MG132-sensitive (RGR < 90%; dark blue) or mildly MG132-sensitive (RGR 90-95%; light blue). (D) Canavanine-sensitivity assay. Cells are spotted in five-fold serial dilutions on solid media with or without canavanine. Images are after

proteasome regulon genes to all other genes. A p -value cut-off of <0.05 was used to exclude mutants with global expression changes, leaving 51 mutants with significantly changed proteasome regulon expression (Figure 6A, Supplementary Table S3). This group of mutants is likely to be highly enriched for mutants with UPS defects.

Only three mutants, including *rpn4Δ*, *mkk2Δ* and *tom1Δ*, show downregulation of the proteasome regulon. Mkk2 is a mitogen-activated kinase kinase of the protein kinase C signalling pathway, which is required for the maintenance of cellular integrity^{44,45}. Tom1 is a ubiquitin E3 ligase with a role in mRNA export, histone degradation and transcription regulation^{46–48}. Neither of them has been implicated in proteasome function before, but our data suggests that they promote transcription activation of the proteasome regulon through an as yet unknown mechanism. Alternatively, the downregulated proteasome regulon in *mkk2Δ* and *tom1Δ* may indicate disruption of processes resulting in feedback to downregulate proteasome activity.

The remaining 48 mutants, with elevated proteasome regulon expression levels, are associated with different functional categories (Table 2). The mutants with the highest p -values for proteasome regulon expression changes are mutants that have previously been implicated in proteasome function or regulation of Rpn4 turnover (Figure 6B). They include mutants of proteasome subunits (*pre9Δ*, *rpn10Δ* and *sem1Δ*), proteasome assembly factors (*add66Δ*, *hsm3Δ*, *irc25Δ*, *mot2Δ*, *pba1Δ* and *poc4Δ*), and the E2 and E3 enzymes that ubiquitinate Rpn4 (*rad6Δ*, *mub1Δ* and *ubr2Δ*). Strikingly, four mutants implicated in proteasome function, including *rpn13Δ*, *rpn14Δ*, *hsc82Δ* and *nas6Δ*, do not display the characteristic proteasome regulon expression signature (Figure 6C). This suggests that deletion of

these components does not interfere with the stability and function of the proteasome. Another possibility is redundancy among the components. For example, Rpn10 may relieve the defect of *rpn13Δ* by partially taking over its function as ubiquitin receptor⁴⁹.

Ten mutants, representing components of the urmylation system and Elongator complex, are also identified as having increased expression of proteasome genes (Figure 6A, Table 2). Urmylation is a poorly characterised ubiquitin-like system that is based on the modification of proteins with the ubiquitin-related modifier Urm1. Several Elongator mutants are known to affect the urmylation system, but it is still unclear how they are functionally linked^{50,51}. Although urmylation is thought to function mostly independently of the ubiquitin system, urmylation mutants have been shown to suffer from defective proteasome function, which interferes with ubiquitin-dependent protein degradation⁵². Surprisingly unlike the proteasome mutants, urmylation mutants have increased expression of only a subset of the proteasome genes (Figure 6C). This may indicate the existence of an alternative proteasome complex that may be specific for proteolysis of Urm1-modified substrates⁷. This alternative complex may consist of the core subunits Pre1, Pre2, Pre3, Pre10, Pup3 and the regulatory particle subunits Rpn1, Rpn2, Rpn3, Rpn6, Rpn11, Rpt1, Rpt2, Rpt3 and Rpt4.

The two largest groups of mutants with elevated proteasome regulon expression are mutants implicated in transcription and mRNA processing (Table 2). It is unlikely that these expression changes result from a global transcriptional or translational defect, as they specifically affect proteasome regulon genes. For *med18Δ* and *swd3Δ* sensitivity to MG132 was confirmed (Figure 5F), which places them as new members in the UPS. The identification of several

three days growth at 25°C. Mutants are categorised as strongly sensitive (++), mildly sensitive (+) or insensitive (0) to canavanine compared to wt. (E) Venn diagram, showing the overlap of mutants with proteasome regulon expression changes and mutants with sensitivity to MG132 and/or canavanine. (F) Overview of the mutant proteasome regulon expression and drug sensitivity phenotypes. Mutants are sorted from those with the highest to lowest average proteasome regulon expression changes (M_p). Right hand panel shows the negative controls (wt, *med5Δ*, *rpn14Δ* and *hog1Δ*). Mutants with mild or strong sensitivity to MG132 or canavanine are indicated in blue.

are able to modulate the transcription of proteasome genes in response to proteotoxic stress. Therefore we have analysed the expression of proteasome components and other genes implicated in the ubiquitin and ubiquitin-like systems to understand how ubiquitin(-like) systems are transcriptionally regulated in *S. cerevisiae*.

DNA microarray expression profiles were employed to screen a large collection of yeast deletion mutants for expression changes of genes encoding ubiquitin(-like) system components. Most mutants can be distinguished by the presence of one of two expression responses that involve ubiquitin(-like) system genes: 1) the upregulation of genes implicated in the general stress response, 2) the upregulation of genes involved in proteasome function. Surprisingly, deletion of genes encoding enzymatic components, such as E1, E2, E3 and deconjugating enzymes, was observed to have little impact on the expression of ubiquitin(-like) system genes. We attribute this to possible redundancy or a conditional function of these genes.

The focus of this study is to understand the expression response involving the proteasome. A cluster of 80 coexpressed genes was identified that comprised proteasome genes, as well as genes with roles in protein degradation, protein folding and DNA repair. These genes can be separated in two groups: genes that are directly targeted by Rpn4 and genes that change in expression as a secondary

response to UPS dysfunction. The first group of genes can be distinguished based on the presence of PACE elements in their promoters to which Rpn4 can bind for transcription activation of these genes¹⁵. Indeed, the majority of the genes that are part of the signature contain PACE elements and largely represent subunits of the proteasome complex and proteasome assembly factors, which are known targets of Rpn4. The second group of coexpressed genes without PACE elements represents genes with various cellular roles, including protein folding, ubiquitination, ERAD and DNA repair. The induction of these genes is likely a consequence of accumulation of misfolded proteins. Yeast may counteract further proteotoxic stress by increasing the expression of chaperone proteins to promote protein folding and by increasing the expression of ubiquitination and ERAD factors to stimulate protein degradation. The transcriptional response described in this study is distinct from the unfolded protein response (UPR). The UPR regulates a distinct set of genes in response to proteotoxic stress in the endoplasmic reticulum, which is coordinated by the transcription factor Hac1⁵⁵. This indicates that UPS dysfunction is not necessarily accompanied with activation of the UPR. The expression changes upon UPS activation therefore represent a separate transcriptional regulatory pathway, mediated by Rpn4.

The expression changes of the proteasome

Table 2. Classification of mutants with proteasome regulon expression changes

Function	Mutants
Proteasome complex subunits	<i>pre9Δ rpn10Δ sem1Δ</i>
Proteasome complex assembly	<i>add66Δ hsm3Δ irc25Δ mot2Δ pba1Δ poc4Δ</i>
Rpn4 ubiquitination	<i>mub1Δ rad6Δ ubr2Δ</i>
Transcription	<i>asf1Δ bre1Δ bur2Δ cdc73Δ ino2Δ ino4Δ iwr1Δ med18Δ med20Δ med31Δ mga2Δ rpn4Δ* swd3Δ opi1Δ</i>
mRNA processing	<i>brr1Δ bud13Δ cdc40Δ ist3Δ snt309Δ thp1Δ tgs1Δ tom1Δ*</i>
Urmylation, Elongator complex	<i>elp2Δ elp3Δ elp6Δ iki1Δ iki3Δ kti12Δ ncs2Δ ncs6Δ uba4Δ urm1Δ</i>
DNA damage response	<i>def1Δ met18Δ rad50Δ rad52Δ</i>
Mitosis, meiosis	<i>kar3Δ mck1Δ</i>
Cell wall integrity	<i>mkk2Δ*</i>

* Mutants marked with an asterisk show downregulation of the proteasome regulon. All other mutants show upregulation of the proteasome regulon

regulon were used as a signature to identify mutants with UPS defects. In total, we have found 48 mutants that are characterised by an elevated expression of the proteasome regulon. We can distinguish three groups of mutants: mutants with defects in posttranslational modification of Rpn4, proteasome (-assembly) mutants and mutants that suffer from a certain cellular stress that requires UPS activation. We use these mutants to delineate a model that explains the mechanisms through which cells modulate the expression of the proteasome regulon, integrating the Rpn4 transcription regulatory pathway. This model is visualised in Figure 7 and described in detail below.

The *RPN4* gene itself is transcriptionally regulated. The promoter of *RPN4* contains binding sites for the transcription factors Hsf1, Pdr1, Pdr3 and Yap1, involved in response to heat shock, oxidative stress and multidrug resistance^{56,57}. It is thought that a variety of cellular stresses can act on these transcription factors to connect to the transcription regulatory network of *RPN4*. Transcription activation of *RPN4* results in the formation of Rpn4. Rpn4 subsequently activates the transcription of PACE-bearing genes. In parallel, a specific set of genes without PACE elements are also coinduced, possibly via transcription activation by an undefined transcription factor. The combined expression of these genes, representing the proteasome regulon, promotes proteasome complex formation, ubiquitination, protein folding, etc, which suppresses proteotoxic stress in the cell. Intriguingly, the three transcription factor genes *HSF1*, *PDR1* and *YAP1* are also part of the expression signature associated with UPS dysfunction (Figure 4, Table 1). This suggests that there is also possible feedback to the transcription activation of *RPN4*.

The Rpn4 protein is subjected to ubiquitination by the E2 enzyme Rad6 and the E3 ligase Ubr2/Mub1. Consequently, Rpn4 is targeted to the proteasome for degradation, which suppresses the activation of the proteasome regulon. Rpn4 can also be targeted to the proteasome by a ubiquitin-independent pathway. This reduces the transcription

and formation of proteasome complexes, resulting in a negative feedback loop between Rpn4 and the proteasome¹⁸⁻²¹. We have observed that deletion of *RAD6*, *UBR2* and *MUB1* results in an elevated proteasome regulon expression. This is likely a consequence of Rpn4 overstabilisation due to loss of Rpn4 ubiquitination. Ubiquitination of Rpn4 is also stimulated by phosphorylation⁵⁸. An *in vitro* phosphorylation assay has revealed that Rpn4 can be phosphorylated by casein kinase 2 (Cka2)⁵⁸. However, a *cka2Δ* mutant did not show changed proteasome regulon expression (data not shown). This may indicate that Rpn4 is not an *in vivo* substrate of Cka2 or that redundant kinases can compensate for the loss of Cka2-dependent Rpn4 phosphorylation. A potential candidate for further investigation is the kinase Mck1. Deletion of *MCK1* results in a mild upregulation of the proteasome regulon, suggesting that Mck1 may directly target Rpn4 *in vivo* (Figure 6A). In contrast, the kinase Mkk2 may have an inhibitory function as *mkk2Δ* shows proteasome regulon downregulation (Figure 6A).

The proteasome is constituted of many subunits that are mostly essential. We have profiled three nonessential deletion mutants, representing proteasome subunits of the regulatory and core particle, and found that all three of them were characterised by an upregulation of the proteasome signature. Similarly, mutants implicated in proteasome assembly showed the presence of the same signature. In all these cases, we attribute the upregulation to a proteasome dysfunction, resulting in a perturbation of Rpn4 degradation. This will lead to overstabilisation of Rpn4 and overactivation of the proteasome regulon genes.

Rpn4 is required for the constitutive transcription of proteasome genes, but is also induced under certain stress conditions²². We have identified several mutants that are likely to suffer from distinct cellular stresses, which may explain their increased expression of the proteasome regulon. The first class of mutants include mutants with increased oxidative stress. They include mutants implicated in

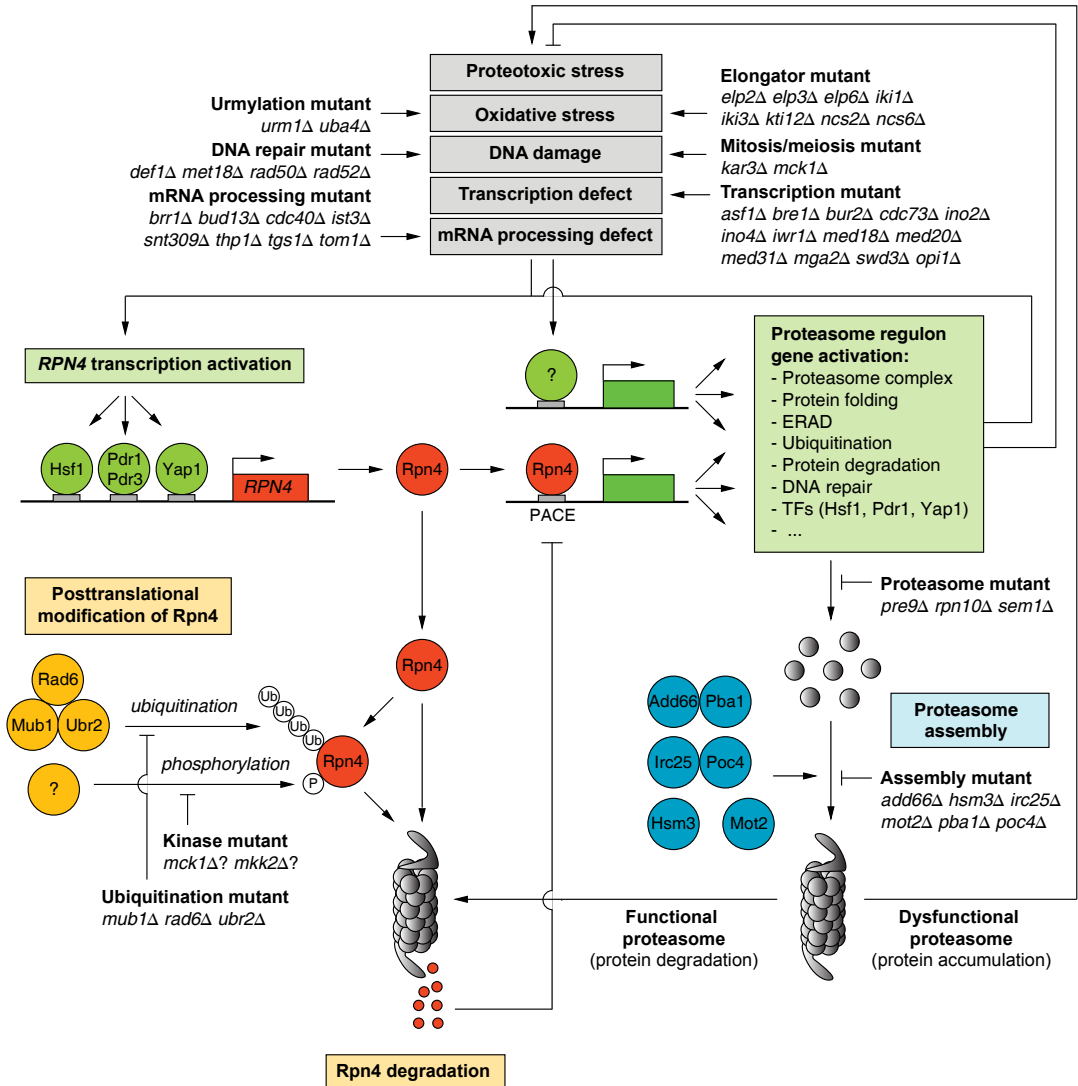


Figure 7. Model of proteasome regulon transcription activation.

Schematic representation of the adaptive transcriptional response to proteotoxic stress. Specific stress conditions that induce proteotoxic stress (grey boxes) activate the transcription factors Hsf1, Pdr1, Pdr3 and Yap1. The promoter of *RPN4* is bound by Hsf1, Pdr1, Pdr3 and Yap1 (green), which stimulates the expression of the transcription activator Rpn4 (orange). Rpn4 binds and activates PACE-bearing genes. In parallel, the stress conditions induce other genes without PACE elements. These coexpressed genes, representing the proteasome regulon (green box), promote the formation of proteasome complexes and factors that stimulate ubiquitination, protein folding, protein degradation, DNA repair, ERAD, etc, in order to suppress proteotoxic stress. The transcribed and translated proteasome subunits are assembled into a functional proteasome complex by several chaperone proteins (blue). Deletion of proteasome subunits or assembly factors results in a dysfunctional proteasome and proteotoxic stress. Rpn4 controls proteasome levels via a negative feedback loop. Rpn4 is transported to the proteasome via a phosphorylation-dependent ubiquitination pathway (yellow) and a ubiquitin-independent pathway, both resulting in Rpn4 degradation. Rpn4 degradation inhibits the transcription activation of proteasome genes. This represses the formation of proteasome complexes and consequently leads to Rpn4 stabilisation. All mutants identified in this study with significant proteasome regulon expression changes are annotated. See 'Discussion' for a detailed description of the underlying molecular mechanisms.

urmylation and Elongator function^{50,51}. Urmylation is a ubiquitin-like modification that is stimulated during oxidative stress and is dependent on the Elongator complex^{59,60}. Intriguingly, the urmylation and Elongator mutants are found to affect a subset of the proteasome genes, suggesting the existence of an alternative proteasome complex. A proteomics study aimed at the isolation and characterisation of this proteasome complex in urmylation mutants may confirm this hypothesis.

The second class of mutants are implicated in DNA damage. They include mutants involved in DNA repair, such as the mutants *rad50Δ* and *rad52Δ*, members of the *RAD52* epistasis group with a role in double strand DNA repair⁶¹. Moreover, four genes involved in DNA repair (*IRC20*, *MAG1*, *RAD23* and *RAD52*) are part of the proteasome regulon, suggesting a transcriptional feedback mechanism to DNA repair systems.

The third and fourth class of represent a large variety of mutants with roles in transcription and mRNA processing. It is unclear at what level they intersect with the Rpn4 transcription regulatory pathway, but we suspect that a defect in either process is accompanied with proteotoxic stress. In order to answer this question one has to dissect the function of the individual components in the context of UPS dysfunction. A first line of evidence for a direct role of these components in proteasome regulation may be obtained by using a similar approach as described in this study, namely confirming mutant sensitivity to either MG132 or canavanine. This way we have already confirmed that *med18Δ* is likely to suffer from a disturbed UPS. Med18 is one of the 25 subunits of the transcriptional coregulator Mediator complex⁶². Intriguingly, we have identified several more Mediator mutants to have the proteasome regulon expression signature, including *med20Δ* and *med31Δ*. *Med2Δ* was also found to be MG132- and canavanine-sensitive, however, the presence of the proteasome expression signature was annotated as insignificant due to the large number of expression changes in this mutant. Typically, *med5Δ* is not sensitive to either MG132 or canavanine,

which agrees with the absence of the proteasome expression signature in this mutant. These combined observations suggest that specific Mediator subunits have a direct function in the UPS. The Med8 subunit of mammalian Mediator is reported to be part of a ubiquitin ligase complex⁶³. Similar roles may exist for the yeast Mediator subunits.

The model shown in Figure 7 summarises most of the observations in this study. The transcription regulatory pathway of Rpn4 and its feedback loop with the proteasome are reasonably well-established²². We have extended the existing model with additional signalling pathways that appear to have feedback to Rpn4, which may represent novel components of the adaptive transcription response to proteotoxic stress. Our study demonstrates that the proteasome has a central role in a variety of cellular pathways that directly act on Rpn4 or indirectly contribute to the UPS via feedback mechanisms that trigger the activation of proteasome regulon genes. Further research will be needed to demonstrate at what level these more indirect feedback effects contribute to the UPS.

MATERIALS and METHODS

Expression profiling

The DNA microarray expression data was obtained from two microarray studies and a large collection of unpublished microarray profiles of yeast deletion mutants, which were grown under one identical experimental condition alongside a wt strain^{23,25}. All strains are isogenic to S288c (BY4742; MATa *his3Δ1 leu2Δ lys2Δ lys2Δ ura3Δ*). Strains are from the *Saccharomyces* Genome Deletion libraries of Open Biosystems (Huntsville, USA) and Euroscarf (Frankfurt, Germany). Technical issues with strains from the commercial collections, such as aneuploidy, no downregulation of the deleted gene or deletion of the wrong gene, were occasionally encountered. In these cases, the strains were remade by PCR-based gene disruption using the pFA6a-KanMX6 or pFA6aNatMX6 deletion cassettes in the genetic background of the wt parental strain BY4742 and reprofiled⁶⁴. The strains were grown in liquid synthetic complete (SC) medium (US Biologicals, Swampscott, USA) containing 2% D-glucose. Yeast cultures were grown from OD₆₀₀ 0.15 to 0.6 and harvested in mid-log phase. RNA was extracted, amplified and labelled as described previously^{23,25}. RNA was hybridised on two-channel DNA microarrays containing 70-mer oligonucleotides from the Operon Array-Ready Oligo Set (Operon Biotechnologies,

Huntsville, USA). RNA isolated from a single, large culture of wt yeast was used as common reference, which was used in one of the channels for each hybridisation and used in the statistical analysis to obtain an average expression profile for each deletion mutant relative to the wt. Per mutant, two independent cultures were hybridised on two separate microarrays. Each gene probe is represented twice on the microarray, resulting in four measurements per mutant. For each mutant the replicate hybridisations were compared to wt cultures grown on the same day to assess day-to-day variance and compared to a pool of 200 wt replicates grown throughout the project through a common reference. The data was normalised using a print-tip LOESS algorithm and corrected for gene-specific dye bias effects^{13,65}. *P*-values were obtained (*limma* R package version 2.12.0) after Benjamini-Hochberg FDR correction⁶⁶. A set of 58 genes ('wt variable genes') that changes frequently irrespective of the targeted deletion and in the collection of wt profiles was excluded from further downstream analysis²⁵.

Expression data analyses

Unsupervised clustering of the microarray expression profiles was performed using the cosine correlation, including all genes that passed the FC and *p*-value thresholds as indicated, after replacing insignificant or deleted genes with zero and excluding wt variable genes. For the identification of the proteasome regulon, a cluster was generated based on 533 different mutant expression profiles, including all mutants with at least one significant expression change in any gene (FC > 1.5, *p* < 0.01). The proteasome regulon subcluster included all genes with a cosine correlation < 0.25. The data is visualised using JavaTreeview⁶⁷. The disruption network is generated in Cytoscape (v2.8.2)⁶⁸. Enrichment analysis of the proteasome regulon genes for GO terms or Rpn4 binding transcription factor binding sites was performed using a background gene population that was set to 6,182 (the number of genes represented on the microarray)^{35,36}. *P*-values are Bonferroni-corrected for multiple testing. PACE elements were identified by a BLAST search of the 5'-GGTGGCAAA-3' sequence in the 600 bp promoter regions of all genes, using the Regulatory Sequence Analysis Tools (RSAT)⁶⁹.

MG132- and canavanine-sensitivity assays

Mutants were grown overnight in standard liquid SC medium: 2 g/L drop-out mix complete and 6.71 g/L yeast nitrogen base (YNB) without amino acids, carbohydrate and with ammonium sulphate, from US Biologicals (Swampscott, USA) with 2% D-glucose. Per mutant at least three liquid cultures were inoculated with independent yeast colonies. Sensitivity to MG132 was assessed in liquid SC medium: 1.7 g/L YNB without amino acids, carbohydrate and ammonium sulphate (US Biologicals, Swampscott, USA), 1 gr L-glutamic acid (Sigma), 2 gr drop-out mix complete without YNB (US Biologicals) with 2% D-glucose, 0.01% SDS and 50 µM MG132 (Sigma) that was dissolved in DMSO (Merck). Control medium contained no MG132 and an equal amount of DMSO. Mutants were inoculated at OD₆₀₀ of 0.15 in 0.5 ml medium

and grown in 48-wells plates (Corning) at 30°C in a Tecan Infinite F200 incubator under continuous shaking. Growth rate was calculated in the exponential growth phase over a time period of 2 days. Sensitivity to canavanine was assessed by spot assays on solid SC medium: 6.7 gr YNB, without amino acids, carbohydrate and with ammonium sulphate (US Biologicals), 2 gr drop-out mix without arginine and YNB (US Biologicals), 2% D-glucose, 2% standard SC medium with arginine and 2 µg/ml L-canavanine (Sigma). Images were taken after three days growth at 30°C.

REFERENCES

- Hough, R., Pratt, G. & Rechsteiner, M. Purification of two high molecular weight proteases from rabbit reticulocyte lysate. *J. Biol. Chem.* **262**, 8303–8313 (1987).
- Waxman, L., Fagan, J. M. & Goldberg, A. L. Demonstration of two distinct high molecular weight proteases in rabbit reticulocytes, one of which degrades ubiquitin conjugates. *J. Biol. Chem.* **262**, 2451–2457 (1987).
- Tanaka, K. *et al.* Proteasomes (multi-protease complexes) as 20 S ring-shaped particles in a variety of eukaryotic cells. *J. Biol. Chem.* **263**, 16209–16217 (1988).
- Heinemeyer, W., Kleinschmidt, J. A., Sadowsky, J., Escher, C. & Wolf, D. H. Proteasome yscE, the yeast proteasome/multicatalytic-multifunctional proteinase: mutants unravel its function in stress induced proteolysis and uncover its necessity for cell survival. *EMBO J.* **10**, 555–562 (1991).
- Pickart, C. M. & Cohen, R. E. Proteasomes and their kin: proteases in the machine age. *Nat. Rev. Mol. Cell Biol.* **5**, 177–187 (2004).
- Wolf, D. H. & Hilt, W. The proteasome: a proteolytic nanomachine of cell regulation and waste disposal. *Biochim. Biophys. Acta* **1695**, 19–31 (2004).
- Hanna, J. & Finley, D. A proteasome for all occasions. *FEBS Lett.* **581**, 2854–2861 (2007).
- Ikeda, F. & Dikic, I. Atypical ubiquitin chains: new molecular signals. 'Protein Modifications: Beyond the Usual Suspects' review series. *EMBO Rep.* **9**, 536–542 (2008).
- Komander, D. & Rape, M. The Ubiquitin Code. *Annual review of biochemistry* (2012).doi:10.1146/annurev-biochem-060310-170328
- Leggett, D. S. *et al.* Multiple associated proteins regulate proteasome structure and function. *Mol. Cell* **10**, 495–507 (2002).
- Xie, Y. & Varshavsky, A. UFD4 lacking the proteasome-binding region catalyses ubiquitination but is impaired in proteolysis. *Nat. Cell Biol.* **4**, 1003–1007 (2002).
- Groll, M. *et al.* Structure of 20S proteasome from yeast at 2.4 Å resolution. *Nature* **386**, 463–471 (1997).
- Margaritis, T. *et al.* Adaptable gene-specific dye bias correction for two-channel DNA microarrays. *Mol. Syst. Biol* **5**, 266 (2009).
- Lasker, K. *et al.* Molecular architecture of the 26S proteasome holocomplex determined by an integrative approach. *Proc. Natl. Acad. Sci. U.S.A.* **109**, 1380–1387 (2012).
- Mannhaupt, G., Schnall, R., Karpov, V., Vetter, I. & Feldmann, H. Rpn4p acts as a transcription factor by

- binding to PACE, a nonamer box found upstream of 26S proteasomal and other genes in yeast. *FEBS Lett.* **450**, 27–34 (1999).
16. Meiners, S. *et al.* Inhibition of proteasome activity induces concerted expression of proteasome genes and de novo formation of Mammalian proteasomes. *J. Biol. Chem.* **278**, 21517–21525 (2003).
 17. Lundgren, J., Masson, P., Mirzaei, Z. & Young, P. Identification and characterization of a *Drosophila* proteasome regulatory network. *Mol. Cell. Biol.* **25**, 4662–4675 (2005).
 18. Xie, Y. & Varshavsky, A. RPN4 is a ligand, substrate, and transcriptional regulator of the 26S proteasome: a negative feedback circuit. *Proc. Natl. Acad. Sci. U.S.A.* **98**, 3056–3061 (2001).
 19. Ju, D. & Xie, Y. Proteasomal degradation of RPN4 via two distinct mechanisms, ubiquitin-dependent and -independent. *J. Biol. Chem.* **279**, 23851–23854 (2004).
 20. Wang, L., Mao, X., Ju, D. & Xie, Y. Rpn4 is a physiological substrate of the Ubr2 ubiquitin ligase. *J. Biol. Chem.* **279**, 55218–55223 (2004).
 21. Ju, D., Wang, X., Xu, H. & Xie, Y. Genome-wide analysis identifies MYND-domain protein Mub1 as an essential factor for Rpn4 ubiquitylation. *Mol. Cell. Biol.* **28**, 1404–1412 (2008).
 22. Dohmen, R. J., Willers, I. & Marques, A. J. Biting the hand that feeds: Rpn4-dependent feedback regulation of proteasome function. *Biochim. Biophys. Acta* **1773**, 1599–1604 (2007).
 23. van Wageningen, S. *et al.* Functional overlap and regulatory links shape genetic interactions between signaling pathways. *Cell* **143**, 991–1004 (2010).
 24. Benschop, J. J. *et al.* A consensus of core protein complex compositions for *Saccharomyces cerevisiae*. *Mol. Cell* **38**, 916–928 (2010).
 25. Lenstra, T. L. *et al.* The specificity and topology of chromatin interaction pathways in yeast. *Mol. Cell* **42**, 536–549 (2011).
 26. Seufert, W. & Jentsch, S. Ubiquitin-conjugating enzymes UBC4 and UBC5 mediate selective degradation of short-lived and abnormal proteins. *EMBO J.* **9**, 543–550 (1990).
 27. Ohsumi, Y. Molecular dissection of autophagy: two ubiquitin-like systems. *Nat. Rev. Mol. Cell Biol.* **2**, 211–216 (2001).
 28. Regelmann, J. *et al.* Catabolite degradation of fructose-1,6-bisphosphatase in the yeast *Saccharomyces cerevisiae*: a genome-wide screen identifies eight novel GID genes and indicates the existence of two degradation pathways. *Mol. Biol. Cell* **14**, 1652–1663 (2003).
 29. Knop, M. & Strasser, K. Role of the spindle pole body of yeast in mediating assembly of the prospore membrane during meiosis. *EMBO J.* **19**, 3657–3667 (2000).
 30. Mizushima, N., Yoshimori, T. & Ohsumi, Y. The role of Atg proteins in autophagosome formation. *Annu. Rev. Cell Dev. Biol.* **27**, 107–132 (2011).
 31. Cohen, M., Stutz, F., Belgareh, N., Haguenaer-Tsapis, R. & Dargemont, C. Ubp3 requires a cofactor, Bre5, to specifically de-ubiquitinate the COPII protein, Sec23. *Nat. Cell Biol.* **5**, 661–667 (2003).
 32. Cohen, M., Stutz, F. & Dargemont, C. Deubiquitination, a new player in Golgi to endoplasmic reticulum retrograde transport. *J. Biol. Chem.* **278**, 51989–51992 (2003).
 33. Lam, M. H. Y. *et al.* Interaction of the deubiquitinating enzyme Ubp2 and the e3 ligase Rsp5 is required for transporter/receptor sorting in the multivesicular body pathway. *PLoS ONE* **4**, e4259 (2009).
 34. He, F., Brown, A. H. & Jacobson, A. Upf1p, Nmd2p, and Upf3p are interacting components of the yeast nonsense-mediated mRNA decay pathway. *Mol. Cell. Biol.* **17**, 1580–1594 (1997).
 35. MacIsaac, K. D. *et al.* An improved map of conserved regulatory sites for *Saccharomyces cerevisiae*. *BMC Bioinformatics* **7**, 113 (2006).
 36. Ashburner, M. *et al.* Gene ontology: tool for the unification of biology. The Gene Ontology Consortium. *Nat. Genet.* **25**, 25–29 (2000).
 37. Ye, Y., Meyer, H. H. & Rapoport, T. A. The AAA ATPase Cdc48/p97 and its partners transport proteins from the ER into the cytosol. *Nature* **414**, 652–656 (2001).
 38. Alberts, S. M., Sonntag, C., Schäfer, A. & Wolf, D. H. Ubx4 modulates cdc48 activity and influences degradation of misfolded proteins of the endoplasmic reticulum. *J. Biol. Chem.* **284**, 16082–16089 (2009).
 39. Chen, X., Sullivan, D. S. & Huffaker, T. C. Two yeast genes with similarity to TCP-1 are required for microtubule and actin function in vivo. *Proc. Natl. Acad. Sci. U.S.A.* **91**, 9111–9115 (1994).
 40. Jelinsky, S. A., Estep, P., Church, G. M. & Samson, L. D. Regulatory networks revealed by transcriptional profiling of damaged *Saccharomyces cerevisiae* cells: Rpn4 links base excision repair with proteasomes. *Mol. Cell. Biol.* **20**, 8157–8167 (2000).
 41. Panasenko, O. O. & Collart, M. A. Not4 E3 ligase contributes to proteasome assembly and functional integrity in part through Ecm29. *Mol. Cell. Biol.* **31**, 1610–1623 (2011).
 42. Liu, C., Apodaca, J., Davis, L. E. & Rao, H. Proteasome inhibition in wild-type yeast *Saccharomyces cerevisiae* cells. *BioTechniques* **42**, 158, 160, 162 (2007).
 43. Le Tallec, B. *et al.* 20S proteasome assembly is orchestrated by two distinct pairs of chaperones in yeast and in mammals. *Mol. Cell* **27**, 660–674 (2007).
 44. Irie, K. *et al.* MKK1 and MKK2, which encode *Saccharomyces cerevisiae* mitogen-activated protein kinase-kinase homologs, function in the pathway mediated by protein kinase C. *Mol. Cell. Biol.* **13**, 3076–3083 (1993).
 45. Heinisch, J. J., Lorberg, A., Schmitz, H. P. & Jacoby, J. J. The protein kinase C-mediated MAP kinase pathway involved in the maintenance of cellular integrity in *Saccharomyces cerevisiae*. *Mol. Microbiol.* **32**, 671–680 (1999).
 46. Duncan, K., Umen, J. G. & Guthrie, C. A putative ubiquitin ligase required for efficient mRNA export differentially affects hnRNP transport. *Curr. Biol.* **10**, 687–696 (2000).
 47. Saleh, A. *et al.* TOM1p, a yeast hect-domain protein which mediates transcriptional regulation through the ADA/SAGA coactivator complexes. *J. Mol. Biol.* **282**, 933–946 (1998).
 48. Singh, R. K., Kabbaj, M.-H. M., Paik, J. & Gunjan, A. Histone levels are regulated by phosphorylation and ubiquitylation-dependent proteolysis. *Nat. Cell Biol.* **11**, 925–933 (2009).
 49. Husnjak, K. *et al.* Proteasome subunit Rpn13 is a novel ubiquitin receptor. *Nature* **453**, 481–488 (2008).
 50. Furukawa, K., Mizushima, N., Noda, T. & Ohsumi, Y. A

- protein conjugation system in yeast with homology to biosynthetic enzyme reaction of prokaryotes. *J. Biol. Chem* **275**, 7462–7465 (2000).
51. Goehring, A. S., Rivers, D. M. & Sprague, G. F., Jr Urm1: a ubiquitin-like pathway that functions during invasive growth and budding in yeast. *Mol. Biol. Cell* **14**, 4329–4341 (2003).
 52. Hoyt, M. A. *et al.* A genetic screen for *Saccharomyces cerevisiae* mutants affecting proteasome function, using a ubiquitin-independent substrate. *Yeast* **25**, 199–217 (2008).
 53. Wilmes, G. M. *et al.* A genetic interaction map of RNA-processing factors reveals links between Sem1/Dss1-containing complexes and mRNA export and splicing. *Mol. Cell* **32**, 735–746 (2008).
 54. Faza, M. B. *et al.* Sem1 is a functional component of the nuclear pore complex-associated messenger RNA export machinery. *J. Cell Biol.* **184**, 833–846 (2009).
 55. Travers, K. J. *et al.* Functional and genomic analyses reveal an essential coordination between the unfolded protein response and ER-associated degradation. *Cell* **101**, 249–258 (2000).
 56. Hahn, J.-S., Neef, D. W. & Thiele, D. J. A stress regulatory network for co-ordinated activation of proteasome expression mediated by yeast heat shock transcription factor. *Mol. Microbiol.* **60**, 240–251 (2006).
 57. Owsianik, G., Balzi I, L. & Ghislain, M. Control of 26S proteasome expression by transcription factors regulating multidrug resistance in *Saccharomyces cerevisiae*. *Mol. Microbiol.* **43**, 1295–1308 (2002).
 58. Ju, D., Xu, H., Wang, X. & Xie, Y. Ubiquitin-mediated degradation of Rpn4 is controlled by a phosphorylation-dependent ubiquitylation signal. *Biochim. Biophys. Acta* **1773**, 1672–1680 (2007).
 59. Van der Veen, A. G. *et al.* Role of the ubiquitin-like protein Urm1 as a noncanonical lysine-directed protein modifier. *Proc. Natl. Acad. Sci. U.S.A* **108**, 1763–1770 (2011).
 60. Goehring, A. S., Rivers, D. M. & Sprague, G. F., Jr Attachment of the ubiquitin-related protein Urm1p to the antioxidant protein Ahp1p. *Eukaryotic Cell* **2**, 930–936 (2003).
 61. Symington, L. S. Role of RAD52 epistasis group genes in homologous recombination and double-strand break repair. *Microbiol. Mol. Biol. Rev.* **66**, 630–670, table of contents (2002).
 62. Björklund, S. & Gustafsson, C. M. The yeast Mediator complex and its regulation. *Trends Biochem. Sci.* **30**, 240–244 (2005).
 63. Brower, C. S. *et al.* Mammalian mediator subunit mMED8 is an Elongin BC-interacting protein that can assemble with Cul2 and Rbx1 to reconstitute a ubiquitin ligase. *Proc. Natl. Acad. Sci. U.S.A.* **99**, 10353–10358 (2002).
 64. Longtine, M. S. *et al.* Additional modules for versatile and economical PCR-based gene deletion and modification in *Saccharomyces cerevisiae*. *Yeast* **14**, 953–961 (1998).
 65. Yang, Y. H. *et al.* Normalization for cDNA microarray data: a robust composite method addressing single and multiple slide systematic variation. *Nucleic Acids Res.* **30**, e15 (2002).
 66. Smyth, G. K., Michaud, J. & Scott, H. S. Use of within-array replicate spots for assessing differential expression in microarray experiments. *Bioinformatics* **21**, 2067–2075 (2005).
 67. Saldanha, A. J. Java Treeview--extensible visualization of microarray data. *Bioinformatics* **20**, 3246–3248 (2004).
 68. Smoot, M. E., Ono, K., Ruscheinski, J., Wang, P.-L. & Ideker, T. Cytoscape 2.8: new features for data integration and network visualization. *Bioinformatics* **27**, 431–432 (2011).
 69. Thomas-Chollier, M. *et al.* RSAT 2011: regulatory sequence analysis tools. *Nucleic Acids Res.* **39**, W86–91 (2011).

SUPPLEMENTAL INFORMATION

Supplementary Table S1. Selection criteria of genes with a (putative) role in ubiquitin(-like) modification

GO term or protein domain ¹	Description	Number of associated genes
GO:0006511	Ubiquitin-dependent protein catabolic process	195
GO:0070647	Protein modification by small protein conjugation	147
GO:0019787	Small conjugating protein ligase activity	89
GO:0000151	Ubiquitin ligase complex	64
GO:0000502	Proteasome complex	50
GO:0032182	Small conjugating protein binding	43
GO:0043248	Proteasome assembly	27
GO:0019783	Small conjugating protein-specific protease activity	22
GO:0004221	Ubiquitin thiolesterase activity	19
GO:0031386	Protein tag	9
GO:0008641	Small protein activating activity	7
GO:0008180)	Signalosome	7
GO:0033588	Elongator holoenzyme complex	6
GO:0019776	ATG8 ligase activity	4
IPR001841	RING-type zinc finger domain	40
IPR001810	F-box domain	11
IPR000569	HECT domain	5
IPR004181	MIZ-type zinc finger domain	4
IPR003613	U-box domain	2
Other ²		10
Total		361

¹GO terms related to ubiquitin(-like) modification are obtained from the AmiGO Gene Ontology (GO) project (www.amigo.geneontology.org). E3 ligase-specific protein domains are obtained from the InterPro (IPR) database (www.ebi.ac.uk/interpro/).

²Ten genes categorised as 'Other' did not meet the GO term or protein domain criteria, but were included after manual curation of the gene list

Supplementary Table S2. Identification and position of PACE (GGTGGCAA) elements, relative to the start site of transcription

Gene	Start	End	Gene	Start	End	Gene	Start	End
AAD6	-439	-431	NCA3 ¹	-311	-303	RPN9 ^{1,2}	-110	-102
ABZ1	-143	-135	NOP14	-209	-201	RPN11 ^{1,2}	-125	-117
ACS1	-168	-160	NRD1	-422	-414	RPN12 ^{1,2}	-98	-90
AHC2 ²	-115	-107	NSG2	-366	-358	RPS27B	-310	-302
ALG13	-191	-183	OST1	-403	-395	RPT1 ^{1,2}	-156	-148
ATG13	-528	-520	PDI1 ¹	-195	-187	RPT2 ^{1,2}	-132	-124
BDF2 ¹	-158	-150	PIM1 ^{1,2}	-200	-192	RPT3 ^{1,2}	-177	-169
BMH1 ¹	-312	-304	PMT1	-260	-252	RPT4 ^{1,2}	-113	-105
BUD27	-493	-485	PRD1 ²	-90	-82	RPT5 ^{1,2}	-165	-157
BUD27	-261	-253	PRE1 ^{1,2}	-143	-135	RPT6 ^{1,2}	-85	-77
CCT6 ^{1,2}	-176	-168	PRE2 ^{1,2}	-156	-148	SCL1 ^{1,2}	-109	-101
CDC48 ^{1,2}	-142	-134	PRE3 ^{1,2}	-119	-111	SGT2 ²	-98	-90
CEG1 ¹	-235	-227	PRE4 ^{1,2}	-112	-104	SNT2	-61	-53
DEF1	-243	-235	PRE6 ^{1,2}	-110	-102	UBA1 ^{1,2}	-130	-122
DOC1	-37	-29	PRE7 ^{1,2}	-88	-80	UBI4 ¹	-161	-153
ECM12 ¹	-256	-248	PRE8 ^{1,2}	-121	-113	YAP1 ^{1,2}	-47	-39
ECM29 ^{1,2}	-132	-124	PRE9 ^{1,2}	-160	-152	YBR284W	-116	-108
EPL1	-390	-382	PRE10 ^{1,2}	-129	-121	YCL042W	-178	-170
EPL1	-158	-150	PUP2 ^{1,2}	-105	-97	YCL057C-A	-363	-355
ERG25	-359	-351	PUP3 ^{1,2}	-184	-176	YCR061W	-232	-224
GCD1	-173	-165	RAD51	-460	-452	YET3	-430	-422
GOS1	-476	-468	REB1 ¹	-239	-231	YGL010W ²	-199	-191
GSM1	-373	-365	RIM4	-329	-321	YJL045W	-165	-157
HUA1	-237	-229	RPL11A	-455	-447	YML007C-A	-539	-531
HUB1	-38	-30	RPL8B	-504	-496	YNL155W ²	-192	-184
IOC2	-264	-256	RPN1 ^{1,2}	-146	-138	YOL038C-A	-216	-208
KIN2 ¹	-221	-213	RPN2 ^{1,2}	-120	-112	YOR052C ²	-252	-244
LSB3 ²	-41	-33	RPN3 ^{1,2}	-96	-88	YPI1 ²	-154	-146
MCM3	-475	-467	RPN5 ¹	-139	-131	YTA7 ¹	-490	-482
MEF2	-57	-49	RPN6 ^{1,2}	-114	-106	YTH1 ²	-245	-237
NAB2 ¹	-121	-113	RPN7 ²	-155	-147			

¹PACE element identified by Mannhaupt *et al.* (1999)

²Gene is part of the proteasome regulon expression signature

Supplementary Table S3. Overview of mutants with significant proteasome regulon expression changes

Mutant	Gene	M_{pr}	P-value	Mutant	Gene	M_{pr}	P-value
<i>add66</i> Δ	<i>YKL206C</i>	0.28	8.75E-26	<i>met18</i> Δ	<i>YIL128W</i>	0.24	2.26E-13
<i>asf1</i> Δ	<i>YJL115W</i>	0.27	1.80E-06	<i>mga2</i> Δ	<i>YIR033W</i>	0.34	2.47E-07
<i>bre1</i> Δ	<i>YDL074C</i>	0.23	9.19E-04	<i>mkk2</i> Δ	<i>YPL140C</i>	-0.23	7.18E-35
<i>brr1</i> Δ	<i>YPR057W</i>	0.22	1.74E-21	<i>mot2</i> Δ	<i>YER068W</i>	0.55	5.44E-06
<i>bud13</i> Δ	<i>YGL174W</i>	0.27	1.41E-16	<i>mub1</i> Δ	<i>YMR100W</i>	0.49	9.34E-113
<i>bur2</i> Δ	<i>YLR226W</i>	0.42	7.74E-08	<i>ncs2</i> Δ	<i>YNL119W</i>	0.28	8.24E-18
<i>cdc40</i> Δ	<i>YDR364C</i>	0.53	6.21E-26	<i>ncs6</i> Δ	<i>YGL211W</i>	0.34	6.95E-24
<i>cdc73</i> Δ	<i>YLR418C</i>	0.26	2.45E-04	<i>opi1</i> Δ	<i>YHL020C</i>	0.35	7.00E-05
<i>def1</i> Δ	<i>YKL054C</i>	0.35	1.03E-04	<i>pba1</i> Δ	<i>YLR199C</i>	0.29	2.89E-68
<i>elp2</i> Δ	<i>YGR200C</i>	0.33	2.35E-19	<i>poc4</i> Δ	<i>YPL144W</i>	0.52	1.92E-65
<i>elp3</i> Δ	<i>YPL086C</i>	0.27	1.77E-10	<i>pre9</i> Δ	<i>YGR135W</i>	0.82	3.25E-67
<i>elp6</i> Δ	<i>YMR312W</i>	0.34	1.05E-11	<i>rad6</i> Δ	<i>YGL058W</i>	0.43	1.01E-09
<i>hsm3</i> Δ	<i>YBR272C</i>	0.23	5.97E-61	<i>rad50</i> Δ	<i>YNL250W</i>	0.23	0.012
<i>iki1</i> Δ	<i>YHR187W</i>	0.29	3.57E-17	<i>rad52</i> Δ	<i>YML032C</i>	0.21	3.17E-03
<i>iki3</i> Δ	<i>YLR384C</i>	0.23	4.83E-13	<i>rpn4</i> Δ	<i>YDL020C</i>	-0.62	3.72E-61
<i>ino2</i> Δ	<i>YDR123C</i>	0.35	3.83E-04	<i>rpn10</i> Δ	<i>YHR200W</i>	0.30	1.56E-19
<i>ino4</i> Δ	<i>YOL108C</i>	0.38	8.98E-04	<i>sem1</i> Δ	<i>YDR363W-A</i>	0.59	2.24E-51
<i>irc25</i> Δ	<i>YLR021W</i>	0.60	2.79E-100	<i>snt309</i> Δ	<i>YPR101W</i>	0.38	9.14E-17
<i>ist3</i> Δ	<i>YIR005W</i>	0.29	7.60E-21	<i>swd3</i> Δ	<i>YBR175W</i>	0.32	3.62E-13
<i>iwr1</i> Δ	<i>YDL115C</i>	0.21	2.86E-09	<i>tgsl</i> Δ	<i>YPL157W</i>	0.30	1.55E-23
<i>kar3</i> Δ	<i>YPR141C</i>	0.22	1.42E-03	<i>thp1</i> Δ	<i>YOL072W</i>	0.36	2.27E-04
<i>ktr12</i> Δ	<i>YKL110C</i>	0.23	1.14E-15	<i>tom1</i> Δ	<i>YDR457W</i>	-0.22	8.22E-10
<i>mck1</i> Δ	<i>YNL307C</i>	0.25	2.77E-10	<i>uba4</i> Δ	<i>YHR111W</i>	0.35	2.88E-26
<i>med18</i> Δ	<i>YGR104C</i>	0.22	1.07E-04	<i>ubr2</i> Δ	<i>YLR024C</i>	0.52	4.63E-64
<i>med20</i> Δ	<i>YHR041C</i>	0.25	6.41E-06	<i>urm1</i> Δ	<i>YIL008W</i>	0.35	3.96E-14
<i>med31</i> Δ	<i>YGL127C</i>	0.21	7.26E-07				



4

Centromere binding and a conserved role in chromosome stability for SUMO-dependent ubiquitin ligases

Loes A.L. van de Pasch, Antony J. Miles, Wilco Nijenhuis, Nathalie A.C.H. Brabers, Dik van Leenen, Philip Lijnzaad, Markus K. Brown, Jimmy Ouellet, Yves Barral, Geert J.P.L. Kops and Frank C.P. Holstege

Centromere binding and a conserved role in chromosome stability for SUMO-dependent ubiquitin ligases

Loes A.L. van de Pasch¹, Antony J. Miles¹, Wilco Nijenhuis¹, Nathalie A.C.H. Brabers¹, Dik van Leenen¹, Philip Lijnzaad¹, Markus K. Brown¹, Jimmy Ouellet², Yves Barral², Geert J.P.L. Kops¹ and Frank C.P. Holstege¹

¹Molecular Cancer Research, University Medical Centre Utrecht, Universiteitsweg 100, 3508 AB, Utrecht, the Netherlands

²Institute of Biochemistry, Swiss Federal Institute of Technology, ETH-Hönggerberg, 8093, Zürich, Switzerland
Manuscript under revision

ABSTRACT

The *Saccharomyces cerevisiae* Slx5/8 complex is the founding member of a recently defined class of SUMO-targeted ubiquitin ligases (STUbLs). Slx5/8 has been implicated in genome stability and transcription, but the precise contribution is unclear. To characterise Slx5/8 function, we determined genome-wide changes in gene expression upon loss of either subunit. The majority of mRNA changes are part of a general stress response, also exhibited by mutants of other genome integrity pathways and therefore indicative of an indirect effect on transcription. Genome-wide binding analysis reveals a uniquely centromeric location for Slx5. Detailed phenotype analyses of *slx5*Δ and *slx8*Δ mutants show severe mitotic defects that include aneuploidy, spindle mispositioning, fish hooks and aberrant spindle kinetics. This is associated with accumulation of the PP2A regulatory subunit Rts1 at centromeres prior to entry into anaphase. Knockdown of the human STUbL orthologue RNF4 also results in chromosome segregation errors due to chromosome bridges. The study shows that STUbLs have a conserved role in maintenance of chromosome stability and links SUMO-dependent ubiquitination to a centromere-specific function during mitosis.

INTRODUCTION

Accurate inheritance of chromosomes during each cell division is crucial for cell survival. Genome instability is disadvantageous and directly associated with many diseases including cancer¹. Cells have a wide variety of regulatory mechanisms that monitor the fidelity of DNA replication and mitosis. At a molecular level, control of genome stability is an intrinsic process that depends on proper posttranslational modification of many proteins. This includes ubiquitination and sumoylation. Ubiquitin and SUMO (small ubiquitin-like modifier) are small peptides that can be covalently attached to substrates through a three-step enzymatic cascade that activates (E1), conjugates (E2) and ligates (E3) the peptide to

a substrate²⁻⁴. In *S. cerevisiae*, the genes *SLX5* and *SLX8* encode the heterodimeric protein complex Slx5/8, which is required for maintenance of genome integrity in yeast^{5,6}. Biochemical characterisation of the complex has revealed that Slx5/8 is a SUMO-dependent ubiquitin E3 ligase^{7,8}. Both Slx5 and Slx8 have a C-terminal zinc finger RING domain, commonly found in many ubiquitin E3 ligases⁹. Slx5/8 also has multiple SUMO-interaction motifs, which confers a unique ability to ubiquitinate and degrade sumoylated proteins^{7,8}. This indicates that SUMO-targeted ubiquitin ligases (STUbLs) control the turnover of sumoylated proteins via ubiquitin-dependent protein degradation to ensure appropriate cellular levels of sumoylated proteins¹⁰.

The cellular role of STUbLs is less well

characterised. *SLX5* and *SLX8* were originally identified in a screen for genes that are synthetic lethal with deletion of *SGS1*, a DNA helicase of the RecQ family, indicating a role for Slx5/8 in genome stability⁵. Inactivation of STUbLs leads to a broad spectrum of genome instability phenotypes in *S. cerevisiae* and *S. pombe*. These include a strong cell cycle delay, DNA damage checkpoint activation, sensitivity to genotoxic stress, gross chromosomal rearrangements and increased rates of DNA mutation and recombination^{6,11–15}. The Slx5/8 complex resides at sites of DNA damage and replication, and contributes to DNA repair by relocating double stranded DNA breaks to the nuclear pore^{11,12,16}. How the role of Slx5/8 in genome stability ties in with its function as STUbL is unclear and other cellular roles have also been proposed. STUbL orthologues have now been identified from fission yeast (Rfp1, Rfp2, spSlx8) to human (RNF4), indicating an evolutionarily conserved and important function for ubiquitin-dependent degradation of sumoylated proteins^{14,15,17,18}. In humans, there is evidence that RNF4 regulates transcription with several transcription regulators identified as targets for SUMO-dependent ubiquitination^{19–21}. In yeast, Slx5/8 has also been implicated in transcription regulation^{8,22–24}, indicating that STUbL function may extend beyond genome stability.

To better characterise the function of STUbLs, the phenotypes of *slx5Δ* and *slx8Δ* deletion mutants in transcription and genome stability were investigated in detail. We show that changes in mRNA expression in *slx5/8* mutants are largely associated with a general stress response that is likely due to genome instability rather than a direct transcriptional defect. Determination of the genomic location of the Slx5/8 complex reveals that Slx5 locates at centromeres. Loss of *SLX5* or *SLX8* is accompanied by accumulation of Rts1 at centromeres during metaphase. Moreover, the *slx5Δ* and *slx8Δ* mutants display a variety of mitotic defects, supporting a role for Slx5/8 in chromosome stability. This is distinct from previously reported roles of Slx5/8 and gives a better insight into how genome instability arises

in *slx5/8* mutants. Analysis of human RNF4 shows that the role of Slx5/8 in chromosome stability is evolutionarily conserved, further underscoring the importance of STUbL function in genome stability during mitosis.

RESULTS

***Slx5Δ* and *slx8Δ* display a general stress response that is shared with mutants of various genome integrity pathways**

To investigate the role of Slx5/8 in transcription, genome-wide mRNA levels in *SLX5* and *SLX8* deletion strains were compared to wild type (wt), all grown to mid-log phase under standard growth conditions. A strong transcriptional response is observed upon *SLX5* deletion, resulting in changed expression of 321 genes (fold change (FC) > 1.7, $p < 0.05$, Figure 1A). The response in *slx8Δ* is quantitatively weaker (132 genes, FC > 1.7, $p < 0.05$), but correlates highly with *slx5Δ* ($r = 0.81$, Figure 1A). The similarity is also readily observed upon visual inspection of individual genes and consists largely of upregulated expression (Figure 1B; rows 1–2). The differentially expressed genes are enriched for various Gene Ontology (GO) terms (Supplementary Table S1), some of which have previously also been associated with the environmental stress response in yeast²⁵. The *slx5Δ* and *slx8Δ* mutant profiles were therefore compared with previously published DNA microarray datasets of various stress responses, which all share a similar expression response²⁵. This reveals a significant correlation between *slx5Δ* and *slx8Δ* expression profiles and stress responses such as heat shock ($r = 0.48$, $p = 2.95E-200$), indicating constitutive activation of a stress response in both *slx5Δ* and *slx8Δ* under normal growth conditions.

Although Slx5/8 have previously been implicated in regulating transcription, one interpretation of the observed changes in gene expression is that these are indirectly caused by cellular stress as a consequence of the genome instability known to occur in *slx5Δ* and *slx8Δ*. To investigate this, DNA microarray expression profiles

were generated for deletion mutants of various genome integrity pathways (Figure 1B). These mutants include components of the Sgs1-Rmi1-Top3 DNA helicase complex (*sgs1Δ*, *rmi1Δ*), DNA repair factors (*rad18Δ*, *rad50Δ*, *rad52Δ*), Cohesin components (*ctf4Δ*, *ctf18Δ*), a component of the anaphase promoting complex (*cdc26Δ*), a kinesin motor protein (*cin8Δ*), kinetochore-associated proteins (*csml1Δ*, *ctf19Δ*, *mcm21Δ*, *ybp2Δ*) and

protein phosphatase 2A subunits (*pph22Δ*, *rts1Δ*). The transcription responses of all these mutants show a high degree of similarity to each other and to *slx5Δ* and *slx8Δ*, differing mainly in the degree of upregulation, rather than in the affected genes (Figure 1B). The differentially expressed genes are enriched in DNA binding sites for the stress response transcription factors Msn2 and Msn4 (Supplementary Table S1)^{26,27}. Perturbation of

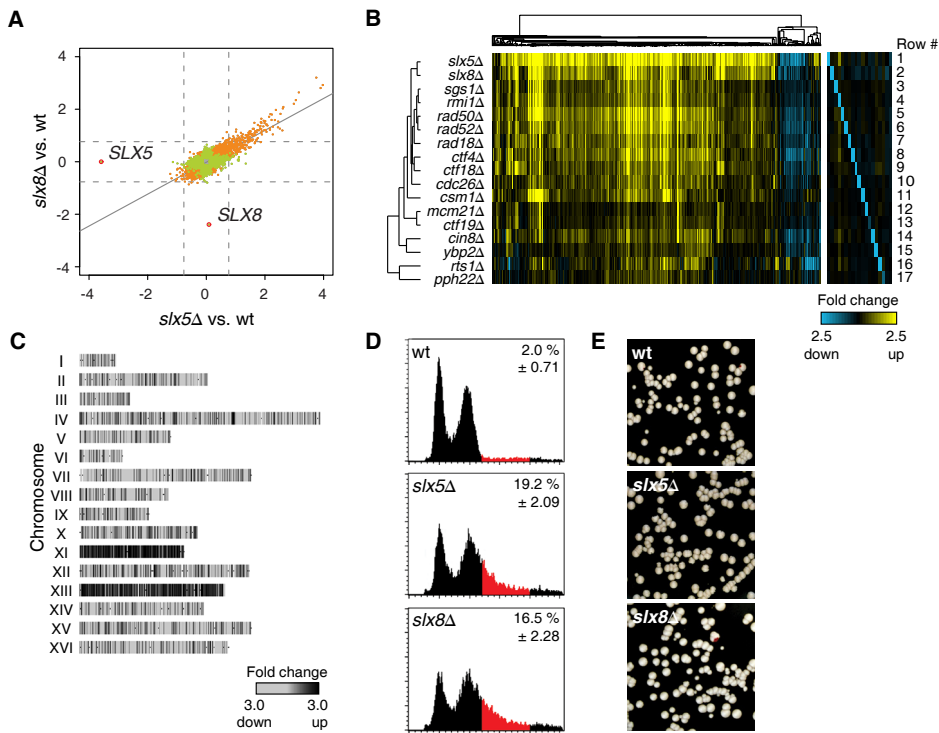


Figure 1. *Slx5Δ* and *slx8Δ* display a genome instability-induced stress response.

(A) Scatter plot comparing the changes in mRNA expression levels in *slx5Δ* and *slx8Δ* mutants. Fold change (FC) in expression is the average of four measurements for each mutant (two independent cultures each measured twice), plotted as \log_2 values of mutant over wt. Genes changing significantly ($p < 0.05$) are indicated in orange (significant in both mutants) or green (significant in one mutant). Deleted genes are indicated. Solid line indicates the regression line. Dashed lines mark a 1.7 FC threshold. (B) Heatmap and cluster diagram of the gene expression profiles of deletion mutants, showing all significant genes ($FC > 1.7$, $p < 0.05$) that change at least once in any mutant. FC expression of mutant over wt is indicated by the colour scale, with yellow for upregulation and blue for downregulation and black for no change. Deleted genes are depicted in the right-hand panel. (C) Microarray expression profile of an aneuploid *slx8Δ* mutant with duplications of chromosome XI and XIII. Genes are mapped per chromosome. The grey scale indicates FC expression in the *slx8Δ* strain versus wt. (D) Flow cytometric profiles of asynchronous populations of wt, *slx5Δ* and *slx8Δ*. Cell population with a $> 2N$ DNA content, indicated in red, is quantified (\pm s.d., $n = 3$). (E) Chromosome loss assay of wt, *slx5Δ* and *slx8Δ* cells. Red-sectoring of colonies reflects loss of the reporter chromosome. Frequency of chromosome missegregation events is 0.03%, 0.06% and 0.11% in wt, *slx5Δ* and *slx8Δ* respectively ($n > 3000$), as quantified by colony half-sector analysis.

several different genome integrity pathways therefore result in a similar gene expression response that is related to stress. A likely explanation for a large part of the gene expression response in *slx5Δ* and *slx8Δ* is therefore that this results indirectly from genome instability-induced stress rather than from a direct defect at the level of transcription of all these genes.

***Slx5Δ* and *slx8Δ* mutants are aneuploid**

The DNA microarray analyses of *slx5Δ* and *slx8Δ* also reveals a second unanticipated phenotype, the occurrence of whole chromosome aneuploidy, an example of which is shown in Figure 1C. Microarray analyses were performed on liquid cultures derived from independent colonies for each mutant. In *slx5Δ* and *slx8Δ*, aneuploidy of various chromosomes (VII, XI, XII and XIII) was observed in the form of an apparent upregulation of all genes from one or more of these chromosomes. Detection of aneuploidy in this way has been described before²⁸. Note that the expression profiles shown in Figure 1A and B are the average of two independent colonies per mutant where no aneuploidy was observed. Since the detection of aneuploidy in DNA microarray experiments depends on singular events in the starting colonies, flow cytometric profiles were generated to examine the DNA content of individual cells (Figure 1D). In asynchronous cell cultures, *slx5Δ* and *slx8Δ* mutants are characterised by a large fraction of the cell population having a DNA content higher than 2N (19.2%, 16.5% and 2% in *slx5Δ*, *slx8Δ* and wt respectively). The flow cytometry therefore agrees with the aneuploidy observed in individual *slx5Δ* and *slx8Δ* microarray experiments. A colony colour assay was performed to measure the chromosome stability in *slx5Δ* and *slx8Δ*²⁹. Wt, *slx5Δ* and *slx8Δ* cells, bearing the *ochre* mutation *ade2-101*, were complemented with a reporter chromosome bearing the *SUP11* gene that suppresses the red colour (Figure 1E). Neither *slx5Δ* nor *slx8Δ* show increased red-sectoring compared to wt, indicating that the reporter chromosome segregates normally. The aneuploidy in *slx5Δ* and *slx8Δ* is therefore not caused by chromosome loss or nondisjunction.

Slx5 resides at the centromere

To further elucidate the function of Slx5/8, their location on DNA was investigated by genome-wide chromatin immunoprecipitation (ChIP-chip). This was motivated by the observation that previously reported roles of Slx5/8, such as transcription^{8,22-24} and DNA repair^{11,12,16}, may be associated with location on DNA. Slx5 and Slx8 were C-terminally fused to GFP by genomic integration, resulting in expression at endogenous levels. ChIP-chip reveals the presence of 17 distinct binding peaks for Slx5 (Figure 2A). Strikingly, each Slx5 peak maps to a different chromosome and coincides exactly with the location of the centromere. One exception is chromosome IV, where a second smaller Slx5 peak is detected (Figure 2A). As opposed to Slx5, Slx8 did not show enrichment at centromeres. For example, whereas chromosome I shows a single centromeric Slx5 peak, we did not detect any coinciding Slx8 signal (Figure 2B and C). Other genomic locations, such as ORFs, promoters, (sub-)telomeres, ARS, or rDNA, do not show notable enrichment for Slx5 or Slx8.

Centromeres play a key role in chromosome segregation. They provide the binding site for the kinetochore, which physically connects centromeres to microtubules, allowing segregation of sister chromatids during mitosis and meiosis³⁰. The centromeres of budding yeast are small (~120 bp) and known as point centromeres. Each Slx5 peak is characterised by enriched signals on three to five consecutive microarray probes that span a centromere (e.g. Figure 2C). An average centromere binding profile was generated by mapping all (peri-) centromeric probes relative to their respective centromere (Figure 2D). Slx5 enrichment is centred on the core centromere, without global enrichment of the entire 10 kb pericentromeric region. We compared the binding profile of Slx5 to a known kinetochore component, Ndc10, which is the centromere DNA binding subunit of the kinetochore³¹. Strikingly, the binding pattern of Slx5 is equivalent to Ndc10, showing that Slx5 is preferentially located at the core centromere (Figure 2D). Centromeric

location of Slx5 was further confirmed by ChIP quantitative real-time PCR. Slx5 and Ndc10 are highly enriched at all centromeres tested (Figure 2E and F), in agreement with the genome-wide experiments. Mock ChIPs, Slx8 and an untagged wt strain show no centromeric enrichment (Figure 2E-H), confirming the specific location of Slx5 to centromeres.

The subcellular localisation of Slx5 was investigated further by fluorescence microscopy (Figure 3A). Slx5 has a diffuse nuclear location with occasional subnuclear foci. This is similar to other studies, where Slx5 is shown to have a diffuse nuclear location with DNA foci at DNA repair centres¹⁶. We investigated whether Slx5 foci also colocalise with centromeric regions, as marked by kinetochore

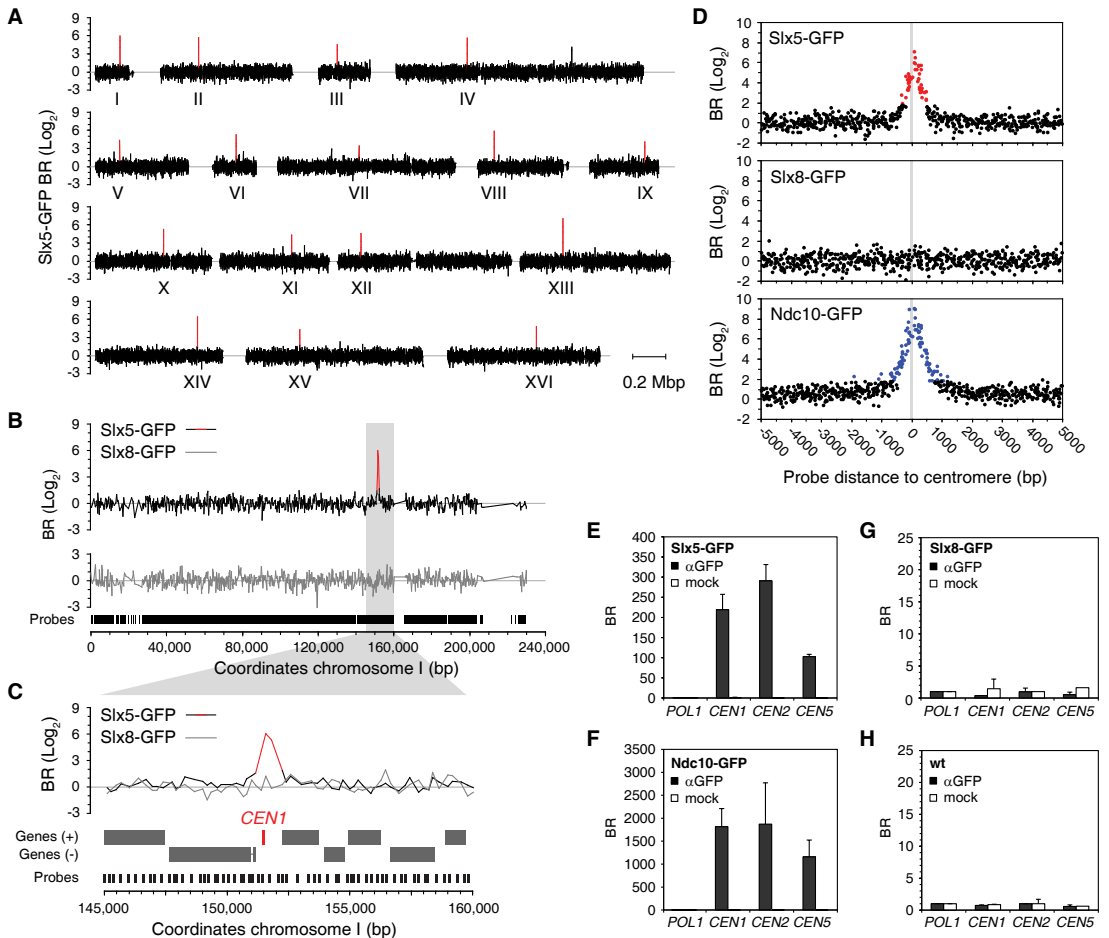


Figure 2. Slx5 resides at centromeres.

(A) ChIP-chip analysis of Slx5. Binding ratios (BR) of individual probes are mapped to the 16 chromosomes of the *S. cerevisiae* genome. BR is expressed as log₂ value of αGFP ChIP/input with subtraction of the mock/input signal. The positions of the centromeres are marked I to XVI. (B) Binding profile of Slx5 and Slx8 at chromosome 1. The genomic region shown in grey is magnified in (C). (D) Average centromeric binding profiles of Slx5, Slx8 and Ndc10. Signals from microarray probes are mapped relative to their position to the centromere and all probes are included that map to within 5000 bp of all 16 centromeres. Probes with a BR (log₂) >2 are shown in red (Slx5) or blue (Ndc10). (E-H) ChIP-qPCR of Slx5 (E), Ndc10 (F), Slx8 (G) and wt (H). BRs at centromere 1, 2, and 5 are normalised to the control gene *POL1* (± s.d., n = 3).

subunit Nnf1 (Figure 3A). Strict colocalisation of the Slx5 foci with Nnf1 was not observed. Although in rare cases Slx5 foci do overlap with the kinetochore (Figure 3A, cell a) it cannot be ruled out that they may represent cases where a DNA break is in close proximity to the centromere. This indicates that the centromeric pool of Slx5 cannot be distinguished visually by fluorescence microscopy and that it is likely part of the diffuse nuclear Slx5 pool (Figure 3A, cell b).

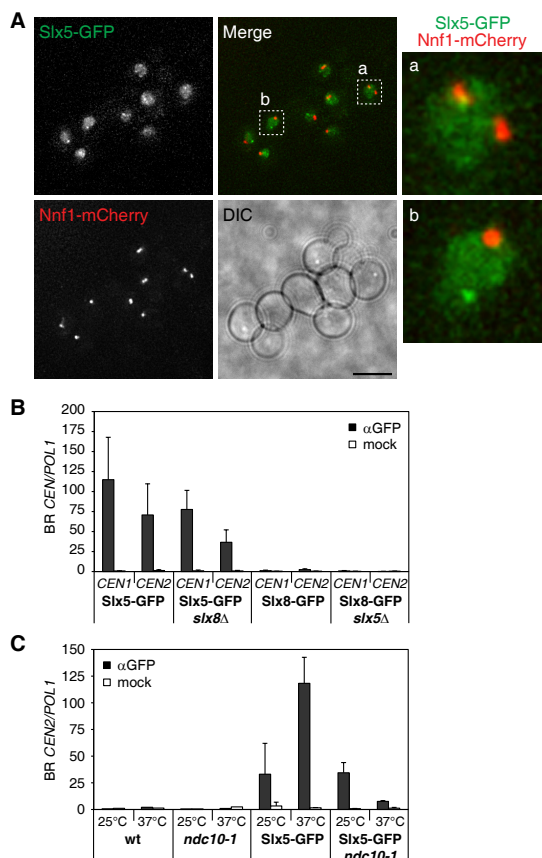


Figure 3. Slx5 binding to centromeres is largely kinetochore-dependent.

(A) Live cell microscopy of cells coexpressing Slx5-GFP and kinetochore protein Nnf1-mCherry. Right-hand panel shows a magnification of two nuclei, indicated in the merged image. Scale bars, 5 μ m. (B) ChIP-qPCR of Slx5-GFP and Slx8-GFP in wt, *slx5Δ* or *slx8Δ* strains. Binding ratios (BR) at *CEN1* and *CEN2* are represented as enrichment over the control gene *POL1* (\pm s.d., $n = 4$), based on two independent biological replicate experiments. (C) ChIP-qPCR of Slx5-GFP in wt and *ndc10-1* strains at permissive (25°C) and nonpermissive (37°C) temperatures. Data is represented as enrichment at *CEN2* over *POL1* (Slx5-GFP and Slx5-GFP *ndc10-1*: \pm s.d., $n = 2$) (wt and *ndc10-1*: $n = 1$, no enrichment).

We next tested the dependency of the Slx5 centromeric location on other proteins by ChIP. Slx5 binding to centromeres is hardly reduced in the absence of *SLX8* (Figure 3B). This agrees with previous observations showing that Slx5 still forms nuclear foci and binds to DNA breaks without Slx8¹⁶. Slx8 also remains absent from centromeres upon deletion of *SLX5* (Figure 3B). To investigate whether centromere location of Slx5 is kinetochore-dependent, a ChIP was performed in the *ndc10-1* mutant, which is defective in kinetochore assembly at a nonpermissive temperature³¹. Centromeric binding of Slx5 is nearly completely eliminated when shifting Slx5-GFP *ndc10-1* cells from 25°C to 37°C (Figure 3C). There is some residual binding, indicating that although centromere location of Slx5 is largely kinetochore-dependent, additional kinetochore-independent interactions may also be involved.

Rts1 accumulates at kinetochores in *slx5Δ* and *slx8Δ* metaphase cells

A role for Slx5/8 that is associated with a centromeric location is particularly interesting since this may better explain the genome stability defects of *slx5Δ* and *slx8Δ* mutants. Since many different regulatory pathways influence chromosome segregation, a candidate-based approach was adopted to determine factors that may be involved in the same pathway as Slx5/8, focusing in particular on potential targets. In yeast, kinetochore proteins Ndc10, Cep3 and Bir1 are sumoylated and Ndc10 interacts with Slx5 by yeast two-hybrid³². Changes in protein levels or subcellular location in *slx5/8* mutants were not found for any of these candidates (Supplementary Figure S1). Mutations in most centromere components display either no or only weak negative synthetic

genetic interactions with *slx5Δ* and *slx8Δ*^{33,34}. Positive genetic interactions are more likely indicative of gene products functioning in the same protein complex or pathway. It was therefore of interest that *RTS1*, a regulatory subunit of the PP2A phosphatase³⁵, was

found to have positive genetic interactions with both *SLX5* and *SLX8* in a high-throughput genetic interaction map³³. *Rts1Δ* also has a similar mRNA expression phenotype as *slx5Δ* and *slx8Δ* (Figure 1B). To confirm the genetic interaction, single and

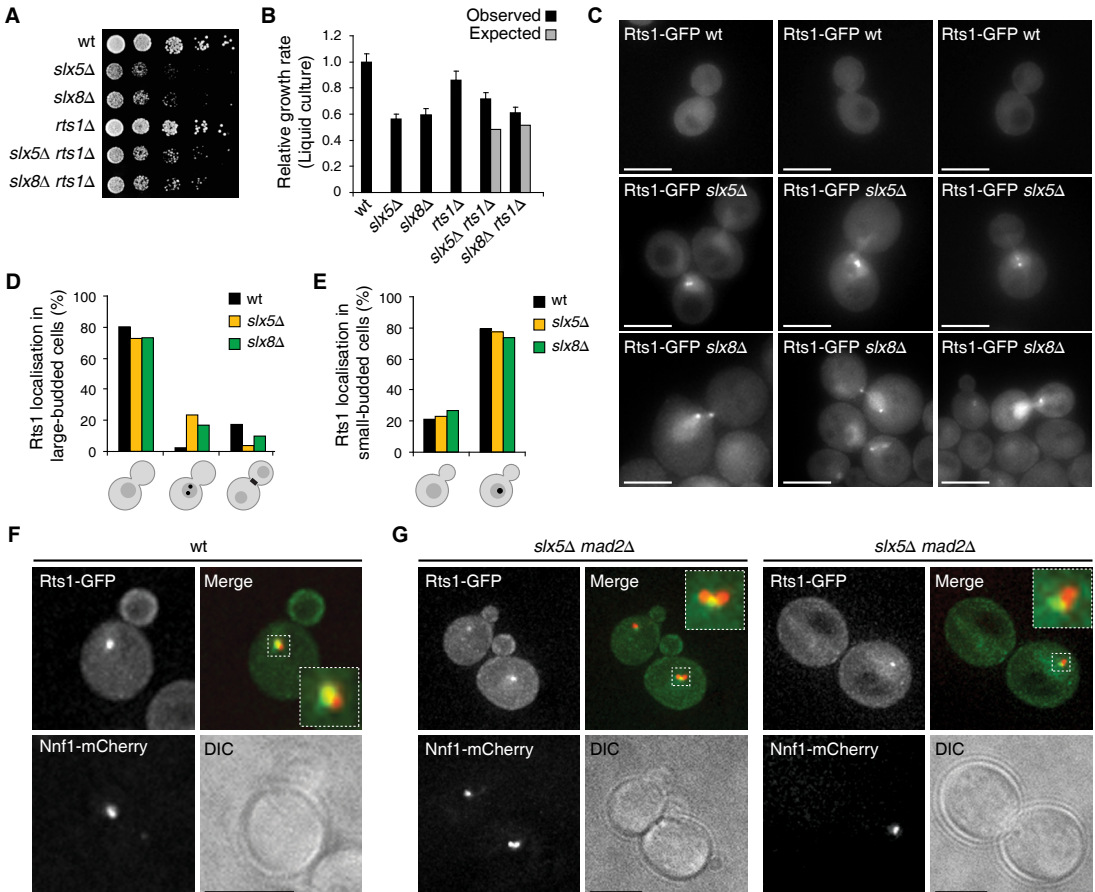


Figure 4. *Slx5Δ* and *slx8Δ* mutants accumulate *Rts1* at kinetochores during metaphase.

(A) Growth rate of cells spotted in five-fold serial dilutions on YPD plates. Images are after two days of growth at 25°C. (B) Growth rate of yeast in liquid YPD media. Relative growth rate (mutant/wt) was quantified during mid-log phase (\pm s.d., $n = 6$). Expected relative growth rates (RGR) of the double deletion mutants are calculated by multiplying the observed RGRs of the single deletion mutants. (C) Live cell microscopy of large-budded wt, *slx5Δ* and *slx8Δ* cells expressing *Rts1*-GFP. Nuclear *Rts1* foci are detected in *slx5Δ* and *slx8Δ*, which are absent in large-budded wt cells. Scale bars, 5 μ m. (D-E) Quantification of subcellular *Rts1* location in wt, *slx5Δ* and *slx8Δ* cells. An asynchronous cell population ($n > 200$ cells) was morphologically divided in small-budded (G1-S phase) and large-budded (G2/M phase) cells. Diffuse *Rts1* location in nucleus and cytoplasm is schematically indicated in grey. Presence of one or two *Rts1* foci is schematically indicated as black nuclear dots. Enrichment of *Rts1* at the bud neck is indicated as a black bar. *Rts1* foci were not detected in nonbudded cells. (F-G) Live cell fluorescence microscopy of wt (F) and *slx5Δ mad2Δ* cells (G), expressing *Rts1*-GFP and kinetochore protein *Nnf1*-mCherry. The small-budded wt has a normal centromeric *Rts1* focus. Note that *Rts1* is also enriched at the bud membrane. The left panel in (G) shows two small-budded *slx5Δ mad2Δ* cells with normal *Rts1* foci that colocalise with kinetochores. The right panel in (G) shows a large-budded *slx5Δ mad2Δ* cell with an aberrant, mislocalised centromeric *Rts1* focus during metaphase. Scale bars, 5 μ m.

double deletion strains were generated and growth was examined on solid medium (Figure 4A) and quantified in liquid cultures (Figure 4B). The double mutants *slx5Δ rts1Δ* and *slx8Δ rts1Δ* indeed grow better than is expected from the growth of single deletion mutants, confirming the positive synthetic genetic interactions of the pairs *RTS1-SLX5* and *RTS1-SLX8*.

Rts1 is a very dynamic centromeric protein that localises to specific subcellular sites in mitotic cells in a cell cycle-dependent manner^{36,37}. Rts1 localises to kinetochores in small-budded cells, then disappears and relocates to the bud neck in large-budded cells during cytokinesis³⁷. We investigated the localisation of Rts1-GFP in asynchronous wt, *slx5Δ* and *slx8Δ* cells using live cell fluorescence microscopy. Strikingly, a subpopulation of large-budded *slx5Δ* and *slx8Δ* cells are characterised by the presence of aberrant Rts1 foci (Figure 4C and D). These Rts1 foci are rarely observed in large-budded wt cells. The cells presenting these foci appear arrested in metaphase and typically have one or two Rts1 foci. The Rts1 foci in small-budded *slx5Δ* and *slx8Δ* cells are indistinguishable from wt (Figure 4E). The foci colocalise with the kinetochore protein Nnf1 (Figure

4F and G), demonstrating that Rts1 accumulates at centromeres during metaphase in *slx5Δ* and *slx8Δ* cells. Deletion of the Spindle Assembly Checkpoint (SAC) component *MAD2* does not affect the location of Rts1 (Figure 4G), indicating that the centromeric location of Rts1 during metaphase is independent of the SAC.

The centromeric accumulation of Rts1 in metaphase suggests the presence of a defect in *slx5/8* mutants that prevents the removal of centromeric Rts1 after recruitment during S-phase. Since the recruitment of Rts1 in meiotic cells is dependent on the centromere cohesion regulator Shugoshin (Sgo1)³⁸, we also investigated whether this is the case in mitotic cells. Deletion of *SGO1* results in a slow growth phenotype (Figure 5A). The Rts1 foci in *sgo1Δ* cells are less bright, indicating that Sgo1 promotes Rts1 recruitment to kinetochores in mitotic cells too (Figure 5B and C). Similarly, deletion of *SGO1* in *slx5Δ* cells results in Rts1 foci in large-budded cells that are less bright and also reduced in number (Figure 5B and C), showing that the aberrant Rts1 foci in *slx5Δ* are also partially Shugoshin-dependent.

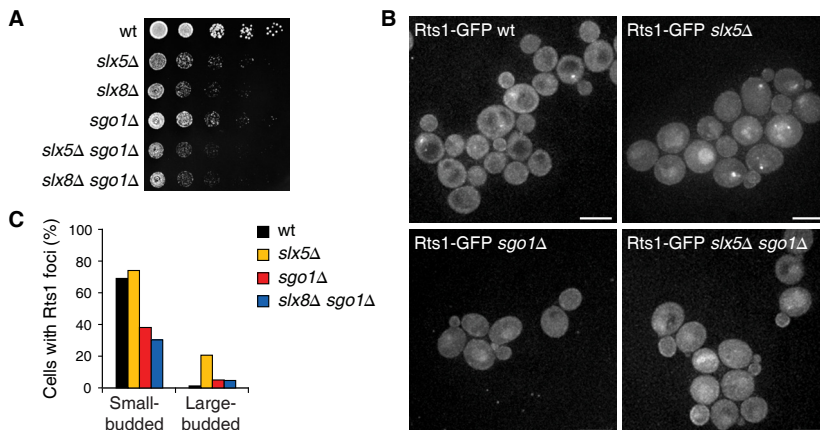


Figure 5. Rts1 foci are partially Shugoshin (Sgo1)-dependent.

(A) Growth rate assay of cells spotted in five-fold serial dilutions on YPD plates. Images are after two days growth at 25°C. (B) Live cell fluorescence microscopy of asynchronous wt, *slx5Δ*, *sgo1Δ* and *slx5Δ sgo1Δ* cells expressing Rts1-GFP. Scale bars, 5 μm. (C) Quantification of Rts1 foci in cells, shown in (B). Quantification is based on an asynchronous cell population (n = 89–203), that was morphologically divided in a small-budded and large-budded cell population.

***Slx5*Δ and *slx8*Δ have aberrant spindle positioning, morphology and elongation kinetics**

In addition to the accumulation of Rts1 at the kinetochore during metaphase, a change in mitotic spindle morphology was observed in both *slx5*Δ and *slx8*Δ. The spindle morphology and

dynamics were investigated in more detail using time-lapse video microscopy of asynchronous cell populations expressing GFP-Tub1 (Figure 6A). Cells were imaged at 2 minute intervals to capture the progression from metaphase into anaphase. *Slx5*Δ and *slx8*Δ arrest temporarily in mitosis as large-budded cells with short mitotic spindles and have an

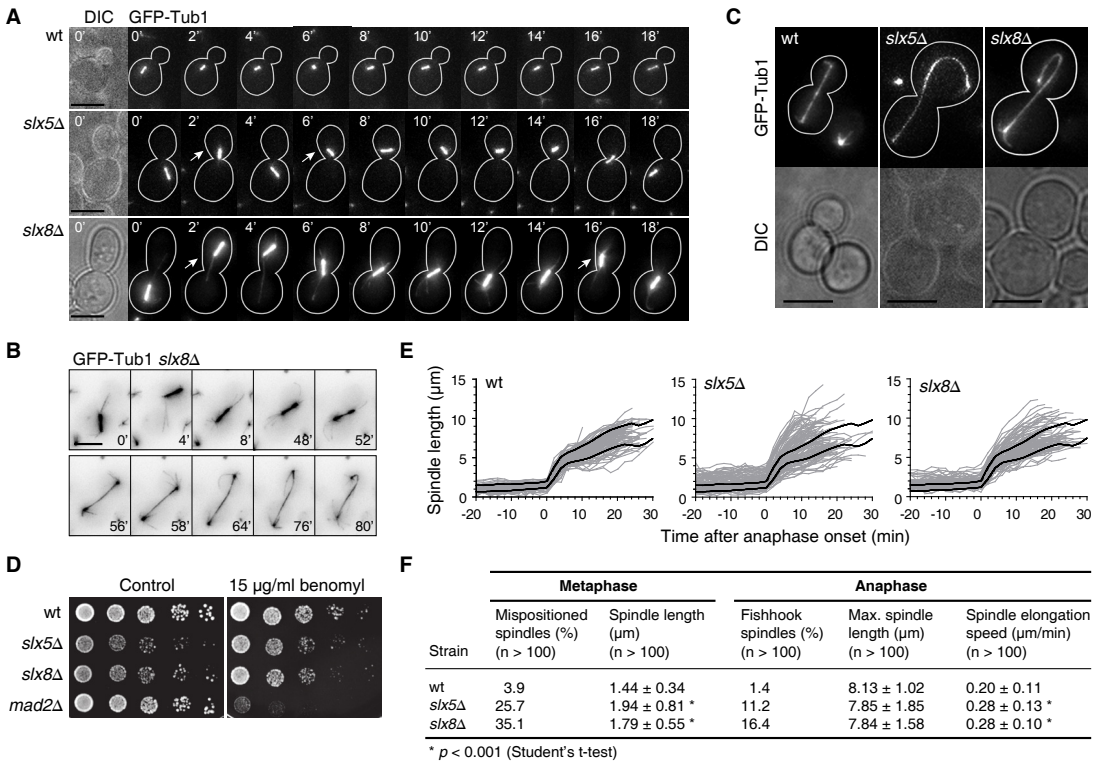


Figure 6. Mitotic spindle defects in *slx5*Δ and *slx8*Δ mutants.

(A) Time-lapse video microscopy of wt, *slx5*Δ and *slx8*Δ cells expressing GFP-Tub1. The upper panel shows a metaphase spindle in a wt cell at 2 minute intervals. Spindle elongation is initiated at t = 18'. The two panels below show examples of aberrant positioning of metaphase spindles in *slx5*Δ and *slx8*Δ cells during a temporary metaphase arrest. Arrows indicate spindle dislocation from the bud neck. Contours of cells are marked with a white line and are based on the DIC image. Scale bars, 5 μm. (B) Example of a spindle in *slx8*Δ, followed from metaphase to late anaphase. Colours are inverted to increase visibility of the astral microtubules at the outer tips of the spindle. The cell has a prolonged metaphase (t = 0'-52') during which the spindle dislocates into the bud (t = 4'). Entry into anaphase is initiated at t = 52', followed by spindle extension (t = 54'-80'). Formation of a fish hook spindle is apparent during late anaphase (t = 76'-80'). Scale bar, 5 μm. (C) Examples of fish hook spindles in *slx5*Δ and *slx8*Δ and a normal elongated spindle in wt during late anaphase. Scale bars, 5 μm. (D) Benomyl sensitivity assay. Growth rate of yeast cells is measured on YPD plates complemented with benomyl or DMSO (control). Images are after two days growth at 30°C. The benomyl-sensitive SAC mutant *mad2*Δ is included as control. (E) Quantification of spindle length, defined as the distance between two spindle pole bodies in wt, *slx5*Δ and *slx8*Δ expressing Spc42-GFP. Spindle length (n > 100) was quantified from 20 minutes before anaphase onset to completion of anaphase. Grey lines depict the spindle length of individual cells. Black lines represent the average wt spindle length ± s.d., which is also shown as reference in the *slx5*Δ and *slx8*Δ plots. (F) Quantifications of spindle phenotypes in wt, *slx5*Δ and *slx8*Δ during metaphase and anaphase.

average mitotic delay of 80 minutes compared to wt (Supplementary Figure 2A). During mitotic arrest, the cells are characterised by a spindle positioning defect in which the mitotic spindle fails to position itself stably at the bud neck (Figure 6A). Instead, the spindle oscillates heavily and frequently dislocates completely away from the bud neck, either shooting back into the mother cell or into the daughter bud. The mispositioned spindles are often accompanied by elongated astral microtubules (Figure 6A and B), which contribute to spindle positioning³⁹. Around 30% of the *slx5Δ* and *slx8Δ* cells show spindle dislocation prior to entry into anaphase. This suggests that the mitotic delay in *slx5Δ* and *slx8Δ* is due to a failure in spindle positioning.

A second aberrant spindle phenotype was observed during anaphase. So-called ‘fish hook’ spindles form in 11% and 16% of the *slx5Δ* and *slx8Δ* anaphase cells respectively (Figure 6C). The formation of fish hook spindles can be a consequence of overstable microtubules and are observed in mutants of microtubule-associated proteins and kinetochore components⁴⁰. Neither *slx5Δ* nor *slx8Δ* shows sensitivity or resistance to treatment with the microtubule-destabilising agent benomyl, suggesting that the stability of microtubules is actually normal (Figure 6D). Also the duration of anaphase in the mutants is not significantly different from wt (Supplementary Figure S2B). Moreover, *slx5Δ* and *slx8Δ* do not interact genetically with SAC component *MAD2* and deletion of *MAD2* is not sufficient to overcome the mitotic arrest in *slx5Δ* and *slx8Δ* (Supplementary Figure S2C and D). This indicates that microtubule-kinetochore interactions in *slx5Δ* and *slx8Δ* are normal and that Slx5/8 does not take part in the SAC signalling pathway.

The aberrant spindle morphology in *slx5Δ* and *slx8Δ* cells prompted us to investigate spindle dynamics. To analyse spindle elongation dynamics during chromosome segregation, strains expressing Spc42-GFP were imaged by time-lapse video microscopy. Spc42-GFP fluorescently labels the spindle pole bodies at the outer ends of the spindle. The spindle length was measured by determining

the spindle pole body distance from metaphase until late anaphase (Figure 6E and F). The average wt spindle length in metaphase is $1.44 \mu\text{m} \pm 0.34$. Upon entry into anaphase this quickly increases to a maximum length of $8.13 \mu\text{m} \pm 1.02$ after ~20 minutes. In contrast, the spindle length in *slx5Δ* and *slx8Δ* is very heterogeneous during metaphase and anaphase (Figure 6E). In metaphase, the average spindle length is 30% longer than wt, $1.94 \mu\text{m} \pm 0.81$ and $1.79 \mu\text{m} \pm 0.55$ for *slx5Δ* and *slx8Δ* respectively. During anaphase, the maximum spindle length measured in *slx5Δ* and *slx8Δ* is on average not significantly different from wt, but in mid-anaphase, the spindle length clearly deviates (Figure 6E and F). In *S. cerevisiae*, spindle elongation during anaphase B occurs in two phases, a quick elongation during early anaphase and a slower elongation during mid- and late anaphase³⁹. Interestingly, *slx5Δ* and *slx8Δ* mutants show a continuous quick spindle elongation during mid-anaphase, whereas the wt reduces its spindle elongation speed (Figure 6E). The average spindle elongation speed was measured during mid-anaphase and is $0.28 \mu\text{m}/\text{min} \pm 0.13$ and $0.28 \mu\text{m}/\text{min} \pm 0.10$ for *slx5Δ* and *slx8Δ* respectively. This is 40% faster than wt, which has a spindle elongation rate of $0.20 \mu\text{m}/\text{min} \pm 0.11$ (Figure 6F). The duration of anaphase in the mutants was not significantly different from wt (Supplementary Figure S2B). The aberrant spindle morphology in *slx5/8* mutants is therefore associated with changes in spindle kinetics during anaphase.

Loss of hRNF4 results in chromosome missegregation due to chromosome bridges

The changes in spindle morphology and elongation dynamics in *slx5/8* mutants indicate a defect during anaphase. Since the microtubule stability itself is unaffected, it suggests that this phenotype is more likely a response to a defect during chromosome segregation. The formation of fish hook spindles, in combination with an increase in spindle elongation speed, suggests that *slx5Δ* and *slx8Δ* cells have an increased need for spindle pulling force in order to separate their sister chromatids during anaphase.

The small size of *S. cerevisiae* does not readily allow high-resolution morphological examination of the sister chromatids during chromosome segregation to test this hypothesis. We therefore used human HeLa cells, also to investigate whether the STuBL orthologue hRNF4 has a related role in chromosome segregation. Biochemically, hRNF4 functions in a manner that is analogous to the Slx5/8 complex in *S. cerevisiae*^{17,18}, but there is as yet little evidence for a role of hRNF4 in genome stability. RNF4 was depleted from H2B-EYFP expressing HeLa cells (Figure 7A and B). While there are no discernible defects in chromosome alignment, mitotic timing or mitotic checkpoint function, the frequency of lagging chromosomes in anaphase increased three-

to six-fold with different siRNA oligos (Figure 7C). Though most segregation defects are minor, anaphase bridges persisting into telophase can be discerned (Figure 7A). More detailed examination in fixed cells shows lagging chromosomes in early anaphase, with persistent chromosome bridges in late anaphase (Figure 7D). The percentage of anaphases with lagging chromosomes in fixed cells resembles that observed in live cell imaging (Supplementary Figure S3). The genomic instability during anaphase and telophase upon RNF4 knockdown agrees with the phenotypes of yeast *slx5Δ* and *slx8Δ* mutants. This demonstrates that Slx5/8 and hRNF4 have an evolutionarily conserved role in maintaining genome integrity during mitosis.

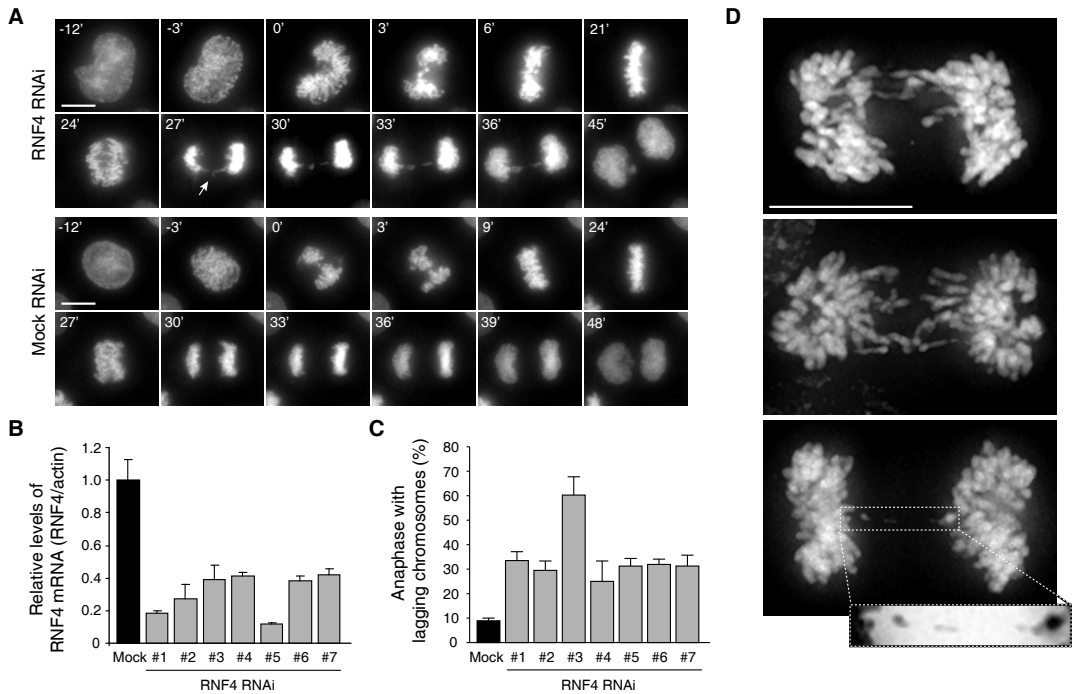


Figure 7. RNF4 depletion causes chromosome segregation errors.

(A) Time-lapse video microscopy of H2B-EYFP HeLa cells transfected with RNF4 siRNA or mock. Arrow indicates a chromosome bridge. Time (minutes) is given relative to the first time frame in prometaphase. Scale bars, 10 μ m. (B) RNF4 knockdown efficiency determined by reverse transcription qPCR. cDNA was prepared from H2B-EYFP HeLa cells transfected with siRNAs targeting RNF4 or mock siRNA. mRNA levels of *RNF4* and β -*ACTIN* were analysed by qPCR. Graph represents a single experiment, showing three technical replicates (\pm s.d.). (C) Quantification of chromosome segregation defects of H2B-EYFP HeLa cells, as shown in (A), transfected with different siRNAs as indicated. Graph represents the average of two independent experiments per siRNA (\pm s.d.) and at least 72 cells per siRNA. (D) Three examples of anaphase cells with lagging chromosomes in fixed HeLa cells transfected with RNF4 siRNA oligos. Inset (negative stain) shows a persistent chromatin bridge. Scale bars, 10 μ m.

DISCUSSION

STuBLs such as Slx5/8 and RNF4 are a relatively new class of modifying enzymes, special in their ability to ubiquitinate proteins that have already been modified through sumoylation^{7,8}. Key questions regarding their cellular function and mechanism of action are unanswered. The results presented here address the cellular role of Slx5/8 in particular. Previous studies have postulated a role for Slx5/8 in regulation of transcription, through contributions to silencing²² and turnover of transcription factors^{8,23,24}. Although the DNA microarray analyses show that loss of either *SLX5* or *SLX8* results in upregulation of numerous genes, the majority of this transcriptional response is similar to the environmental stress response²⁵ and is in fact also common to inactivation of several different genome integrity pathways. Although this does not completely rule out a role for Slx5/8 in regulating gene expression, an important conclusion is that under the conditions of these experiments, the majority of gene expression changes observed upon deletion of *SLX5* or *SLX8* is likely an indirect effect of genome instability-induced stress.

An important finding presented here is the location of Slx5 at centromeres, since this may provide more focus for seeking relevant *in vivo* substrates. Interestingly, RNF4 has recently been shown to regulate the turnover of the human kinetochore protein CENP-I⁴¹. In yeast, the kinetochore protein Ndc10 has been reported to be sumoylated and to interact with Slx5³². We have already undertaken several candidate-based approaches to find *in vivo* targets, focusing on candidates with roles at centromeres, with synthetic genetic interactions with *SLX5* and *SLX8*, and that are known to be ubiquitinated and/or sumoylated. Changes in protein levels, modifications or subcellular location in *slx5Δ* and *slx8Δ* mutants were not found for any of the candidates tested, including the kinetochore proteins Ndc10, Cep3 or Bir1. The PP2A regulatory subunit *RTS1* was found to genetically interact with *SLX5/8* and aberrantly accumulates at kinetochores during metaphase in *slx5Δ* and *slx8Δ*. Rts1 is

involved in different cellular pathways, including the Spindle Position Checkpoint (SPOC)⁴². The SPOC is important for inhibiting mitotic exit when the anaphase spindle is misaligned along the polarity axis of the yeast cell⁴³. Both *slx5Δ* and *slx8Δ* display aberrant spindle elongation kinetics and fish hook spindles in anaphase, but the positioning of the anaphase spindle is normal. There is also no delay in mitotic exit. The spindle positioning defects are exclusively observed during metaphase, which makes it unlikely that SPOC activation by PP2A^{Rts1} explains the anaphase defects of *slx5Δ* and *slx8Δ*. A more likely hypothesis is that the centromeric accumulation of PP2A^{Rts1}, which is partly dependent on Sgo1, involves the tension sensing pathway. Sgo1 senses whether cells have established correct kinetochore-microtubule interactions and regulates their progression into mitosis. Cells with unattached sister chromatids lack tension at the centromeres, leading to activation of the spindle assembly checkpoint and inhibition of entry into anaphase⁴⁴. Rts1 is recruited to the centromere by Sgo1 to protect centromeric sister chromatid cohesion³⁸. Possibly, *slx5Δ* and *slx8Δ* activate the tension sensing pathway to prevent cleavage of cohesion and thereby arrest in mitosis. Indeed, observation of the Rts1 foci in *slx5Δ* and *slx8Δ* metaphase cells reveal that there is a large variability in the distance between the centromeric Rts1 foci of the sister chromatids (Figure 4C), which suggests that there is loss of centromere tension. The underlying cause that potentially triggers the tension checkpoint in *slx5Δ* and *slx8Δ* is still unclear. Slx5/8 themselves are unlikely to take part as mitotic checkpoint components, since they do not show genetic interactions with *MAD2* and are insensitive to benomyl treatment.

Several studies point to a role for Slx5/8 in the DNA damage response^{5,6,11,12,16}. Loss of Slx5/8 function is thought to predominantly affect DNA replication, as this process greatly depends on accurate repair of DNA lesions that naturally occur during replication. It is therefore striking to see that the *slx5Δ* and *slx8Δ* mutant phenotypes revealed here, such as aberrant spindles and Rts1 retention,

are exclusively observed during mitosis. High-resolution morphological examination of HeLa cells after RNF4 knockdown reveals the presence of lagging chromosomes and chromosome bridges, indicating that DNA damage arises during mitosis. It is unclear whether chromosome bridges also form in *slx5Δ* and *slx8Δ*. However, the altered kinetics of spindle elongation in *slx5Δ* and *slx8Δ* is suggestive of a defective separation of sister chromatids, reminiscent of chromosome bridges upon RNF4 knockdown. The source of DNA damage in *slx5Δ* and *slx8Δ* may therefore actually be the impaired segregation of chromosomes rather than defective repair of DNA replication-associated damage. We do not rule out that the origin of the defects may lie in S-phase. For instance, defective DNA decatenation during DNA replication may go unnoticed until the DNA is physically pulled apart during mitosis, ultimately leading to chromosome breaks⁴⁵. Given the synthetic lethal genetic interactions of *SLX5/8* with members of the RecQ family of DNA helicases⁵, *Slx5/8* may contribute to DNA decatenation, which may lead to chromosome segregation errors and DNA breaks. Moreover, the *slx5Δ* and *slx8Δ* mutants arrest in metaphase, which clearly indicates a cellular defect that precedes the separation of sister chromatids. Previously reported roles of *Slx5/8* in DNA repair and replication may therefore be directly linked to the mitotic defects observed in this study.

It is also possible that defects in DNA repair or replication and the mitotic defects represent distinct functions of *Slx5/8*. Whereas ChIP analysis shows that *Slx5* resides at centromeres, localisation studies using fluorescence microscopy show a predominantly diffuse nuclear localisation with occasional occurrence of subnuclear foci that do not strictly colocalise with kinetochores. The foci likely represent DNA replication and repair centres¹⁶, which would agree with distinct functions for *Slx5/8* in various cellular processes. Loss of *Slx5/8* function also results in general accumulation of SUMO-conjugated protein species^{7,8}, suggesting that *Slx5/8* targets multiple substrates for proteasomal degradation, rather than controlling

a single substrate or pathway. The lack of *Slx5* and *Slx8* colocalisation at centromeres is unexpected given that *Slx5/8* is thought to function as a heterodimeric complex^{7,8}. It suggests that only *Slx5* is stably associated with the centromere, where it may function independently of *Slx8* or serve to recruit *Slx8* in a transient manner. We favour the latter hypothesis, based on the complete overlap of mitotic phenotypes of *slx5Δ* and *slx8Δ* mutants. Regulatory control of proteins through sumoylation is well-established to be important for several (nuclear) processes, including transcription, DNA repair and chromosome organisation³. The results presented here will therefore also aid future studies aimed at identification of relevant *in vivo* substrates of *Slx5/8* and RNF4, by focusing on the centromere-specific location and mitotic defects reported here.

MATERIALS and METHODS

Yeast strains and media

All strains are isogenic with S288c. Yeast strains and their genotypes are listed in Supplementary Table S2. Deletion strains used for microarray expression profiling were from the *Saccharomyces* Genome Deletion library (Open Biosystems; Euroscarf) and are in the genetic background of the wt parental strain BY4742. *SLX5* and *SLX8* deletion mutants were generated by PCR-based gene disruption using pFA6a deletion cassettes⁴⁶. Single and double deletion mutants used for assaying synthetic genetic interactions were created by PCR-based gene disruption of *SLX5* or *SLX8* in the heterozygote diploid deletion strains *MAD2/mad2Δ*, *RTS1/rtslΔ* and *SGO1/sgo1Δ* (BY4743; Open Biosystems), followed by tetrad dissection of sporulated diploids using standard genetic techniques. We noted that spores derived from *SGO1/sgo1Δ* had a strong reduction in viability and aberrant segregation of the mutant alleles. Accurate gene disruption and absence of wt alleles were confirmed by PCR. *Slx5*-GFP and *Slx8*-GFP strains were constructed by C-terminal genomic integration of a pFA6a-GFP-His3MX6 cassette⁴⁶. All epitope- or fluorescent-tagged strains exhibited wt growth with the exception of *Slx5*-GFP. All attempts to fuse *SLX5* to a variety of tags, either C- or N-terminally, resulted in strains with slow growth. All other epitope-tagged strains exhibited wt growth. *Rts1*-GFP was obtained from the GFP-tagged yeast collection⁴⁷. *Nnf1*-mCherry was constructed by replacing the GFP tag from *NNF1-GFP::His3MX6*⁴⁷ for mCherry::KanMX4. *Ndc10*-GFP, *Cep3*-GFP and *Bir1*-GFP strains were a kind gift of B. Montpetit³². *Spc42*-GFP (YYB3283) and GFP-Tub1 (YYB2327) are derived from previously described strains^{48,49}. The *ndc10-1* mutation was described previously³¹. Coloured

colony strains were generated by backcrossing *slx5Δ* and *slx8Δ* (BY4742) twice in the genetic background of strain YJB3085⁵⁰. Experiments were performed in synthetic complete (SC) or yeast extract-peptone-dextrose (YPD) media (US Biologicals) containing 2% glucose.

Gene expression profiling

Microarray expression profiling was performed as described previously⁵¹. In brief, mutant and wt strains were grown at 30°C in SC media with 2% glucose and harvested in early mid-log phase. Dual-channel 70-mer oligonucleotide arrays were employed with a common reference wt RNA. All steps after RNA isolation were automated using robotic liquid handlers. After quality control, normalisation and dye-bias correction⁵², statistical analysis was performed for each mutant versus a collection of 200 wt cultures. The reported FC is an average of four replicate mutant gene expression profiles versus the average of all wts. Fifty-eight genes that showed stochastic changes in wt profiles (wt variable genes)⁵³ were excluded from further downstream analyses. Clustering of the microarray expression profiles was performed using an unsupervised hierarchical cosine correlation, based on all significant genes (FC > 1.7, $p < 0.05$), excluding wt variable genes and deleted genes. The data is visualised using JavaTreeview⁵⁴ and GeneSpring (Agilent) software. Microarray data has been deposited in the public data repositories ArrayExpress and GEO under accession numbers E-TABM-1221 and GSE33929. The data are also available in flat-file from http://www.holstegelab.nl/publications/slx5_slx8.

Functional enrichment analyses

Enrichment analysis of GO-terms⁵⁵ and transcription factor binding sites²⁷ was performed on all significant genes in *slx5Δ* and *slx8Δ* (FC > 1.7, $p < 0.05$), excluding wt variable genes and deleted genes. The background gene population was set to 6,182 (the number of genes represented on the microarray) and p values are Bonferroni-corrected for multiple testing. Comparison with the general stress response is performed by a Pearson correlation analysis of the average *slx5Δ* and *slx8Δ* profile with a 30-minute heat shock condition²⁵.

ChIP-chip analysis

ChIP-chip was performed essentially as described previously⁵⁶, with minor modifications. Cells were grown in 500 ml SC medium to mid-log phase at 30°C. For analysis of the temperature sensitive *ndc10-1* mutant, cells were grown overnight at 25°C and subsequently for 6 hours at either 25°C or 37°C. Cells were crosslinked with 1% formaldehyde for 20 min at room temperature (RT). Glycine (300 mM) was added for 5 min at RT. Cells were harvested by centrifugation for 5 min at 4000 rpm at 4°C. The cell pellet was washed twice with cold TBS pH 7.5 (150 mM NaCl, 10 mM Tris), once with cold FA lysis buffer (50 mM HEPES-KOH pH 7.5, 150 mM NaCl, 1 mM EDTA, 1% Triton X-100, 0.1% sodium deoxycholate, 0.1% SDS), and resuspended in 1.5 ml FA lysis buffer complemented with Complete Protease Inhibitor Cocktail (Roche). Cells were disrupted with the Disrupter Genie (Scientific Industries)

using 0.5 ml zirconia beads (BioSpec Products Inc; Ø 0.5 mm) at 4°C. The cell lysate was centrifuged 2 min at 4000 rpm at 4°C. The supernatant was centrifuged 15 min at 14,000 rpm at 4°C to collect the chromatin. The chromatin pellet was washed 30 min in 1.5 ml FA lysis buffer at 4°C, resuspended in 1.5 ml FA lysis buffer, and sonicated (Bioruptor, Diagenode: 10 cycles, 30 sec on/off, medium setting) to an average DNA fragment size of ~400 bp. The lysate was centrifuged 20 min at 14,000 rpm at 4°C after which the supernatant (chromatin extract; CE) was collected for ChIP. ChIPs were performed by incubating 200 µl chromatin extract and 125 µg BSA to 20 µl Protein G-Agarose beads (Roche), coupled to rabbit polyclonal αGFP antibodies, for 2 h at RT. In parallel, mock ChIPs (no antibody) were performed on the same extracts. The beads were washed twice with 0.5 ml FA lysis buffer, twice in wash buffer 1 (FA lysis buffer, 500 mM NaCl), twice in wash buffer 2 (10 mM Tris pH, 0.25 mM LiCl, 0.5% Nonidet P-40, 0.5% sodium deoxycholate, 1 mM EDTA), and once in TE 10/1 (10 mM Tris pH 8, 1 mM EDTA). The beads were eluted twice in 50 µl TE 1% SDS (10 mM Tris pH 8, 1 mM EDTA, 1% SDS) for 10 min at 65°C. CHIP and input (20 µl CE) samples were incubated overnight in 100 µl TE 1% SDS and 10 µg ribonuclease A (Sigma) to reverse the formaldehyde cross-links. Samples were incubated with 400 µg proteinase K (Roche) for 2 hours at 37°C. For ChIP-chip, the proteinase K step was preceded by shrimp alkaline phosphatase (SAP) treatment by adding 1 ul of SAP (Roche) for 2 hours at 37°C. DNA was extracted with phenol-chloroform-isoamylalcohol (Sigma) and cleaned on PCR purification columns (Qiagen). Input and ChIP DNA was amplified using a robotically automated double-round T7 RNA polymerase-based amplification procedure⁵⁶. Cy5-labelled ChIP samples were hybridised with cy3-labelled input DNA to a high-resolution 44K 4-pack yeast array (Agilent Technologies). The microarray data was quantified and normalised using a density lowess-normalisation algorithm⁵⁷. ChIP/input and mock/input binding ratios were mapped to the ENSEMBL yeast genome EF 3 (February, 2011).

ChIP quantitative real-time PCR

Non-amplified input and ChIP DNA were analysed by qPCR using the iQ SYBR Green Supermix (Bio-Rad) in a CFX96 Real-Time PCR detection system (Bio-Rad). The PCR program was 95°C/10 min, 2 cycles of 95°C/15 sec, 50°C/30 sec, 72°C/30 sec and 45 cycles of 95°C/15 sec, 58°C/30 sec, 72°C/30 sec, followed by a melting curve to check for primer specificity. Primer sequences are listed in Supplementary Table S3. Binding ratios at centromeres are based on ΔCt-values (Ct ChIP/Ct input) and are presented as fold occupancy over the control gene *POLI*.

Flow cytometry

Cells were grown to early mid-log phase and either harvested directly as asynchronous cell population or synchronised in G1-phase by α-factor treatment (5 µg/ml; Zymo Research). Cells were released after 2.5 h in pre-warmed SC medium and harvested at 30 minute intervals. Cells (OD₆₀₀ 1.0) were washed twice in 1 ml FACS buffer (200 mM Tris, 20 mM

EDTA), resuspended in 100 μ l ribonuclease A (1 mg/ml in FACS buffer; Sigma) and incubated for 2 h at 37°C at 800 rpm. Cells were washed in phosphate-buffered saline (PBS) and stained in 100 μ l propidium iodide (50 μ g/ml in PBS; Molecular Probes) for 1 h at RT. Sample volume was increased to 1 ml with PBS and sonicated for 10 sec at 25% amplitude (Hielscher UP200S). DNA content was quantified by flow cytometry (FACSCalibur) and analysed using CellQuest 5.2.

Chromosome loss assay

Strains were grown in selective SC media lacking uracil for maintenance of the reporter chromosome and plated to single colonies on nonselective YPD plates. Colonies were allowed to grow for four days at 30°C. Red colour development was stimulated by incubating the plates one week at 4°C. The frequency of chromosome missegregation was quantified by colony half-sector analysis⁵⁸.

Yeast live cell imaging

Cells were grown asynchronously in SC medium to early mid-log phase at 30°C. Cells were transferred to a pre-warmed 8-well chambered glass-bottom Lab-TEK slide (Nunc) and covered with pre-warmed solid SC medium (5% agar). Cells were imaged on a DeltaVision RT system (Applied Precision), equipped with a heated chamber at 30°C, using a 100x/1.42-numerical aperture (NA) PlanApoN objective (Olympus). Images were acquired using Softworx software for deconvolution and are maximum intensity projections of all Z planes stacked at 0.3 μ m distance. Time-lapse video microscopy was performed by acquiring Z-stacks at 2 minute intervals for 2 - 3 hours. Images are processed in ImageJ and Adobe Photoshop CS2. Spindle length was quantified in ImageJ and defined as the distance between two spindle pole bodies (Spc42-GFP) from pixel to pixel with the highest intensity using Z-stack maximum intensity projections. Only cells for which a complete mitosis was captured were included in the analyses. Measurements were started 20 minutes before entry into anaphase and continued for maximally one hour. Metaphase cells are scored to have mispositioned spindles if the spindle showed one or more dislocation events from the bud neck into the bud or mother cell. Spindle oscillation at the bud neck without full dislocation was scored as normal. Spindle length in metaphase cells was measured 2-4 minutes before entry into anaphase. Cells displaying a bended spindle for at least two time frames were scored as having a fish hook spindles. Maximum spindle length in anaphase cells is measured in the last time frame before spindle shortening. Spindle elongation speed was measured in mid-anaphase from 4 to 12 minutes after start of anaphase.

Tissue culture, transfections and treatments

HeLa cells and HeLa cells stably expressing H2B-EYFP were grown in DMEM supplemented with 9% FBS and pen/strep (50 μ g/ml). Asynchronous cells were transfected twice with 40 nM siRNA (Supplementary Table S4) using HiPerfect (Qiagen). Following the first transfection, cells were treated with 2 mM thymidine (Sigma) for 24 h. Subsequently, cells

were transfected a second time and released into regular culture medium for 10 h. Cells were then treated with thymidine for 24 h and subsequently released into regular culture medium. For immunofluorescence microscopy, cells were fixed 12 h after the second release. RNF4 knockdown efficiency was measured by reverse transcription qPCR. Total rRNA was extracted using the RNeasy kit (Qiagen) including a DNase treatment step. Total RNA (250 ng) was used for cDNA synthesis (SuperScript II, Invitrogen). Expression of *RNF4* and β -*ACTIN* was analysed by qPCR (Supplementary Table S3) and normalised against a standard reference cDNA from untreated H2B-EYFP HeLa cells.

Immunofluorescence microscopy and live cell imaging of HeLa cells

Cells, plated on 12-mm coverslips, were fixed in 3.7% Shandon Zinc Formal-Fixx (Thermo Scientific) for 10 min and permeabilised for 15 min with 0.5% Triton X-100 in PBS and washed with 0.1% Triton X-100 in PBS. Coverslips were washed and submerged in PBS containing DAPI, then washed again and mounted using ProLong antifade (Molecular Probes). Image acquisition was done using a DeltaVision RT system with a 60x/1.40NA UPlanSApo objective (Olympus) for acquiring images and SoftWorx software for deconvolution and projections. Images are maximum intensity projections of deconvolved stacks. For live cell imaging, cells were plated in eight-well chambered glass-bottomed slides (LabTek), transfected, and imaged in a heated chamber (37°C and 5% CO₂) using a 60x/1.40NA UPlanSApo objective on an Olympus IX-81 microscope, controlled by Cell-M software (Olympus). Sixteen-bit yellow fluorescent images were acquired every 3 minutes using a Hamamatsu ORCA-ER camera. Images of H2B-EYFP were maximum intensity projections of all Z-planes and were processed using Cell-M software.

ACKNOWLEDGEMENTS

We thank L. Kleij and M. Groot Koerkamp for technical assistance; J. Benschop and T. Lenstra for contributing microarray data; P. Kemmeren, S. van Hooff and K. Sameith for bioinformatics.

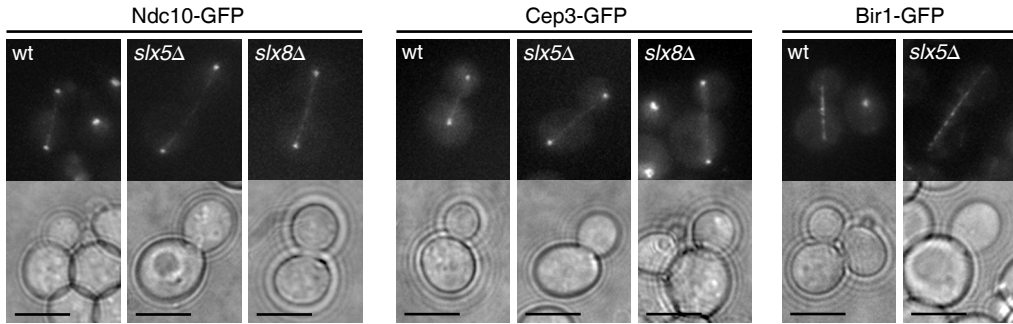
REFERENCES

1. Hoeijmakers, J. H. Genome maintenance mechanisms for preventing cancer. *Nature* **411**, 366–374 (2001).
2. Kerscher, O., Felberbaum, R. & Hochstrasser, M. Modification of proteins by ubiquitin and ubiquitin-like proteins. *Annu. Rev. Cell Dev. Biol.* **22**, 159–180 (2006).
3. Johnson, E. S. Protein modification by SUMO. *Annu. Rev. Biochem.* **73**, 355–382 (2004).
4. Geiss-Friedlander, R. & Melchior, F. Concepts in sumoylation: a decade on. *Nat. Rev. Mol. Cell Biol.* **8**, 947–956 (2007).
5. Mullen, J. R., Kaliraman, V., Ibrahim, S. S. & Brill, S. J.

- Requirement for three novel protein complexes in the absence of the Sgs1 DNA helicase in *Saccharomyces cerevisiae*. *Genetics* **157**, 103–118 (2001).
6. Zhang, C., Roberts, T. M., Yang, J., Desai, R. & Brown, G. W. Suppression of genomic instability by SLX5 and SLX8 in *Saccharomyces cerevisiae*. *DNA Repair (Amst.)* **5**, 336–346 (2006).
 7. Uzunova, K. *et al.* Ubiquitin-dependent proteolytic control of SUMO conjugates. *J. Biol. Chem* **282**, 34167–34175 (2007).
 8. Xie, Y. *et al.* The yeast Hex3.Slx8 heterodimer is a ubiquitin ligase stimulated by substrate sumoylation. *J. Biol. Chem* **282**, 34176–34184 (2007).
 9. Ii, T., Fung, J., Mullen, J. R. & Brill, S. J. The yeast Slx5-Slx8 DNA integrity complex displays ubiquitin ligase activity. *Cell Cycle* **6**, 2800–2809 (2007).
 10. Perry, J. J. P., Tainer, J. A. & Boddy, M. N. A SIM-ultaneous role for SUMO and ubiquitin. *Trends Biochem. Sci* **33**, 201–208 (2008).
 11. Burgess, R. C., Rahman, S., Lisby, M., Rothstein, R. & Zhao, X. The Slx5-Slx8 complex affects sumoylation of DNA repair proteins and negatively regulates recombination. *Mol. Cell. Biol* **27**, 6153–6162 (2007).
 12. Nagai, S. *et al.* Functional targeting of DNA damage to a nuclear pore-associated SUMO-dependent ubiquitin ligase. *Science* **322**, 597–602 (2008).
 13. Kosoy, A., Calonge, T. M., Outwin, E. A. & O'Connell, M. J. Fission yeast Rnf4 homologs are required for DNA repair. *J. Biol. Chem* **282**, 20388–20394 (2007).
 14. Sun, H., Levenson, J. D. & Hunter, T. Conserved function of RNF4 family proteins in eukaryotes: targeting a ubiquitin ligase to SUMOylated proteins. *EMBO J* **26**, 4102–4112 (2007).
 15. Prudden, J. *et al.* SUMO-targeted ubiquitin ligases in genome stability. *EMBO J* **26**, 4089–4101 (2007).
 16. Cook, C. E., Hochstrasser, M. & Kerscher, O. The SUMO-targeted ubiquitin ligase subunit Slx5 resides in nuclear foci and at sites of DNA breaks. *Cell Cycle* **8**, 1080–1089 (2009).
 17. Tatham, M. H. *et al.* RNF4 is a poly-SUMO-specific E3 ubiquitin ligase required for arsenic-induced PML degradation. *Nat. Cell Biol* **10**, 538–546 (2008).
 18. Lallemand-Breitenbach, V. *et al.* Arsenic degrades PML or PML-RARalpha through a SUMO-triggered RNF4/ubiquitin-mediated pathway. *Nat. Cell Biol* **10**, 547–555 (2008).
 19. Guo, B. & Sharrocks, A. D. Extracellular signal-regulated kinase mitogen-activated protein kinase signaling initiates a dynamic interplay between sumoylation and ubiquitination to regulate the activity of the transcriptional activator PEA3. *Mol. Cell. Biol* **29**, 3204–3218 (2009).
 20. Martin, N. *et al.* PARP-1 transcriptional activity is regulated by sumoylation upon heat shock. *EMBO J* **28**, 3534–3548 (2009).
 21. van Hagen, M., Overmeer, R. M., Abolvardi, S. S. & Vertegaal, A. C. O. RNF4 and VHL regulate the proteasomal degradation of SUMO-conjugated Hypoxia-Inducible Factor-2alpha. *Nucleic Acids Res* **38**, 1922–1931 (2010).
 22. Darst, R. P., Garcia, S. N., Koch, M. R. & Pillus, L. Slx5 promotes transcriptional silencing and is required for robust growth in the absence of Sir2. *Mol. Cell. Biol* **28**, 1361–1372 (2008).
 23. Wang, Z. & Prelich, G. Quality control of a transcriptional regulator by SUMO-targeted degradation. *Mol. Cell. Biol* **29**, 1694–1706 (2009).
 24. Nixon, C. E., Wilcox, A. J. & Laney, J. D. Degradation of the *Saccharomyces cerevisiae* mating-type regulator alpha1: genetic dissection of cis-determinants and trans-acting pathways. *Genetics* **185**, 497–511 (2010).
 25. Gasch, A. P. *et al.* Genomic expression programs in the response of yeast cells to environmental changes. *Mol. Biol. Cell* **11**, 4241–4257 (2000).
 26. Martínez-Pastor, M. T. *et al.* The *Saccharomyces cerevisiae* zinc finger proteins Msn2p and Msn4p are required for transcriptional induction through the stress response element (STRE). *EMBO J* **15**, 2227–2235 (1996).
 27. MacIsaac, K. D. *et al.* An improved map of conserved regulatory sites for *Saccharomyces cerevisiae*. *BMC Bioinformatics* **7**, 113 (2006).
 28. Hughes, T. R. *et al.* Widespread aneuploidy revealed by DNA microarray expression profiling. *Nat. Genet* **25**, 333–337 (2000).
 29. Hieter, P., Mann, C., Snyder, M. & Davis, R. W. Mitotic stability of yeast chromosomes: a colony color assay that measures nondisjunction and chromosome loss. *Cell* **40**, 381–392 (1985).
 30. McAinsh, A. D., Tytell, J. D. & Sorger, P. K. Structure, function, and regulation of budding yeast kinetochores. *Annu. Rev. Cell Dev. Biol* **19**, 519–539 (2003).
 31. Goh, P. Y. & Kilmartin, J. V. NDC10: a gene involved in chromosome segregation in *Saccharomyces cerevisiae*. *J. Cell Biol.* **121**, 503–512 (1993).
 32. Montpetit, B., Hazbun, T. R., Fields, S. & Hieter, P. Sumoylation of the budding yeast kinetochore protein Ndc10 is required for Ndc10 spindle localization and regulation of anaphase spindle elongation. *J. Cell Biol* **174**, 653–663 (2006).
 33. Collins, S. R. *et al.* Functional dissection of protein complexes involved in yeast chromosome biology using a genetic interaction map. *Nature* **446**, 806–810 (2007).
 34. Costanzo, M. *et al.* The genetic landscape of a cell. *Science* **327**, 425–431 (2010).
 35. Zhao, Y., Boguslawski, G., Zitomer, R. S. & DePaoli-Roach, A. A. *Saccharomyces cerevisiae* homologs of mammalian B and B' subunits of protein phosphatase 2A direct the enzyme to distinct cellular functions. *J. Biol. Chem* **272**, 8256–8262 (1997).
 36. Gentry, M. S. & Hallberg, R. L. Localization of *Saccharomyces cerevisiae* protein phosphatase 2A subunits throughout mitotic cell cycle. *Mol. Biol. Cell* **13**, 3477–3492 (2002).
 37. Dobbelaere, J., Gentry, M. S., Hallberg, R. L. & Barral, Y. Phosphorylation-dependent regulation of septin dynamics during the cell cycle. *Dev. Cell* **4**, 345–357 (2003).
 38. Riedel, C. G. *et al.* Protein phosphatase 2A protects centromeric sister chromatid cohesion during meiosis I. *Nature* **441**, 53–61 (2006).
 39. Straight, A. F., Marshall, W. F., Sedat, J. W. & Murray, A. W. Mitosis in living budding yeast: anaphase A but no metaphase plate. *Science* **277**, 574–578 (1997).
 40. Vizeacoumar, F. J. *et al.* Integrating high-throughput genetic interaction mapping and high-content screening to explore yeast spindle morphogenesis. *J. Cell Biol* **188**, 69–81 (2010).

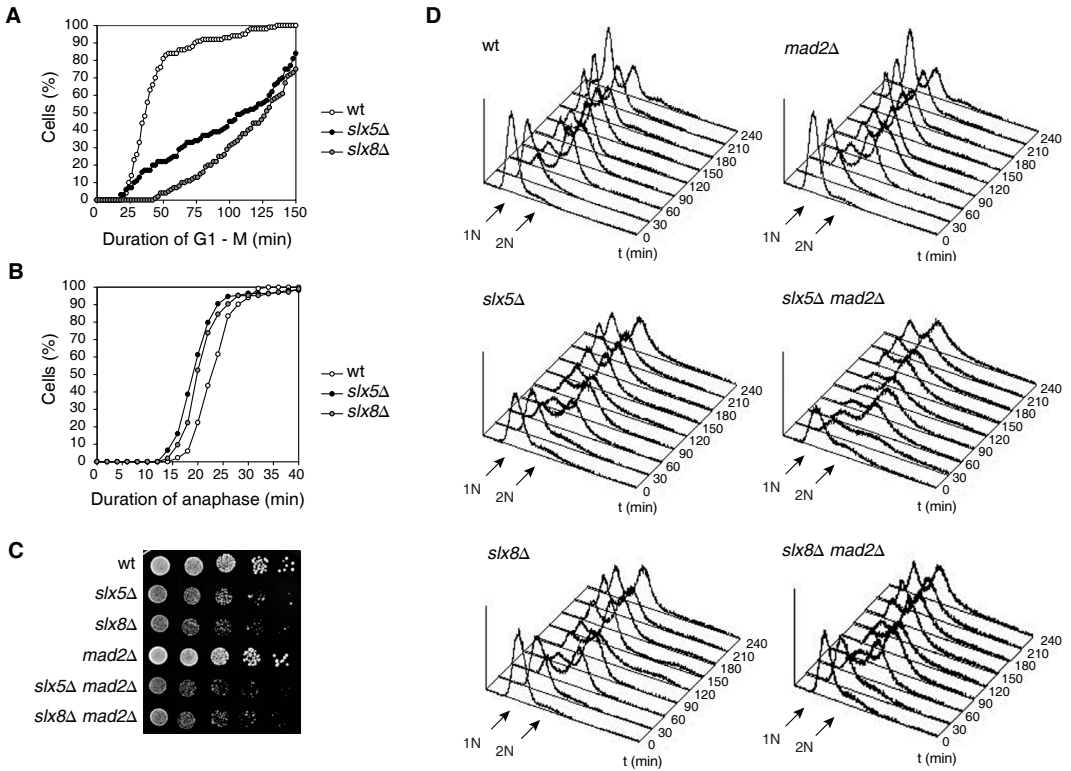
41. Mukhopadhyay, D., Arnaoutov, A. & Dasso, M. The SUMO protease SENP6 is essential for inner kinetochore assembly. *J. Cell Biol* **188**, 681–692 (2010).
42. Chan, L. Y. & Amon, A. The protein phosphatase 2A functions in the spindle position checkpoint by regulating the checkpoint kinase Kin4. *Genes Dev* **23**, 1639–1649 (2009).
43. Caydasi, A. K., Ibrahim, B. & Pereira, G. Monitoring spindle orientation: Spindle position checkpoint in charge. *Cell Div* **5**, 28 (2010).
44. Indjeian, V. B., Stern, B. M. & Murray, A. W. The centromeric protein Sgo1 is required to sense lack of tension on mitotic chromosomes. *Science* **307**, 130–133 (2005).
45. Wang, J. C. Cellular roles of DNA topoisomerases: a molecular perspective. *Nat. Rev. Mol. Cell Biol.* **3**, 430–440 (2002).
46. Longtine, M. S. *et al.* Additional modules for versatile and economical PCR-based gene deletion and modification in *Saccharomyces cerevisiae*. *Yeast* **14**, 953–961 (1998).
47. Huh, W.-K. *et al.* Global analysis of protein localization in budding yeast. *Nature* **425**, 686–691 (2003).
48. Grava, S., Schaerer, F., Faty, M., Philippsen, P. & Barral, Y. Asymmetric recruitment of dynein to spindle poles and microtubules promotes proper spindle orientation in yeast. *Dev. Cell* **10**, 425–439 (2006).
49. Neurohr, G. *et al.* A midzone-based ruler adjusts chromosome compaction to anaphase spindle length. *Science* **332**, 465–468 (2011).
50. Spencer, F., Gerring, S. L., Connelly, C. & Hieter, P. Mitotic chromosome transmission fidelity mutants in *Saccharomyces cerevisiae*. *Genetics* **124**, 237–249 (1990).
51. Lenstra, T. L. *et al.* The specificity and topology of chromatin interaction pathways in yeast. *Mol. Cell* **42**, 536–549 (2011).
52. Margaritis, T. *et al.* Adaptable gene-specific dye bias correction for two-channel DNA microarrays. *Mol. Syst. Biol* **5**, 266 (2009).
53. van Wageningen, S. *et al.* Functional overlap and regulatory links shape genetic interactions between signaling pathways. *Cell* **143**, 991–1004 (2010).
54. Saldanha, A. J. Java Treeview--extensible visualization of microarray data. *Bioinformatics* **20**, 3246–3248 (2004).
55. Ashburner, M. *et al.* Gene ontology: tool for the unification of biology. The Gene Ontology Consortium. *Nat. Genet* **25**, 25–29 (2000).
56. van Bakel, H. *et al.* Improved genome-wide localization by ChIP-chip using double-round T7 RNA polymerase-based amplification. *Nucleic Acids Res* **36**, e21 (2008).
57. van Werven, F. J. *et al.* Cooperative action of NC2 and Mot1p to regulate TATA-binding protein function across the genome. *Genes Dev* **22**, 2359–2369 (2008).
58. Hyland, K. M., Kingsbury, J., Koshland, D. & Hieter, P. Ctf19p: A novel kinetochore protein in *Saccharomyces cerevisiae* and a potential link between the kinetochore and mitotic spindle. *J. Cell Biol* **145**, 15–28 (1999).

SUPPLEMENTAL INFORMATION



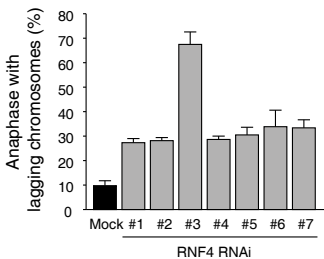
Supplementary Figure S1. Live cell fluorescence microscopy of wt, *slx5Δ* and *slx8Δ*.

Slx5Δ and *slx8Δ* have longer anaphase spindles and normal localisation of kinetochore components Ndc10, Cep3 and Bir1 at the centromeres and along the mitotic spindle. Scale bars, 5 μ m.



Supplementary Figure S2. *Slx5Δ* and *slx8Δ* have a mitotic delay that cannot be relieved by deletion of *MAD2*.

(A) Cumulative frequency graph of the duration of G1- to M-phase. Calculation is based on the time from spindle duplication in G1-phase to spindle pole body separation in anaphase, as measured by time-lapse video microscopy of cells (n = 100) expressing Spc42-GFP. (B) Cumulative frequency graph of the duration of anaphase. Calculation is based on the time from start of spindle elongation to spindle depolymerisation, as measured by time-lapse video microscopy of cells (n = 100) expressing Tub1-GFP. (C) Growth rate assay of cells spotted in five-fold serial dilutions on YPD plates. Images are after two days growth at 30°C. (D) Cell cycle rate progression of synchronized cells. DNA content was measured by flow cytometry at 30 minute intervals over a period of four hours after release from α -factor arrest in G1-phase. Arrows indicate cell populations with 1N (G1-phase) and 2N (G2/M-phase) DNA content.



Supplementary Figure S3. Quantification of chromosome segregation defects in fixed HeLa cells.

Graph represents the average of two independent experiments (\pm s.d.) and at least 110 cells per siRNA. Anaphases with chromosome segregation defects other than lagging chromosomes were infrequent in both mock and RNF4 knockdown situation and not considered for these analyses.

Supplementary Table S1. Gene Ontology (GO) and transcription factor binding site (TFBS) enrichment analyses of differentially expressed genes (mutant vs. wt, FC > 1.7, p < 0.05)

Mutant	Significant genes	Enrichment type	Enrichment description	P-value	Hits
<i>cdc26Δ</i>	36	GO-BP	regulation of ATPase activity (GO:0043462)	1.15E-03	3
<i>cdc26Δ</i>	36	GO-BP	negative regulation of hydrolase activity (GO:0051346)	2.43E-03	3
<i>cdc26Δ</i>	36	GO-MF	aldehyde dehydrogenase (NAD) activity (GO:0004029)	7.83E-03	2
<i>cdc26Δ</i>	36	TFBS	MSN4	4.45E-04	8
<i>cin8Δ</i>	34	GO-MF	structural constituent of cell wall (GO:0005199)	2.72E-03	3
<i>cin8Δ</i>	34	GO-CC	extracellular region (GO:0005576)	1.21E-06	8
<i>cin8Δ</i>	34	GO-CC	fungus-type cell wall (GO:0009277)	8.39E-03	5
<i>cin8Δ</i>	34	TFBS	MSN2	7.35E-04	8
<i>csmlΔ</i>	54	GO-BP	monosaccharide catabolic process (GO:0046365)	1.23E-03	6
<i>csmlΔ</i>	54	GO-BP	alcohol catabolic process (GO:0046164)	2.74E-03	6
<i>csmlΔ</i>	54	GO-BP	cellular carbohydrate catabolic process (GO:0044275)	3.87E-03	7
<i>csmlΔ</i>	54	GO-BP	NADPH regeneration (GO:0006740)	5.10E-03	4
<i>csmlΔ</i>	54	GO-BP	carbohydrate catabolic process (GO:0016052)	6.40E-03	7
<i>csmlΔ</i>	54	GO-BP	oxidation-reduction process (GO:0055114)	8.77E-03	13
<i>csmlΔ</i>	54	GO-BP	NADP metabolic process (GO:0006739)	8.88E-03	4
<i>csmlΔ</i>	54	GO-CC	plasma membrane enriched fraction (GO:0001950)	4.88E-03	6
<i>csmlΔ</i>	54	TFBS	MSN4	1.53E-06	12
<i>csmlΔ</i>	54	TFBS	MSN2	6.51E-06	12
<i>ctf4Δ</i>	87	GO-BP	oxidation-reduction process (GO:0055114)	1.28E-03	19
<i>ctf4Δ</i>	87	GO-BP	trehalose metabolic process (GO:0005991)	3.20E-03	4
<i>ctf4Δ</i>	87	GO-BP	carbohydrate catabolic process (GO:0016052)	4.86E-03	9
<i>ctf4Δ</i>	87	GO-MF	hydrolase activity, acting on glycosyl bonds (GO:0016798)	5.79E-04	8
<i>ctf4Δ</i>	87	GO-MF	hydrolase activity, hydrolyzing O-glycosyl compounds (GO:0004553)	2.54E-03	7
<i>ctf4Δ</i>	87	GO-CC	extracellular region (GO:0005576)	5.70E-07	12
<i>ctf4Δ</i>	87	GO-CC	fungus-type cell wall (GO:0009277)	1.21E-05	11
<i>ctf4Δ</i>	87	GO-CC	cell wall (GO:0005618)	1.97E-05	11
<i>ctf4Δ</i>	87	GO-CC	external encapsulating structure (GO:0030312)	1.97E-05	11
<i>ctf4Δ</i>	87	TFBS	MSN2	8.38E-08	17
<i>ctf4Δ</i>	87	TFBS	MSN4	5.39E-05	13
<i>ctf4Δ</i>	87	TFBS	NRG1	7.49E-04	11
<i>ctf18Δ</i>	53	GO-BP	response to pheromone involved in conjugation with cellular fusion (GO:0000749)	4.66E-07	9
<i>ctf18Δ</i>	53	GO-BP	response to pheromone (GO:0019236)	9.27E-06	9
<i>ctf18Δ</i>	53	GO-BP	conjugation with cellular fusion (GO:0000747)	2.50E-05	9
<i>ctf18Δ</i>	53	GO-BP	conjugation (GO:0000746)	2.95E-05	9
<i>ctf18Δ</i>	53	GO-BP	cellular response to chemical stimulus (GO:0070887)	3.23E-05	13
<i>ctf18Δ</i>	53	GO-BP	multi-organism process (GO:0051704)	1.24E-04	9
<i>ctf18Δ</i>	53	GO-BP	response to organic substance (GO:0010033)	1.76E-04	10
<i>ctf18Δ</i>	53	GO-BP	response to chemical stimulus (GO:0042221)	2.53E-04	14
<i>ctf18Δ</i>	53	GO-BP	agglutination involved in conjugation with cellular fusion (GO:0000752)	3.95E-04	3
<i>ctf18Δ</i>	53	GO-BP	agglutination involved in conjugation (GO:0000771)	3.95E-04	3
<i>ctf18Δ</i>	53	GO-BP	heterophilic cell-cell adhesion (GO:0007157)	3.95E-04	3
<i>ctf18Δ</i>	53	GO-BP	pheromone-dependent signal transduction involved in conjugation with cellular fusion (GO:0000750)	5.20E-04	5
<i>ctf18Δ</i>	53	GO-BP	signal transduction involved in conjugation with cellular fusion (GO:0032005)	5.20E-04	5
<i>ctf18Δ</i>	53	GO-BP	cell-cell adhesion (GO:0016337)	9.82E-04	3
<i>ctf18Δ</i>	53	GO-BP	sexual reproduction (GO:0019953)	1.17E-03	10
<i>ctf18Δ</i>	53	GO-BP	G-protein coupled receptor signaling pathway (GO:0007186)	1.90E-03	5
<i>ctf18Δ</i>	53	GO-BP	cell surface receptor signaling pathway (GO:0007166)	2.18E-03	5
<i>ctf18Δ</i>	53	GO-BP	reproductive process (GO:0022414)	5.19E-03	13
<i>ctf18Δ</i>	53	GO-BP	cellular process involved in reproduction (GO:0048610)	5.19E-03	13
<i>ctf18Δ</i>	53	GO-MF	cell adhesion molecule binding (GO:0050839)	4.10E-05	3
<i>ctf18Δ</i>	53	GO-MF	mating pheromone activity (GO:0000772)	1.63E-04	3
<i>ctf18Δ</i>	53	GO-MF	pheromone activity (GO:0005186)	1.63E-04	3
<i>ctf18Δ</i>	53	GO-MF	receptor binding (GO:0005102)	8.05E-04	3

Supplementary Table S1. Continued

Mutant	Significant genes	Enrichment type	Enrichment description	P-value	Hits
<i>ctf18Δ</i>	53	GO-CC	extracellular region (GO:0005576)	2.91E-07	10
<i>ctf18Δ</i>	53	GO-CC	fungus-type cell wall (GO:0009277)	1.04E-04	8
<i>ctf18Δ</i>	53	GO-CC	cell wall (GO:0005618)	1.49E-04	8
<i>ctf18Δ</i>	53	GO-CC	external encapsulating structure (GO:0030312)	1.49E-04	8
<i>ctf18Δ</i>	53	TFBS	MSN4	8.82E-03	8
<i>mcm21Δ</i>	7	GO-BP	response to stimulus (GO:0050896)	4.03E-03	6
<i>rad18Δ</i>	64	GO-BP	glycogen biosynthetic process (GO:0005978)	1.13E-03	4
<i>rad18Δ</i>	64	GO-BP	glycogen metabolic process (GO:0005977)	1.60E-03	5
<i>rad18Δ</i>	64	GO-BP	energy reserve metabolic process (GO:0006112)	2.32E-03	5
<i>rad18Δ</i>	64	GO-BP	cellular glucan metabolic process (GO:0006073)	9.12E-03	5
<i>rad18Δ</i>	64	GO-BP	glucan metabolic process (GO:0044042)	9.12E-03	5
<i>rad18Δ</i>	64	GO-MF	ribonucleoside-diphosphate reductase activity (GO:0004748)	2.65E-04	3
<i>rad18Δ</i>	64	GO-MF	oxidoreductase activity, acting on CH or CH2 groups, disulfide as acceptor (GO:0016728)	2.65E-04	3
<i>rad18Δ</i>	64	GO-MF	oxidoreductase activity, acting on CH or CH2 groups (GO:0016725)	6.57E-04	3
<i>rad18Δ</i>	64	GO-CC	ribonucleoside-diphosphate reductase complex (GO:0005971)	2.86E-04	3
<i>rad18Δ</i>	64	GO-CC	extracellular region (GO:0005576)	3.83E-03	7
<i>rad18Δ</i>	64	TFBS	MSN2	4.76E-05	12
<i>rad18Δ</i>	64	TFBS	MSN4	7.95E-04	10
<i>rad18Δ</i>	64	GO-BP	trehalose metabolic process (GO:0005991)	4.85E-06	6
<i>rad18Δ</i>	64	GO-BP	oxidation-reduction process (GO:0055114)	1.03E-05	26
<i>rad18Δ</i>	64	GO-BP	carbohydrate catabolic process (GO:0016052)	2.11E-05	13
<i>rad18Δ</i>	64	GO-BP	pyridine nucleotide metabolic process (GO:0019362)	1.80E-04	9
<i>rad18Δ</i>	64	GO-BP	energy reserve metabolic process (GO:0006112)	2.19E-04	7
<i>rad18Δ</i>	64	GO-BP	pyridine-containing compound metabolic process (GO:0072524)	2.47E-04	9
<i>rad18Δ</i>	64	GO-BP	glycogen biosynthetic process (GO:0005978)	4.62E-04	5
<i>rad18Δ</i>	64	GO-BP	cellular carbohydrate catabolic process (GO:0044275)	5.84E-04	11
<i>rad18Δ</i>	64	GO-BP	oxidoreduction coenzyme metabolic process (GO:0006733)	1.01E-03	9
<i>rad18Δ</i>	64	GO-BP	carbohydrate metabolic process (GO:0005975)	1.09E-03	20
<i>rad18Δ</i>	64	GO-BP	glycoside metabolic process (GO:0016137)	1.16E-03	6
<i>rad18Δ</i>	64	GO-BP	response to stress (GO:0006950)	1.28E-03	31
<i>rad18Δ</i>	64	GO-BP	nicotinamide nucleotide metabolic process (GO:0046496)	1.50E-03	8
<i>rad18Δ</i>	64	GO-BP	glycogen metabolic process (GO:0005977)	2.45E-03	6
<i>rad18Δ</i>	64	GO-BP	cellular carbohydrate metabolic process (GO:0044262)	3.24E-03	18
<i>rad18Δ</i>	64	GO-BP	alcohol catabolic process (GO:0046164)	5.64E-03	8
<i>rad18Δ</i>	64	GO-BP	cellular response to oxidative stress (GO:0034599)	6.70E-03	9
<i>rad18Δ</i>	64	GO-BP	negative regulation of catalytic activity (GO:0043086)	6.95E-03	6
<i>rad18Δ</i>	64	GO-BP	negative regulation of hydrolase activity (GO:0051346)	7.07E-03	4
<i>rad18Δ</i>	64	GO-BP	arabinose metabolic process (GO:0019566)	8.12E-03	3
<i>rad18Δ</i>	64	GO-BP	arabinose catabolic process (GO:0019568)	8.12E-03	3
<i>rad18Δ</i>	64	GO-BP	D-xylose catabolic process (GO:0042843)	8.12E-03	3
<i>rad18Δ</i>	64	GO-MF	alditol:NADP+ 1-oxidoreductase activity (GO:0004032)	1.61E-04	4
<i>rad18Δ</i>	64	GO-MF	alcohol dehydrogenase (NADP+) activity (GO:0008106)	1.29E-03	4
<i>rad18Δ</i>	64	GO-MF	aldo-keto reductase (NADP) activity (GO:0004033)	2.12E-03	4
<i>rad18Δ</i>	64	GO-MF	endopeptidase inhibitor activity (GO:0004866)	6.02E-03	3
<i>rad18Δ</i>	64	GO-MF	peptidase inhibitor activity (GO:0030414)	6.02E-03	3
<i>rad18Δ</i>	64	GO-CC	plasma membrane enriched fraction (GO:0001950)	2.11E-03	9
<i>rad18Δ</i>	64	GO-CC	fungus-type cell wall (GO:0009277)	9.78E-03	9
<i>rad18Δ</i>	64	TFBS	MSN2	2.95E-09	21
<i>rad18Δ</i>	64	TFBS	MSN4	1.35E-07	18
<i>rad18Δ</i>	64	TFBS	SKN7	3.53E-04	15
<i>rad18Δ</i>	64	TFBS	NRG1	2.10E-03	12
<i>rad18Δ</i>	64	TFBS	MOT3	6.45E-03	9
<i>rad52Δ</i>	93	GO-BP	oxidation-reduction process (GO:0055114)	5.26E-05	22
<i>rad52Δ</i>	93	GO-BP	glycogen biosynthetic process (GO:0005978)	1.47E-04	5

Supplementary Table S1. Continued

Mutant	Significant genes	Enrichment type	Enrichment description	P-value	Hits
<i>rad52Δ</i>	93	GO-BP	pyridine nucleotide metabolic process (GO:0019362)	3.74E-04	8
<i>rad52Δ</i>	93	GO-BP	pyridine-containing compound metabolic process (GO:0072524)	4.96E-04	8
<i>rad52Δ</i>	93	GO-BP	oxidoreduction coenzyme metabolic process (GO:0006733)	1.73E-03	8
<i>rad52Δ</i>	93	GO-BP	cellular response to chemical stimulus (GO:0070887)	2.21E-03	15
<i>rad52Δ</i>	93	GO-BP	negative regulation of hydrolase activity (GO:0051346)	2.78E-03	4
<i>rad52Δ</i>	93	GO-BP	glucan biosynthetic process (GO:0009250)	3.40E-03	5
<i>rad52Δ</i>	93	GO-BP	nicotinamide nucleotide metabolic process (GO:0046496)	3.49E-03	7
<i>rad52Δ</i>	93	GO-BP	carbohydrate catabolic process (GO:0016052)	8.67E-03	9
<i>rad52Δ</i>	93	GO-MF	ribonucleoside-diphosphate reductase activity (GO:0004748)	1.19E-03	3
<i>rad52Δ</i>	93	GO-MF	oxidoreductase activity, acting on CH or CH2 groups, disulfide as acceptor (GO:0016728)	1.19E-03	3
<i>rad52Δ</i>	93	GO-MF	endopeptidase inhibitor activity (GO:0004866)	2.93E-03	3
<i>rad52Δ</i>	93	GO-MF	oxidoreductase activity, acting on CH or CH2 groups (GO:0016725)	2.93E-03	3
<i>rad52Δ</i>	93	GO-MF	peptidase inhibitor activity (GO:0030414)	2.93E-03	3
<i>rad52Δ</i>	93	GO-MF	structural constituent of cell wall (GO:0005199)	5.20E-03	4
<i>rad52Δ</i>	93	GO-CC	extracellular region (GO:0005576)	1.31E-05	11
<i>rad52Δ</i>	93	GO-CC	ribonucleoside-diphosphate reductase complex (GO:0005971)	1.10E-03	3
<i>rad52Δ</i>	93	TFBS	MSN2	3.04E-08	18
<i>rad52Δ</i>	93	TFBS	MSN4	2.88E-07	16
<i>rad52Δ</i>	93	TFBS	SKN7	3.97E-03	12
<i>rmi1Δ</i>	57	GO-BP	monosaccharide catabolic process (GO:0046365)	1.77E-03	6
<i>rmi1Δ</i>	57	GO-BP	alcohol catabolic process (GO:0046164)	3.93E-03	6
<i>rmi1Δ</i>	57	GO-BP	cellular carbohydrate catabolic process (GO:0044275)	5.83E-03	7
<i>rmi1Δ</i>	57	GO-BP	carbohydrate catabolic process (GO:0016052)	9.60E-03	7
<i>rmi1Δ</i>	57	GO-MF	endopeptidase inhibitor activity (GO:0004866)	5.15E-04	3
<i>rmi1Δ</i>	57	GO-MF	peptidase inhibitor activity (GO:0030414)	5.15E-04	3
<i>rmi1Δ</i>	57	GO-MF	endopeptidase regulator activity (GO:0061135)	1.78E-03	3
<i>rmi1Δ</i>	57	GO-MF	peptidase regulator activity (GO:0061134)	2.83E-03	3
<i>rmi1Δ</i>	57	GO-CC	extracellular region (GO:0005576)	1.47E-03	7
<i>rmi1Δ</i>	57	TFBS	MSN4	2.96E-05	11
<i>rmi1Δ</i>	57	TFBS	MSN2	1.09E-04	11
<i>rts1Δ</i>	41	GO-BP	mitochondrial electron transport, ubiquinol to cytochrome c (GO:0006122)	7.35E-03	3
<i>sgs1Δ</i>	55	GO-BP	monosaccharide catabolic process (GO:0046365)	1.51E-03	6
<i>sgs1Δ</i>	55	GO-BP	alcohol catabolic process (GO:0046164)	3.36E-03	6
<i>sgs1Δ</i>	55	GO-BP	cellular carbohydrate catabolic process (GO:0044275)	4.84E-03	7
<i>sgs1Δ</i>	55	GO-BP	NADPH regeneration (GO:0006740)	6.05E-03	4
<i>sgs1Δ</i>	55	GO-BP	carbohydrate catabolic process (GO:0016052)	7.99E-03	7
<i>sgs1Δ</i>	55	GO-MF	endopeptidase inhibitor activity (GO:0004866)	4.48E-04	3
<i>sgs1Δ</i>	55	GO-MF	peptidase inhibitor activity (GO:0030414)	4.48E-04	3
<i>sgs1Δ</i>	55	GO-MF	endopeptidase regulator activity (GO:0061135)	1.55E-03	3
<i>sgs1Δ</i>	55	GO-MF	peptidase regulator activity (GO:0061134)	2.46E-03	3
<i>sgs1Δ</i>	55	TFBS	MSN4	1.91E-06	12
<i>sgs1Δ</i>	55	TFBS	MSN2	8.10E-06	12
<i>slx5Δ</i>	321	GO-BP	oxidation-reduction process (GO:0055114)	3.18E-11	60
<i>slx5Δ</i>	321	GO-BP	biological_process (GO:0008150)	5.39E-03	92
<i>slx5Δ</i>	321	GO-BP	glutamate metabolic process (GO:0006536)	5.67E-03	7
<i>slx5Δ</i>	321	GO-MF	oxidoreductase activity (GO:0016491)	1.69E-08	47
<i>slx5Δ</i>	321	GO-MF	endopeptidase inhibitor activity (GO:0004866)	6.42E-03	4
<i>slx5Δ</i>	321	GO-MF	peptidase inhibitor activity (GO:0030414)	6.42E-03	4
<i>slx5Δ</i>	321	GO-CC	extracellular region (GO:0005576)	4.43E-09	24
<i>slx5Δ</i>	321	GO-CC	fungal-type cell wall (GO:0009277)	3.38E-06	21
<i>slx5Δ</i>	321	GO-CC	cell wall (GO:0005618)	8.10E-06	21
<i>slx5Δ</i>	321	GO-CC	external encapsulating structure (GO:0030312)	8.10E-06	21
<i>slx5Δ</i>	321	GO-CC	anchored to membrane (GO:0031225)	1.74E-04	14
<i>slx5Δ</i>	321	TFBS	MSN4	1.58E-07	30

Supplementary Table S1. Continued

Mutant	Significant genes	Enrichment type	Enrichment description	P-value	Hits
<i>slx5Δ</i>	321	TFBS	MSN2	4.74E-05	28
<i>slx5Δ</i>	321	TFBS	CAD1	9.31E-03	8
<i>slx8Δ</i>	132	GO-BP	oxidation-reduction process (GO:0055114)	4.46E-05	27
<i>slx8Δ</i>	132	GO-BP	nicotinamide nucleotide metabolic process (GO:0046496)	3.89E-04	9
<i>slx8Δ</i>	132	GO-BP	pyridine nucleotide metabolic process (GO:0019362)	5.38E-04	9
<i>slx8Δ</i>	132	GO-BP	pyridine-containing compound metabolic process (GO:0072524)	7.35E-04	9
<i>slx8Δ</i>	132	GO-BP	response to pheromone involved in conjugation with cellular fusion (GO:0000749)	2.58E-03	9
<i>slx8Δ</i>	132	GO-BP	conjugation with cellular fusion (GO:0000747)	2.80E-03	11
<i>slx8Δ</i>	132	GO-BP	oxidoreduction coenzyme metabolic process (GO:0006733)	2.93E-03	9
<i>slx8Δ</i>	132	GO-BP	conjugation (GO:0000746)	3.37E-03	11
<i>slx8Δ</i>	132	GO-MF	oxidoreductase activity (GO:0016491)	7.19E-04	21
<i>slx8Δ</i>	132	GO-MF	cell adhesion molecule binding (GO:0050839)	1.07E-03	3
<i>slx8Δ</i>	132	GO-MF	mating pheromone activity (GO:0000772)	4.23E-03	3
<i>slx8Δ</i>	132	GO-MF	ribonucleoside-diphosphate reductase activity (GO:0004748)	4.23E-03	3
<i>slx8Δ</i>	132	GO-MF	pheromone activity (GO:0005186)	4.23E-03	3
<i>slx8Δ</i>	132	GO-MF	oxidoreductase activity, acting on CH or CH2 groups, disulfide as acceptor (GO:0016728)	4.23E-03	3
<i>slx8Δ</i>	132	GO-CC	extracellular region (GO:0005576)	5.86E-05	12
<i>slx8Δ</i>	132	GO-CC	ribonucleoside-diphosphate reductase complex (GO:0005971)	3.18E-03	3
<i>slx8Δ</i>	132	GO-CC	fungus-type cell wall (GO:0009277)	4.58E-03	10
<i>slx8Δ</i>	132	GO-CC	cell wall (GO:0005618)	6.88E-03	10
<i>slx8Δ</i>	132	GO-CC	external encapsulating structure (GO:0030312)	6.88E-03	10
<i>slx8Δ</i>	132	TFBS	MSN4	4.77E-05	16
<i>slx8Δ</i>	132	TFBS	MSN2	2.72E-04	16
<i>ybp2Δ</i>	3	GO-CC	extracellular region (GO:0005576)	2.17E-03	2

Supplementary Table S2. Yeast strains

Name	Genotype	Source
BY4741	<i>MATa his3-Δ1 leu2-Δ0 lys2-Δ0 ura3-Δ0</i>	OBS
BY4742	<i>MATα his3-Δ1 leu2-Δ0 met15-Δ0 ura3-Δ0</i>	OBS
TL5001	<i>MATα his3-Δ1 leu2-Δ0 met15-Δ0 ura3-Δ0 slx5::KanMX6</i>	This study
YTM006	<i>MATα his3-Δ1 leu2-Δ0 met15-Δ0 ura3-Δ0 slx8::KanMX6</i>	This study
YFR036W	<i>MATα his3-Δ1 leu2-Δ0 met15-Δ0 ura3-Δ0 cdc26::KanMX4</i>	OBS
YEL061C	<i>MATα his3-Δ1 leu2-Δ0 met15-Δ0 ura3-Δ0 cin8::KanMX4</i>	Euroscarf
YCR086W	<i>MATα his3-Δ1 leu2-Δ0 met15-Δ0 ura3-Δ0 csm1::KanMX4</i>	OBS
YPR135W	<i>MATα his3-Δ1 leu2-Δ0 met15-Δ0 ura3-Δ0 ctf4::KanMX4</i>	Euroscarf
YMR078C	<i>MATα his3-Δ1 leu2-Δ0 met15-Δ0 ura3-Δ0 ctf18::KanMX4</i>	OBS
YPL018W	<i>MATα his3-Δ1 leu2-Δ0 met15-Δ0 ura3-Δ0 ctf19::KanMX4</i>	OBS
YDR318W	<i>MATα his3-Δ1 leu2-Δ0 met15-Δ0 ura3-Δ0 mcm21::KanMX4</i>	OBS
YDL188C	<i>MATα his3-Δ1 leu2-Δ0 met15-Δ0 ura3-Δ0 pph22::KanMX4</i>	OBS
YCR066W	<i>MATα his3-Δ1 leu2-Δ0 met15-Δ0 ura3-Δ0 rad18::KanMX4</i>	OBS
YNL250W	<i>MATα his3-Δ1 leu2-Δ0 met15-Δ0 ura3-Δ0 rad50::KanMX4</i>	OBS
YML032C	<i>MATα his3-Δ1 leu2-Δ0 met15-Δ0 ura3-Δ0 rad52::KanMX4</i>	OBS
YPL024W	<i>MATα his3-Δ1 leu2-Δ0 met15-Δ0 ura3-Δ0 rmi1::KanMX4</i>	Euroscarf
YMR190C	<i>MATα his3-Δ1 leu2-Δ0 met15-Δ0 ura3-Δ0 sgs1::KanMX4</i>	OBS
YGL060W	<i>MATα his3-Δ1 leu2-Δ0 met15-Δ0 ura3-Δ0 ybp2::KanMX4</i>	OBS
YLP522	<i>MATα his3-Δ1 leu2-Δ0 ura3-Δ0 slx5::His3MX6</i>	This study
YLP524	<i>MATa his3-Δ1 leu2-Δ0 met15-Δ0 ura3-Δ0 slx5::His3MX6</i>	This study
YLP534	<i>MATa his3-Δ1 leu2-Δ0 lys2-Δ0 ura3-Δ0 slx5::NatMX6</i>	This study
YLP536	<i>MATα his3-Δ1 leu2-Δ0 met15-Δ0 ura3-Δ0 slx5::NatMX6</i>	This study
YLP525	<i>MATa his3-Δ1 leu2-Δ0 met15-Δ0 ura3-Δ0 slx8::His3MX6</i>	This study
YLP527	<i>MATα his3-Δ1 leu2-Δ0 lys2-Δ0 met15-Δ0 ura3-Δ0 slx8::His3MX6</i>	This study
YLP504	<i>MATα his3-Δ1 leu2-Δ0 ura3-Δ0 slx8::NatMX6</i>	This study
YLP505	<i>MATa his3-Δ1 leu2-Δ0 ura3-Δ0 slx8::NatMX6</i>	This study
YLP538	<i>MATa his3-Δ1 leu2-Δ0 met15-Δ0 ura3-Δ0 rts1::KanMX4</i>	This study
YLP540	<i>MATα his3-Δ1 leu2-Δ0 lys2-Δ0 ura3-Δ0 rts1::KanMX4</i>	This study
YLP543	<i>MATa his3-Δ1 leu2-Δ0 met15-Δ0 ura3-Δ0 rts1::KanMX4 slx5::NatMX6</i>	This study
YLP545	<i>MATα his3-Δ1 leu2-Δ0 lys2-Δ0 ura3-Δ0 rts1::KanMX4 slx5::NatMX6</i>	This study
YLP547	<i>MATa his3-Δ1 leu2-Δ0 met15-Δ0 lys2-Δ0 ura3-Δ0 rts1::KanMX4 slx8::His3MX6</i>	This study
YLP550	<i>MATα his3-Δ1 leu2-Δ0 met15-Δ0 lys2-Δ0 ura3-Δ0 rts1::KanMX4 slx8::His3MX6</i>	This study
YLP530	<i>MATα his3-Δ1 leu2-Δ0 met15-Δ0 lys2-Δ0 ura3-Δ0 sgo1::KanMX4</i>	This study
YLP531	<i>MATα his3-Δ1 leu2-Δ0 met15-Δ0 ura3-Δ0 sgo1::KanMX4 slx5::NatMX6</i>	This study
YLP533	<i>MATα his3-Δ1 leu2-Δ0 lys2-Δ0 ura3-Δ0 sgo1::KanMX4 slx8::NatMX6</i>	This study
YLP512	<i>MATα his3-Δ1 leu2-Δ0 met15-Δ0 ura3-Δ0 mad2::KanMX4</i>	This study
YLP514	<i>MATa his3-Δ1 leu2-Δ0 met15-Δ0 ura3-Δ0 mad2::KanMX4</i>	This study
YLP516	<i>MATα his3-Δ1 leu2-Δ0 met15-Δ0 ura3-Δ0 mad2::KanMX4 slx5::His3MX6</i>	This study
YLP518	<i>MATa his3-Δ1 leu2-Δ0 met15-Δ0 ura3-Δ0 mad2::KanMX4 slx5::His3MX6</i>	This study
YLP519	<i>MATα his3-Δ1 leu2-Δ0 met15-Δ0 ura3-Δ0 mad2::KanMX4 slx8::His3MX6</i>	This study
YLP521	<i>MATa his3-Δ1 leu2-Δ0 met15-Δ0 ura3-Δ0 mad2::KanMX4 slx8::His3MX6</i>	This study
YLP033	<i>MATα his3-Δ1 leu2-Δ0 met15-Δ0 ura3-Δ0 SLX8-GFP::His3MX6</i>	This study
YLP034	<i>MATα his3-Δ1 leu2-Δ0 met15-Δ0 ura3-Δ0 SLX5-GFP::His3MX6</i>	This study
YYB2168	<i>MATa ade2-101 his3-Δ200 leu2 lys2-801 trp1-Δ63 ura3-52 ndc10-1</i>	This study
YLP437	<i>MATa ade2-101 his3-Δ200 leu2 lys2-801 trp1-Δ63 ura3-52 SLX5-GFP::His3MX6 ndc10-1</i>	This study
YLP438	<i>MATα his3-Δ1 leu2-Δ0 met15-Δ0 ura3-Δ0 SLX5-GFP::His3MX6 slx8::NatMX6</i>	This study
YLP439	<i>MATα his3-Δ1 leu2-Δ0 met15-Δ0 ura3-Δ0 SLX8-GFP::His3MX6 slx5::NatMX6</i>	This study
YYB3085	<i>MATa ade2-101 his3-Δ200 leu2-Δ1 lys2-801 trp1-Δ63 ura3-52 CFIII (CEN3.LYPH278) URA3 SUP11</i>	Spencer et al., 1990
YLP440	<i>MATa ade2-101 his3-Δ200 leu2-Δ1 lys2-801 trp1-Δ63 ura3-52 CFIII (CEN3.LYPH278) URA3 SUP11 slx5::His3MX6</i>	This study
YLP441	<i>MATa ade2-101 his3-Δ200 leu2-Δ1 lys2-801 trp1-Δ63 ura3-52 CFIII (CEN3.LYPH278) URA3 SUP11 slx8::His3MX6</i>	This study
YBM556	<i>MATα ura3-52 ade2-101 trp1-Δ63 his3-Δ200 leu2-Δ1 NDC10-GFP::His3MX6</i>	Montpetit et al., 2006
YLP578	<i>MATa his3-Δ200 leu2-Δ1 lys2-801 ura3-52 NDC10-GFP::His3MX6 slx5::KanMX6</i>	This study
YLP580	<i>MATa his3-Δ200 leu2-Δ1 lys2-801 trp1-Δ63 ura3-52 NDC10-GFP::His3MX6 slx8::NatMX6</i>	This study
YPH1819	<i>MATa ade2-101 his3-Δ200 leu2-Δ1 lys2-801 trp1-Δ63 ura3-52 CEP3-GFP::His3MX6</i>	Montpetit et al., 2006
YLP583	<i>MATa his3-Δ200 leu2-Δ1 lys2-801 ura3-52 CEP3-GFP::His3MX6 slx5::KanMX6</i>	This study
YLP585	<i>MATα his3-Δ200 leu2-Δ1 lys2-801 trp1-Δ63 ura3-52 CEP3-GFP::His3MX6 slx8::NatMX6</i>	This study
YPH1821	<i>MATa ade2-101 his3-Δ200 leu2-Δ1 lys2-801 trp1-Δ63 ura3-52 BIR1-GFP::His3MX6</i>	Montpetit et al., 2006
YLP553	<i>MATa his3-Δ200 leu2-Δ1 lys2-801 ura3-52 BIR1-GFP::His3MX6 slx5::KanMX6</i>	This study

Supplementary Table S2. Continued

Name	Genotype	Source
YYB3820	<i>MATα his3-Δ1 leu2-Δ0 met15-Δ0 ura3-Δ0 Nnf1-mCherry::KanMX4</i>	This study
YLP225	<i>MATα his3-Δ1 leu2-Δ0 met15-Δ0 ura3-Δ0 Nnf1-mCherry::KanMX4 SLX5-GFP::His3MX6</i>	This study
YLP160	<i>MATα his3-Δ1 leu2-Δ0 met15-Δ0 ura3-Δ0 RTS1-GFP::His3MX6</i>	Huh et al., 2003
YLP161	<i>MATα his3-Δ1 leu2-Δ0 ura3-Δ0 RTS1-GFP::His3MX6 slx5::KanMX6</i>	This study
YLP162	<i>MATα his3-Δ1 leu2-Δ0 lys2-Δ0 ura3-Δ0 RTS1-GFP::His3MX6 slx5::KanMX6</i>	This study
YLP163	<i>MATα his3-Δ1 leu2-Δ0 met15-Δ0 ura3-Δ0 RTS1-GFP::His3MX6 slx8::KanMX6</i>	This study
YLP165	<i>MATα his3-Δ1 leu2-Δ0 lys2-Δ0 ura3-Δ0 RTS1-GFP::His3MX6 slx8::KanMX6</i>	This study
YLP422	<i>MATα his3-Δ1 leu2-Δ0 met15-Δ0 ura3-Δ0 RTS1-GFP::His3MX6 sgo1::KanMX6</i>	This study
YLP426	<i>MATα his3-Δ1 leu2-Δ0 met15-Δ0 ura3-Δ0 RTS1-GFP::His3MX6 sgo1::KanMX6 slx5::NatMX6</i>	This study
YLP427	<i>MATα his3-Δ1 leu2-Δ0 ura3-Δ0 Nnf1-mCherry::KanMX4 RTS1-GFP::His3MX6</i>	This study
YLP429	<i>MATα his3-Δ1 leu2-Δ0 ura3-Δ0 Nnf1-mCherry::KanMX4 RTS1-GFP::His3MX6 slx5::KanMX6 mad2::URA3</i>	This study
YYB2327	<i>MATα ura3-52 lys2-801 ade2-101 trp1-Δ63 his3-Δ200 leu2-Δ1 GFP-TUB1::URA3</i>	Grava et al., 2006
YLP144	<i>MATα ura3-52 lys2-801 ade2-101 trp1-Δ63 his3-Δ200 leu2-Δ1 GFP-TUB1::URA3 slx8::KanMX6</i>	This study
YLP146	<i>MATα ura3-52 lys2-801 ade2-101 trp1-Δ63 his3-Δ200 leu2-Δ1 GFP-TUB1::URA3 slx5::His3MX6</i>	This study
YYB3283	<i>MATα ura3-52 lys2-801 ade2-101 trp1-Δ63 his3-Δ200 leu2-Δ1 SPC42-GFP::hphNT1</i>	Neurohr et al., 2011
YLP076	<i>MATα ura3-52 lys2-801 ade2-101 trp1-Δ63 his3-Δ200 leu2-Δ1 SPC42-GFP::hphNT1 slx5::KanMX6</i>	This study
YLP077	<i>MATα ura3-52 lys2-801 ade2-101 trp1-Δ63 his3-Δ200 leu2-Δ1 SPC42-GFP::hphNT1 slx8::KanMX6</i>	This study

Supplementary Table S3. Primer sequences

Name	Direction	Sequence (5' – 3')
CEN1	Forward	AACTTCAAAACCTTTTATGTAA
	Reverse	AGGCGCTTGAAATGAAAGCTCCG
CEN2	Forward	CTTGAGCAAATTGATCCTACATAAT
	Reverse	GCAAGAAATATATTGATACTTC
CEN5	Forward	CTATGAAACATCAAATTAATCA
	Reverse	CGGAAATCTAATACTGCTACAA
POL1	Forward	TGCACCAGTTAATTCTAAAAAGGCA
	Reverse	AAAACACCCTGATCCACCTCTGAA
RNF4	Forward	CTCGTGGAACCTGCTGGAGATGAAATTG
	Reverse	ATTCCTCCTTGGTCTTCTTCTTTCGTCAAC
β-Actin	Forward	GACATGGAGAAAATCTGGCA
	Reverse	AATGTCACGCACGATTTCCC

Supplementary Table S4. SiRNA sequences

Name	#	Sequence (5' – 3')
Luciferase	Mock	CGTACGCGGAATACTTCGA
RNF4-2	#1	GAATGGACGTCTCATCGTTTT
RNF4-5	#2	CCCTGTTTCCTAAGAACGAAA
RNF4-8	#3	AAGACTGTTTCGAAACCAACA
RNF4-D7	#4	GCTAATACTTGCCCAACTT
RNF4-D8	#5	GAATGGACGTCTCATCGTT
RNF4-D9	#6	GACAGAGACGTATATGTGA
RNF4-D10	#7	GCAATAAATCTAGACAAG



Subunit-specific functions of the SUMO-targeted ubiquitin E3 ligase Slx5/8

Loes A.L. van de Pasch, Antony J. Miles,
Eva Apweiler, Sjoerd J.L. van Wijk, H. Th.
Marc Timmers and Frank C.P. Holstege

Subunit-specific functions of the SUMO-targeted ubiquitin E3 ligase Slx5/8

Loes A.L. van de Pasch, Antony J. Miles, Eva Apweiler, Sjoerd J.L. van Wijk, H. Th. Marc Timmers and Frank C.P. Holstege

Molecular Cancer Research, University Medical Centre Utrecht, Universiteitsweg 100, 3508 AB, Utrecht, the Netherlands

ABSTRACT

The turnover of polysumoylated proteins is under the regulatory control of the ubiquitin-proteasome system. SUMO-targeted ubiquitin ligases (STUbLs) bind to sumoylated proteins and mediate their polyubiquitination, leading to proteasomal protein degradation. The Slx5/8 complex in *Saccharomyces cerevisiae* is a heterodimeric STUbL, which is required for the maintenance of genome stability through an as yet undefined mechanism. The precise contribution of the Slx5 and Slx8 subunits in SUMO-dependent ubiquitination is unclear. We therefore functionally characterised the individual Slx5 and Slx8 subunits to gain a mechanistic insight into STUbL complexes. The spectrum of phenotypic defects of *slx5Δ* analysed here, including accumulation of sumoylated proteins, sensitivity to hydroxyurea and chromosomal instability, is similar to that of that of *slx8Δ*, which agrees with a shared function in the same cellular pathway. Analysis of the individual subunits demonstrates that Slx5 and Slx8 perform different molecular functions. Together with previous studies on Slx5/8, this leads to the proposal that Slx5 is the subunit that binds to sumoylated substrates, whereas Slx8 mediates the interaction with E2 enzymes. We provide a model that explains how combined action of Slx5 and Slx8 is required to function as STUbL and how they may contribute to genome stability.

INTRODUCTION

Ubiquitin and the ubiquitin-like protein SUMO (small ubiquitin-like modifier) are small polypeptides that function as important posttranslational modifications of many proteins in eukaryotes. Molecularly, the processes of ubiquitination and sumoylation are very similar to each other. Both require a three-step enzymatic cascade catalysed by E1, E2 and E3 enzymes to be covalently attached to a protein substrate. These enzymes perform different functions in consecutive order, which are the activation of the modifier (E1), the transfer (E2) and the selection of the substrate (E3). Consecutive rounds of ubiquitin or SUMO protein conjugation results in the formation of polyubiquitin or

polySUMO chains. Ubiquitin and SUMO monomers and polymers modulate the function of the protein substrate by altering its conformation, activity, protein interactions, subcellular localisation and turnover. This plays important roles in many cellular pathways, such as cell cycle progression, genome stability, transcription and vesicular transport¹⁻⁴.

A well-known function of ubiquitination is its key role in protein degradation, which is predominantly mediated by K48-linked polyubiquitin chains^{5,6}. These chains act as a targeting molecule for the proteasome, which is a large multi-subunit protease complex that drives protein degradation⁷. This is crucial for degradation of misfolded proteins, but also for regulated protein degradation in response to specific cellular

signals. The turnover of sumoylated proteins is also regulated by the ubiquitin-proteasome system⁸⁻¹⁰. Eukaryotic cells have SUMO-targeted ubiquitin E3 ligases (STUbLs) that are dedicated to the polyubiquitination of sumoylated substrates, which results in their degradation by the proteasome¹¹⁻¹⁶. *Saccharomyces cerevisiae* has a heterodimeric STUbL complex, consisting of the subunits Slx5 and Slx8 (hereafter referred to as the Slx5/8 complex)¹⁷. Slx5 and Slx8 both have a C-terminal RING domain, which is typically found in many ubiquitin E3 ligases. The RING domain is a type of zinc-finger domain that adopts its protein conformation by folding around two zinc ions. The RING is a binding platform for E2-ubiquitin conjugates and is thought to promote the transfer of ubiquitin to the substrate by allosteric regulation of the E2 enzyme¹⁸. In addition, Slx5 and Slx8 contain several SUMO-interaction motifs (SIMs), which mediate their interaction with sumoylated proteins^{13,14,19,20}. The function of Slx5/8 as a SUMO-targeted ubiquitin E3 ligase requires the simultaneous action of Slx5 and Slx8, where Slx5 is thought to bind the sumoylated substrate and Slx8 to mediate Ubc4-dependent ubiquitination^{13,14}. A hallmark of STUbL mutants is the accumulation of polysumoylated proteins due to a failure of their ubiquitin-dependent degradation by the proteasome. This is associated with a pleiotropic mutant phenotype that includes a severe defect in the maintenance of genome stability^{11,12,21-25}. The aberrant cellular levels of sumoylated proteins are thought to be the direct cause of impaired DNA repair or replication, but as yet no true *in vivo* substrate of Slx5/8 with a role in genome stability has been identified. Only three substrates have been characterised, which are the transcription regulators Mot2, $\alpha 1$ and $\alpha 2$, indicating that Slx5/8 has additional functions in transcription regulation^{20,26,27}. The molecular mechanism that explains the genome instability in STUbL mutants is therefore largely unknown.

Previously, we have demonstrated that Slx5 is physically located at centromeres (Chapter 4, this thesis). A centromere is a single DNA binding

site on a chromosome for the kinetochore, a large structure that physically connects centromeres to microtubules, allowing regulated segregation of sister chromatids during mitosis and meiosis²⁸. Intriguingly, the centromeric location of Slx5 occurs independently of Slx8. This is unexpected given that Slx5 and Slx8 function together as a heterodimeric ubiquitin E3 ligase^{13,14,17}. In contrast to the lack of centromeric colocalisation, the phenotypes of *slx5* Δ and *slx8* Δ mutants are very similar and point to a shared function in genome stability. To separate potential independent cellular functions of Slx5 and Slx8, we aimed to investigate subunit-specific functions of the Slx5/8 complex. Our results point to a shared function of Slx5 and Slx8 in one cellular pathway, in which the subunits perform different molecular functions, being binding to a substrate and an E2 enzyme, respectively. The combination of these two functions in one protein complex is crucial for the maintenance of genome stability.

RESULTS

Slx5 and Slx8 contribute equally to degradation of sumoylated proteins *in vivo*

Slx5 Δ and *slx8* Δ mutants in *S. cerevisiae* and STUbL mutants in other species are characterised by an accumulation of polysumoylated proteins¹¹⁻¹⁶. We investigated whether there are differences in the accumulation of polysumoylated proteins in *slx5* Δ and *slx8* Δ , which would indicate that Slx5 and Slx8 may act on different substrates independently of each other. Our SUMO-antibodies did not detect polySUMO conjugates (data not shown) and therefore strains were generated that expressed epitope-tagged SUMO (*SMT3*). *SMT3* was N-terminally fused to a 3HA-tag and placed under the control of its own endogenous *SMT3* promoter. Constitutive expression of *3HA-SMT3* resulted in a mild growth defect and spores derived of heterozygote diploid *3HA-SMT3* strains were inviable (data not shown). This suggests that N-terminally tagging of *SMT3* results in mitotic and meiotic defects. We therefore set up an inducible

system where 3HA-SMT3 was placed on a low-copy plasmid under the control of an inducible GAL promoter. Upon exposure to galactose, wt strains show overexpression of 3HA-SMT3 in comparison to a strain that constitutively expresses 3HA-SMT3 (Figure 1A). Both *slx5Δ* and *slx8Δ* exhibit a strong accumulation of high-molecular weight SUMO-conjugates, which is absent in the wt (Figure 1B). This agrees with their function in promoting degradation of polysumoylated proteins. Sumoylated proteins in the lower molecular weight range appear unaffected in *slx5Δ* and *slx8Δ* compared to wt. These likely represent mono-sumoylated proteins that are not regulated by SUMO-dependent ubiquitination. There is no detectable difference between *slx5Δ* and *slx8Δ* in sumoylated protein species patterns or levels, suggesting that Slx5 and Slx8 act on the same proteins. They appear to contribute equally to

sumoylated protein degradation, which agrees with a shared function in a single protein complex. These observations are supported by genetic evidence (Figure 1C). The mutants *slx5Δ* and *slx8Δ* have a similar growth defect. Combination of the two mutations in the double mutant *slx5Δ slx8Δ* does not result in an additional growth inhibition. This indicates that Slx5 and Slx8 are less likely to have independent cellular functions, as this would lead to aggravation of the growth defect in the double mutant. In addition the entire spectrum of synthetic genetic interactions of *SLX5* and *SLX8* with other genes in high-throughput studies is highly similar^{29,30}. These epistatic relationships therefore confirm that Slx5 and Slx8 function in the same cellular pathway and as a single protein complex and therefore likely target the same sumoylated proteins as demonstrated above.

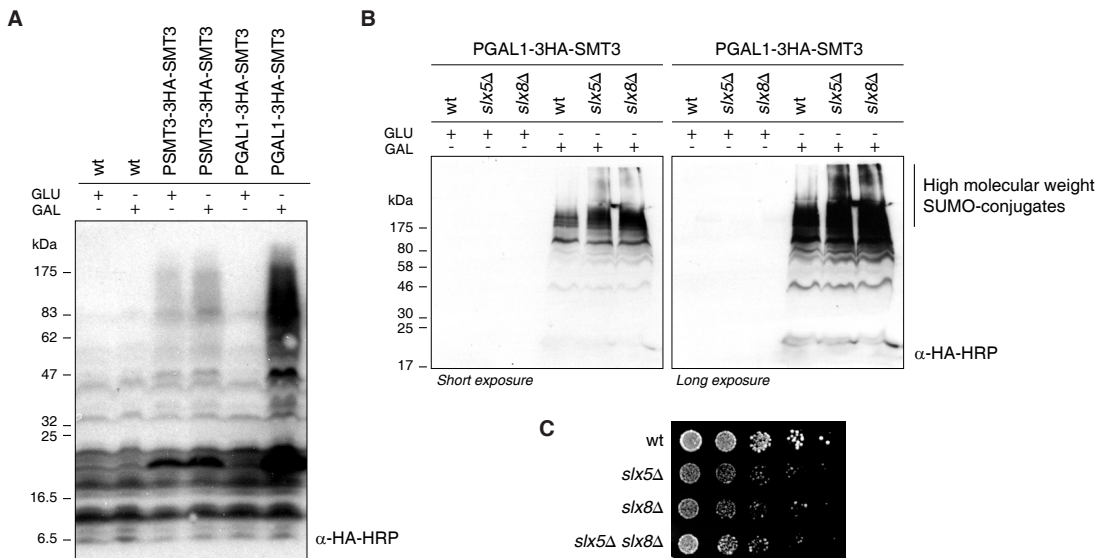


Figure 1. Slx5 and Slx8 contribute equally to SUMO-dependent ubiquitination.

(A) Immunoblot analysis of sumoylated proteins in yeast whole cell lysates of wt strains expressing epitope-tagged SUMO (3HA-SMT3). 3HA-SMT3 was expressed from a low-copy plasmid under the control of the endogenous, constitutive SMT3 promoter (PSMT3) or the inducible GAL promoter (PGAL) in the presence of glucose (GLU: non-inducing) or galactose (GAL: inducing). (B) Immunoblot analysis of 3HA-tagged sumoylated proteins in yeast whole cell lysates of wt, *slx5Δ* and *slx8Δ* strains. 3HA-SMT3 was expressed from a low-copy plasmid under control of the GAL promoter (PGAL) in the presence of glucose or galactose. Accumulation of high-molecular weight SUMO-conjugates (HMW-SC) in *slx5Δ* and *slx8Δ* can be observed in the stacking gel. (C) Growth rate assay of wt, *slx5Δ*, *slx8Δ* and *slx5Δ slx8Δ* cells spotted in five-fold serial dilutions on YPD plates. Images are after two days growth at 30°C.

RING domains of Slx5 and Slx8 are both required for *in vivo* function in genome stability

To distinguish whether the phenotype of STUbL mutants is exclusively due to ubiquitination defects, Slx5 and Slx8 RING mutants were generated to inactivate the function of the RING (Figure 2A and 2B). The RING domain consists in general of 40–60 residues, including a Cys-X₂-Cys-X_{9–39}-Cys-X_{1–3}-His-X_{2–3}-Cys-X₂-Cys-X_{4–48}-Cys-X₂-Cys motif (where X can be any amino acid; histidines and cysteines are sometimes exchanged). The cysteines and histidines are zinc-coordinating residues, which adopt loop structures in the RING. These loops are required

for binding to E2 enzymes¹⁸. Introduction of two cysteine to serine mutations in the RING of either Slx5 or Slx8 has previously been shown to be sufficient for complete disruption of *in vitro* ubiquitination by Slx5/8¹⁴. Phenotype characterisation of *slx5*Δ and *slx8*Δ, transformed with plasmids expressing either wt or RING mutant Slx5 and Slx8, reveals that the mutant growth defect is fully RING-dependent (Figure 2C). Moreover, the RING mutants show an increased sensitivity to hydroxyurea (HU), as previously reported, which indicates that both RING mutants have a reduced resistance to genotoxic stress¹⁴. Previously, we have demonstrated that

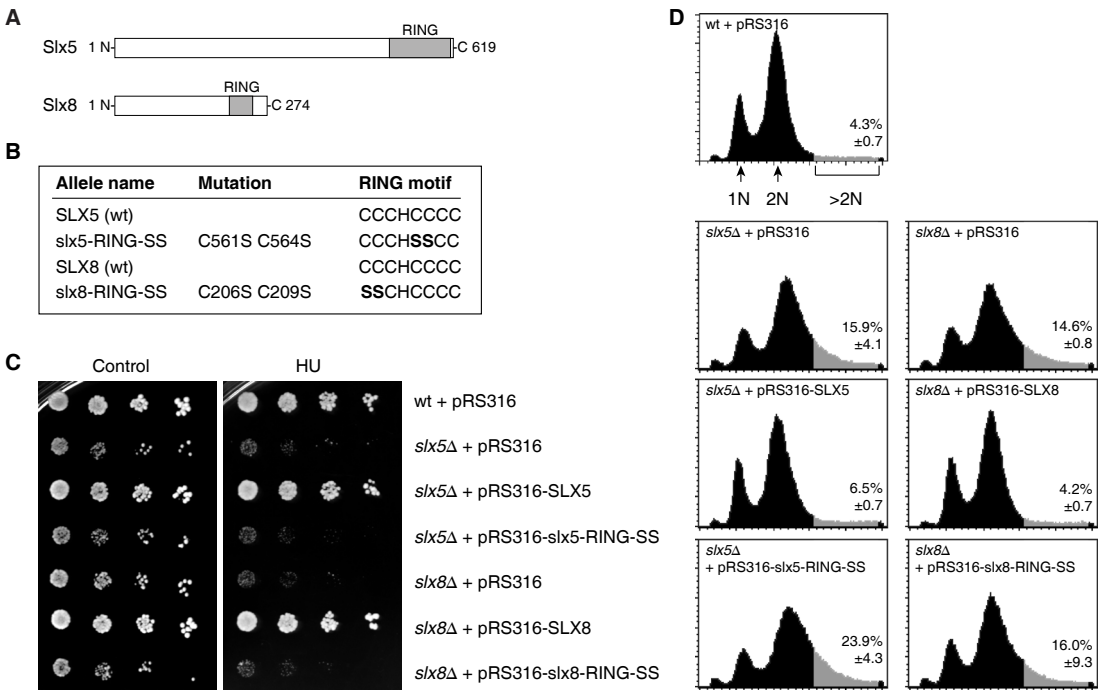


Figure 2. RING domains of Slx5 and Slx8 are both required for Slx5/8 function.

(A) Schematic representation of the Slx5 and Slx8 proteins. The position of the C-terminal RING domain is indicated. (B) Overview of RING motifs in wild type *SLX5* and *SLX8* and mutant *slx5* and *slx8*, in which two cysteine (C) to serine (S) point mutations were introduced in the RING domain. (C) Phenotype characterisation of wt, *slx5*Δ and *slx8*Δ, complemented with the low copy *CEN URA3* vector (pRS316), expressing wt or RING mutant Slx5 and Slx8, as shown in (B). Empty vector (pRS316) was used as control. Growth properties of the strains were assayed by growing the cells on solid media lacking uracil for plasmid maintenance. Sensitivity to hydroxy urea (HU) was measured on plates complemented with 100 mM HU. Cells were spotted in five-fold serial dilutions and grown for two days at 30°C. (D) Flow cytometric profiles of asynchronous cell populations, expressing wt or RING mutant Slx5 or Slx8 on a low copy pRS316 vector, as shown in (B). Cells were grown in selective media under normal growth conditions and harvested in the exponential growth phase. The DNA content was measured and the cell population with a >2N DNA content, indicated in grey, was quantified (\pm s.d., $n = 3$).

slx5Δ and *slx8Δ* are highly chromosomally unstable and are characterised by an aberrant DNA content. Flow cytometric analyses reveals that also this phenotype is characteristic for *slx5* and *slx8* RING mutants (Figure 2D). Asynchronous *slx5Δ* and *slx8Δ* cell cultures, transformed with an empty vector (pRS316) or expressing *slx5* or *slx8* RING mutants, are characterised by a large fraction of the cell population having a DNA content higher than 2N, indicating chromosomal aneuploidy. The defect can be rescued upon expression of wt *SLX5* or *SLX8* (Figure 2D). This indicates that the role of Slx5/8 in genome stability, whether in DNA repair, replication or chromosome segregation, is dependent on a functional RING of both Slx5 and Slx8.

In addition to a RING domain, Slx5 also contains multiple SIM domains, which are required for interacting with SUMOylated proteins. The SIM domains in Slx5 are characterised by a short stretch of 3-4 hydrophobic residues, that is sometimes followed by a stretch of 3-4 acidic residues^{13,20}. The SIM domains in Slx5 are poorly characterised and current estimates are that Slx5 has at least five redundant SIMs (Figure 4A)²⁰. Simultaneous mutation of the two most N-terminal SIMs is known to result in a weak loss of sumoylated protein degradation¹⁴. Simultaneous mutation of the first and third SIM results in loss of binding to SUMO in a yeast two-hybrid assay¹³. To investigate whether the SIM domains in Slx5 contribute to the *in vivo*

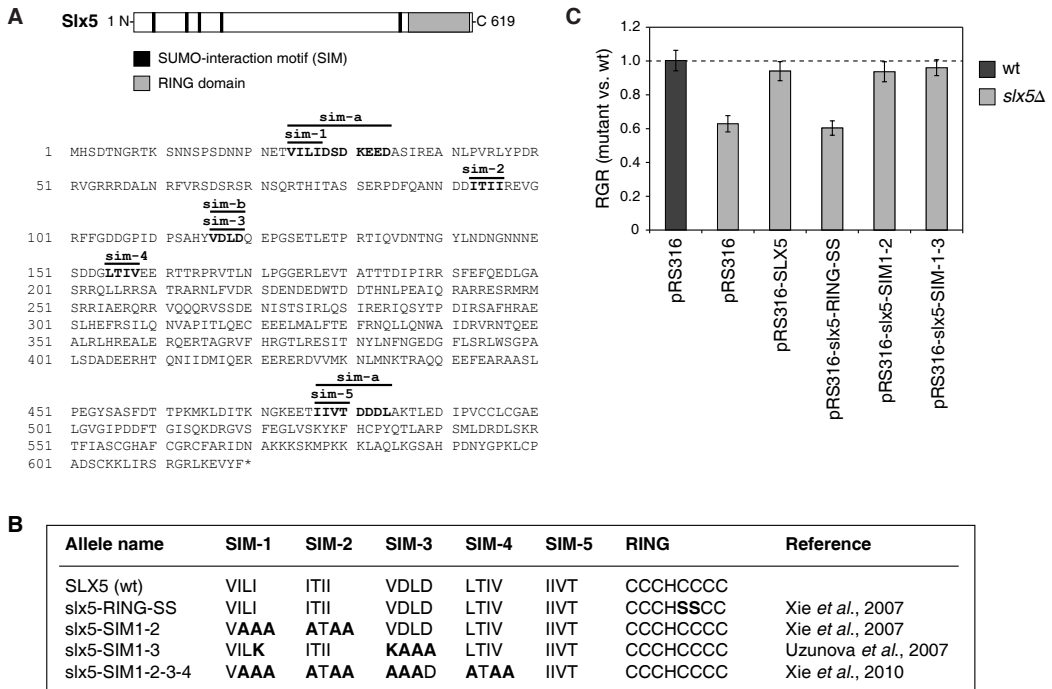


Figure 3. Slx5 contains multiple redundant SIM domains.

(A) Schematic representation of the Slx5 protein. Slx5 has a C-terminal RING domain and five SIM domains. The bottom panel shows the amino acid sequence of Slx5 with the (putative) SIM domains indicated as described by Uzunova *et al.* (sim-a and sim-b) and Xie *et al.* (sim1-5)^{13,14,20}. (B) Overview of the Slx5 mutants, bearing point mutations in the RING domain or SIM domains. (C) Growth rate assay of wt and *slx5Δ*, complemented with the low copy *CEN URA3* vector (pRS316), expressing wt, RING or SIM point mutants of Slx5. An empty vector was used as negative control. The relative growth rate (mutant vs. wt) was quantified during mid-log phase at 30°C in liquid synthetic media lacking uracil for plasmid maintenance (\pm s.d., n = 4). Note that the quadruple SIM mutant (*slx5*-SIM1-2-3-4), shown in (B), is not tested.

function of Slx5/8, we generated two different *slx5* SIM mutants. In these mutants, the hydrophobic cores of two SIMs are substituted with alanine or lysine residues, as described by Xie *et al.* and Uzunova *et al.* (Figure 4B)^{13,14}. Both SIM mutants have a wt-like growth rate and do not display any phenotypic defects that are characteristic for Slx5/8 loss of function (Figure 4C). Extended analyses of additional putative Slx5 SIMs by others have revealed that combined mutation of four SIMs is required to achieve complete loss of SUMO-binding and accumulation of sumoylated proteins, which is associated with sensitivity to hydroxyurea²⁰. This demonstrates that Slx5/8 function is dependent on the SIM domains of Slx5 and the RING domains of Slx5 and Slx8 to perform its *in vivo* function as STUBL.

Slx8 interacts with UBC-fold domains of human ubiquitin E2 enzymes

Slx5/8 as a heterodimeric complex can stimulate *in vitro* ubiquitination, but the individual subunits cannot or only do so with little efficiency^{13,14,31}. This indicates that Slx5 and Slx8 are interdependent for mediating the ubiquitination of substrates. However, both Slx5 and Slx8 possess a RING domain, which potentially mediates the interaction with an E2 enzyme. Both RING domains are required for the *in vivo* function of Slx5/8, but it is unclear whether one or both RING domains of Slx5 and Slx8 are involved in E2-binding. We therefore investigated whether Slx5 and Slx8 possess the capacity to interact with specific E2 conjugating enzymes using a yeast two-hybrid approach (Figure 4A). An array of EGY48a yeast strains was used that expressed UBC-fold domains derived from 36 different human E2 enzymes fused to a LexA DNA binding domain. The highly conserved UBC-fold domain of E2 enzymes is crucial for selective interaction with RING domains of E3 ligases³². The strains were systematically mated to EGY48a strains, bearing either full length *SLX5* or *SLX8* that were N-terminally fused to a galactose-inducible B42-activation domain. Yeast two-hybrid interactions were visualised by X-Gal induced blue-

colouring of yeast spots upon galactose-dependent activation of the LacZ reporter. Each E2-SLX pair was tested in triplicate and in parallel an empty LexA vector was taken along as control (Figure 4A). For unclear reasons, Slx8 was capable of LacZ activation in the presence of an empty LexA vector, but not when it was co-transformed with most LexA-E2 fusion vectors, allowing us to investigate all UBC-fold interactions with Slx5 and Slx8 (Figure 4B).

Four different interactions were identified between Slx8 and UBC-fold domains. Strikingly, Slx5 did not reveal yeast two-hybrid interactions with any of the 36 E2s (Figure 4B). This indicates that Slx8 and not Slx5 is the subunit that mediates the interaction with E2 enzymes. The interactions that were found for Slx8 are with the UBC-fold domains of UBE2D2, UBE2E2, UBE2G2 and UBE2U (Figure 3C). The interaction of Slx8 with UBE2D2 is lost upon K36E mutation (Figure 4C). Similar loss of E2-E3 interaction in the UBE2D2 K36E mutant is described for the human ubiquitin E3 ligase CNOT4 and for the human Slx5/8 orthologue RNF4 (SNURF)^{32,33}. UBE2D2 is a member of the highly conserved Ubch5 family of E2 enzymes, which catalyses the attachment of K48 poly-ubiquitin chains to substrates for proteasomal degradation³⁴. The orthologous E2s in *S. cerevisiae* are Ubc4 and Ubc5. Indeed, ubiquitination of transcription factor $\alpha 2$ by Slx5/8 is dependent on Ubc4²⁰, suggesting that the interaction of Slx8 with the UBC-fold of UBE2E2 represents a functional interaction with Ubc4 in yeast. Slx8 did not interact with the UBC-fold of the SUMO-specific E2 enzyme UBE2I (Figure 4C). This supports the theory that Slx5/8 functions as a ubiquitin E3 ligase^{13,14,20}, rather than being a SUMO E3 ligase as previously proposed³⁵.

Formation of subnuclear Slx8 foci is dependent on Slx5

Slx5 and Slx8 are nuclear proteins. Investigation of the subcellular localisation of Slx5 and Slx8 has revealed that their subnuclear location does not fully overlap, suggesting potential separate cellular functions for Slx5 and Slx8. Microscopy revealed

that Slx5 is enriched at the nuclear pore and frequently in subnuclear foci, which represent sites of DNA replication and DNA damage^{22,24,25}. The subcellular location of Slx8 is less well characterised and contradictory. The number of Slx8 foci are fewer in number compared to Slx5 foci or are reported not to be existent at all^{22,25}. Moreover, chromatin immunoprecipitation showed that Slx5 resides at centromeric DNA, whereas Slx8 does not (Chapter 4, this thesis). The subcellular location of Slx8 was

therefore investigated in more detail to gain insight into potential separate *in vivo* functions of Slx5 and Slx8.

Cells expressing Slx8-GFP were studied by live cell fluorescence microscopy. All cells show a diffuse nuclear location of Slx8 with an occasional punctuate location. Slx8 foci vary in size and number per cell (Figure 5A). The subcellular location of Slx8 resembles that of Slx5, in having a diffuse nuclear location with foci^{22,25}. The location of Slx8 was further

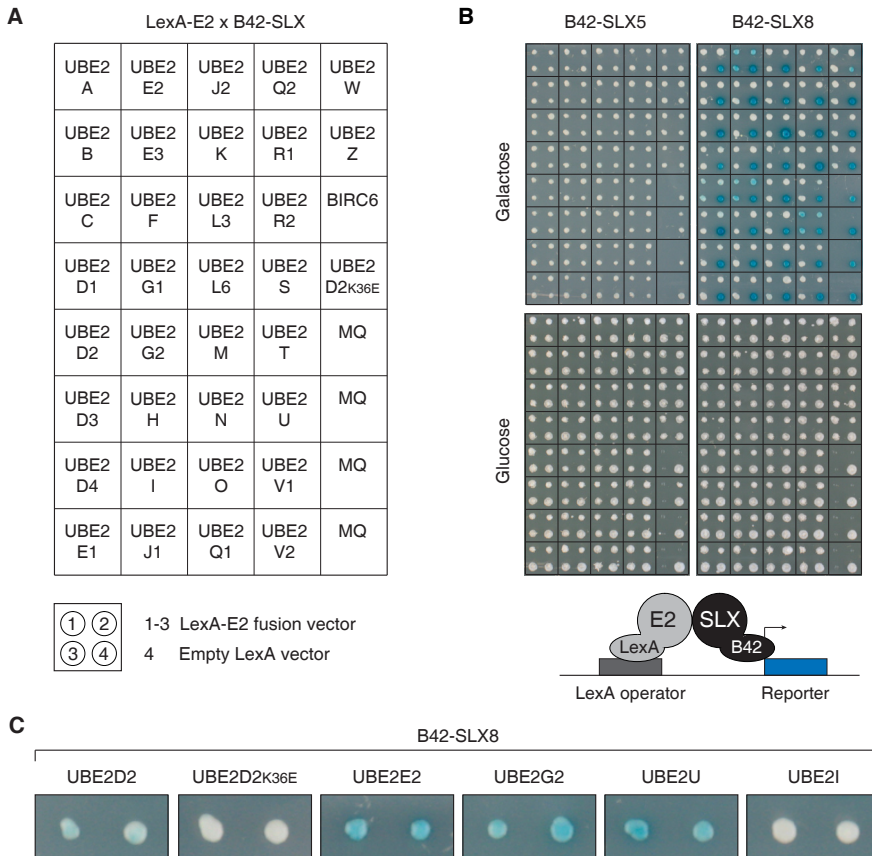


Figure 4. Slx8 interacts with specific UBC-fold domains of human ubiquitin E2 enzymes.

(A) Outline of LexA-E2 yeast two-hybrid array used for pair-wise screening for interactions with B42-Slx5 and B42-Slx8. The LexA-E2 fusion constructs comprised 36 different UBC-fold domains derived from human E2 enzymes (Van Wijk *et al.*, 2009). The UBC-fold domains were N-terminally fused to a LexA DNA binding domain (LexA-E2) and were co-expressed with full length Slx5 or Slx8 that were N-terminally fused to a B42 activation domain. Each E2-SLX interaction was tested in triplicate, with an empty LexA vector and Milli-Q water (MQ) as negative controls. (B) Yeast two-hybrid assays for B42-Slx5 and B42-Slx8 under B42-inducing (galactose) and B42-repressing (glucose) conditions. SLX-E2 interactions were visualised after three days growth on SC X-Gal plates. (C) Magnification of selected Slx8-E2 yeast two-hybrid interactions illustrated in (B), showing two biological replicates under inducing conditions. Slx8 interacts with UBE2-D2, UBE2-E2 and UBE2-U, but not with UBE2-D2_{K36E} or UBE2-I.

studied in *slx5Δ* cells to investigate whether the subcellular location of Slx8 is dependent on Slx5. In contrast to wt cells, Slx8 is homogeneously dispersed throughout the nucleus in *slx5Δ* cells and Slx8 foci are completely absent (Figure 5B). This indicates that Slx5 is required for the correct subcellular location of Slx8. This supports the hypothesis that Slx5 and

Slx8 function together as a heterodimeric complex, where Slx5 is the subunit that binds to sumoylated proteins that may be present in the foci.

Previously, we have shown by chromatin immunoprecipitation that Slx5 resides at centromeres, whereas Slx8 does not, suggesting a Slx8-independent function of Slx5 at the kinetochore (Chapter 4, this

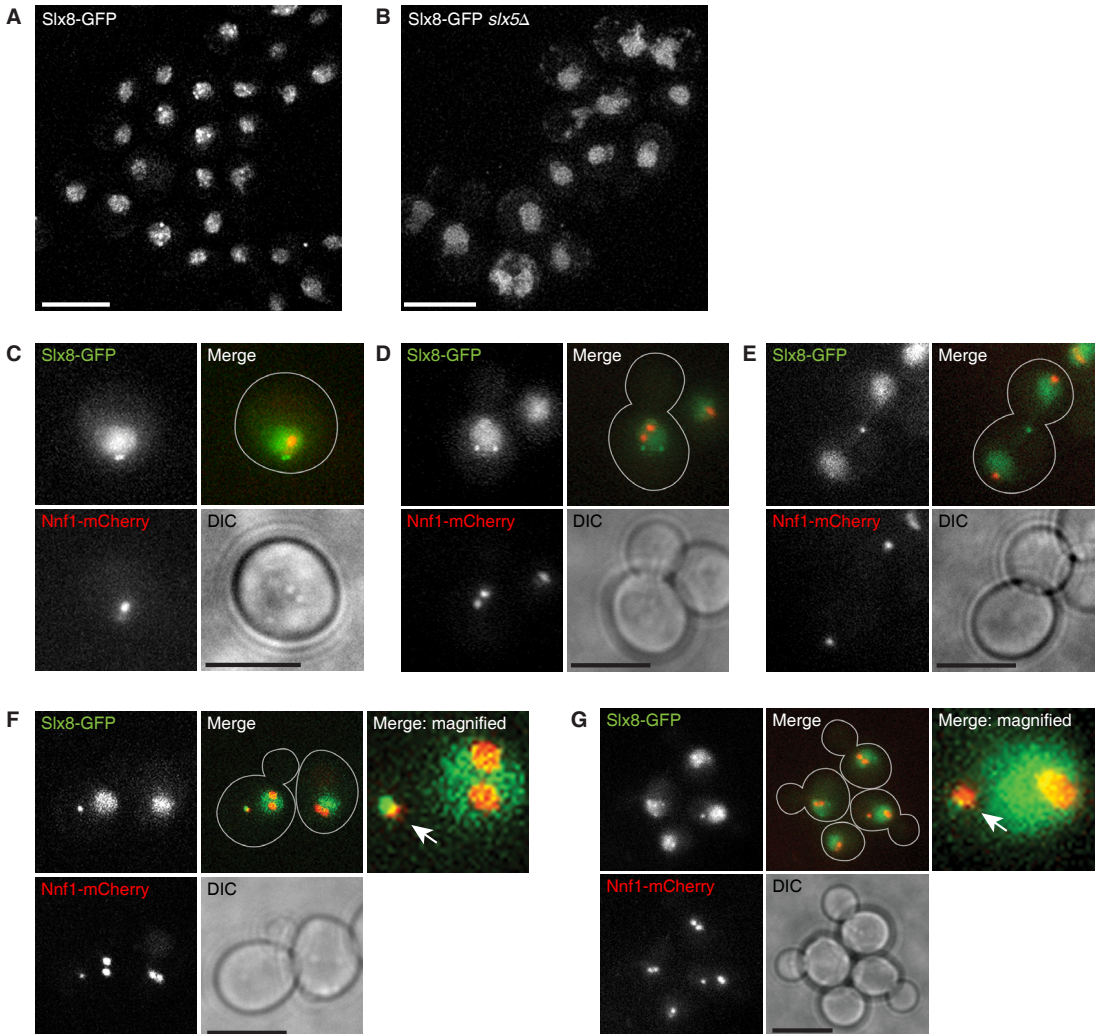


Figure 5. Slx8 resides in subnuclear foci, which is dependent on Slx5.

(A-B) Live cell fluorescence microscopy of asynchronous wt (A) and *slx5Δ* (B) cell populations that express Slx8-GFP. (C-E) Representative examples of wt cells that display Slx8-GFP foci in G1 phase (C), G2/M phase (D) and in anaphase/telophase (E). Kinetochore protein Nnf1-mCherry is used as a centromeric marker. (F-G) Two examples of metaphase cells with a misattached chromosome. A Slx8 focus is located at the centromere of the misattached chromosome, which is indicated with an arrow. Scale bars, 5 μm.

thesis). The location of Slx8 and kinetochore protein Nnf1 was therefore studied to investigate whether Slx8 foci colocalise with centromeres. While Slx8 foci can be discerned during all cell cycle stages, they do not strictly colocalise with Nnf1 (Figure 5C-E). Strikingly, those cells that do show centromeric Slx8 foci appear to have a misaligned chromosome during metaphase. In these cells, Slx8 is clearly enriched at a small Nnf1 focus that is outside of the two normal kinetochore foci in metaphase cells. This suggests that Slx8 is recruited to centromeres upon chromosome misattachment during metaphase. Although the molecular mechanism remains unresolved, it demonstrates that the role of Slx5/8 in genome stability extends beyond DNA repair and is likely to contribute directly to regulation of chromosome segregation.

DISCUSSION

Slx5 and Slx8 form a heterodimeric STUbL complex, which is crucial for the maintenance of genome stability in yeast. Localisation studies of Slx5 and Slx8 have demonstrated that both reside at various subnuclear locations, including the nuclear pore, double strand DNA breaks, DNA damage foci and DNA replication foci^{22,24,25}. A more recent finding is the association of Slx5 with centromeric DNA (Chapter 4, this thesis). Intriguingly, Slx8 does not colocalise with Slx5 at centromeres as analysed by ChIP. This instigated the hypothesis that Slx5 and Slx8 may function as monomers with independent cellular functions. The function of the Slx5 and Slx8 subunits was therefore investigated to gain insight into the contribution of the individual subunits in SUMO-targeted ubiquitination and maintenance of genome stability.

Characterisation of *slx5Δ* and *slx8Δ* mutants has revealed several hallmarks of STUbL mutants, including accumulation of high-molecular weight SUMO conjugates, sensitivity to genotoxic stress and general genome instability^{13,14,17,21}. Our assays have demonstrated that there are virtually no differences between the type and severity of the mutant

phenotypes of *slx5Δ* and *slx8Δ*. This agrees with the theory that Slx5 and Slx8 have a shared function in one protein complex, rather than functioning in separate cellular pathways. One should bear in mind that the assays used here are based on finding STUbL defects. If either Slx5 or Slx8 has a second independent function that is not related to SUMO-targeted ubiquitin ligation, then a more suitable approach would be to focus on other characteristics. However, the similarity in genome-wide synthetic genetic interactions of *SLX5* and *SLX8* with other genes indicate that it is more likely that Slx5 and Slx8 have completely overlapping cellular functions^{29,30}.

While the cellular function of Slx5 and Slx8 appears to be the same, the molecular function of the subunits is different. The presence of SIM and RING domains leads us to speculate that Slx5 and Slx8 may both be involved in binding to substrates and to E2 enzymes *in vivo*. *In vitro* ubiquitination assays have demonstrated that Slx5 and Slx8 are interdependent for mediating ubiquitination of substrates. The presence of two functional RING domains in both subunits was an absolute requirement. Indeed, we have shown that mutation of either RING results in genome instability. However, the yeast two-hybrid experiments revealed that only the RING of Slx8 is involved in binding to E2 enzymes. The function of the RING of Slx5 remains unknown, but it may be involved in the heterodimerisation of the Slx5 and Slx8 subunits. Besides the RING domain, Slx5 has multiple SIM domains, but Slx8 also bears one uncharacterised SIM domain¹³. The presence of a SIM domain in Slx8 suggests that it may also contribute to substrate recognition. Moreover, Slx8 is reported to have a DNA-binding domain, which is thought to be required for Slx5/8 binding to DNA³⁶. Although we did not generate *slx8* SIM or DNA-binding domain mutants, it is unlikely that either the SIM or DNA-binding domain has a functional role *in vivo* in either substrate recognition or Slx5/8 recruitment to DNA. Deletion of *SLX5* results in complete mislocation of Slx8, indicating that the presence of a SIM or DNA-binding domain in Slx8 is not sufficient for the correct subcellular location

of Slx8. Slx8 is fully dependent on Slx5, which again argues for a shared function in one complex.

How can a shared function be reconciled with the results of the ChIP-chip experiments where Slx5 is found to be enriched at centromeres and Slx8 is not (Chapter 4, this thesis)? Closer examination of the subcellular location of Slx8 by live cell microscopy demonstrates that Slx8 is located at centromeres in a small number of cells (Figure 5F and 5G). This suggests that Slx8 has also a centromeric function, which is likely shared with Slx5. Intriguingly, Slx8 appears to be exclusively located on centromeres of cells in metaphase with misattached chromosomes. These cells represent a very small fraction of the entire cell population in a normal cell culture, which may explain why Slx8 is not detected on centromeres by ChIP-chip. In contrast, Slx5 is highly enriched on centromeres. This either indicates that Slx5 is constitutively located on centromeres or that Slx5 is present in a subpopulation of the asynchronous cell culture, e.g. during a specific cell cycle phase. The exciting observation that Slx8 is located on centromeres of misattached chromosomes in fraction of cells begs for more experiments to investigate a potential function of Slx8 (and Slx5) in mitotic checkpoint signalling prior to chromosome segregation. Preliminary experiments in which chromosome misattachment was induced,

using the spindle destabilising drug benomyl or a temperature-sensitive kinetochore mutant, did not reveal centromeric location Slx8 on misattached chromosomes (data not shown). The molecular function of Slx5/8 on centromeres remains therefore unclear. More ChIP experiments on synchronised cell populations and identification of (centromeric) substrates of Slx5/8 will be of great importance for delineating the molecular mechanism that explains the centromeric location of Slx5/8.

The observations presented here, and reported by others, allow us to propose a model where Slx5 interacts directly with a substrate on DNA (Figure 6). The interaction is mediated by the SIM domains of Slx5 in case of a sumoylated substrate. However, Slx5/8 has also been reported to be capable of ubiquitination in a SUMO-independent fashion²⁰. For these substrates, an alternative mechanism may exist. The (sumoylated) substrate is likely a component of the DNA repair or DNA replication system, or may constitute a centromeric protein, such as the kinetochore. A specific cellular signal, such as DNA damage or chromosome misattachment, may activate the recruitment of Slx8 to Slx5. Upon heterodimerisation, Slx5/8 forms a functional STUbL complex that provides a binding platform for the E2 enzyme at the RING of Slx8. The E2 for SUMO-targeted ubiquitination is Ubc4, but *in vitro* ubiquitination assays and our yeast two-hybrid assays suggest that Slx8 may also interact with other E2s^{13,14,31}. By simultaneously binding to the substrate and the E2 enzyme, Slx5/8 allows the transfer of ubiquitin to the substrate, which ultimately becomes polyubiquitinated with K48-linked ubiquitin chains and targeted to the proteasome for degradation. Controlled degradation of polysumoylated substrates via this mechanism is important for cell viability in yeast. The molecular mechanism is conserved and parallels may be drawn to other species as well, including humans. Future studies of Slx5/8 will therefore help in unravelling the general molecular mechanism of STUbLs.

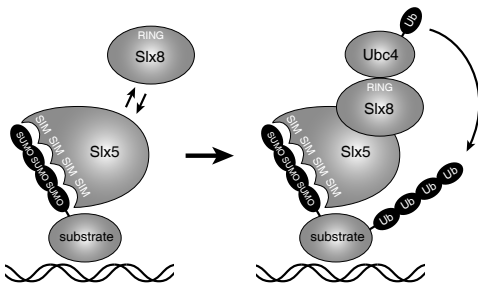


Figure 6. Proposed model of the mechanism of SUMO-targeted ubiquitination by Slx5/8.

This model takes into account distinct molecular functions of Slx5 and Slx8 that together contribute to a single cellular role. See 'Discussion' for details.

MATERIALS and METHODS

Yeast media and strains

Experiments were performed in synthetic complete (SC) or yeast extract-peptone-dextrose (YPD) media (US Biologicals) containing 2% glucose, unless indicated otherwise. All strains are in the genetic background of S288C. The genotype and source of the strains are listed in Supplementary Table S1. *SLX5* and *SLX8* deletion mutants were generated by PCR-based gene disruption using pFA6a deletion cassettes³⁷. Slx8-GFP strains were constructed by C-terminal genomic integration of a pFA6a-GFP-His3MX6 cassette³⁷. Nfn1-mCherry was constructed by replacing the GFP tag from NFN1-GFP::His3MX6 for mCherry::KanMX4³⁸. Strains were mated, followed by tetrad dissection of sporulated diploids to combine different mutations. Strains were transformed with pRS316 expression plasmids using standard genetic techniques. All plasmids are listed in Supplementary Table S2.

Construction of 3HA-Smt3 plasmids

Plasmid pFA6a-KanMX6-PGAL1-HBH-SMT3, containing N-terminally histidine-biotin-tagged *SMT3* with a *GAL1* promoter was a kind gift of P. Kaiser³⁹. The endogenous promoter of *SMT3* was PCR amplified from wt genomic DNA, using primers Smt3p-500-Bgl2 and Smt3p-500-Xho2, containing a BglII site and XhoI site respectively. All primer sequences are supplied in Supplementary Table S3. PSMT3 was BglII/XhoI digested and cloned into pFA6a-KanMX6-PGAL1-HBH-SMT3 to create pFA6a-KanMX6-PSMT3-HBH-SMT3. PFA6a-KanMX6-PSMT3-HBH-SMT3 was NcoI/PacI digested and cloned into pFA6a-KanMX6-PGAL1-3HA³⁷ to create pFA6a-KanMX6-PSMT3-3HA. Plasmid pFA6a-NatMX6 was NcoI/EcoRI digested and cloned into pFA6a-KanMX6-PSMT3-3HA to create pFA6a-NatMX6-PSMT3-3HA. Plasmid pFA6a-His3MX6-PGAL1-3HA was PCR amplified using primers SMT3-F4 and SMT3-R3³⁷. The PCR product was transformed into wt strains YYB384 and YYB386 to fuse *SMT3* N-terminally to a 3HA epitope tag under the control of the inducible *GAL1* promoter. Plasmid pFA6a-NatMX6-PSMT3-3HA was PCR amplified using primers SMT3-F4 and SMT3-R3. The 3HA-SMT3 strains underwent a second round of transformation with this PCR product, resulting in strains that constitutively expressed 3HA-SMT3. Genomic DNA was isolated from the strains with integrated 3HA-SMT3 constructs with a *GAL1* or *SMT3* promoter. The DNA was PCR amplified using primers Smt3-Clal and NatMX-R to obtain the full length *GAL1* or *SMT3* promoter, the 3HA tag, the *SMT3* gene and *SMT3* terminator. The PCR fragments were digested with Asp718/Clal and cloned into the low copy expression vector pRS316, resulting in plasmids pRS316-PGAL1-3HA-3SMT3 and pRS316-PSMT3-3HA-3SMT3. The plasmids were transformed into wt, *slx5Δ* and *slx8Δ* strains.

Construction of *slx5* and *slx8* point mutants

The *SLX5* and *SLX8* genes with their complete endogenous promoter and terminator regions were PCR amplified with T3 and T7 sequence overhangs, using primers SLX5M.F1,

SLX5M.R.2.2, TL.SLX8M.F1 and TL.SLX8M.R.2. The low copy expression vector pRS316 was BamHI/EcoRI digested and cotransformed with the *SLX5* or *SLX8* PCR products in yeast strain BY4272. Recombined plasmids were isolated from yeast, transformed into DH5α bacteria and sequence verified. *Slx5* and *slx8* RING and SIM domain point mutants on plasmid were created using constructs of synthesised DNA fragments (GeneArt). DNA sequences of the GeneArt constructs are listed in Supplementary Table S4. Fragment SLX5-C561S-C564S was AvaI/HindIII digested and cloned into pRS316-SLX5 to create pRS316-slx5-RING-SS. Fragment SLX8-C206S-C209S was SphI/NheI digested and cloned into pRS316-SLX8 to create pRS316-slx8-RING-SS. Fragment SLX5-I25A-L26A-I27A-I93A-I95A-I96A was ClaI/BglII digested and cloned into pRS316-SLX5 to create pRS316-slx5-SIM1-2. Fragment SLX5-I27K-V260A-D261A-L262A was ClaI/BglIII digested and cloned into pRS316-SLX5 to create pRS316-slx5-SIM1-3.

Immunoblot analyses of yeast whole cell lysates

Strains transformed with pRS316-PGAL1-3HA-3SMT3 or pRS316-PSMT3-3HA-SMT3 were grown at 30°C from OD₆₀₀ 0.3 to 1.0 (mid-log phase) in SC medium with 2% raffinose and lacking uracil for plasmid maintenance. Strains with genomically integrated 3HA-SMT3 constructs were grown to mid-log in YEP with 2% raffinose. Cells were induced with either 2% galactose or 2% glucose and harvested after 90 minutes. Exactly 30 OD units were spun down for 2 minutes at 4000 rpm at RT. The cell pellet was snapfrozen in liquid nitrogen and stored at -80°C. Whole cell lysates were prepared using an adapted protocol originally described by Yaffe *et al.*^{40,41}. Cell pellets were resuspended in 0.75 ml cold 1.85 M NaOH/7.4% 2-mercaptoethanol and incubated for 10 minutes on ice. The lysate was precipitated 10 minutes with 0.75 ml cold 50% trichloroacetic acid on ice and centrifuged for 2 minutes at 14,000 rpm at 4°C. The cell pellet was washed in 0.75 ml ice-cold acetone. The pellet was air-dried for 2 minutes and resuspended in 0.1 ml 0.5 Tris base, 6.5% SDS, 100 mM DTT, 12% glycerol and 0.002% bromophenol blue. The samples were denatured for 20 minutes at 65°C and centrifuged 1 minute at 14,000 rpm to remove cellular debris. The supernatant (10 μl) was analysed by SDS-PAGE (12.5% gel) and subsequent electroblotting of the running and stacking gel on nitrocellulose membranes. The blots were immunoprobed with αHA-HRP antibodies (3F10, Roche), followed by chemoluminescent detection.

Yeast two-hybrid analysis

Slx5 and Slx8 yeast two-hybrid interactions with human UBC-fold domains were investigated as described before³². In brief, E2-fold domains were PCR amplified and N-terminally fused to a LexA DNA binding domain the pEG202-NLS vector. Full-length *SLX5* and *SLX8* genes were cloned (EcoRI, XhoI) into vector pJG4-5 (2μ, *GAL1p* NLS-B42-HAtag, MCS, ADH1t, *TRP1*) for N-terminal fusion to the B42 activation domain. Yeast strain EGY48α was transformed with the LexA-E2 fusion vectors together with a LacZ reporter plasmid

(LexAop)₈ pSH18-34. Strain EGY48a was transformed with the B42-SLX fusion vectors. LexA-E2 transformed EGY48a strains were mated to B42-SLX transformed cells and grown under auxotrophic selection to generate diploids. To assess E2-E3 yeast two-hybrid interactions, diploids were transferred to X-Gal plates either complemented with galactose (inducing) or glucose (non-inducing). Blue-colouring was measured after 3 days growth at 30°C.

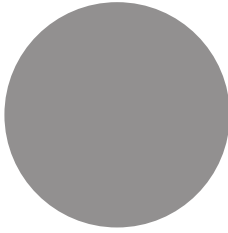
Yeast live cell imaging

Cells were grown asynchronously in SC medium to early mid-log phase at 30°C. Cells were transferred to a pre-warmed 8-well chambered glass-bottom Lab-TEK slide (Nunc) and covered with pre-warmed solid SC medium (5% agar). Cells were imaged on a DeltaVision RT system (Applied Precision), equipped with a heated chamber at 30°C, using a 100x/1.42-numerical aperture (NA) PlanApoN objective (Olympus). Images were acquired using Softworx software for deconvolution and are maximum intensity projections of all Z planes stacked at 0.3 µm distance. Images are processed in ImageJ and Adobe Photoshop CS2.

REFERENCES

- Pickart, C. M. Mechanisms underlying ubiquitination. *Annu. Rev. Biochem.* **70**, 503–533 (2001).
- Johnson, E. S. Protein modification by SUMO. *Annu. Rev. Biochem.* **73**, 355–382 (2004).
- Kerscher, O., Felberbaum, R. & Hochstrasser, M. Modification of proteins by ubiquitin and ubiquitin-like proteins. *Annu. Rev. Cell Dev. Biol.* **22**, 159–180 (2006).
- Geiss-Friedlander, R. & Melchior, F. Concepts in sumoylation: a decade on. *Nat. Rev. Mol. Cell Biol.* **8**, 947–956 (2007).
- Hochstrasser, M. Ubiquitin-dependent protein degradation. *Annu. Rev. Genet.* **30**, 405–439 (1996).
- Pickart, C. M. & Eddins, M. J. Ubiquitin: structures, functions, mechanisms. *Biochim. Biophys. Acta* **1695**, 55–72 (2004).
- Pickart, C. M. & Cohen, R. E. Proteasomes and their kin: proteases in the machine age. *Nat. Rev. Mol. Cell Biol.* **5**, 177–187 (2004).
- Perry, J. J. P., Tainer, J. A. & Boddy, M. N. A SIM-ultaneous role for SUMO and ubiquitin. *Trends Biochem. Sci.* **33**, 201–208 (2008).
- Geoffroy, M.-C. & Hay, R. T. An additional role for SUMO in ubiquitin-mediated proteolysis. *Nat. Rev. Mol. Cell Biol.* **10**, 564–568 (2009).
- Miteva, M., Keusekotten, K., Hofmann, K., Praefcke, G. J. K. & Dohmen, R. J. Sumoylation as a signal for polyubiquitylation and proteasomal degradation. *Subcell. Biochem.* **54**, 195–214 (2010).
- Prudden, J. *et al.* SUMO-targeted ubiquitin ligases in genome stability. *EMBO J* **26**, 4089–4101 (2007).
- Sun, H., Leverson, J. D. & Hunter, T. Conserved function of RNF4 family proteins in eukaryotes: targeting a ubiquitin ligase to SUMOylated proteins. *EMBO J* **26**, 4102–4112 (2007).
- Uzunova, K. *et al.* Ubiquitin-dependent proteolytic control of SUMO conjugates. *J. Biol. Chem.* **282**, 34167–34175 (2007).
- Xie, Y. *et al.* The yeast Hex3.Slx8 heterodimer is a ubiquitin ligase stimulated by substrate sumoylation. *J. Biol. Chem.* **282**, 34176–34184 (2007).
- Lallemant-Breitenbach, V. *et al.* Arsenic degrades PML or PML-RARalpha through a SUMO-triggered RNF4/ubiquitin-mediated pathway. *Nat. Cell Biol.* **10**, 547–555 (2008).
- Tatham, M. H. *et al.* RNF4 is a poly-SUMO-specific E3 ubiquitin ligase required for arsenic-induced PML degradation. *Nat. Cell Biol.* **10**, 538–546 (2008).
- Mullen, J. R., Kaliraman, V., Ibrahim, S. S. & Brill, S. J. Requirement for three novel protein complexes in the absence of the Sgs1 DNA helicase in *Saccharomyces cerevisiae*. *Genetics* **157**, 103–118 (2001).
- Budhidarmo, R., Nakatani, Y. & Day, C. L. RINGs hold the key to ubiquitin transfer. *Trends Biochem. Sci.* **37**, 58–65 (2012).
- Song, J., Durrin, L. K., Wilkinson, T. A., Krontiris, T. G. & Chen, Y. Identification of a SUMO-binding motif that recognizes SUMO-modified proteins. *Proc. Natl. Acad. Sci. U.S.A.* **101**, 14373–14378 (2004).
- Xie, Y., Rubenstein, E. M., Matt, T. & Hochstrasser, M. SUMO-independent *in vivo* activity of a SUMO-targeted ubiquitin ligase toward a short-lived transcription factor. *Genes Dev.* **24**, 893–903 (2010).
- Zhang, C., Roberts, T. M., Yang, J., Desai, R. & Brown, G. W. Suppression of genomic instability by SLX5 and SLX8 in *Saccharomyces cerevisiae*. *DNA Repair (Amst.)* **5**, 336–346 (2006).
- Burgess, R. C., Rahman, S., Lisby, M., Rothstein, R. & Zhao, X. The Slx5-Slx8 complex affects sumoylation of DNA repair proteins and negatively regulates recombination. *Mol. Cell. Biol.* **27**, 6153–6162 (2007).
- Kosoy, A., Calonge, T. M., Outwin, E. A. & O'Connell, M. J. Fission yeast Rnf4 homologs are required for DNA repair. *J. Biol. Chem.* **282**, 20388–20394 (2007).
- Nagai, S. *et al.* Functional targeting of DNA damage to a nuclear pore-associated SUMO-dependent ubiquitin ligase. *Science* **322**, 597–602 (2008).
- Cook, C. E., Hochstrasser, M. & Kerscher, O. The SUMO-targeted ubiquitin ligase subunit Slx5 resides in nuclear foci and at sites of DNA breaks. *Cell Cycle* **8**, 1080–1089 (2009).
- Wang, Z. & Prelich, G. Quality control of a transcriptional regulator by SUMO-targeted degradation. *Mol. Cell. Biol.* **29**, 1694–1706 (2009).
- Nixon, C. E., Wilcox, A. J. & Laney, J. D. Degradation of the *Saccharomyces cerevisiae* mating-type regulator alpha: genetic dissection of cis-determinants and trans-acting pathways. *Genetics* **185**, 497–511 (2010).
- McAinsh, A. D., Tytell, J. D. & Sorger, P. K. Structure, function, and regulation of budding yeast kinetochores. *Annu. Rev. Cell Dev. Biol.* **19**, 519–539 (2003).
- Collins, S. R. *et al.* Functional dissection of protein complexes involved in yeast chromosome biology using a genetic interaction map. *Nature* **446**, 806–810 (2007).
- Costanzo, M. *et al.* The genetic landscape of a cell. *Science* **327**, 425–431 (2010).
- Ii, T., Fung, J., Mullen, J. R. & Brill, S. J. The yeast Slx5-Slx8 DNA integrity complex displays ubiquitin ligase activity. *Cell Cycle* **6**, 2800–2809 (2007).

32. van Wijk, S. J. L. *et al.* A comprehensive framework of E2-RING E3 interactions of the human ubiquitin-proteasome system. *Mol. Syst. Biol* **5**, 295 (2009).
33. Winkler, G. S. *et al.* An altered-specificity ubiquitin-conjugating enzyme/ubiquitin-protein ligase pair. *J. Mol. Biol.* **337**, 157–165 (2004).
34. Finley, D. *et al.* Inhibition of proteolysis and cell cycle progression in a multiubiquitination-deficient yeast mutant. *Mol. Cell. Biol.* **14**, 5501–5509 (1994).
35. Ii, T., Mullen, J. R., Slagle, C. E. & Brill, S. J. Stimulation of in vitro sumoylation by Slx5-Slx8: evidence for a functional interaction with the SUMO pathway. *DNA Repair (Amst.)* **6**, 1679–1691 (2007).
36. Yang, L., Mullen, J. R. & Brill, S. J. Purification of the yeast Slx5-Slx8 protein complex and characterization of its DNA-binding activity. *Nucleic Acids Res* **34**, 5541–5551 (2006).
37. Longtine, M. S. *et al.* Additional modules for versatile and economical PCR-based gene deletion and modification in *Saccharomyces cerevisiae*. *Yeast* **14**, 953–961 (1998).
38. Huh, W.-K. *et al.* Global analysis of protein localization in budding yeast. *Nature* **425**, 686–691 (2003).
39. Tagwerker, C. *et al.* A tandem affinity tag for two-step purification under fully denaturing conditions: application in ubiquitin profiling and protein complex identification combined with in vivocross-linking. *Mol. Cell Proteomics* **5**, 737–748 (2006).
40. Yaffe, M. P. & Schatz, G. Two nuclear mutations that block mitochondrial protein import in yeast. *Proc. Natl. Acad. Sci. U.S.A.* **81**, 4819–4823 (1984).
41. Johnson, E. S. & Blobel, G. Cell cycle-regulated attachment of the ubiquitin-related protein SUMO to the yeast septins. *J. Cell Biol.* **147**, 981–994 (1999).



General discussion

General discussion

Posttranslational modification is an efficient way for a cell to expand the functionality of proteins. In this thesis we describe investigations into a class of proteinaceous modifications that involves the attachment of ubiquitin and ubiquitin-like modifiers to other proteins. Ubiquitin(-like) modifiers regulate the activity, localisation and turnover of many different proteins, thereby playing crucial roles in diverse cellular processes, such as cell cycle progression, intracellular transport, metabolism, transcription, DNA replication and repair. An important aspect of ubiquitin(-like) modification is that it depends on a large number of enzymes and adapter proteins, which mediate the attachment or removal of the ubiquitin(-like) modifier to and from substrates. The combined function of these enzymes and adapter proteins forms intricate enzymatic systems that are able to target specific proteins in the cell. For many of these enzymes it is unclear how they cooperate to achieve ubiquitin(-like) modification and which proteins and cellular processes they regulate. The studies described in this thesis address these questions in particular. The findings shed new light on many functional relationships between the ubiquitin(-like) system components in the yeast *Saccharomyces cerevisiae*, but also raise several questions which are discussed here.

Functional characterisation of yeast mutants by microarray expression profiling

The importance of ubiquitin(-like) systems becomes evident when the genes encoding these system components are deleted. Mutation of genes in *S. cerevisiae* is often associated with phenotypic defects, such as temperature sensitivity, cell cycle progression defects, metabolic defects or abnormalities in cell morphology¹. These phenotypes are in general indicative for the cellular function of the product of the mutated gene. Importantly, mutants with similar phenotypes are therefore likely to have a shared cellular role. This observation is widely

used as a genetic tool to associate genes to specific biological processes in yeast and other species. In Chapter 2 of this thesis we aimed to characterise all genes encoding ubiquitin(-like) system components. However, rather than using classical phenotype assays, we employed microarray expression profiles to analyse the yeast mutants. Genome-wide expression profiling provides detailed information about the transcriptional responses of the mutants, representing specific phenotypes. The advantage of microarray expression profiling over classical phenotype screens is that many different phenotypes can be measured in a single assay. The use of large-scale microarray expression profiling to study yeast mutants is not new. The first compendium of yeast mutant expression profiles dates back from 2000². Such a collection of expression profiles is highly suitable for the identification of mutants with similar expression profiles and therefore with shared cellular functions. The application of a similar strategy to study posttranslational modification systems, as illustrated by the compendium of expression profiles of the yeast phosphorylation system, has proven to give valuable insights in the functional relationships between kinases and phosphatases³. We therefore aimed to extend this approach to the ubiquitin and ubiquitin-like systems.

S. cerevisiae contains 361 genes that encode (putative) ubiquitin(-like) system components of which 224 deletion mutants of the nonessential genes were profiled. It is not easy to generate a data set of this scale. The downside of microarray expression profiling is that it is a complicated, expensive and labour-intensive technology. However, the long-time experience with microarray technology in our laboratory and the technical optimisation of a robotics-based, high-throughput method of expression profiling has allowed the relatively quick generation of high-quality expression data for a large number of yeast mutants under a single growth condition³⁻⁵. The microarrays prove to be a powerful method for the detection and characterisation of yeast phenotypes. The perturbation of distinct cellular pathways is accompanied with highly

specific transcriptional responses, allowing the annotation of new functions to genes and to delineate relationships between genes that may take part in the same cellular pathway. This data gives a unique insight in the functional role of ubiquitin(-like) system components at the level of mRNA expression changes and is a valuable addition to our current knowledge about ubiquitin(-like) systems, as this is mostly based on biochemical approaches.

Delineating functional relationships and gene functions of ubiquitin(-like) system components

In essence, the ubiquitin(-like) systems can be summarised as follows. There are multiple enzymes that target specific substrates in various cellular processes for the attachment or removal of a ubiquitin(-like) modifier. Many enzymes require adapter proteins or are part of multi-subunit complexes essential for their function. The enzymes function in a hierarchical order in a sequential E1-E2-E3 signalling cascade. These characteristics are reflected by the microarray expression data. We have specified twenty groups of mutants with a distinct expression phenotype representing a specific ubiquitin(-like)-dependent biological process. The mutants that fall within one group represent highly functionally related mutants with a shared function in one protein complex or cellular pathway. Several protein complexes are identified, including catalytic components and noncatalytic adaptor proteins, representing ubiquitin E3 ligases and heterodimeric DUBs. Furthermore, we find E2 and E3 enzyme pairs that are known to have a joint function in ubiquitination. Strikingly, we could not link the expression profiles of the DUB mutants to any of the E2 or E3 mutants. We anticipated that the mutant profiles of DUBs involved in ubiquitin-processing would overlap and DUBs involved in ubiquitin-deconjugation would be opposite to those of the E2 and E3 enzymes that target the same protein. The lack of functional relationships between conjugating and deconjugating enzymes may be related to the fact that expression profiles for several key enzymes

in ubiquitin(-like) modification are missing due to their essentiality. For example, we could not profile the deletion mutants of the essential ubiquitin- and SUMO-specific E1 and E2 enzymes *UBA1*, *UBA2*, *AOS1*, *CDC34*, *UBC1* and *UBC9*, as well as several essential E3 ligases, which hampers the delineation of pathways involving specific combinations of E1s, E2s, E3s and DUBs. A way to bypass this problem is the use of mutants with temperature-sensitive (ts) alleles for these genes, for example *ubc9-1* and *cdc34-2*, which will confer an expression phenotype when shifting the mutant to a semi-permissive temperature^{6,7}. Extension of the current data set with expression profiles of ts mutants or other point mutants is needed to obtain the full spectrum of phenotypes for ubiquitin(-like) system mutants, which will improve the delineation of functional relationships among genes.

The investigation of mutant expression profiles has provided insight into the many different transcriptional responses that are elicited upon disruption of specific cellular pathways. We have discovered expression responses for distinct cellular processes, such as histone modification, various ubiquitin-dependent secretory pathways, urmylation, ERAD and proteasome function. For some mutants, the affected cellular process can be instantly delineated from the responding genes. For example, Chapter 3 describes an expression signature of proteasome genes that is associated with an underlying ubiquitin-proteasome system defect. However, the delineation of function from differentially expressed genes is not clear-cut for most mutants. This is due to the fact that the observed expression changes are a combination of direct and indirect effects. This is not a problem for the delineation of interactions between genes. After all, the indirect effects in a mutant are the same for any other mutant with a similar function. However, it does complicate the functional characterisation of these mutants. How can we distinguish which cellular processes are directly affected by a ubiquitin(-like) defect and which affected processes are secondary? Direct effects can perhaps better be investigated by

the use of conditional mutants, such as *ts* mutants or by use of the anchors-away method¹⁸. The expression changes that occur early after inactivation of a protein, by shifting to a nonpermissive temperature or by nuclear depletion, will be representative for the primary affected cellular processes.

The differentially expressed genes of mutants were analysed for GO enrichment in order to delineate the cellular role(s) of the product of the deleted gene. This was fairly straightforward for mutants with a small number of expression changes, which likely represents the disruption of a single biological process. However, for those mutants with a pleiotropic phenotype, the large numbers of associated gene expression changes are more difficult to interpret, as they reflect the simultaneous disruption of multiple biological processes. Intriguingly, we have several cases where mutant expression profiles are only partially overlapping. These cases likely represent different pleiotropic mutants that share one affected cellular process, which potentially indicates a functional interaction. This is nicely illustrated by the example of the DUB mutants *ubp3Δ* and *bre5Δ*, which share part of their expression phenotype with MAP kinase mutants. This reflects that Ubp3/Bre5 has a functional role in the pheromone response and osmotic stress pathways in cooperation with these kinases (Chapter 2, Figure 6)^{8,9}. This example also underscores the possibilities of exploring regulatory relationships across other modification systems. Nevertheless, it is generally difficult to establish what kind of interaction is represented by an overlap in expression phenotype. For this we are dependent on prior knowledge of established interactions in order to interpret the associated expression changes in these mutants. The rapid increase of expression profiles for a large number of mutants in our lab only increases the number of overlapping expression phenotypes. A great challenge lies ahead in the identification of novel functional regulatory interactions between these mutants and especially in unravelling the nature of these interactions. A suitable approach to address these issues is to

incorporate other high-throughput data sets, such as proteomics studies, genome-wide synthetic genetic interaction maps and epistatic miniarray profiles (E-MAPs)¹¹⁻¹⁴. A reported protein-protein interaction is strongly indicative for a direct functional interaction between two gene products that upon deletion result in a (partial) overlap in expression phenotype. Further confirmation about potentially direct functional interactions between two genes with shared expression phenotypes can be obtained from synthetic genetic interactions. The presence of a positive synthetic genetic interaction between two genes in combination with a (partial) overlap in expression phenotype likely represents a direct functional interaction between these genes in the same cellular pathway. In contrast, a negative synthetic genetic interaction in combination with a (partial) overlap in expression phenotype may reflect that these two genes are likely to function in parallel pathways. Integration of other data sets may therefore help in pinpointing the molecular mechanism to explain the (partial) overlap in expression phenotype upon deletion of these components. This is required because the generation of hypotheses from high-throughput functional genomic data sets vastly surpasses the rate of which they can be tested by conventional means. Such investigations would serve to increase the ability of individual high-throughput data sets, some of which on their own are prone to various degrees of false-positives.

Studying uncharacterised ubiquitin(-like) system components

The genome of *S. cerevisiae* contains 6383 annotated protein-coding genes of which 31% has as yet not been associated with any biological process¹⁴. One of our aims was to functionally characterise mutants of unknown function with a putative role in ubiquitin(-like) modification. A striking observation is that only half of the ubiquitin(-like) system components display a significant expression phenotype upon deletion. These largely include mutants that have already been characterised before,

leaving the remaining uncharacterised mutants virtually untouched. A lack of phenotype can be due to the occurrence of redundancy among genes. This is for instance the case for the E2 enzyme Ubc5, whose function can be taken over by Ubc4, or for the ubiquitin protein, which is encoded by four genes¹⁵⁻¹⁷. In order to study the phenotype of a redundant gene, one can combine multiple deletions in one strain. It is currently not feasible to generate expression profiles for all pair-wise combinations of gene deletions. The availability of increasing numbers of high-throughput synthetic genetic interaction maps provides many starting points for the selection of genes with potentially interesting redundancy effects and also offers opportunities for further studying epistatic relationships between genes^{10,11}.

Another reason for a lack of expression phenotype is that the gene may have a conditional function. The mutant phenotype may therefore only be detected upon perturbation of the standard growth condition, for example by limiting certain nutrients, treatment with chemicals or temperature shift. All our microarray experiments are carried out at 30°C in rich media with high levels of glucose, which is the optimal growth condition for yeast. We limited ourselves to a single growth condition to allow direct comparison of mutants. The benefit of this approach is that we are able to systematically compare the expression phenotypes of hundreds of yeast mutants and also allows comparison to other high-throughput data sets³⁻⁵. However, the chosen condition is fairly standard and widely used for research of *S. cerevisiae*. It is therefore not surprising that most of the uncovered functional relationships described in this thesis have already been described by others. Shifting to a suboptimal growth condition may be more appropriate for analysing the poorly characterised ubiquitin(-like) system components. Ubiquitination is particularly important for the induced degradation of proteins in stress conditions, for example during heat shock or DNA damage. A mutant strain, deleted for a gene required for DNA repair, may therefore not display any signs

of genome instability under optimal growth conditions, whereas chemical treatment with DNA damaging drugs will lead to a phenotype, which can be detected by expression profiling. Annotation of new functions to mutants without a phenotype may therefore still be feasible when assaying these mutants under a different growth condition. This is of particular importance for the study of the neddylation and Atg8/Atg12 modification systems. We have not found a single mutant phenotype for these two systems, which we attribute to a conditional function.

From 'Synthetic Lethal Unknown' to 'STUbl'

The expression profiles of *slx5Δ* and *slx8Δ* were uncovered in an early stage of our project where we aimed to profile all mutants of the ubiquitin(-like) systems. At that stage, very little was known about the Synthetic Lethal Unknown (SLX) genes. Slx5/8 was first identified as a protein complex essential for cell viability in the absence of the DNA helicase *SGS1* and was shown to be required for maintenance of genome stability^{19,20}. Slx5 and Slx8 were also reported to have a RING domain¹⁹. We therefore speculated that Slx5 and Slx8 may function as a ubiquitin E3 ligase complex. Our efforts to confirm this hypothesis by *in vitro* ubiquitination assays stranded, because we were unable to purify recombinant Slx5 from bacteria. However, the notion that Slx5/8 is a ubiquitin ligase was strengthened by the yeast two-hybrid experiments, revealing that Slx8 is able to bind to the UBC-fold domain of several human ubiquitin-conjugating enzymes (Chapter 5, Figure 4). Meanwhile, several studies reported unsuspected links between Slx5/8 and the sumoylation system, contradicting the hypothesis of Slx5/8 being a ubiquitin ligase²¹⁻²³. This was shortly after reconciled by multiple studies revealing that Slx5/8 is the founding member of a novel class of SUMO-targeted ubiquitin ligases (STUbls), which is evolutionary conserved from yeast to human²⁴⁻³⁰. STUbls are required for the polyubiquitination of sumoylated proteins, which leads to their degradation by the proteasome. This is an important

regulatory mechanism for the maintenance of accurate intracellular levels of sumoylated proteins ^{31–34}.

STuBLs and transcription

Deletion of *SLX5* or *SLX8* results in the accumulation of sumoylated proteins, which is accompanied with a strong upregulation of many genes (Chapter 4). Initially, this was interpreted as a direct effect on transcription, leading to the idea that Slx5/8 may function as a transcriptional repressor. There are several lines of evidence that Slx5/8 is directly involved in transcription regulation. Slx5/8 is a nuclear protein complex that has *in vitro* double-stranded DNA binding-activity, mediated by Slx8 ³⁵. Slx5 contributes to silencing of telomeric and rDNA loci ³⁶. Moreover, three transcription regulators (Mot1, MAT α 1 and MAT α 2) are presently known to be ubiquitinated by Slx5/8 for the regulation of their turnover ^{37–39}. Also the human STuBL orthologue RNF4 targets several transcription factors ^{28,29,40–42}. Strikingly, none of these functions could be derived from the expression changes observed in *slx5 Δ* and *slx8 Δ* . In fact, the expression responses of *slx5 Δ* and *slx8 Δ* are very similar to those of mutants with various functions in the maintenance of genome stability. We concluded that the expression changes in *slx5 Δ* and *slx8 Δ* are the result of the activation of a general stress response due to genome instability and therefore do not reflect a direct transcription defect in the mutants.

It is unclear why direct effects on transcription cannot be detected by expression profiling of *slx5 Δ* and *slx8 Δ* . It suggests that SUMO-dependent ubiquitination of transcription factors has a minor or even no role in transcription regulation. Secondly, the turnover of transcription factors may be altered in the mutants without having an immediate effect on the efficiency of transcription activation or repression. Thirdly, the experimental setup may be unsuitable for measuring transcription defects in these mutants. All microarray experiments conducted in this thesis are performed in a steady-state situation of cells growing exponentially. An

alternative approach would be the performance of kinetic experiments in which expression changes are measured while shifting the mutants to a growth condition that requires transcriptional reprogramming, for example α -factor treatment to induce or repress mating genes regulated by MAT α 1 and MAT α 2. Possible changes in the dynamics of the transcriptional response may reveal a direct role of Slx5/8 in transcription regulation.

STuBLs and the maintenance of genome stability

Deletion of Slx5 or Slx8 nevertheless results in a grown defect under standard growth conditions. In Chapter 4 and Chapter 5 we aimed to investigate this. ChIP-chip of Slx5 and Slx8 in standard growth conditions revealed that Slx5 resides exclusively at centromeric DNA, which is largely kinetochore-dependent. This suggests a novel function for Slx5, and possibly Slx8, in the maintenance of genome stability by contributing directly to accurate chromosome segregation. Other studies have pointed to a role of Slx5/8 in DNA repair and showed that Slx5 and Slx8 locate to DNA breaks, DNA damage foci and DNA replication centres ^{19,20,22,43,44}. Binding of Slx5/8 to these genomic locations is likely undetectable by conventional ChIP-chip assays, assuming that DNA replication forks and sites of DNA damage are randomly scattered across the genome in a small subpopulation of asynchronously growing cells. Localisation studies of Slx5 and Slx8 using microscopy revealed little about their potential centromeric function. Preliminary results suggest that Slx8 is recruited to centromeres in the fraction of cells with misattached chromosomes (Chapter 5, Figure 5). Follow-up studies are required to assess whether chromosome misattachment directly induces the recruitment of Slx8 and Slx5 to centromeres. More insight in the centromeric location of Slx5 and Slx8 can also be gained from ChIP-chip experiments of synchronised cell populations to determine the timing of Slx5/8 binding to centromeres in the different cell cycle phases. We also tried to investigate whether human RNF4 locates

to centromeres by expressing GFP-tagged RNF4 in HeLa cells. However, cells transformed with RNF4-GFP were unable to proliferate, suggesting a cellular defect due to RNF dysfunction resulting from the tag or protein overexpression (W. Nijenhuis, personal communication). Similarly, we noticed that tagging or overexpression of Slx5 (but not Slx8) resulted in a *slx5Δ*-like mutant phenotype in yeast (data not shown). This problem can be solved by generating Slx5- and RNF4-specific antibodies, which will facilitate future research of Slx5/8 and RNF4.

An important question is whether the centromere binding of Slx5 is SUMO-dependent, as this may indicate a direct role for SUMO-dependent ubiquitination at centromeres. This can either be done by mutating the SIM domains of Slx5, resulting in loss of the SUMO-interaction with the substrate, or by mutating the lysine residue in the substrate that is sumoylated. Our initial attempts to generate Slx5-SIM mutants were unsuccessful because of redundancy among the five SIM domains (Chapter 4, Figure 3). Recently a new *slx5* mutant was described in which four out of five SIM domains were mutated, resulting in complete loss of SUMO-binding³⁹. This mutant will be highly suitable for further investigation of the SUMO-dependency of Slx5 for its subcellular location. We also attempted to identify the putative centromeric substrate that is targeted by Slx5. We used a candidate-based approach of various centromeric proteins, aiming to find changes in the protein level of the targeted substrate, or changes in the levels of sumoylated or ubiquitinated protein species upon deletion of Slx5 or Slx8. The proteins were selected based on their reported physical or genetic interactions with Slx5 and/or Slx8, or because they were reported to be sumoylated or ubiquitinated. Similar protein level changes were described for DNA repair proteins in *slx5Δ* and *slx8Δ*²². Unfortunately, none of the tested proteins showed any aberrant protein levels, making them unlikely *in vivo* substrates (data not shown). Furthermore, we could not detect any increased sumoylated protein species. Estimates are that <1% of a protein population is sumoylated, making it

difficult to distinguish sumoylated protein species in the pool of unsumoylated proteins⁴⁵. We therefore set up a strategy to express epitope-tagged SUMO (Chapter 5). Pull-down experiments with tagged SUMO may help in finding the *in vivo* substrate of Slx5/8 that is responsible for the centromeric location of Slx5.

The approach described above is quite similar to finding a needle in a haystack due to the large number of centromeric proteins⁴⁶. A more efficient method would be to first establish which proteins in *S. cerevisiae* are actually modified by a polySUMO chain. Recently, a new method was developed for the isolation of polysumoylated proteins from HeLa cells and their identification by mass spectrometric analysis⁴⁷. The method is based on an affinity purification strategy using a fragment of RNF4 that bears four SIM domains. This way many putatively polysumoylated proteins were identified, including the centromeric proteins CENP-B, CENP-V and KIF2C⁴⁷. Proteomic analyses of *slx5Δ* and *slx8Δ* mutants will help to determine the identity of the polysumoylated proteins in yeast and to establish which of them are responsible for the mitotic defects. The pleiotropic phenotype of *slx5Δ* and *slx8Δ* suggests that Slx5/8 may actually target multiple substrates. The modification of proteins with SUMO or ubiquitin is often a carefully timed process that occurs in a very specific cell cycle stage, such as seen for the sumoylation of septin proteins during cytokinesis⁴⁸. The use of synchronised cell populations is therefore of fundamental importance for the elucidation of the molecular processes underlying the mutant phenotypes of Slx5/8.

Substrates of ubiquitin(-like) enzymes

As pointed out for Slx5/8, the identification of *in vivo* substrates of ubiquitin(-like) enzymes is crucial for understanding the molecular mechanisms of ubiquitin(-like) systems. Microarray expression profiling has the potential to identify substrates, but has also its limitations. Characterisation of the genes that change in expression in a mutant is helpful for delineating the affected cellular processes and greatly

narrows down the number of candidate substrates. However, as for example seen for *slx5Δ* and *slx8Δ*, the expression profile does not necessarily reflect the affected cellular processes. Another approach is the inclusion of additional expression profiles of mutants, whose deleted gene product represents a (putative) substrate. The phenotype of the substrate deletion mutant is expected to resemble the phenotype of the corresponding E2, E3 or deconjugating enzyme mutant, as they take part in the same cellular process. For enzymes that target multiple substrates, the expression profiles of the substrate and enzyme mutants may only partially overlap. In rare cases, we observed that the expression of substrates is changed upon deletion of the corresponding enzyme, as for example seen for the deletion mutants of the DUB complex Ubp3/Bre5, which displays changed expression of its two substrates Sec23 and Sec27 (Chapter 2, Figure 6A). However, the expression of other known substrates are generally not affected by enzyme gene disruption (data not shown), which complicates the delineation of substrates from gene expression changes. A comparative study of the expression profiles of yeast mutants in combination with proteomics analyses of these same mutants may give more insight in potential substrates. Deletion of a gene can also be associated with numerous protein level changes, as for example seen for DUB deletion mutants⁴⁹. Any deviations between the expression of a gene and the level or modification of a protein may be indicative for the gene product being a direct substrate of ubiquitin(-like) systems.

Concluding remarks

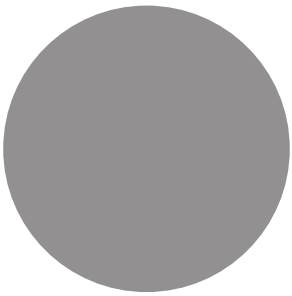
The microarray studies described in this thesis have demonstrated that expression profiling of yeast mutants is a powerful method for uncovering the functional role of ubiquitin(-like) system components. Gene expression changes can be used to place ubiquitin(-like) system components in specific biological pathways and illustrate the complexity of these systems in terms of protein complexes and regulatory interactions between pathway components. The examples in Chapter 2 and

3 provide many starting points for future studies to gain mechanistic insight in the molecular events that underlie these expression phenotypes. Nonetheless, microarray studies do not answer all questions, as shown for the SUMO-targeted ubiquitin ligase complex Slx5/8 in Chapter 4 and 5. Extensive follow-up studies are required to understand the molecular mechanism of the Slx5/8 complex. In order to achieve a complete biological network of all functional relationships between ubiquitin(-like) system components, it is therefore necessary to systematically perform similar follow-up studies for all these components. This demonstrates that high-throughput methods, such as microarray expression profiling, require high-throughput follow-ups.

REFERENCES

- Hampsey, M. A review of phenotypes in *Saccharomyces cerevisiae*. *Yeast* 13, 1099–1133 (1997).
- Hughes, T. R. *et al.* Functional discovery via a compendium of expression profiles. *Cell* 102, 109–126 (2000).
- van Wageningen, S. *et al.* Functional overlap and regulatory links shape genetic interactions between signaling pathways. *Cell* 143, 991–1004 (2010).
- Apweiler, E. *et al.* Yeast glucose pathways converge on the transcriptional regulation of trehalose biosynthesis. *BMC genomics* 13, 239 (2012).
- Lenstra, T. L. *et al.* The specificity and topology of chromatin interaction pathways in yeast. *Mol. Cell* 42, 536–549 (2011).
- Betting, J. & Seufert, W. A yeast Ubc9 mutant protein with temperature-sensitive *in vivo* function is subject to conditional proteolysis by a ubiquitin- and proteasome-dependent pathway. *J. Biol. Chem.* 271, 25790–25796 (1996).
- Varelas, X., Stuart, D., Ellison, M. J. & Ptak, C. The Cdc34/SCF ubiquitination complex mediates *Saccharomyces cerevisiae* cell wall integrity. *Genetics* 174, 1825–1839 (2006).
- Haruki, H., Nishikawa, J. & Laemmli, U. K. The anchor-away technique: rapid, conditional establishment of yeast mutant phenotypes. *Mol. Cell* 31, 925–932 (2008).
- Solé, C. *et al.* Control of Ubp3 ubiquitin protease activity by the Hog1 SAPK modulates transcription upon osmostress. *EMBO J* (2011).doi:10.1038/emboj.2011.227
- Wang, Y. & Dohlmans, H. G. Pheromone-dependent ubiquitination of the mitogen-activated protein kinase Ste7. *J. Biol. Chem* 277, 15766–15772 (2002).
- Costanzo, M. *et al.* The genetic landscape of a cell. *Science* 327, 425–431 (2010).
- Collins, S. R. *et al.* Functional dissection of protein complexes involved in yeast chromosome biology using a genetic interaction map. *Nature* 446, 806–810 (2007).
- Gavin, A.-C. *et al.* Proteome survey reveals modularity of the yeast cell machinery. *Nature* 440, 631–636 (2006).
- Collins, S. R. *et al.* Toward a comprehensive atlas of the physical interactome of *Saccharomyces cerevisiae*. *Mol. Cell Proteomics* 6, 439–450 (2007).
- Ashburner, M. *et al.* Gene ontology: tool for the unification of biology. The Gene Ontology Consortium. *Nat. Genet* 25, 25–29 (2000).
- Seufert, W. & Jentsch, S. Ubiquitin-conjugating enzymes UBC4 and UBC5 mediate selective degradation of short-lived and abnormal proteins. *EMBO J.* 9, 543–550 (1990).
- Ozkaynak, E., Finley, D. & Varshavsky, A. The yeast ubiquitin gene: head-to-tail repeats encoding a polyubiquitin precursor protein. *Nature* 312, 663–666 (1984).
- Ozkaynak, E., Finley, D., Solomon, M. J. & Varshavsky, A. The yeast ubiquitin genes: a family of natural gene fusions. *EMBO J.* 6, 1429–1439 (1987).
- Mullen, J. R., Kaliraman, V., Ibrahim, S. S. & Brill, S. J. Requirement for three novel protein complexes in the absence of the Sgs1 DNA helicase in *Saccharomyces cerevisiae*. *Genetics* 157, 103–118 (2001).
- Zhang, C., Roberts, T. M., Yang, J., Desai, R. & Brown, G. W. Suppression of genomic instability by SLX5 and SLX8 in *Saccharomyces cerevisiae*. *DNA Repair (Amst.)* 5, 336–346 (2006).
- Wang, Z., Jones, G. M. & Prelich, G. Genetic analysis connects SLX5 and SLX8 to the SUMO pathway in *Saccharomyces cerevisiae*. *Genetics* 172, 1499–1509 (2006).
- Burgess, R. C., Rahman, S., Lisby, M., Rothstein, R. & Zhao, X. The Slx5-Slx8 complex affects sumoylation of DNA repair proteins and negatively regulates recombination. *Mol. Cell. Biol* 27, 6153–6162 (2007).
- Ii, T., Mullen, J. R., Slagle, C. E. & Brill, S. J. Stimulation of *in vitro* sumoylation by Slx5-Slx8: evidence for a functional interaction with the SUMO pathway. *DNA Repair (Amst.)* 6, 1679–1691 (2007).
- Prudden, J. *et al.* SUMO-targeted ubiquitin ligases in genome stability. *EMBO J* 26, 4089–4101 (2007).
- Sun, H., Leveson, J. D. & Hunter, T. Conserved function of RNF4 family proteins in eukaryotes: targeting a ubiquitin ligase to SUMOylated proteins. *EMBO J* 26, 4102–4112 (2007).
- Uzunova, K. *et al.* Ubiquitin-dependent proteolytic control of SUMO conjugates. *J. Biol. Chem* 282, 34167–34175 (2007).
- Xie, Y. *et al.* The yeast Hex3.Slx8 heterodimer is a ubiquitin ligase stimulated by substrate sumoylation. *J. Biol. Chem* 282, 34176–34184 (2007).
- Lallemand-Breitenbach, V. *et al.* Arsenic degrades PML or PML-RARalpha through a SUMO-triggered RNF4/ubiquitin-mediated pathway. *Nat. Cell Biol* 10, 547–555 (2008).
- Tatham, M. H. *et al.* RNF4 is a poly-SUMO-specific E3 ubiquitin ligase required for arsenic-induced PML degradation. *Nat. Cell Biol* 10, 538–546 (2008).
- Weisshaar, S. R. *et al.* Arsenic trioxide stimulates SUMO-2/3 modification leading to RNF4-dependent proteolytic targeting of PML. *FEBS Lett* 582, 3174–3178 (2008).
- Perry, J. J. P., Tainer, J. A. & Boddy, M. N. A SIM-ultaneous role for SUMO and ubiquitin. *Trends Biochem. Sci* 33, 201–208 (2008).
- Geoffroy, M.-C. & Hay, R. T. An additional role for SUMO in ubiquitin-mediated proteolysis. *Nat. Rev. Mol. Cell Biol.* 10, 564–568 (2009).
- Miteva, M., Keusekotten, K., Hofmann, K., Praefcke, G. J. K. & Dohmen, R. J. Sumoylation as a signal for polyubiquitylation and proteasomal degradation. *Subcell. Biochem.* 54, 195–214 (2010).
- Praefcke, G. J. K., Hofmann, K. & Dohmen, R. J. SUMO playing tag with ubiquitin. *Trends Biochem. Sci.* 37, 23–31 (2012).
- Yang, L., Mullen, J. R. & Brill, S. J. Purification of the yeast Slx5-Slx8 protein complex and characterization of its DNA-binding activity. *Nucleic Acids Res* 34, 5541–5551 (2006).
- Darst, R. P., Garcia, S. N., Koch, M. R. & Pillus, L. Slx5 promotes transcriptional silencing and is required for robust growth in the absence of Sir2. *Mol. Cell. Biol* 28, 1361–1372 (2008).
- Wang, Z. & Prelich, G. Quality control of a transcriptional regulator by SUMO-targeted degradation. *Mol. Cell. Biol* 29, 1694–1706 (2009).
- Nixon, C. E., Wilcox, A. J. & Laney, J. D. Degradation of

- the *Saccharomyces cerevisiae* mating-type regulator alpha: genetic dissection of cis-determinants and trans-acting pathways. *Genetics* 185, 497–511 (2010).
39. Xie, Y., Rubenstein, E. M., Matt, T. & Hochstrasser, M. SUMO-independent in vivo activity of a SUMO-targeted ubiquitin ligase toward a short-lived transcription factor. *Genes Dev* 24, 893–903 (2010).
 40. Guo, B. & Sharrocks, A. D. Extracellular signal-regulated kinase mitogen-activated protein kinase signaling initiates a dynamic interplay between sumoylation and ubiquitination to regulate the activity of the transcriptional activator PEA3. *Mol. Cell. Biol* 29, 3204–3218 (2009).
 41. van Hagen, M., Overmeer, R. M., Abolvardi, S. S. & Vertegaal, A. C. O. RNF4 and VHL regulate the proteasomal degradation of SUMO-conjugated Hypoxia-Inducible Factor-2alpha. *Nucleic Acids Res* 38, 1922–1931 (2010).
 42. Martin, N. *et al.* PARP-1 transcriptional activity is regulated by sumoylation upon heat shock. *EMBO J* 28, 3534–3548 (2009).
 43. Nagai, S. *et al.* Functional targeting of DNA damage to a nuclear pore-associated SUMO-dependent ubiquitin ligase. *Science* 322, 597–602 (2008).
 44. Cook, C. E., Hochstrasser, M. & Kerscher, O. The SUMO-targeted ubiquitin ligase subunit Slx5 resides in nuclear foci and at sites of DNA breaks. *Cell Cycle* 8, 1080–1089 (2009).
 45. Johnson, E. S. Protein modification by SUMO. *Annu. Rev. Biochem* 73, 355–382 (2004).
 46. McAinsh, A. D., Tytell, J. D. & Sorger, P. K. Structure, function, and regulation of budding yeast kinetochores. *Annu. Rev. Cell Dev. Biol* 19, 519–539 (2003).
 47. Bruderer, R. *et al.* Purification and identification of endogenous polySUMO conjugates. *EMBO Rep.* 12, 142–148 (2011).
 48. Johnson, E. S. & Blobel, G. Cell cycle-regulated attachment of the ubiquitin-related protein SUMO to the yeast septins. *J. Cell Biol.* 147, 981–994 (1999).
 49. Poulsen, J. W. *et al.* Comprehensive profiling of proteome changes upon sequential deletion of deubiquitylating enzymes. *Journal of proteomics* (2012).doi:10.1016/j.jprot.2012.04.055



Nederlandse samenvatting

Curriculum vitae

Publications

Dankwoord

Nederlandse samenvatting

In alle eukaryote organismen, van gist tot mens, komt het eiwit ubiquitine voor. Ubiquitine is een klein eiwit dat gekoppeld kan worden aan andere eiwitten. De modificatie van eiwitten met ubiquitine wordt daarom ook wel 'ubiquitinatie' genoemd. Ubiquitinatie is uitermate belangrijk voor het reguleren van allerlei cellulaire processen, zoals celdeling, intracellulair transport, metabolisme, transcriptie, DNA replicatie en reparatie. Deze processen vinden plaats in bijna iedere cel en worden uitgevoerd door een scala aan eiwitten. De koppeling van een of meerdere ubiquitinemoleculen aan een eiwit kan allerlei veranderingen in de functie van dat eiwit teweegbrengen. Hierdoor is de cel in staat om deze biologische processen aan te sturen. Ubiquitinatie wordt verzorgd door tientallen verschillende enzymen. Zo zijn er enzymen die ubiquitine aan eiwitten koppelen, ook wel E1, E2 en E3 enzymen genoemd, en zijn er enzymen die ubiquitine weer van een eiwit afhalen oftewel deubiquitineren. Elk enzym heeft zijn eigen plek en functie in de cel en weet onder de juiste cellulaire omstandigheden die eiwitten te vinden die geubiquitineerd moeten worden. Naast het ubiquitine systeem zijn er nog andere ubiquitine-achtige systemen, zoals sumoylatie, neddylatie en urmylatie. Deze zijn ook betrokken bij eiwitmodificatie met behulp van vergelijkbare enzymssystemen. De functies van deze systemen zijn nog relatief onbekend. Voor veel enzymen is het onduidelijk hoe ze samenwerken om ubiquitine(-achtige) modificatie van een eiwit voor elkaar te krijgen en vooral op welke eiwitten en cellulaire processen ze precies aangrijpen. Om deze vragen te beantwoorden hebben we gebruik gemaakt van de bakkersgist *Saccharomyces cerevisiae*. De ubiquitine(-achtige) systemen van een gistcel functioneren op een vergelijkbare manier als iedere andere cel, zoals die van een mens. Een groot voordeel van gist voor wetenschappelijk onderzoek is dat er een grote collectie van gistmutanten bestaat. Elke mutant mist een specifiek gen in zijn DNA, wat

tot gevolg kan hebben dat er een eiwit ontbreekt die een bepaalde cellulaire functie zou moeten uitvoeren. In dit proefschrift beschrijven we hoe we door de studie van deze mutanten tot nieuwe inzichten zijn gekomen over de functies van de verschillende ubiquitine(-achtige) systemen.

Hoofdstuk 2 beschrijft een uitgebreide studie van de fenotypes van 224 gistmutanten met deleties van verschillende componenten van ubiquitine(-achtige) systemen. Deleties van genen zijn vaak geassocieerd met een fenotype als gevolg van een of meerdere cellulaire defecten. Deze fenotypes zijn meetbaar op het niveau van veranderingen in genexpressie. Voor elke mutant is een expressieprofiel gemaakt door middel van een microarray, die alle veranderingen in genexpressie weergeeft. In de helft van de mutanten werd een significante expressieverandering gemeten. Het karakteriseren van de veranderingen in genexpressie van mutanten bleek zeer nuttig voor het achterhalen van de aangedane cellulaire processen en het ontrafelen van de functie van ubiquitine(-achtige) systeem componenten. Er werden ten minste twintig verschillende expressiepatronen ontdekt die representatief zijn voor een specifieke groep mutanten met een gezamenlijke functie in een cellulair proces. Zo werden er onder andere fenotypes ontdekt voor mutanten betrokken bij ubiquitine-afhankelijk transport, histon modificatie, urmylatie en proteasoomfunctie. Op basis van gelijkenis in expressiepatronen konden bekende en nieuwe functionele relaties afgeleid worden. Deze omvatten de identificatie van verschillende eiwitcomplexen, het herleiden van functionele interacties tussen E2 en E3 enzymen, en het onderscheiden van signaleringsroutes tussen ubiquitinatie, urmylatie en fosforylatie systemen.

In **hoofdstuk 3** lichten we één van de gevonden fenotypes verder uit, gerelateerd aan het ubiquitine-proteasoom systeem (UPS). De proteasoom is een eiwitcomplex dat betrokken is bij de afbraak van geubiquitineerde eiwitten. We laten zien dat mutanten met een proteasoomdefect een verhoogde expressie

hebben van genen betrokken bij proteasoomfunctie, ubiquitinatie en eiwitvouwing. De aanwezigheid van deze expressiesignatuur is een goede indicator voor een algemeen UPS-defect en kan gebruikt worden voor het screenen van mutanten. Uit onze screen wordt duidelijk dat de proteasoom een zeer centrale rol heeft in meer cellulaire processen dan eerder werd aangenomen.

In **hoofdstuk 4** richten we ons op een nieuwe en relatief onbekende klasse van SUMO-afhankelijke ubiquitine E3 ligases, ook wel STUbLs genoemd. STUbLs zijn verantwoordelijk voor de afbraak van gesumoyeerde eiwitten, maar het is onbekend welke bijdrage dit levert aan het functioneren van een cel. De mens heeft één STUbL, genaamd RNF4. Gist heeft twee STUbL componenten, Slx5 en Slx8, die gezamenlijk het Slx5/8 complex vormen. Het uitschakelen van de functie van Slx5/8 heeft zeer negatieve gevolgen voor een cel. Deze cellen hebben een verminderde levensvatbaarheid door genominstabiliteit, o.a. ophoping van DNA-schade, waarvan de oorzaak onbekend is. Daarnaast is Slx5/8 betrokken bij het ubiquitineren en afbreken van verschillende transcriptiefactoren. Ons doel was om uit te zoeken hoe Slx5/8 het behoud van genomstabiliteit en transcriptie reguleert en om te onderzoeken of RNF4 een vergelijkbare functie heeft in de mens. Genexpressieprofielen van Slx5/8 mutanten lieten zien dat er een groot effect op transcriptie is, maar dat dit waarschijnlijk toegeschreven kan worden aan een stressgerelateerde celreactie als gevolg van DNA-schade. Er kon geen bewijs geleverd worden voor een verandering in genexpressie als gevolg van een afwijkende afbraak van transcriptiefactoren. Studie van de localisatie van Slx5 en Slx8 wees echter uit dat Slx5 zelf gebonden is aan het DNA. Slx5 is specifiek gebonden aan centromeer DNA, de plek waar een structuur van eiwitten, ook wel 'kinetochoor' genoemd, bindt om chromosomen te scheiden tijdens de celdeling. De centromeerbinding van Slx5 is afhankelijk van het kinetochoor, wat suggereert dat Slx5 direct aangrijpt op een onderdeel van het kinetochoor en betrokken

is bij de verdeling van chromosomen. Verdere studie van Slx5/8 mutanten liet verschillende mitotische defecten zien, waaronder een vertraagde mitose, een afwijkende vorm en positionering van het spoelfiguur, een abnormaal aantal chromosomen en ophoping van het eiwit Rts1 op centromeren. We vermoeden dat Slx5/8 een directe rol heeft bij de afbraak van een of meerdere gesumoyeerde eiwitten op de centromeer, wat mogelijk bijdraagt aan de correcte verdeling van de chromosomen over de moeder en dochtercel tijdens de celdeling. Verder onderzoek zal moeten uitwijzen welk substraat dit precies is.

Hoofdstuk 4 laat verder zien dat rol van Slx5/8 in het behoud chromosoomstabiliteit tijdens mitose evolutionair geconserveerd is in de mens. Studie van de humane STUbL RNF4 wees uit dat het uitschakelen van RNF4 ook leidt tot een afwijkende chromosoomsegregatie. Microscopie van delende cellen liet zien dat de segregatie van chromosomen verhinderd wordt doordat de twee chromatiden niet altijd volledig van elkaar losgemaakt worden. Hierdoor worden zogeheten 'chromosoombruggen' gevormd. Het geforceerd uit elkaar trekken van deze chromosoombruggen kan uiteindelijk leiden tot breuken in het DNA. Waarschijnlijk verklaart dit hoe DNA-schade ontstaat als gevolg van een defecte STUbL in zowel gist als mens.

In **hoofdstuk 5** gaan we dieper in op de individuele moleculaire functies van Slx5 en Slx8 als onderdeel van een STUbL-complex. Beide eiwitten hebben verschillende functies: Slx5 is verantwoordelijk voor de herkenning en binding van de gesumoyeerde eiwitten, terwijl Slx8 zorgt voor de interactie met het E2 enzym. Door deze twee moleculaire functies te combineren in één eiwitcomplex is de cel in staat om gesumoyeerde eiwitten te ubiquitineren en vervolgens af te breken.

Ten slotte in **hoofdstuk 6** worden de bevindingen van het bovenstaand onderzoek samengevat en bediscussieerd in het licht van de huidige literatuur.

Curriculum Vitae

Loes Andrea Leonora van de Pasch werd geboren op 1 februari 1982 te Horst. In 2000 behaalde zij haar VWO diploma aan het Dendron College te Horst. Vervolgens begon zij de bacheloropleiding Biomedische Wetenschappen aan de Universiteit Utrecht. Deze werd vervolgd met de master Developmental Biology and Biomedical Genetics. Gedurende deze master werden twee onderzoeksstages gedaan. Bij de afdeling Fysiologische Chemie aan het Universitair Medisch Centrum Utrecht (UMCU) werd onderzoek gedaan naar de DNA locatie van het eiwitcomplex Mediator onder begeleiding van dr. Jean-Christophe Andrau en dr. Frank Holstege. Bij de afdeling Celbiologie in het Nijmegen Center for Molecular Life Sciences (NCMLS) werd onderzoek verricht naar de rol van ATP productie tijdens celmigratie onder begeleiding van dr. Edwin Janssen en prof.dr. Bé Wieringa. In februari 2006 studeerde zij *cum laude* af aan de Universiteit Utrecht. In datzelfde jaar begon zij als Onderzoeker in Opleiding aan haar promotieonderzoek naar ubiquitine en ubiquitine-achtige systemen op de afdeling Molecular Cancer Research (UMCU). De resultaten van dat onderzoek, onder begeleiding van promotor prof.dr. Frank Holstege, staan beschreven in dit proefschrift.

Publications

Van de Pasch LAL*, Margaritis T*, Kashani M, Ampatziadis G, Van Wageningen S, Lenstra TL, Van Leenen D, Groot Koerkamp MJA, Holstege FCP. **Delineating ubiquitin and ubiquitin-like systems in *Saccharomyces cerevisiae* by gene expression profiling.** *Manuscript in preparation*

Van de Pasch LAL, Miles AJ, Nijenhuis W, Brabers NACH, Van Leenen D, Lijnzaad P, Brown MK, Ouellet J, Barral Y, Kops GJPL, Holstege FCP. **Centromere binding and a conserved role in chromosome stability for SUMO-dependent ubiquitin ligases.** *Manuscript under revision*

Apweiler E*, Sameith K*, Margaritis T, Brabers N, **Van de Pasch LAL**, Bakker LV, Van Leenen D, Holstege FCP, Kemmeren P. **Yeast glucose pathways converge on the transcriptional regulation of trehalose biosynthesis.** *BMC Genomics* 13(1):239 (2012)

Lenstra TL, Benschop JJ, Kim T, Schulze JM, Brabers NA, Margaritis T, **Van de Pasch LAL**, Van Heesch SA, Brok MO, Groot Koerkamp MJ, Ko CW, Van Leenen D, Sameith K, Van Hooff SR, Lijnzaad P, Kemmeren P, Hentrich T, Kobor MS, Buratowski S, Holstege FCP. **The specificity and topology of chromatin interaction pathways in yeast.** *Molecular Cell* 42(4):536-539 (2011)

Van Wageningen S*, Kemmeren P*, Lijnzaad P, Margaritis T, Benschop JJ, De Castro IJ, Van Leenen D, Groot Koerkamp MJ, Ko CW, Miles AJ, Brabers N, Brok MO, Lenstra TL, Fiedler D, Fokkens L, Aldecoa R, Apweiler E, Taliadouros V, Sameith K, **Van de Pasch LAL**, Van Hooff SR, Bakker LV, Krogan NJ, Snel B, Holstege FCP. **Functional overlap and regulatory links shape genetic interactions between signaling pathways.** *Cell* 143(6):991-1004 (2010)

Van Horssen R, Janssen E, Peters W, **Van de Pasch LAL**, Lindert MM, Van Dommelen MM, Linssen PC, Hagen TL, Franssen JA, Wieringa B. **Modulation of cell motility by spatial repositioning of enzymatic ATP/ADP exchange capacity.** *Journal of Biological Chemistry* 284(3):1620-1627 (2009)

Larivière L*, Seizl M*, Van Wageningen S, Röther S, **Van de Pasch LAL**, Feldmann H, Strässer K, Hahn S, Holstege FCP, Cramer P. **Structure-system correlation identifies a gene regulatory Mediator submodule.** *Genes and Development* 22(7):872-877 (2008)

Andrau JC, **Van de Pasch LAL**, Lijnzaad P, Bijma T, Koerkamp MG, van de Peppel J, Werner M, Holstege FCP. **Genome-wide location of the coactivator Mediator: Binding without activation and transient Cdk8 interaction on DNA.** *Molecular Cell* 22(2):179-192 (2006)

* Equally contributing authors

Dankwoord

De afgelopen jaren zijn er vele mensen voorbij gekomen die hebben bijgedragen aan dit proefschrift. Ik wil hierbij iedereen bedanken en een aantal mensen in het bijzonder. Allereerst mijn promotor Frank. Bedankt dat je me alle vrijheid gaf om vorm te geven aan mijn onderzoeksprojecten. Terugkijkend in dit proefschrift zie ik dat ik verrassend weinig aan transcriptie heb gewerkt, maar des te meer aan allerlei andere uitdagende onderwerpen. Ik heb bewondering hoe je mij altijd hebt weten te ondersteunen met goed advies dankzij je brede kennis, kritische blik en oneindige optimisme. Het voltooiën van mijn promotietraject was niet makkelijk met alle tegenslagen van het afgelopen jaar. Bedankt voor je hulp, geduld en vertrouwen dat het allemaal goed zou komen.

De leden van de beoordelingscommissie: Emmanuel Wiertz, Marc Timmers, Wouter de Laat en Geert Kops. Bedankt voor het lezen en de razendsnelle beoordeling van dit proefschrift. Geert Kops en Susanne Lens, jullie expertise op het gebied van mitose hebben mij erg geholpen bij het Slx5/8 project. Bedankt voor de samenwerking en alle discussies. Yves Barral and Jimmy Ouellet, thank you very much for our collaboration. The opportunity to come to Zürich and to learn how to perform microscopy experiments on yeast has given me so many new insights in yeast biology and gave a boost to the Slx5/8 project. Your knowledge and enthusiasm have been inspiring

Ik wil al mijn (oud-)collega's bedanken voor hun support. Sandy, je bent een organisatorisch wonder. Bedankt voor het regelen van al het papierwerk rondom mijn promotie en voor de organisatie van geweldige retreats! Wat fijn dat bij jou altijd de deur openstaat om even bij te kletsen en om daarna weer vrolijk naar buiten te lopen. Tony, ik kan je onmogelijk in een paar regels bedanken voor alles wat je de afgelopen jaren hebt gedaan. Jouw jarenlange hulp was een enorme steun. Het was fijn om alle grote en kleine succesjes en crisismomenten rond Slx5/8 met iemand te kunnen delen die precies begrijpt waar ik het over heb. Heel veel succes met al je toekomstplannen! Mariel, de laatste tijd heb ik jouw gezelligheid als buurvrouw erg gemist. Bij jou vond ik altijd een luisterend oor en goed advies. Ik hoop dat je snel weer zingend in het lab staat. Katrin, thank you so much for your friendship in- and outside the lab. Our conversations were the best stress-relieving medicine. Thank you for your help with all kinds of dry lab issues, from data analyses to picking colours for figures. Good luck with the completion of your thesis. I'm sure it's going to be filled with beautiful figures. You're next! Eoghan, you still have a few years to go, but keep up the good work! Soon you'll be on your own, but I'm sure you will be successful. Take good care of the yeasties. Tineke, wat jij allemaal in korte tijd voor elkaar hebt gekregen is een geweldige prestatie. Maak er een mooie tijd van in Washington! Eva, the lab is not the same anymore without you. It has been a time with many ups and downs, but at least we had each other. Thank you for always putting a smile on my face with your comments, sense of humour and adventures. Good luck in Chile! Thanasis, you have helped me out with many things, thank you so much for that! With joint forces we completed the huge task of generating microarray expression for a lot of ubiquitin(-like) system mutants. Thank you for your support and for always providing me with pizza and cookies. Joris, ik heb een enorme waardering voor je betrokkenheid. Op werkgebied, maar ook op persoonlijk vlak heb ik veel van je geleerd. Alhoewel ik met mijn eigenwijsheid jouw adviezen niet altijd opvolgde, moet ik toch toegeven dat je wel vaak gelijk had (maar niet altijd!). Met jouw humor en nuchtere kijk op de zaken wist je me altijd op te beuren als de proeven tegensaten of weer met beide benen op de grond te krijgen als proeven meezaten. Bedankt voor de geweldige tijd in het lab en fijn dat je me wil bijstaan als paranimf!

Sake, vanaf dag één liepen we samen rond in het Stratenum. Je was echt de (muzikale) sferemaker van het lab. Bedankt! Nathalie, bedankt voor de fijne samenwerking. De ontelbare tetrade-dissecties, spotassays en microscoopsessies waren een stuk gezelliger met z'n tweeën! Philip, Patrick, Sander en Linda, zonder jullie bioinformatici was ik nergens. Philip, dankzij jou is mijn onderzoek in ieder geval significant! Bedankt voor al je hulp! Patrick, bedankt dat je altijd de tijd nam om me te helpen met scripts en andere onbegrijpelijke zaken. Ik wens je veel succes toe in de toekomst! Sander, qua werk hadden we niet vaak direct met elkaar te maken, maar bedankt voor de plezierige 'samenwerking' tijdens lunches, pauzes en retreats. Linda, voor een 'nerd' was je toch wel heel gezellig ;-)! Leuk dat we onze muziekliefde konden delen. Als jullie kleintje er is, wordt het weer eens hoog tijd om samen naar een concert te gaan. Marian, Dik, Cheuk en Diane, jullie hebben een ongelooflijke berg aan microarray en ChIP experimenten verwerkt en de data die er uit kwam rollen is prachtig! Marian, bedankt dat je ondanks alle drukte altijd voor me klaarstond. Ik heb genoten van alle brainstormsessies en je enthousiasme voor de gistjes en microarrays! Dik, je hebt me regelmatig uit de brand geholpen als ik weer eens een 'computerprobleem' had veroorzaakt. Bedankt voor je hulp en voor alles wat je achter de schermen doet! Cheuk, je bent terug! Bedankt voor je vrolijke gezelschap in het Holstege lab en voor alle hulp in het lab en daarbuiten. Diane, het is al weer een hele tijd geleden, maar bedankt voor je hulp bij mijn allereerste microarrayexperimenten. Also a big thank you to all the students that have joined the lab for shorter or longer periods, especially Markus, Giannis and Mehdi for their contribution to this thesis. Ten slotte wil ik mijn oud-collega's van de Holstege generatie 1.0 bedanken: Jean-Christophe, Nynke, Nienke, Paul, Jeroen, Marijana en Harm. Jullie stonden aan de basis van dit proefschrift en ik heb ontzettend veel gehad aan alles wat ik van jullie heb geleerd als masterstudent en eerstejaars OiO.

Daarnaast wil ik alle (oud-)collega's van de afdeling Molecular Cancer Research bedanken voor het draaiende houden van de afdeling en voor de leuke gesprekken en discussies in de wandelgangen, tijdens retraites, borrels en werkbesprekingen. Marjoleine, bedankt voor alle last-minute bestellingen die je voor me gedaan hebt en de gezelligheid mét koekjes. Het IT-team, bedankt voor jullie snelle hulp bij allerlei computergerelateerde problemen en voor het veilig opslaan van mijn data. Marcel, bedankt dat je altijd wel wat Erlenmeyers voor me achter de hand wist te houden als ik weer een groot experiment ging doen. Folkert, Sjoerd and Gianpiero, you were all great company in the yeast lab and thank you all for your helpful discussions about ChIP experiments and ubiquitin. Maria, ik weet zeker dat de gistjes in goede handen zijn bij jou. Petra, jouw peptalks doen me goed! Bedankt voor je adviezen en succes met jouw project! Hetty, bedankt voor het brengen van orde in de chaos van het lab. Jij weet alles en iedereen te vinden en voor vragen kon ik altijd bij je aankloppen. Hopelijk kan je snel met plezier en in goede gezondheid weer aan de slag. Benjamin, tijdens onze enthousiaste discussies wist je me elke keer weer zover te krijgen om nog meer proeven te doen. Jij en Judith veel succes op het NKI. Livio, bedankt dat ik met mijn gistjes in de buurt van je microscopen mocht komen en voor al je hulp met de DeltaVision! Wilco, de overstap naar humane cellen vond ik welkome afwisseling! Bedankt voor het meedenken, al het trouble-shooten rond RNF4, en voor de mooie bijdrage aan hoofdstuk 4. Saskia, Nannette en Banafsheh, mijn gezellige buurvrouwen op de tweede verdieping, bedankt voor jullie interesse en veel succes met jullie projecten. Harmjan, 'is het al af?'. Ik kan eindelijk 'JA!' zeggen. Tijd voor een feestje!

Lieve vriendinnen Esther, Eline, Nga-Chi en Eveline. Het is zo fijn om te merken dat jullie me al sinds mijn studententijd zijn blijven steunen in mijn onderzoek. En beter nog... jullie begrijpen het ook nog (een beetje)! Of jullie nu dichtbij Utrecht zijn of aan de andere kant van de wereld, bedankt dat jullie altijd tijd weten vrij te maken voor gezellige etentjes, skype-sessies en berichtjes. Bedankt voor jullie vriendschap!

Lieve Ineke, ik ben zo blij dat ik jou in de buurt heb voor wat Brabantse gezelligheid. Bedankt dat je altijd voor me klaar staat. Soms lijkt het zo vanzelfsprekend, maar het is heel bijzonder! Wanneer gaan we onze wereldreis vervolgen? Familie van de Pasch, Smits en van Meel, bedankt voor jullie interesse en voor alle leuke afleiding in de vorm van bezoekjes, etentjes en city trips. Lieve zusjes, ik ben altijd weer blij als ik bij jullie ben. Jullie zijn zo gezellig! Anke en Ivo, ik kan kan niet wachten tot december om jullie spruitje te bewonderen! Carla en Nick, het feest is natuurlijk niet compleet zonder jullie twee feestbeesten. Carla, superleuk dat je mijn paranimf bent! Lieve pap en mam, eindelijk kunnen jullie het eindresultaat van zes jaar hard werken in dit kleine boekje terugzien. En dit was niet mogelijk geweest zonder jullie... 'biëstig' bedankt dat jullie me in alles steunen en dat ik altijd op jullie kan terugvallen. Lieve Pieter, met z'n tweeën is het leven zo veel mooier geworden. Bedankt voor alles! Wat de toekomst gaat brengen is nog onbekend, maar dat het samen is met jou dat is zeker!

Loes

